NATIONAL COOPERATIVE
HIGHWAY RESEARCH PROGRAM REPORT **276**

THERMAL EFFECTS IN CONCRETE BRIDGE SUPERSTRUCTURES

TRANSPORTATION RESEARCH BOARD
NATIONAL RESEARCH COUNCIL

NATIONAL COOPERATIVE HIGHWAY RESEARCH PROGRAM
REPORT 276

THERMAL EFFECTS IN CONCRETE BRIDGE SUPERSTRUCTURES

R. A. IMBSEN, D. E. VANDERSHAF, R. A. SCHAMBER, and R. V. NUTT
Engineering Computer Corporation
Sacramento, California

RESEARCH SPONSORED BY THE AMERICAN ASSOCIATION OF STATE HIGHWAY AND TRANSPORTATION OFFICIALS IN COOPERATION WITH THE FEDERAL HIGHWAY ADMINISTRATION

AREAS OF INTEREST:

STRUCTURES DESIGN AND PERFORMANCE
CEMENT AND CONCRETE
(HIGHWAY TRANSPORTATION)
(PUBLIC TRANSIT)
(RAIL TRANSPORTATION)

TRANSPORTATION RESEARCH BOARD
NATIONAL RESEARCH COUNCIL
WASHINGTON, D.C.
SEPTEMBER 1985

NATIONAL COOPERATIVE HIGHWAY RESEARCH PROGRAM

Systematic, well-designed research provides the most effective approach to the solution of many problems facing highway administrators and engineers. Often, highway problems are of local interest and can best be studied by highway departments individually or in cooperation with their state universities and others. However, the accelerating growth of highway transportation develops increasingly complex problems of wide interest to highway authorities. These problems are best studied through a coordinated program of cooperative research.

In recognition of these needs, the highway administrators of the American Association of State Highway and Transportation Officials initiated in 1962 an objective national highway research program employing modern scientific techniques. This program is supported on a continuing basis by funds from participating member states of the Association and it receives the full cooperation and support of the Federal Highway Administration, United States Department of Transportation.

The Transportation Research Board of the National Research Council was requested by the Association to administer the research program because of the Board's recognized objectivity and understanding of modern research practices. The Board is uniquely suited for this purpose as: it maintains an extensive committee structure from which authorities on any highway transportation subject may be drawn; it possesses avenues of communications and cooperation with federal, state, and local governmental agencies, universities, and industry; its relationship to the National Research Council is an insurance of objectivity; it maintains a full-time research correlation staff of specialists in highway transportation matters to bring the findings of research directly to those who are in a position to use them.

The program is developed on the basis of research needs identified by chief administrators of the highway and transportation departments and by committees of AASHTO. Each year, specific areas of research needs to be included in the program are proposed to the National Research Council and the Board by the American Association of State Highway and Transportation Officials. Research projects to fulfill these needs are defined by the Board, and qualified research agencies are selected from those that have submitted proposals. Administration and surveillance of research contracts are the responsibilities of the National Research Council and the Transportation Research Board.

The needs for highway research are many, and the National Cooperative Highway Research Program can make significant contributions to the solution of highway transportation problems of mutual concern to many responsible groups. The program, however, is intended to complement rather than to substitute for or duplicate other highway research programs.

NCHRP REPORT 276

Project 12-22 FY'81

ISSN 0077-5614

ISBN 0-309-03860-X

L. C. Catalog Card No. 85-52305

Price $9.60

NOTICE

The project that is the subject of this report was a part of the National Cooperative Highway Research Program conducted by the Transportation Research Board with the approval of the Governing Board of the National Research Council. Such approval reflects the Governing Board's judgment that the program concerned is of national importance and appropriate with respect to both the purposes and resources of the National Research Council.

The members of the technical committee selected to monitor this project and to review this report were chosen for recognized scholarly competence and with due consideration for the balance of disciplines appropriate to the project. The opinions and conclusions expressed or implied are those of the research agency that performed the research, and, while they have been accepted as appropriate by the technical committee, they are not necessarily those of the Transportation Research Board, the National Research Council, the American Association of State Highway and Transportation officials, or the Federal Highway Administration, U.S. Department of Transportation.

Each report is reviewed and accepted for publication by the technical committee according to procedures established and monitored by the Transportation Research Board Executive Committee and the Governing Board of the National Research Council.

The National Research Council was established by the National Academy of Sciences in 1916 to associate the broad community of science and technology with the Academy's purposes of furthering knowledge and of advising the Federal Government. The Council has become the principal operating agency of both the National Academy of Sciences and the National Academy of Engineering in the conduct of their services to the government, the public, and the scientific and engineering communities. It is administered jointly by both Academies and the Institute of Medicine. The National Academy of Engineering and the Institute of Medicine were established in 1964 and 1970, respectively, under the charter of the National Academy of Sciences.

The Transportation Research Board evolved in 1974 from the Highway Research Board which was established in 1920. The TRB incorporates all former HRB activities and also performs additional functions under a broader scope involving all modes of transportation and the interactions of transportation with society.

Special Notice

The Transportation Research Board, the National Research Council, the Federal Highway Administration, the American Association of State Highway and Transportation Officials, and the individual states participating in the National Cooperative Highway Research Program do not endorse products or manufacturers. Trade or manufacturers' names appear herein solely because they are considered essential to the object of this report.

Published reports of the

NATIONAL COOPERATIVE HIGHWAY RESEARCH PROGRAM

are available from:

Transportation Research Board
National Research Council
2101 Constitution Avenue, N.W.
Washington, D.C. 20418

Printed in the United States of America

FOREWORD

By Staff
Transportation
Research Board

This report contains the findings of a comprehensive study of thermally induced stresses in reinforced and prestressed concrete bridge superstructures. Design guidelines for thermal effects in concrete bridge superstructures, accompanied by a commentary, are included in the report and are of immediate importance, applicability, and interest to bridge engineers, construction engineers, researchers, specification writing bodies, and others concerned with thermal effects in concrete structures.

Bridge design requires consideration of the effects produced by temperature ranges and thermal gradients in the structure. These effects are particularly significant in large concrete bridges but are covered only to a limited extent in the current *AASHTO Standard Specifications for Highway Bridges.* Modern methods of concrete bridge construction require more accurate information for design purposes.

An increasing number of long span, concrete box girder bridges are being constructed in the United States. In large sections, commonly used for segmental or other modern concrete bridge superstructures, the effects of temperature gradients, either across the section or through the thickness of its elements, are important and should be considered in the design. In some cases, stresses caused by temperature gradients may exceed those calculated for design live loads. Some design codes used in other countries provide guidance on these effects, but they are not adequately addressed in the current AASHTO Specifications.

This report contains the findings of NCHRP Project 12-22, "Thermal Effects in Concrete Bridge Superstructures." The objectives of this study were to develop recommended specifications and design procedures for consideration of thermally induced stresses and movements in concrete bridge superstructures.

The first part of the report provides a review and evaluation of existing domestic and foreign codes of practice, research findings, and performance data. On the basis of this information, key parameters for the development and refinement of design procedures for thermal effects are identified. Case studies were performed to investigate the effects produced by thermal gradients on typical bridge configurations. Based on an assessment of the results of these case studies, design guidelines and a corresponding commentary have been developed and are presented along with representative example problems. The guidelines and commentary will be considered for adoption by the AASHTO Subcommittee on Bridges and Structures.

The report also provides a comprehensive bibliography containing detailed reference categories that would be of use to both designers and researchers.

CONTENTS

ACKNOWLEDGMENTS

The research reported herein was performed under NCHRP Project 12-22 by Engineering Computer Corporation (ECC) of Sacramento, California. Roy A. Imbsen, President of ECC, served as principal investigator. He was assisted by David E. Vandershaf, Structural Engineer, and Robert A. Schamber, Research Engineer. Carl Stewart was a consultant to ECC on this project. Richard V. Nutt, Project Manager for ECC, reviewed the work and assisted in preparing the report.

THERMAL EFFECTS IN CONCRETE BRIDGE SUPERSTRUCTURES

SUMMARY

This is a report on a comprehensive study of thermally induced stresses in reinforced and prestressed concrete bridge superstructures. The study includes stresses resulting from variations in average bridge temperature and variations in temperature due to temperature gradients within the superstructure. The former types of stresses have an important effect on the performance of most concrete bridge superstructures, while the latter types of stresses have had an adverse effect on bridge performance in only a few cases—primarily long-span prestressed box girders with design optimized cross sections.

The average bridge temperature varies seasonally and/or diurnally primarily because of fluctuations in ambient temperatures. The resultant expansion and contraction of the bridge superstructure can result in internal stresses if the structure is restrained. Radiational heat gain or loss can result in a nonuniform distribution of temperature through the depth or the width of a superstructure. This temperature variation is not linear and can induce stresses in two ways. First, the variations in the thermal distortions of the concrete will induce deformations perpendicular to the longitudinal axis of the superstructure which, when restrained, will result in internal bending moments. Secondly, the nonlinear variation in temperature will be restrained from inducing nonlinear distortions of the superstructure section because of the tendency for plane sections to remain plane. This will also result in thermally induced stress.

The current AASHTO design specifications contain provisions for the variation in average bridge temperature, but do not provide any guidance for considering the variation in the temperature between different elements of the superstructure. The Post Tensioning Institute (PTI) and the design specifications from several foreign countries provide methods for considering this phenomenon. Most states that consider this temperature variation during design use the methods proposed by PTI.

The methods used by PTI and several foreign countries vary considerably. One of the primary differences in these methods is the assumed variation in temperature through the depth of the superstructure. Case studies performed as part of NCHRP Project 12-22 demonstrated that temperature variations can result in significant thermally induced stress and that the assumed variation in temperature has a large influence on these stresses.

Based on the results of these case studies and the fact that temperature variations in superstructures were verified by field measurement, the temperature gradient shape recently proposed by the University of Illinois is recommended for design purposes in the United States. This temperature gradient shape consists of a multilinear temperature variation for both the loading cases of radiational heating and radiational cooling. A proposed revision to the AASHTO specifications which includes this method of considering temperature variation was drafted as part of this study.

CHAPTER ONE

INTRODUCTION AND RESEARCH APPROACH

Temperature effects on bridges can be classified into effects resulting from the seasonal and/or diurnal variation in the mean bridge temperatures and effects resulting from the variation in temperature between different elements of the bridge at any point in time. Variations in the mean bridge temperature will result in the expansion or contraction of an unrestrained bridge superstructure. If the superstructure is fully or partially restrained by its supporting columns, piers, or abutments, thermally induced stresses will result. The variation in temperature between different elements of the bridge will result in rotational as well as translational distortions of the superstructure.

Rotational distortions caused by a variation in temperature through the depth of the superstructure will result in bending moments in a structure which is continuous over one or more supports. When the temperature variation with depth is nonlinear, stresses will also be induced because of the tendency for plane sections to remain plane.

Traditionally, most bridges have been designed to accommodate only the overall longitudinal movement arising from temperature strain. However, with the recent changes in bridges types, it has become apparent that temperature differentials also exist in bridge superstructures. These temperature differentials cause stresses that should be included in the design procedures. Although the current AASHTO specifications include probable temperature ranges of mean temperature conditions that affect expansion and contraction of concrete bridge superstructures, there is no recommendation for temperature differentials that may occur in superstructure sections.

Several bridge design specifications and guidelines recognize the existence of temperature gradients throughout the depth of a bridge superstructure and recommend that vertical temperature gradients be considered in the design procedure. In addition, some guidelines have also recommended that temperature gradients be used in the transverse direction to reflect the temperature changes that occur between the external and internal surfaces of box girder bridges. To date various approaches have emerged, most of them requiring different shaped temperature gradients and intensities to be used in the gradient. The thermal response of a bridge involves a combination of the shade temperature, the intensity of solar radiation, the absorptivity of the superstructure materials, and the depth of the superstructure. Although many researchers and code writers recognize these factors and have proposed various design specifications that include these thermal effects, they often disagree about the importance and refinement that should be included in the design procedure. In addition, code writers are influenced by local meteorology and construction practices. The objective of NCHRP Project 12-22 is to develop comprehensive specifications and design procedures for consideration of thermally induced stresses and movements in concrete bridge superstructures, and to recommend those procedures that might be the most appropriate for inclusion in the AASHTO Specifications.

To meet this objective, the basic approach taken in this project was to review and evaluate existing domestic and foreign codes of practice, research findings, and performance data; and, on the basis of the information generated, to establish rationales for alternative approaches to the development of guidelines for consideration of thermal effects in the design of major concrete bridge structures. The salient aspects of the research are covered in the succeeding chapters and appendixes of this report. Current research results and performance data are briefly discussed in Chapter Two. Chapter Three gives a comprehensive discussion of the key parameters in the development and refinement of the design procedures for thermal effects. Bridge design codes of different countries and alternative approaches to account for thermal effects are detailed in Chapter Four. Chapter Five describes several case studies that were conducted to investigate the effects produced by thermal gradients on the longitudinal and transverse fiber stresses induced in a selected group of U.S. bridges. The conclusions and recommendations summarized in Chapter Six are based on an assessment of the results of these case studies. Design guidelines and commentary are provided in Appendixes A and B, respectively. Two worked example problems are given in Appendix C. More detailed background information with respect to bridge design codes of the different countries and alternative analysis procedures for calculating thermally induced longitudinal stresses are provided in Appendixes D and E respectively.

CHAPTER TWO

FINDINGS—CURRENT RESEARCH AND PERFORMANCE DATA

There are only a few published accounts of concrete bridges damaged by differential temperature effects. In 1965, Leonhardt et al. (*105*) described the damage in the girders of the Jagst Bridge in Germany. This two-span continuous box girder bridge is shown in Figure 1. Five years after completion of the bridge, cracks were discovered along one of the webs, as shown in the

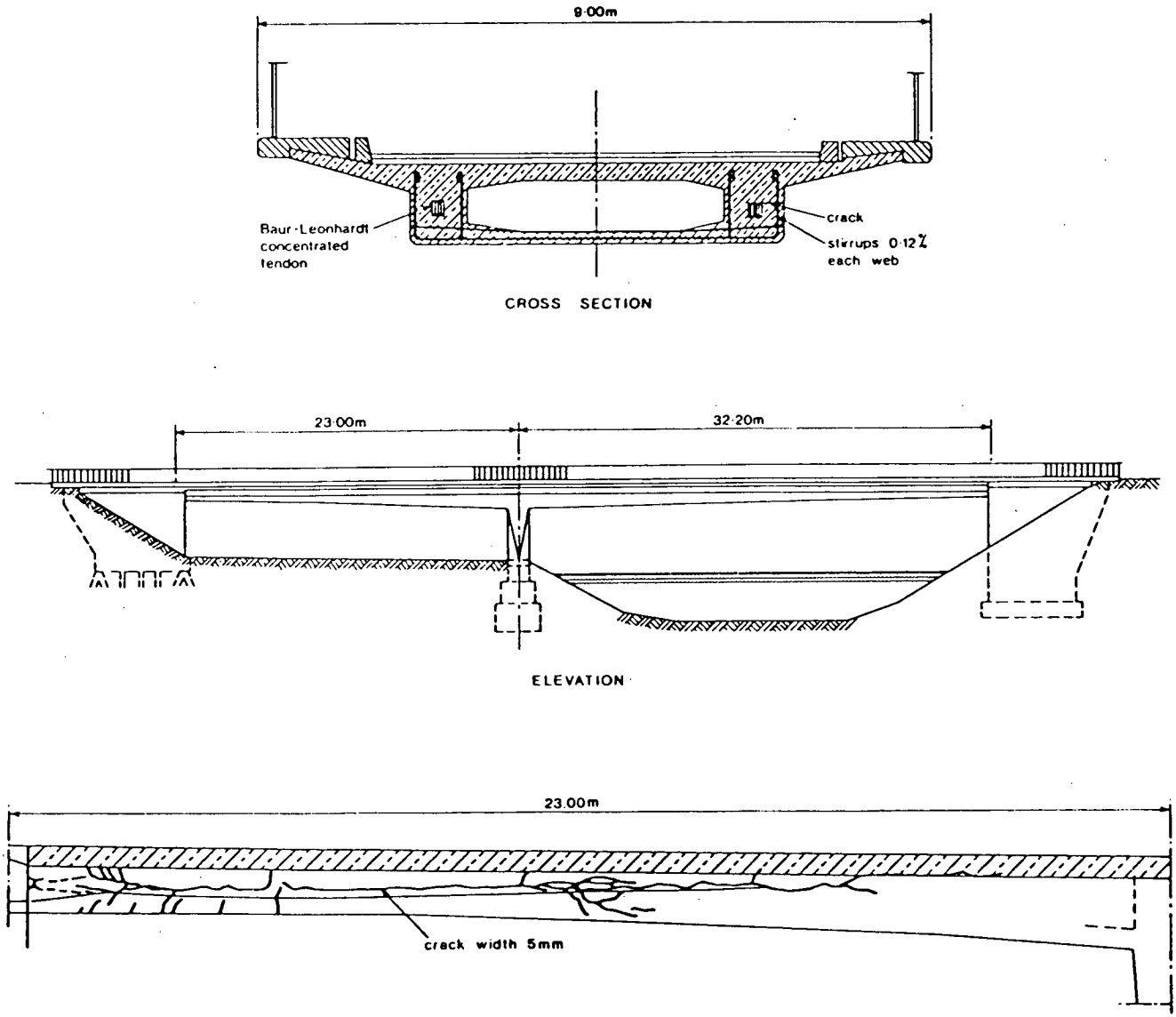

Figure 1. The Jagst Bridge in Germany (105).

figure. Crack widths of 0.2 in. (5 mm) were measured, with lateral displacements of 0.1 in. (2 mm). Initially, the damage was attributed to the effects of nonlinear temperature gradients, but subsequent more detailed investigation revealed that other contributing factors included large, concentrated prestress forces and small amounts of reinforcement to control cracking. Large ducts located in each web produced large concentrated forces which, in turn, induced high, localized tensile stresses. It is possible that a more uniform arrangement of prestressing tendons would have prevented the cracking. The stirrups that were provided in the webs failed to prevent the cracking. In a subsequent publication, Leonhardt and Lippoth (*117*) made recommendations intended to prevent such uncontrolled cracking. They suggested that thick-walled box sections should, if possible, be avoided and that enough secondary reinforcement should be provided to control any cracks that might occur.

In 1981, Zichner (*90*) described the fundamentals for determining temperature effects in concrete bridges and indicated that cracks such as those shown in Figure 2 were observed in the course of thorough inspections of several bridges. The cracks located in the bottom slabs and girder stems of box girder bridges can be attributed to, among other causes, temperature differences that existed within the bridge superstructure.

More recently the State of Colorado experienced cracking in the webs and bottom deck soffits of four cast-in-place, segmental, prestressed bridges. Two of the bridges are approximately 747 ft long, the third about 516 ft long, and the fourth about 449 ft long. The three longer bridges have four spans, while the shorter one has three. The three-span bridge, shown schematically in Figure 3, exhibited the greatest amount of cracking. The crack patterns on the single-cell bottom deck soffit and webs are also shown in Figure 3. The largest crack width reported is approximately 0.13 in. (3 mm). In a report, Ellsworth and Wooley (*130*) state:

> The temperature . . . was measured at 5:00 p.m., August 11, 1982, by the use of a wahl digital heat spy, model DHS-40X.

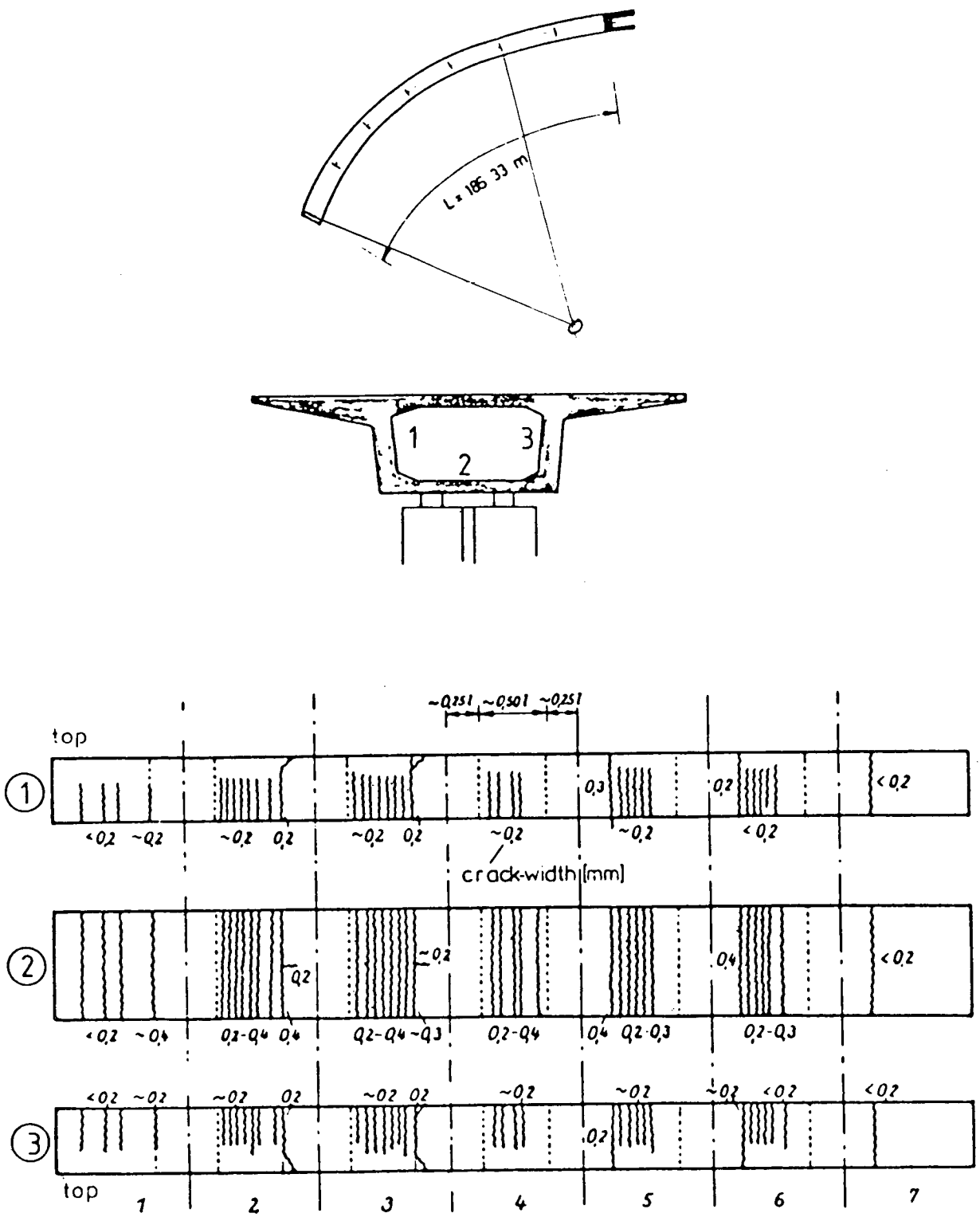

Figure 2. Cracks in a multispan box girder bridge (90).

This device detects infrared radiation and displays a corresponding temperature. Recordings were taken on the riding surface, the barrier wall and the bottom exterior slab. Temperatures were found to be 82, 72, and 60 degrees, respectively. At this time the opening of the joint between segments 203 and 204 was measured at 3/8".

The following morning at 8 a.m. the procedure was repeated. The temperature was recorded as follows: riding surface: 50 degrees F, exterior bottom slab: 47 degrees F.

The joint opening at segment 203 and 204 was recorded at 1/8". This demonstrated that the temperature gradient was noticeably affecting the structure.

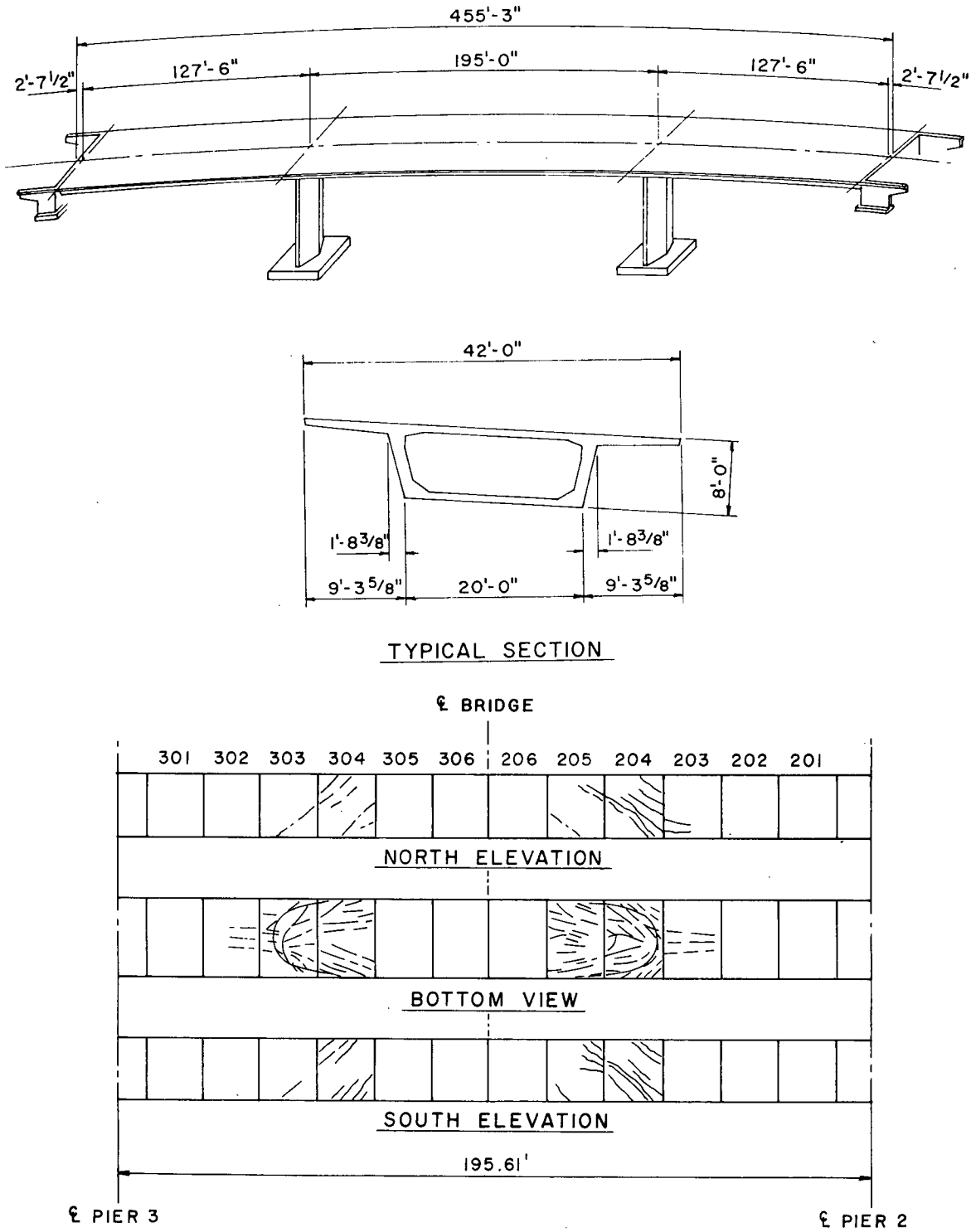

Figure 3. Miller Creek Bridge in Colorado.

The other three structures were reported to "... show the same cracking pattern ... but to a lesser degree."

During an 8-year period, California (*34*) investigated 64 concrete box girder structures that were over 350 ft long and had no expansion joints, i.e., the deck was continuous between the back walls of the abutments (the abutment backwalls were monolithic with the girders).

Twenty of these structures were over 400 ft long with three

extending over 500 ft. The objective of the investigation was to determine if shrinkage, elastic and plastic prestress deformation, and temperature effects adversely affected the serviceability of the structures. The investigators relied on unusual cracking as the primary manifestation of adverse effects.

Unusual cracking was found in only 20 bents, and that only at the top of one or more columns. These cracks were horizontally oriented and in the area that is in tension when the structure shortens. There were also horizontal cracks near the top of 12 abutment walls. None of the cracks measured more than 0.01-in. in width. None of the decks, exterior webs, or soffits showed any signs of unusual cracking.

Temperature probably helped develop these cracks in the columns, but so did shrinkage and prestress deformation. It was not possible to determine how much each of these factors contributed to the unusual cracking.

Other reported cases of thermal-caused stress in structures are included in a report by Lanigan (*109*) on construction joints opening in webs of a box girder bridge and in a report by Huizing et al. (*110*) on the falsework collapse of a continuous box girder bridge.

White (*20*) of Great Britain concluded that the British design practice prior to 1979, which made no specific provisions for temperature differentials, in general resulted in adequate accommodation of temperature effects. While surveying reported problem of temperature differentials in highway structures, he found that there were no recorded cases of temperature-caused distress in his country. He concluded: "It appears that the lack of information in the British Isles is either because any cases of temperature damage which have occurred have not been published or because temperature damage has not occurred, the latter implying that the effects of nonlinear differential temperature distributions have been unintentionally allowed for in the design process (i.e. the other design loadings are too severe and/or the design criteria too conservative)."

CHAPTER THREE

FINDINGS—HEAT EXCHANGE AND THERMAL EFFECTS

HEAT ENERGY EXCHANGE ON CONCRETE BRIDGE SUPERSTRUCTURES

Any structure exposed to the atmosphere is subjected to an exchange of heat energy between the surface of the structure and its surrounding environment. A bridge is continually gaining or losing heat which produces both seasonal and diurnal variations. The amount of heat energy exchanged is dependent on many factors. There are three principal mechanisms of heat transfer: (1) radiation from the sun and reradiation between the surrounding environment and the structure itself, (2) convection of heat between the surface of the structure and its surrounding environment, and (3) conduction of heat between the surface of the structure and its surrounding environment

Heat Transfer by Radiation

Heat transfer by radiation is generally considered to be the most important of the three mechanisms. During the daylight hours when the structure is exposed to the sun, especially during the warm summer months, a net gain of heat energy occurs through the depth of structure, primarily as a result of the solar radiation impinging on the surfaces of the structures. Conversely, primarily as a result of reradiation to the surrounding environment of the heat energy stored in the structure, a net loss of heat energy occurs during the night. During the summer, the temperature in the top surface of the bridge deck is warmer than the soffit, which results in a positive gradient. Negative gradient develops on typical winter nights when the top surface is cooler than the soffit. The intensity of the solar radiation reaching the surface of the earth is dependent on the angle at which the radiation passes through the atmosphere and the length of daylight time. This intensity is dependent on latitude and has an annual variation, as shown in Figure 4. In addition,

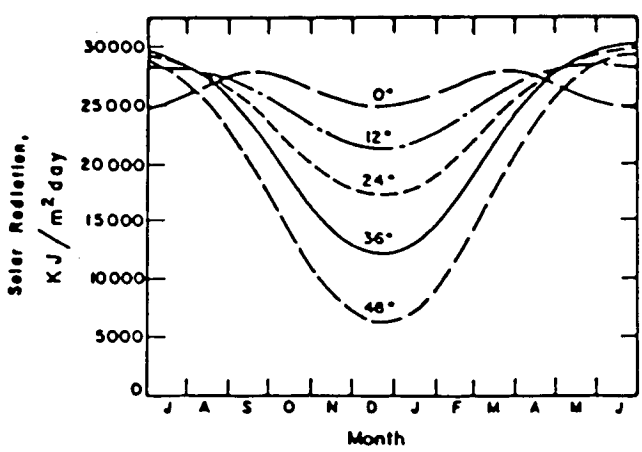

Figure 4. Variation in solar radiation for various latitudes. (Source: Ref. *98*)

the intensity of the solar radiation reaching the surface of a bridge is dependent on several other factors, each pertaining to the condition of the earth's atmosphere. These factors are shown diagrammatically in Figure 5. The intensity of solar radiation varies daily, as shown in Figure 6. Moreover, because of the poor thermal conductivity of concrete, these diurnal variations result in temperature gradients within bridge superstructures.

As shown in Figure 5, the radiation which penetrates the atmosphere and reaches the surface of a bridge deck has two primary effects. It may be reflected or it may penetrate the surface, be absorbed and converted to heat. The amount of absorbed radiation in a bridge structure is dependent on the type of surfacing. Various media absorb different quantities of radiation. Colored bodies are distinguished by their selective

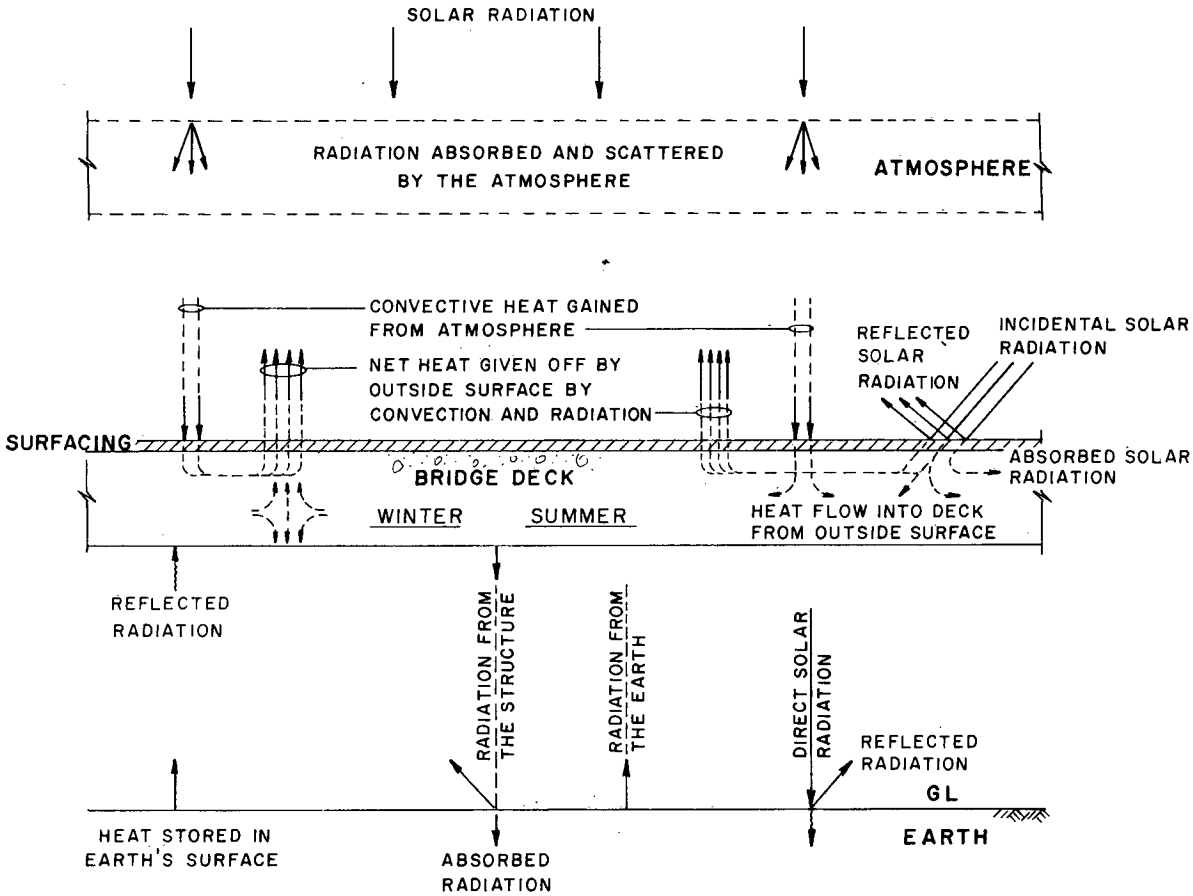

Figure 5. Solar radiation reaching the surface of a bridge.

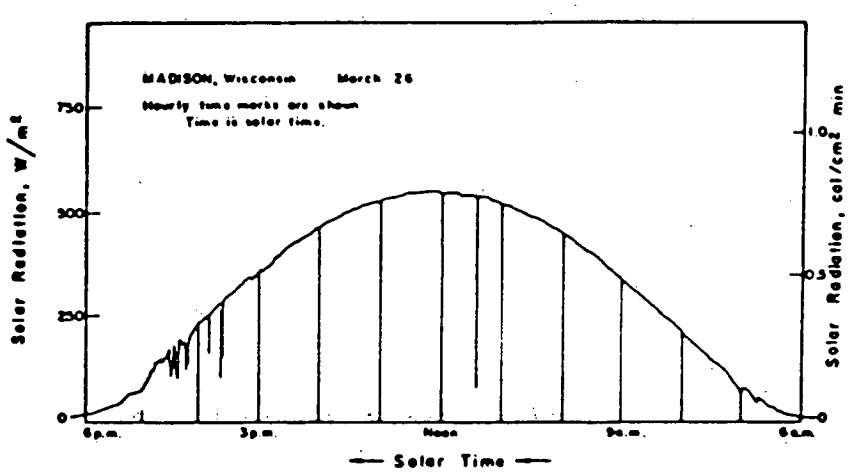

Figure 6. Variation in solar radiation for a clear day. (Source: Ref. *98*)

absorption of different wavelengths of light. A body which absorbs all wavelengths is defined as a "blackbody." Concrete structures function as "gray bodies" because they absorb only a certain amount of wavelength and reflect the remainder. Emerson (*21*) has investigated the amount of radiation absorbed on bridges having various amounts of surfacing. Emerson concluded that the influence of the depth of deck surfacing should also include the shape of the cross section. Priestley (*16*) investigated the effects of white surfacing, black surfacing, and no surfacing on a one-quarter scale model of a box girder bridge. The maximum surface temperatures of the concrete were found when the deck was unsurfaced. The white surfacing was found to yield the lowest temperatures. The temperatures yielded by the black surfacing were about 10 percent lower than those occurring in the unsurfaced concrete. This difference was due to the insulating effect of the top, black layer, even though it had a greater absorptivity of radiation than the base concrete surface.

Heat Transfer by Conduction and Convection

In addition to the heat transfer by radiation heat transfer by conduction and convection also takes place at the structure surface. However, because the heat transfer by conduction alone is small, it is difficult to assess. Therefore, it is normal to allow for heat transfer by conduction and convection by assuming a single, combined coefficient sensitive to wind velocity, ambient air temperature, and surface temperature.

Overall Heat Energy Exchange

Once the variables governing the heat exchange have been defined and quantified and the expressions governing the surface boundary conditions have been developed, the temperature distribution throughout the structure may be calculated. To help the bridge designer establish these boundary conditions, researchers have developed various expressions for the heat-energy exchange at the surface of a structure.

THERMAL EFFECTS ON BRIDGE SUPERSTRUCTURES

Having established the parameters governing the heat exchange at the boundaries of a bridge, the temperatures within the structure may be determined. A bridge superstructure is continually gaining and losing heat which produces both seasonal and diurnal variations in the bridge, variations that are of concern to the bridge designer. Provisions for seasonal variations are included in the design of bearings, hinge seats, and substructure components that are connected to the superstructure. The mean temperature of the superstructure is used in this case.

Thermal Properties of Concrete

The thermal coefficient of expansion for concrete is greatly dependent on its aggregate type and mix proportions (*76, 96, 97*). The cement paste of normal concrete usually has a higher thermal coefficient of expansion than the aggregate in the mix, but because the aggregate occupies about 75 percent of the volume, it is the aggregate's thermal exansion characteristics that dictate the volumetric change during a temperature change. It is believed that a concrete's thermal coefficient of expansion is about equal to the weighted average of the thermal coefficient of its ingredients. Variations in coefficients for a particular mix are caused by the original water/cement ratio, method of curing and moisture content, and age at the time of interest.

Most codes specify an average thermal coefficient of 0.000011 to 0.000012/°C (about 0.000006/°F) for reinforced concrete. Actual coefficients from laboratory tests on concrete samples, given in Table 1, vary as much as 22 percent above and 64 percent below the higher value, depending on the aggregate type.

Aggregates are often complex in terms of mineral content, while the minerals vary widely in thermal characteristics (*96*). For examples of the mineral variations, siliceous minerals such as quartz have a coefficient of approximately 12 microstrain/°C, whereas calcite, which is present in many limestones, has a coefficient from 1 to 5 microstrain/°C. Thus, the thermal expansion coefficient of rocks having a high percentage of siliceous minerals is higher than those having a high percentage of calcite.

Rocks are usually grouped according to their primary mineral. The secondary mineral can vary both in type and amount; hence, rock groups from different sources (parts of the country, or on a more broader base the world) can have different thermal coefficients. Accordingly, rock groups are sometimes listed with a range of thermal coefficients, as given in Table 2.

Table 1. Thermal coefficients of concrete (.000001/°C).

AGGREGATE TYPE	REPORTER			
	PCA[a]	EMERSON[b]	BROWN[c]	ONTARIO[d]
Quartzite		12.7	11.7–14.6	12.8
Quartz	11.9		9.0–13.2	
Sandstone	11.7	11.7	9.2–13.3	11.7
Gravel	10.8	13.2	9.0–13.7	13.1
Granite	9.5	9.6	8.1–10.3	9.5
Dolerite		9.6		9.5
Basalt	8.6		7.9–10.4	
Marble			4.4– 7.4	
Limestone	6.8	7.3	4.3–10.3	7.4

[a] *Building Movements and Joints,* 1st Ed., Portland Cement Association, Skokie, Illinois, 1982.
[b] M. Emerson, "Bridge Temperatures for Setting Bearings and Expansion Joints, *TRRL Supplementary Report 479,* Berkshire, England, ISSN 0305-1315, 1979.
[c] R. D. Brown, "Properties of Concrete in Reactor Vessels," Conference on Prestressed Pressure Vessels, *Proc.,* Institute of Civil Engineers, London, 1968.
[d] *Ontario Highway Bridge Design Code and Commentary,* Ontario Ministry of Transportation and Communications, Ontario, Canada, 1979.

Table 2. Thermal coefficients of aggregates (.000001/°C).

AGGREGATE TYPE	DEPT. OF INTERIOR[a]	REPORTER		
		BROWN[b]	PCA[c]	FHWA[d]
Quartzite	3.4	7.0–13.2	13.1	6–7
Sandstone	3.1	4.3–12.1	11.9	6–8
Gravel			10.6–12.8	4.5–7
Granite	2.4	1.8–11.9	1.8–11.9	4–5.5
Basalt	1.7	4.0–9.7	8.1	4–5
Marble	2.2	2.2–16.0	1.1–16.0	
Limestone	2.4	1.8–11.7	3.4–11.5	2.5–4

[a] *Concrete Manual,* 7th Ed., U.S. Department of the Interior, Bureau of Reclamation.
[b] R. D. Brown, "Properties of Concrete in Reactor Vessels," Conference on Prestressed Pressure Vessels, *Proc.,* Institute of Civil Engineers, London, 1968.
[c] *Building Movements and Joints,* 1st Ed., Portland Cement Association, Skokie, Illinois, 1982.
[d] S. G. Fattal, T. A. Reinhold, and B. Ellingwood, "Analysis of Thermal Stresses in Internally Sealed Concrete Bridge Decks," *Report No. FHWA/RD-80/085,* Center for Building Technology, National Bureau of Standards, April 1981.

Another reason for some of the reported differences by different testers within an aggregate group could be due to the method of testing (*96*). The curing method used on the test sample, the moisture content of the sample at the time of testing, its size, and the rate in which the temperature is changed all influence to some degree the resulting thermal coefficient of expansion. Variability in these factors among the various tests would, in itself, cause some variability in the results.

The presence of reinforcing steel in most in-service concrete because of a possible difference in their thermal coefficients probably causes a composite coefficient of the mass that is unlike either the steel's or the concrete's. It is thought that the maximum effect on the concrete's thermal coefficient by the presence of steel reinforcement is no more than 10 percent (*96*).

Because of the wide range of aggregate's thermal characteristics and the various factors that influence the thermal coefficient of concrete, it is difficult to predict with a high degree of accuracy the actual thermal coefficient of expansion for a concrete without extensive material testing. Even with testing of the materials to be used, it should be recognized that there will likely be a difference between the test and actual field results.

Temperature Range

Mean or effective bridge temperatures are associated with the long-term (seasonal) movements of a bridge. These movements may require the use of expansion joints, but the current trend is to eliminate joints where possible and allow structural elements, such as column and abutments, to absorb temperature-induced movement. The AASHTO Design Specifications provide values for a rise and fall in average bridge temperature as a function of superstructure material and the surrounding type of terrain. Other bridge codes also provide guidelines for calculation of overall longitudinal movements by specifying a range of temperatures that depends on the geographical location and form of construction. The specified range of effective temperature represents the average range to be considered in design. Unusual conditions, such as frost pockets and sheltered, low-lying areas, may require that there be some adjustments to a given range of effective temperatures.

Emerson (*81*) defines the effective temperature of a bridge as that temperature which governs the longitudinal movement of the bridge deck. The effective temperature may be derived by performing a calculation which includes both the product of the areas between isotherms and their mean temperatures divided by the total area of cross section of the deck. Emerson (*43*) and Black (*27*) have correlated the extreme values of the effective bridge temperature with shade temperatures. Emerson correlated the shade temperature with the temperatures obtained from structures instrumented with thermocouples, and Black correlates shade temperature with bridge movements to obtain the extreme values of effective bridge temperatures.

Temperature Differentials and a Review of Analytical Studies to Determine Temperature Distribution

Because of the poor thermal conductivity of concrete, diurnal temperature effects produce temperature gradients in a concrete bridge superstructure. As mentioned earlier and explained in greater detail under "Response Analysis," these gradients will result in rotational distortions that will produce stresses in the superstructures. Large, positive temperature gradients occur during days with high solar radiation, clear skies, a large range of ambient temperatures, and a light wind. Negative temperature gradients develop during periods associated with evening conditions. The temperature gradients that form are governed by heat flow through the body and are a function of the density, specific heat, and thermal conductivity of the concrete.

The general heat flow equation which governs the transient heat flow within the boundaries of the bridge superstructure is expressed as:

$$\frac{\delta T}{\delta t} = \frac{k}{\rho c}\left[\frac{\delta^2 T}{\delta x^2} + \frac{\delta^2 T}{\delta y^2} + \frac{\delta^2 T}{\delta z^2}\right] \quad (1)$$

where

T = temperature of the mass;
t = time;
x,y,z = direction in the Cartesian coordinates;
k = thermal conductivity;
ρ = density; and
c = specific heat.

Various researchers have reduced Eq.1 from the general three-dimensional heat-flow equation to both two-dimensional and one-dimensional heat-flow equations. A two-dimensional heat-flow analysis includes both the vertical and transverse heat flows in the given bridge superstructure. However, one-dimensional heat flow in the vertical direction is generally considered to be sufficiently accurate to conduct most bridge superstructure analyses. Since the 1965 report by Leonhardt, Kolbe, and Peter (*105*), in which they describe the distress apparently caused by nonlinear temperature distribution in the Jagst bridge (see Fig. 1), there have been many research studies on the thermal response of bridges subjected to diurnal temperature variation caused by solar radiation.

Tests conducted in Japan by Narouka, Hirai, and Yamaguti (*62*) in 1955 on a composite steel bridge verified that there were nonlinear temperature gradients through the depth of the concrete deck. The maximum measured temperature gradient was about 16°F.

In 1957, Barber (*63*) presented a formula to estimate the maximum pavement surface temperature. The formulation included the relationships between pavement temperature, air temperature, wind speed, intensity of solar radiation, and the thermal properties of the pavement materials. In 1961, Zuk (*64*) developed a rigorous method for computing thermal stresses and deflections in statically determinate composite steel bridges. This method made it possible to estimate the stresses and strains resulting from linear temperature gradients over the bridge cross section. Liu and Zuk (*65*) extended this work in 1963 to include the temperature effects in simply supported, prestressed concrete bridges. This model included the change in prestressing force caused by the change in temperature of the tendon. Temperatures of the tendon were assumed to experience the same temperature as the surrounding concrete. Results of the study indicated that the change in the prestressing force varied from −3 to 5 percent of the initial prestress. Temperature-induced stresses were computed to be approximately 200 psi in compression and 100 psi in tension.

In 1965, Zuk (*67*) attempted to predict the maximum bridge

surface temperature for the Virginia area by using a modification of the equation originally presented by Barber (*63*). He also presented an equation for determining the maximum temperature differential between the top and bottom of a composite steel bridge. Good correlation was reported between the measured and computed values. Field tests further confirmed the accuracy of Zuk's equation in determining the nonlinear temperature distribution through the concrete deck. Temperature distribution in the steel beams was either uniform or varied. The computed maximum temperature differential was 24°F, compared to the measured temperature differential of 23°F. In addition, good correlation was obtained between the calculated maximum deck temperature of 102°F and the measured value of 98°F.

In 1969, Wah and Kirksey (*66*) reported the results for a study that included the theoretical development experimental model and field tests for a simply supported, reinforced concrete bridge. Equations were developed to predict the thermal stresses and deflections in a beam-slab bridge. Field tests were performed on two summer days and one winter night. A significant discrepancy was found between the measured and the theoretical deflections, which was attributed both to the inability of the theoretical analysis to accurately include the actual temperature distribution and to the deviation of the actual bridge from the model of the bridge. Wah and Kirksey reported that tensile stresses as high as 1,500 psi were computed from measured strains.

Priestley (*57, 58*) analyzed the effects of several assumed thermal gradients and compared the results with measured data available at the time. One of the assumed thermal gradients consisted of a linear temperature distribution through the top deck slab, as proposed by Maher (*56*) and as supported by measured temperatures from three bridges located in the British Isles (*59, 60, 61*). Other assumed thermal gradients included the temperature distribution proposed by the Ministry of Works of New Zealand and distributions in which temperatures vary with depth as second-, fourth-, and sixth-degree parabolas. The sixth-degree parabola was found to be in good agreement with measured data, and its use was recommended for superstructure depths between 3.94 and 4.92 ft (1,200 and 1,500 mm).

In 1973, Emerson (*21, 83*) described a method to calculate the one-dimensional heat flow within a concrete-slab bridge by using an iterative, finite-difference solution scheme. The method related the bridge temperature to solar radiation, ambient air temperature, and wind speed. The model of the structure in this case is composed of several layers, and a starting time is assumed, at which point the equations governing the boundary conditions are applied. The assumption of boundary conditions requires an estimation of the times at which the nonlinear differential distribution is at a minimum. It is further assumed that the temperature throughout the structure is a constant at this time. Emerson (*83*) estimated that for concrete bridges the beginning time was 0800 hours for the heating phase and 1600 hours for the cooling phase. By using these input parameters, a nonlinear differential temperature distribution was computed at 15-min intervals until a maximum gradient was reached at approximately 1500 hours. Temperatures predicted by the model correlated well with measured prototype summer and winter temperature distributions.

In 1973, Lanigan (*109*) developed a two-dimensional, heat-flow, finite element program and found good agreement between theoretical temperature distribution, measurements on laboratory models, and prototype structures. In this case, heat flow along the longitudinal axis of the bridge was ignored.

In 1974, Berwanger (*74*) modified the method presented by Zuk (*64*) in 1961 for the composite girder bridge. The modification was made to account for symmetrically and unsymmetrically reinforced concrete slabs subjected to linear and nonlinear temperature gradients. The investigation included both simple and continuous, composite girder steel bridges. Temperature-induced stresses, resulting from an assumed temperature differential of 45°F, was found to be significant enough to warrant additional studies. In this case, a linear temperature gradient was assumed in the concrete slab and a constant temperature in the steel girder.

In 1976, Priestley (*60, 61*) proposed a revised temperature distribution consisting of three individual parts. In the first part, temperatures were assumed to decrease nonlinearly from a maximum of the top surface of the deck slab to a minimum at a depth of 1,200 mm. The nonlinear variation was represented by a fifth-degree parabola. The second part of the revised distribution applies only to a deck slab over an enclosed cell of a box girder in which case temperatures were assumed to decrease linearly. The third and final part of the revised distribution assumes a linear variation of temperatures over the bottom 200 mm of the cross section. A diagram of this variation in temperature is shown in Appendix D.

Priestley observed that in bridges with bituminous overlaps, the maximum temperature at the top of the concrete deck slab would decrease linearly with the thickness of the overlay because of the insulating properties of this material. Radolli and Green (*55*) and Zuk (*67*) observed that the darker bituminous surface provided greater solar absorptivity. They found that an overlay thickness of 1.6 to 2.0 in. (40 to 50 mm) would be required before the insulating properties of the overlay would offset the effect of the increased solar absorption on the temperature of the underlying concrete. Data obtained by Emerson (*21*), which varifies this phenomenon, are the basis for the provisions of the British Code of Practice, BS 5400.

In 1977, Will et al. (*88*) developed a finite-element program for predicting bridge response under temperature changes. Two programs were developed, one for the transient heat-conduction analysis, and the other for the static thermal stress analysis of bridge-type structures. The transient heat conduction program employed two-dimensional finite elements to predict the internal temperature distribution in the bridge cross section. The temperature distribution obtained from the heat conduction analysis was subsequently used as input into the static analysis to obtain the thermally induced movements and stresses in the bridge. The static analysis program uses two-dimensional finite elements in a three-dimensional, global assemblage with six degrees-of-freedom at each nodal point. This program can handle skew supported bridge structures. The developed analytical procedures were correlated satisfactorily with measured field movements on two bridges. Included in the study were a three-span, continuous, post-tensioned bridge which was skewed at the supports, and a two-span, pedestrian overcrossing with pretensioned beams made continuous for live loads. The measured field movements were slope changes measured with a mechanical inclinometer developed by Matlock et al. (*118*) to measure slope changes on bridges tested for live load effects. Instead of the solar radiation, wind speed, and air temperature used by Emer-

son (*43*) surface temperatures were measured at selected time intervals and input into the transient heat-conduction analysis as boundary conditions.

Thepchatri, Johnson, and Matlock (*87*) conducted analytical studies by using the computer program developed by Will, Johnson, and Matlock (*88*) and assumed diurnal variations in solar radiation, air temperature, and wind speed to predict the transient temperature distribution in three types of bridge cross sections: (1) a post-tensioned concrete slab bridge, (2) a composite, precast, post-tensioned bridge, and (3) a composite steel girder bridge. The environmental conditions, believed to be equal to the extreme summer and winter climatic conditions of Austin, Texas, were used for boundary conditions in the two-dimensional finite element, heat-flow analysis. In addition, the developed mathematical models were verified by conducting correlation studies on a three-span concrete slab bridge and a simply supported, girder-type reinforced concrete bridge. Field measurements of surface temperatures were correlated with the predicted temperature variations by using measured solar radiation, air temperature, and wind velocity in the case of the slab bridge. Extensive field test data throughout the cross-section depth were available for the girder-type bridge (*87*). In this case, extremely good correlation was obtained throughout the structure depth by using the two-dimensional heat-transfer model. Having verified the analytical procedures, the researchers proceeded to determine the temperature distributions on the three selected cross sections by using the extreme summer and winter climatic conditions from Austin, Texas. A maximum temperature differential of 35°F through the depth of the cross section of the 17-in. slab bridge was obtained for an extreme summer condition during the month of August. Extreme winter conditions, on the other hand, produced a reversed gradient of 9°F. Analyses conducted on a three-span, continuous concrete slab bridge indicate that during the extreme summer condition, a compression stress of 1,000 psi would occur on the top surface, whereas during the extreme winter condition, a top tensile stress of 400 psi would occur. The maximum predicted gradient for the 40-in.-deep composite concrete bridge composed of a precast, pretensioned concrete beam and reinforced concrete slab was 27°F for the summer condition. This gradient produced a maximum compressive stress of 477 psi at the deck surface and a maximum tensile stress of approximately 400 psi in the bottom fiber of the pretensioned girder for a two-span continuous bridge. A maximum reversed gradient of 7°F was predicted for the winter condition. This gradient produced a tensile force of approximately 140 psi at the bottom fiber of a simply supported span.

In 1975, Radolli and Green (*55*) developed a one-dimensional heat-flow analysis similar to that used by Emerson (*83*). Although acknowledging that the assumption of one-dimensional heat flow was not strictly correct, they cited comparisons indicating good correlations between observed and predicted temperature gradients obtained from a one-dimensional heat-flow analysis. They were able to use this approach to develop simplified formulas for use in design. Comparisons between the British Standards (*12*), Maher (*56*), the New Zealand Ministry of Works (*16*), and Priestley's sixth-degree parabola to an "I" girder indicate that the resulting stresses are strongly dependent on the temperature difference and temperature gradient. Comparisons between the gradients proposed by Leonhardt, Priestley, Maher and the one-dimensional heat flow were presented for varying superstructure depths. The results were decomposed into continuity and self-equilibrating stresses. Radolli and Green proposed the use of simple design formulas for design that do not require an understanding of the temperature gradient. This is basically the approach used in the Ontario code.

Response Analysis

Having selected a given temperature gradient or loading, the bridge designer is next faced with performing the response analysis. The most significant aspect of ambient thermal response of bridges is the consideration of temperature-induced strains. As with other induced deformations, such as creep and shrinkage, a temperature-induced strain does not induce stress in a member unless the free thermal expansion is restrained in some manner, as would be the case for any statically indeterminate structure. Thermal strain can occur without thermal stress; and thermal stress, without thermal strain. Because neither free movement nor complete restraint conditions exist in bridge structures, a combination of both thermal stress and thermal strain generally prevails. In particular, longitudinal tension stresses induced at the soffit of continuous bridges can be isolated as the single-most troublesome effect, though transverse thermal stresses also need to be considered, especially for box girder bridges.

Assumptions

The following assumptions are made in the development of thermal stress analyses using the one-dimensional beam theory.

1. The material is homogeneous and exhibits isotropic behavior.
2. Material properties are independent of temperature.
3. The material has linear stress-strain and temperature-strain relations. Thus, thermal stresses can be considered independently of stresses or strains imposed by other loading conditions, and the principle of superposition holds.
4. The Navier-Bernoulli hypothesis that initially plane sections remain plane after bending is valid.
5. The temperature varies only with depth, but is constant at all points of equal depth.
6. Longitudinal and transverse thermal responses of the bridge superstructure can be considered independently and the results superimposed; i.e., the longitudinal and transverse thermal stress fields are assumed to be uncoupled.

This final assumption simplifies the analysis, particularly for such complex section geometries as box girders. Because of this assumed uncoupling of the response, the theory and analysis techniques for longitudinal and transverse thermal stresses are treated separately in the following sections.

Longitudinal Response Analysis

It is advantageous to separate the longitudinal thermal responses into two components and superimpose the results. The bridge structure to be analyzed is first made statically deter-

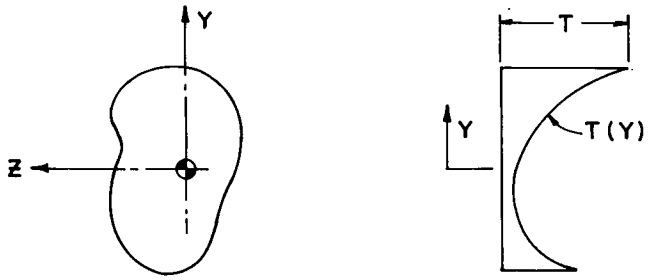

Figure 7. Arbitrary cross section subjected to a nonlinear temperature gradient.

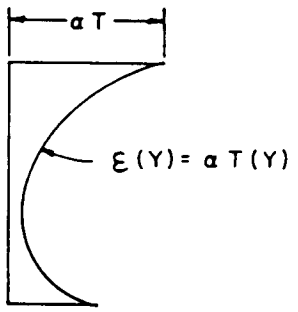

Figure 8. Temperature-induced strain distribution assuming that the section's fibers do not influence one another.

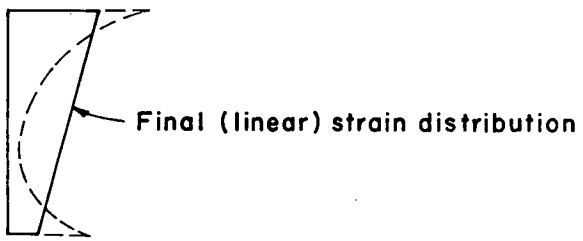

Figure 9. Temperature-induced strain distribution.

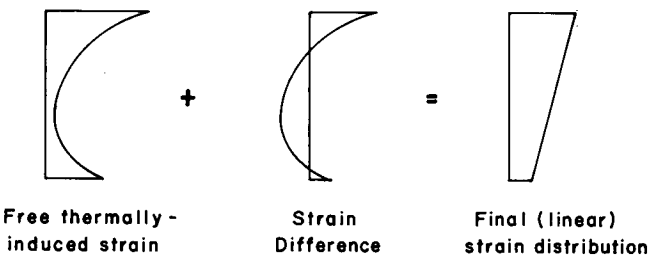

Figure 10. Strain difference that results in the self-equilibrating stresses.

minate by removal of sufficient internal redundancies. The stresses due to the nonlinearity of the temperature profile are also calculated. These stresses are generally called the "self-equilibrating stresses." The compatibility of the structure is then reestablished by applying the appropriate forces and moments to remove the inadmissible deformations introduced at the locations of released redundancy. The stresses resulting from this action are termed "continuity stresses." Each longitudinal stress component is discussed in greater detail in the following sections.

Self-Equilibrating Stresses—Theory. Consider an arbitrary cross section subjected to a temperature field which is not plane (see Fig. 7). If such conditions exist within an unrestrained section, each of the section's fibers will tend to deform in such a way that the section will not remain plane (see Fig. 8). This deformation, however, violates the Navier-Bernoulli hypothesis stated earlier. Because of this, only a portion of the temperature field is responsible for the section's deformation, and the final strain profile must be linear as shown in Figure 9.

The differences between the thermal strains which would result from a free expansion of the section fibers and the strains in the resultant plane section give rise to what are termed self-equilibrating stresses (see Fig. 10). By definition, the sum total of these stresses across a section and the bending moments resulting from these stresses is zero. The procedure for deriving expressions for the self-equilibrating stresses, based on the assumptions discussed under "Assumptions," consists of the stresses in an artificially restrained structure, plus stresses resulting from axial loads and bending moments that would be required to remove the artificial restrains. (Note that in the sequel, compressive stresses are taken as positive.)

Figure 11 shows an arbitrary cross section and vertical temperature distribution of a typical member. As noted under the heading, "Assumptions," it is assumed that the temperature varies only in the vertical direction. Full restraint is provided at the ends of the member by the bending moment M and the axial force P.

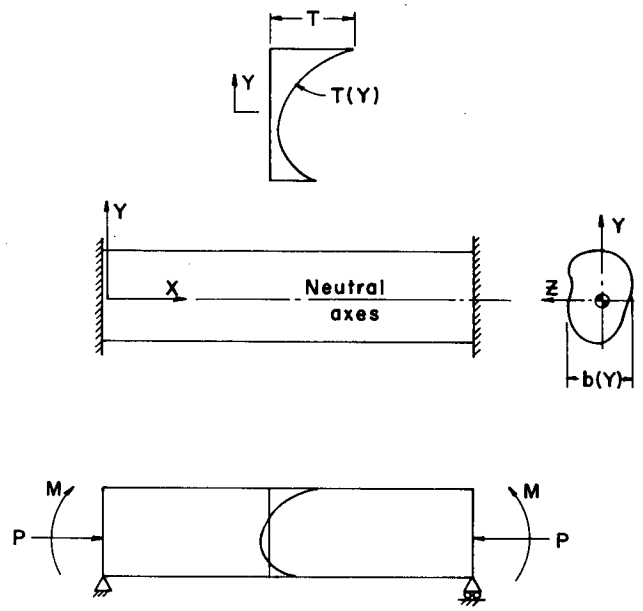

Figure 11. Typical member with an arbitrary cross section and vertical temperature distribution.

For a fully restrained member subjected to a nonlinear temperature-induced strain, the longitudinal stresses are given by

$$\sigma_t(Y) = E\alpha T(Y) \tag{2}$$

where

$\sigma_t(Y)$ = longitudinal stress at a fiber located a distance Y from the center of gravity of the cross section;
E = elastic modulus;
α = coefficient of thermal expansion; and
$T(Y)$ = temperature at a depth Y.

Since the self-equilibrating stresses act only on an unrestrained (statically determinate) structure, the conditions of longitudinal and flexural restraint shown in Figure 11 must be removed. The restraining axial force P, based on the stress distribution given by Eq. 2, is determined from

$$P = \int_Y E\alpha T(Y)\, b(Y) dY = \int_Y \sigma_t(Y)\, b(Y) dY \tag{3}$$

and the stress associated with this axial force acting on the cross-sectional area A is given by

$$\sigma_P(Y) = \frac{P}{A} \tag{4}$$

where $b(Y)$ = net section width at height Y.

The restraining end moment M can be evaluated from

$$M = \int_Y E\alpha T(Y) b(Y) Y dY = \int_Y \sigma_t(Y) b(Y) \mathrm{Y dY} \tag{5}$$

and the longitudinal stress associated with this moment is given by

$$\sigma_m(Y) = \frac{MY}{I} \tag{6}$$

For a long, thin member without end restraints, the longitudinal self-equilibrating stress is obtained by applying the negative of both the restraining axial force and the restraining end moment to the stress distribution given by Eq. 2. Thus using Eqs. 2, 4, and 6 yields

$$\sigma(Y) = \sigma_t(Y) - \sigma_p(Y) - \sigma_m(Y)$$

or

$$\sigma(Y) = E\alpha T(Y) - \frac{P}{A} - \frac{MY}{I} \tag{7}$$

This summation of stresses is shown graphically in Figure 12. Notice that if the temperature variation is linear, no self-equilibrating stresses will exist.

Continuity Stresses. To calculate the continuity stresses, a sufficient number of internal redundancies are first removed for the purpose of making the structure statically determinate. The inadmissible deformations induced at the locations of removed redundancies are then eliminated by the application of appropriate forces and moments. The stresses induced by this reestablishment of compatibility are known as continuity stresses.

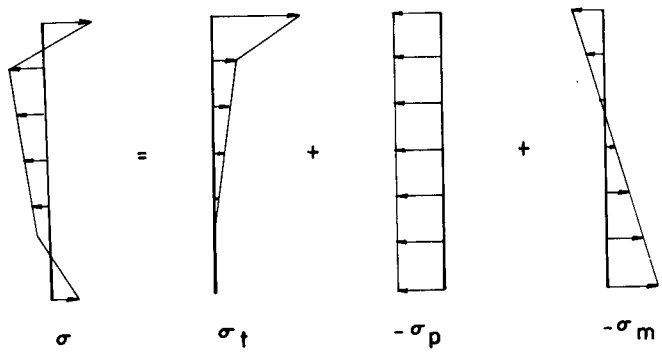

Figure 12. Distribution of self-equilibrating stresses.

The magnitude and distribution of the continuity stresses are, of course, dependent on the particular bridge structure and support conditions being analyzed. Nonetheless, the total state of stresses, which is obtained by the principle of superposition, is the sum total of the self-equilibrating and continuity stress sets.

Transverse Response Analysis

Although transverse thermally induced stresses may be calculated as part of the total solution, for more complex sections it is convenient to "decouple" the transverse and longitudinal stresses, and analyze them separately. Such an approach is consistant with the assumptions made under "Assumptions."

Box girder bridges are the most common types requiring a transverse analysis, and are discussed in the following paragraphs.

In a box girder section, under a vertical temperature gradient, the deck slab will be subjected to greater temperature variation than the soffit. For fairly slender deck slabs (less than about 10 in. in thickness), it is reasonable to assume a linear temperature gradient through the thickness (*16*).

One approach (*16*) to analyzing the transverse response consists of removing the constraints imposed on the deck slab and allowing it to deform freely. As shown in Figure 13, the unrestrained thermal deformation of the heated deck slab may be thought of as consisting of two components: (1) an average transverse increase in length of $\Delta L = [L\alpha(T_1 + T_2)]/(2)$; and (2) a (hogging) curvature of $\psi = [\alpha(T_1 - T_2)]/(h)$, in which T_1 and T_2 are the temperature increases of the top and bottom surfaces of the deck slab relative to the soffit slab; L is the distance between web centerlines; and h is the deck slab thickness.

In this unrestrained state, no primary thermal stresses are induced because the temperature gradient is linear, and the final strain profile is identical to the unrestrained thermal strain profile.

Secondary thermal stresses will, however, be induced by restraint of the deck slab elongation and curvature. The elongation can be treated as an initial lack-of-fit problem, in which the section is in equilibrium with the initial free elongation of the

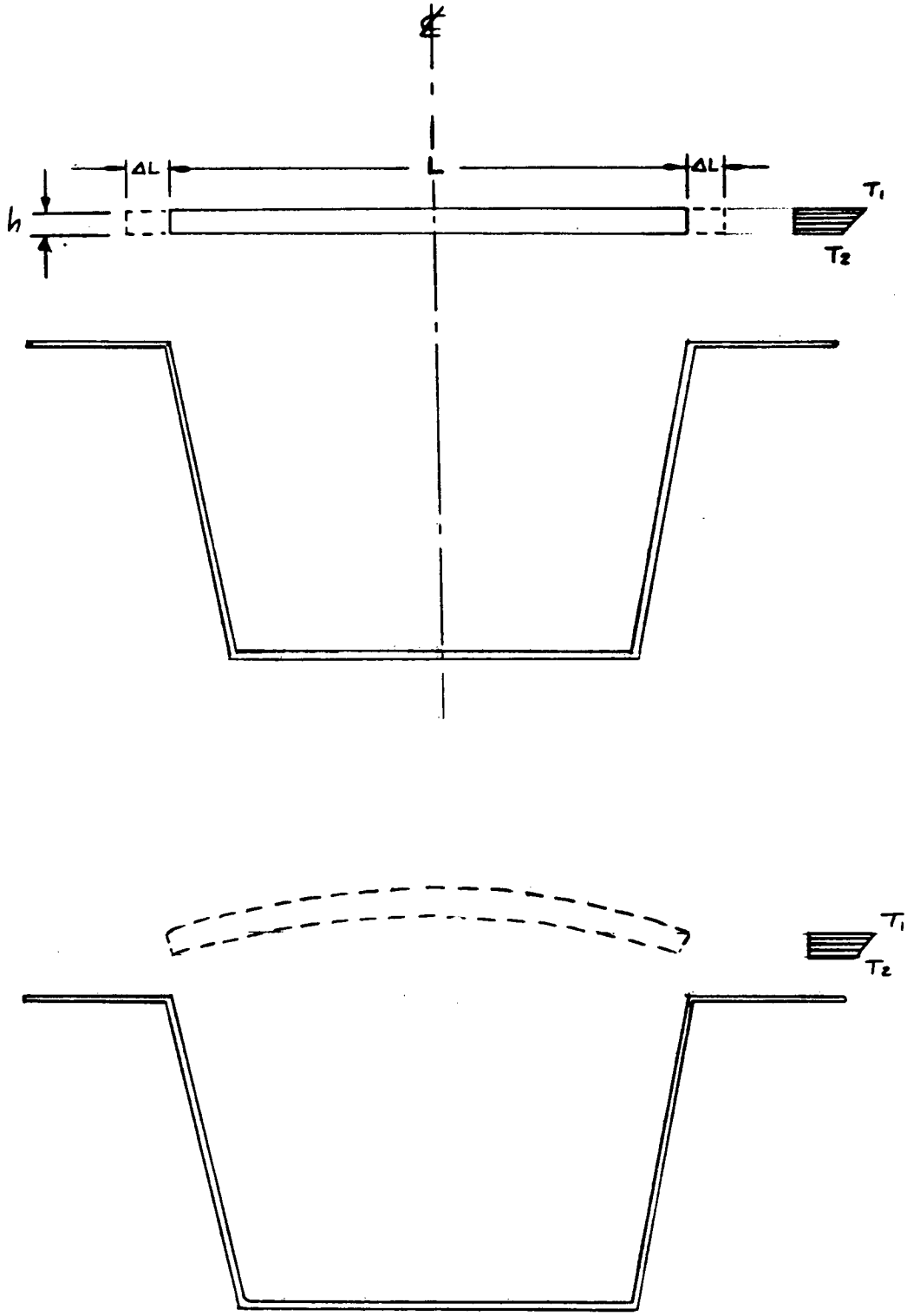

Figure 13. Top figure shows thermally induced deck slab elongation; bottom figure, thermally induced deck slab curvature.

deck slab. Stresses induced by restraint of the curvature are analyzed by calculating the moments required to fully restrain the rotation, then releasing the deck-slab/web joints and performing a moment distribution around the section. Total transverse stresses are the sum of those resulting from restraint of the elongation and the curvature. The relative magnitude of the two effects depends largely on the relative stiffness of the webs and deck slab (*16*), and it must be noted that the section has tacitly been assumed to be uncracked.

A second approach to analyzing the transverse response consists of both hand calculations and computer analyses. The following steps are involved in the procedure.

1. On the basis of the configuration of the bridge cross section, an equivalent mathematical model is developed (using beam elements) for subsequent static plane frame analysis.
2. All degrees of freedom are constrained by imposing artificial restraints at all the nodal points.
3. The thermal gradient is applied to the restrained structure and thermally induced stresses are computed across the member cross section. These calculations are performed by hand.
4. On the basis of the applied thermal gradient, fixed-end forces and fixed-end moments are computed.
5. The negative of the fixed-end forces and that of the moments are applied as concentrated nodal forces and couples. This removes the artificial constraints imposed in step 2.
6. Stresses are obtained from a computer analysis using the applied loadings determined in step 5.
7. The stresses determined in steps 2 and 6 are now summed together.

Interaction Between Longitudinal and Transverse Thermal Stresses

In the foregoing discussion the longitudinal and transverse stresses have been treated separately. The assumed uncoupling is, however, an approximation and the actual thermally induced stresses will be somewhat higher than those computed.

As presented by Priestley and Buckle (*16*), an approximate allowance for the interaction resulting from Poisson's ratio, ν, effects can be obtained by adding ν times the bending component of the longitudinal stress to the transverse stresses, and vice versa. It was further pointed out that these revised longitudinal stresses will have little influence on the curvature, provided the neutral axis of the cross section is a reasonable distance below the deck slab, since the net longitudinal compression in the deck slab remains unaltered.

The interaction of stresses discussed above assumes isotropic material behavior; thus, if the deck slab is conventionally reinforced in the transverse direction, and therefore subject to cracking, the concept of Poisson's ratio no longer has meaning. In such a case it is more reasonable to ignore the interaction between longitudinal and transverse stresses.

Available Meteorological Data

Climate is a measure of the typical atmospheric conditions at a specific location and is determined from meteorological data collected over a period of years. Particular aspects of climate may be quantified in terms of statistical information about temperature, precipitation, wind, solar radiation, or other measurable atmospheric phenomena. This type of information is important for many planning, engineering, and scheduling purposes. Within the United States this information is collected and analyzed by the Environmental Science Services Administration (ESSA). This agency publishes a useful summary of climatic information (*98*). Figures 14 and 15, which are examples of the types of information available, indicate the distribution of normal daily average temperature and normal daily range of temperature, respectively, for the month of January.

Detailed climatic information is important when designing for potential thermal effects on bridges in a country with the climatic diversity of the United States. A similar condition exists in several other countries. Code writers in at least two of these countries have recognized the need to incorporate detailed climatic information in their thermal design procedures. The British Design Standard provides isothermal maps of maximum and minimum shade air temperature, while the Ontario Bridge Code uses isothermal maps of maximum and minimum daily mean temperatures. The climatic information from each of these codes varies; however, methods have been developed in each case for using the climatic data to determine fluctuations in bridge temperature. Although the bridge design specifications of the American Association of State Highway and Transportation Officials do not currently use detailed climatic data, it is desirable to develop bridge design procedures similar to England and Ontario that will use the data compiled by ESSA.

There are many factors that must be considered when converting raw climatic data to thermal loadings for designing bridges. Besides considering factors such as the type of construction and local site conditions, a design code must consider the probability of extreme loading conditions. Because it is generally assumed that new bridges in the United States have a useful life of approximately 50 years, it is reasonable to design bridges for thermal loads that are likely to occur within this time period. Although it may not be possible to obtain climatic data based on a 50-year return period, it is possible to adjust available climatic data to approximate data for a 50-year return period. This should be the approach used in using ESSA data for bridge design.

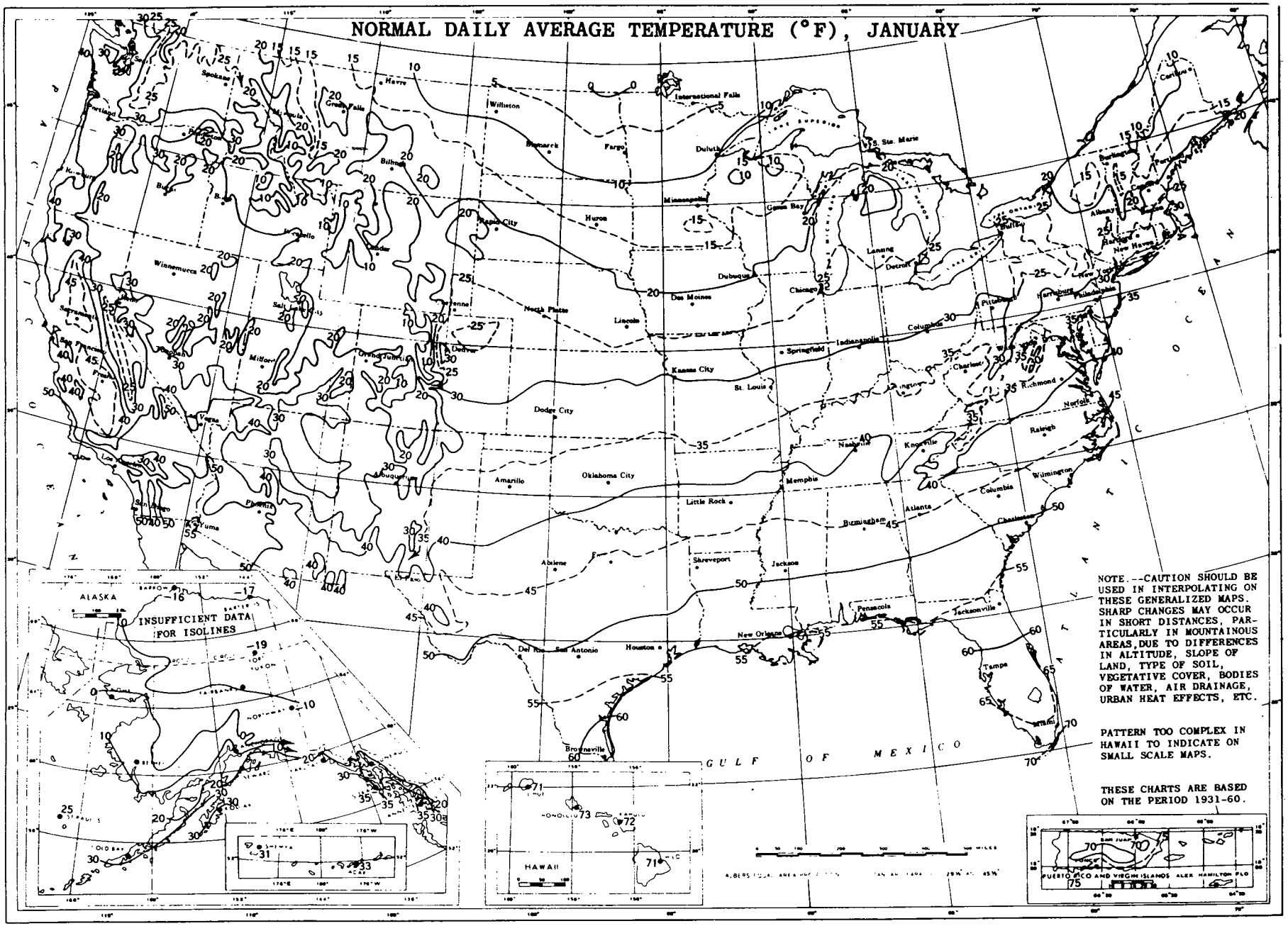

Figure 14. Normal daily temperature, January.

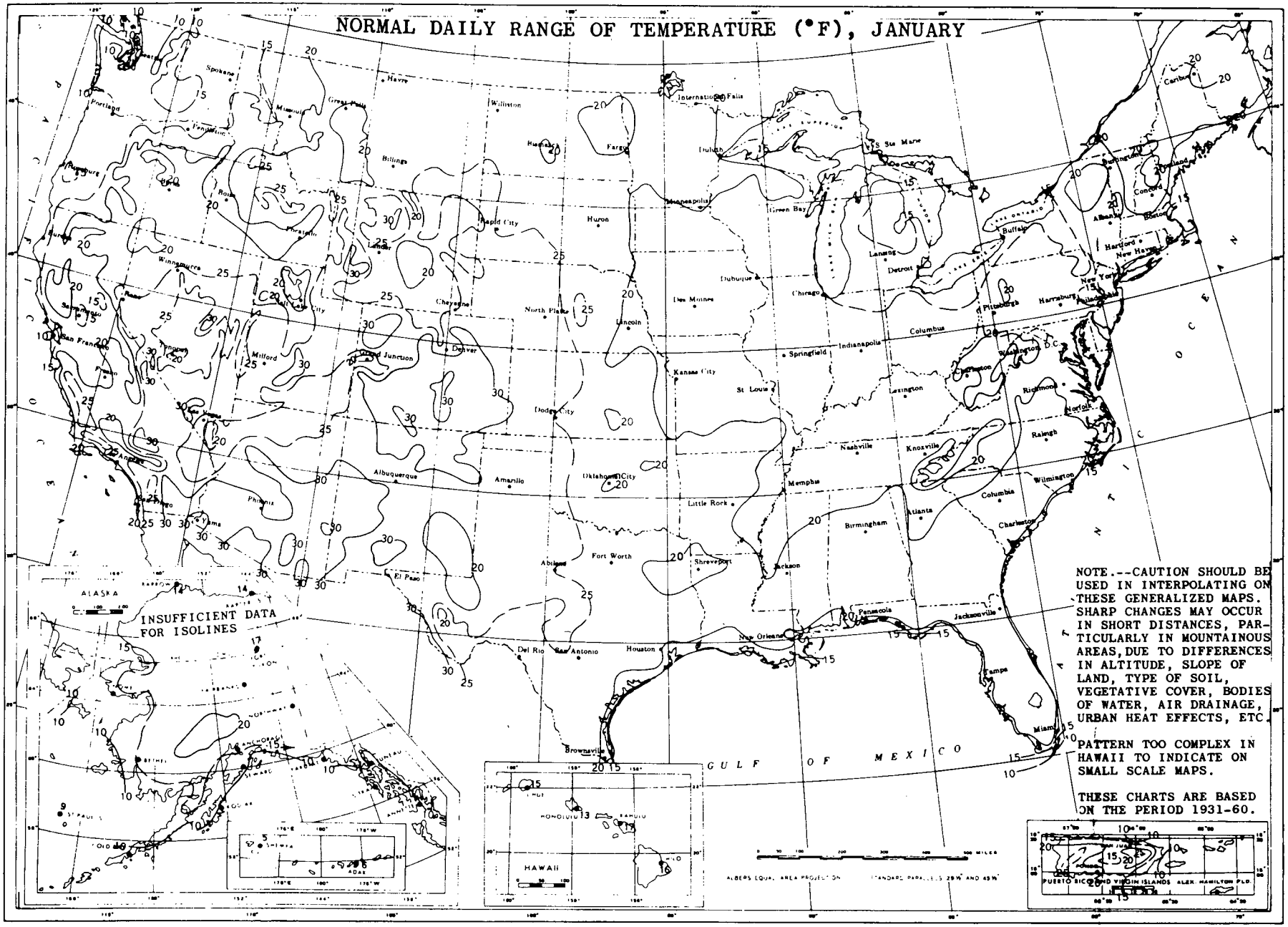

Figure 15. Normal daily range of temperature, January.

FINDINGS—BRIDGE DESIGN CODES AND ALTERNATIVE APPROACHES

Table 3. Summary of international design provisions for thermal effects in concrete bridges.

	EFFECTIVE MEAN STRUCTURE TEMPERATURE				DIFFERENTIAL TEMPERATURE—VERTICAL GRADIENT	
	TEMPERATURE RANGE	VARIABLES AFFECTING TEMPERATURE RANGE	CLIMATIC INFORMATION	NOTES	METHOD USED	GRADIENT USED FOR DECK WARMING
USA (AASHTO)	Based on locality In general use: *Rise* *Fall* Mod. 30°F 40°F Cold 35°F 45°F	• Climate • Temp. lag in massive members • Structure type	Moderate and cold climates are mentioned-No definitions given.		None	None
USA (PTI)				Suggests no improvements to AASHTO	Assumed difference in the temp. of deck slab	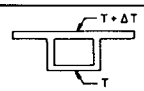
New Zealand	A specified temperature variation is given: *Rise* *Fall* 20°C 20°C	None	None		Nonlinear temp. gradient. Consider longitudinal and transverse effects	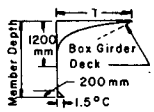
England	Varies Extremes are: −14°C & 37°C	• Climate • Structure type • Deck surfacing	Isothermal maps adjusted for: • return period • elevation • local divergence	Temp. change based on temp. at time of construction	Nonlinear temp. gradient	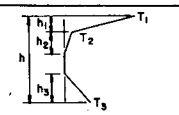
Germany	Minimum: −30°C Maximum: 20°C or 15°C if element thickness ≥ 70 cm Neutral: 10°C	• Structure type • Element thickness	None	Different temp. range used for calculation of movement.	Linear temp. gradient	A temp. differential of 5°C is assumed
Canada (Ontario)	5°C below min. daily mean temp. 10°C above max. daily mean temp.	• Type of superstructure • Depth of superstructure • Climate	Isothermal maps of max. and min. mean daily temp.	A construction temp. of 15°C is usually used.	Unrestrained superstructure curvatures	Nondimensional curvature based on superstructure depth
Canada (CSA)	Based on local temp. record Min. range of 40°C specified.	• Type of superstructure • Temp. lag for massive members • Climate	National Building Code of Canada used as a guide	Temp. rise and fall based on the temp. when constructed.	No specific method is mentioned.	Not specified
Australia	Varies—3 ranges used: 0 to 50°C −5 to 50°C −10 to 40°C	• Climate • Superstructure type	3 climatic regions defined based on latitude and elevation	Mean temp. based on climatic region.	Nonlinear temp. gradient. Both longitudinal & transverse stresses considered.	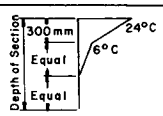
Japan	Based on site. In general ±15°C except ±10°C for structures with thick members	• Climate • Thickness of cross-section elements	None	Different temp. range used for calculation of movement.	Gradient not required for concrete bridges	None
Sweden	Formuli based on superstructure thickness and latitude	• Climate • Thickness of superstructure	Formula based on latitude derived from temperature records.	A temp. of 10°C is assumed at the time of construction	A linear temp. gradient is assumed	A temp. differential of 10°C is assumed
Denmark	Average structure temperatures vary from −15 to 25°C	• Type of structure	Assumed temp. range based on records of past 115 yrs.		A lineare temp. gradient is assumed	A temp. differential of 15°C is assumed
Italy	Based on ambient temp.: Exposed: ±15°C Nonexposed: ±10°C	• Climate data • Exposure	None		Usually ignored. Linear gradient used if measurable differential exists.	Not specified
France	Minimum: −40°C Maximum: 30°C	None Specified	None	Design stresses based on long-term elastic modulus to consider creep.	Linear thermal gradient	Temp. differential of 10°C

Bridge design codes of different countries provide many different approaches to help the designer account for thermal effects. These are summarized in Table 3. While each approach is discussed in detail in this chapter, copies of these codes or pertinent correspondence from the countries surveyed are included in Appendix D. The codes basically differ in the refinement used in determining the meteorological conditions at proposed bridge sites, the types of thermal loadings considered,

DIFFERENTIAL TEMPERATURE—VERTICAL GRADIENT		OTHER DIFFERENTIAL TEMPERATURES		OTHER	
GRADIENT USED FOR DECK COOLING	VARIABLES CONSIDERED	HORIZONTAL TEMPERATURE GRADIENT	TEMPERATURE GRADIENT IN CROSS-SECTION ELEMENTS	MATERIAL & STRUCTURE PROPERTIES FOR THERMAL ANALYSIS	OTHER DESIGN REQUIREMENTS
None	Not applicable	None	None	C_T: Normal concrete .000006 per °F. Lightweight depends on type of aggregate.	Minimum shrinkage and temperature reinforcement.
Considered for transverse stresses when thick bottom slab exists	10°C difference assumed for worked example	None	Cooling of exposed surfaces is considered.		
None	• Depth of member • Thickness of blacktop surface	None	Temp. variation applies to deck slabs	• Crack transformed moment of inertia used	
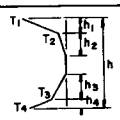	• Deck surfacing thickness • Superstructure thickness • Structure type	None	Temp. gradients apply to deck slabs	C_T: Normal concrete 12×10^{-6}/°C Limestone Agg. 7×10^{-6}/°C	
A temp. differential of 5°C is assumed	None	None	None	Not specified	
Nondimensional curvature based on superstructure depth	• Superstructure thickness	None	A positive linear differential of 15°C in the deck slab.	C_T assumed to vary with aggregate type and curing method.	
Not specified	Not specified	Not specified	Not specified	C_T: Normal density concrete 11×10^{-6}/°C	Min. shrinkage and temp. reinforcement
None	• Superstructure depth	Requires consideration, but gives no further guidance	Temp. gradient applies to deck slabs also.	C_T: Normal weight concrete 11×10^{-6}/°C	
None	None	None	None	C_T: Reinforced concrete - .000010/°C	
A temp. differential of −5°C is assumed	• Type of structure	None	None		
A temp. differential of −10°C is assumed	• Type of structure	None	Temp. differential of 5°C assumed between inside & outside of a box girder.		
Not Specified		Only if measurable differential exists	Only if measurable differential exists	C_T: .00001/°C	
None		None	None	C_T: .00001/°C Long-term elastic modulus used for part of temp. load	

and/or in the methods used to accommodate these thermal loadings. A discussion of the design criteria from each country surveyed follows.

UNITED STATES

The minimum requirements for the design of bridges in the United States is governed by the design specifications of the American Association of State Highway and Transportation Officials (AASHTO). In certain cases, additional, more detailed design criteria may be used. With respect to temperature, the design recommendations of the Post Tensioning Institute (PTI) are often used in the design of prestressed concrete bridges. Many individual states have also developed their own design procedures for considering thermal effects. A survey of states performed as part of this study has made it possible to summarize these practices under "State Practices."

The American Association of State Highway and Transportation Officials

The AASHTO design specifications for bridges provide for a rise and fall in effective mean temperature in concrete structures. The specified normal temperature range varies, based on the type of climate. The specifications require that reduced temperature fluctuations be considered within massive concrete members and/or structures, but no specific guidance is given as to when and how this is to be done. Variations in the mean temperature are used to calculate stresses and movements resulting from the thermal expansion or contraction of the superstructure. A thermal coefficient of expansion for normal-weight concrete is specified. The specifications do not provide for direct consideration of temperature differentials within the superstructure. Minimum reinforcement of all exposed surfaces is required to control cracking due to shrinkage and thermal stresses.

Post Tensioning Institute

The Post Tensioning Institute recommends that temperature differentials be considered in calculating longitudinal and transverse stresses in bridge superstructures. In a worked example presented in their design manual, they assume a 10°C (18°F) temperature difference between the top slab and the remainder of the cross section. This will result in a loading effect, equivalent to that of an applied axial load and longitudinal moment, that will produce longitudinal fiber stresses in both simple and continuous spans. This nonlinear temperature gradient produces self-equilibrating stresses in a bridge superstructure.

The Post Tensioning Institute also recommends that the following temperature phenomena be considered in calculating transverse stress:

1. Rapid cooling of the top slab in relation to the thick bottom slab near the interior supports.
2. Higher temperatures within the interior bays of box girders due to cooling of the exposed surfaces of the cross section. An example of a difference in temperature of 15°C (27°F) is used to illustrate the transverse stresses that will result.
3. Cooling of exposed surfaces in relation to the interior of thick concrete members, which can result in tensile stresses on the concrete surface.

The temperatures used in the illustrative examples of the PTI manual are not necessarily appropriate for all bridge structures. Very little guidance is given for selecting proper temperature differentials.

State Practices

Questionnaires were sent to each of the states to obtain information on their experiences and practices related to the temperature effect on highway structures and the remedial actions taken to accommodate these effects. A summary of the questions and responses is presented in the following paragraphs and in Table 4.

- A. *Question 1: Has your State performed any type of research or studies on temperature effects . . . ?* Research reports were provided by the States of California, Illinois, Indiana, Iowa, Kansas, Missouri, New York, Oklahoma, Oregon, Pennsylvania, Tennessee, Texas, Virginia, and Wisconsin. These reports are included under the "References and Bibliography."
- B. *Question 2: Have you observed any manifestation of temperature-related distress in bridges?* The following states commented as shown:

  Colorado: Major problems have been where multispan bridges up to 400 ft have been constructed without joints. Cracking has developed in the asphalt pavement, in the joint between approach slab and abutment, or cracking of the abutment wall diaphragm due to temperature movements. We have built this type of concrete structure up to 400 ft without joints. The most severe problem has occurred on post-tensioned CIP concrete structure due to shortening added to temperature effects.

  Kansas: Some reinforced concrete rigid frame deck girder bridges (2 girders) have shown serious cracking. Some of this might be due to temperature-related stresses. Cracking between precast segments at epoxy joints appears partially related to thermal stresses.

  South Carolina: Diagonal cracks in RC Tee Beams at bearing areas; spalled narrow bent caps; cracked build-ups.

  Wisconsin: Excessive cracking of concrete decks on long-span steel girders; floorbeam connection failures due to possible moments about y-y axis of floorbeams from differential thermal movements between the tie girder of long-span steel tied arches and the floor system consisting of a reinforced concrete deck on steel stringers.

- C. *Question 3: Do you apply thermal axial and/or nonlinear gradient effects when designing concrete bridge superstructures?* The following states commented as shown:

  Alaska: So far, only on major structures, where the value of the structure justifies the cost of analysis, and the analysis techniques provide for inclusion of temperature effects. Generally, assumed temperature differentials are input into computer analyses.

Table 4. Summary of state responses to questionnaire.

STATE	QUESTION 1		QUESTION 2		QUESTION 3		QUESTION 4	
	YES	NO	YES	NO	YES	NO	YES	NO
Alabama		x		x		x	x	
Alaska	x			x	x			x
Arizona								
Arkansas		x		x	x			x
California	x			x		x		x
Colorado		x	x			x		x
Connecticut		x		x		x		x
Delaware								
Dist. of Columbia		x		x		x		x
Florida								
Georgia								
Hawaii		x		x		x		x
Idaho		x		x	x			
Illinois	x			x		x	x	
Indiana	x			x	x			x
Iowa	x		x			x		x
Kansas		x		x		x		x
Kentucky								
Louisiana		x	x		x			x
Maine								
Maryland		x	x		x			x
Massachusetts								
Michigan		x		x		x		x
Minnesota								
Mississippi		x		x	x			x
Missouri		x		x	x			x
Montana		x		x*		x*		x*
Nebraska		x	x			x		x
Nevada		x		x		x		x
New Hampshire		x		x	?			x
New Jersey		x		x		x		x
New Mexico		x	x			x		x
New York	x			x	x			x
North Carolina		x	x			x		x
North Dakota		x		x		x		x
Ohio		x	x		x			x
Oklahoma	x			x		x		x
Oregon	x		x		x			x
Pennsylvania	x			x	x		x	
Rhode Island		x		x		x		x
South Carolina		x	x		x			x
South Dakota								
Tennessee	x		x			x		x
Texas	x		x			x		x
Utah								
Vermont		x		x		x		x
Virginia	x			x		x		x
Washington	x		x		x		x	
Washington DC								
West Virginia								
Wisconsin	x		x			x		x
Wyoming		x		x		x		x

* Montana's general comment: "Since we do not have any long span concrete structures as described in the second paragraph of your letter, Montana can not provide any useful information to the research project."

Arkansas: Thermal effects determine expansion joint sizes and bearing device type.

Colorado: Current designs for segmental concrete bridges being done by Figg & Muller include provisions for a temperature gradient between top and bottom of segment.

Indiana: Only in long-span concrete box girder procedures (*40*).

Kansas: Monolithic steel beam at abutments—reinforced to handle moment as well as temperature differential.

Louisiana: Thermal effects are considered in the design of beam bearing pads for expansion ends and pile stresses and girder connections for fixed end continuous girder spans. Joint design is also affected.

Maryland: Most structures are for short span. Axial forces taken into account in continuous span structures when determining if bearing at pier should be fixed or expansion. Compare the required force to overcome friction at expansion bearing with force required to move pier column some ΔL for given temperature change.

Missouri: On reinforced concrete box girder bridges with integral columns we include moments from thermal forces in design. No consideration of these forces is made in prestressed I-girder and Double Tee superstructures.

New Hampshire: We will investigate the thermal and/or nonlinear gradient effects in our current long-span concrete bridge design.

New York: On large box superstructures (other than AASHTO boxes) we have applied a linear temperature gradient from top of box to bottom $+18°F$ ($10°C$) and $-9°F$ ($5°C$). These types of structures are very rare so it would

not be correct to say this is policy—just what we have used on two projects.

Ohio: We would expect deep concrete bridges designed for us by consulting firms to be so designed.

Oregon: Slab differential used for stress analysis of transverse frame for box girders.

Pennsylvania: Mostly apply to the expansion and contraction of the bridge superstructures due to temperature change.

South Carolina: Usually only so far as determining expansion joint size. Thermal expansion force taken into account when single span bridges fixed at both ends to vertical abutments are necessary (rare case).

Tennessee: Our policy regarding thermal expansion and contraction is set out in Structures Memorandum 045. A copy is enclosed (see Appendix D).

Texas: We have considered thermal gradients in a brief analysis of a continuous post-tensioned segmented railroad bridge of trough shape.

- D. *Question 4: Other than the nominal light reinforcement placed near the surface in bridge superstructures to minimize shrinkage or thermally caused concrete cracking, does your State's design codes address thermal stresses?* The following states commented as shown:

Illinois: Specifies conditions at expansion joints which may require additional reinforcement in the abutment back wall or piers.

Pennsylvania: Specifies that "Provisions shall be made for stresses and movements resulting in variations in temperature." A range of temperatures is given for steel and concrete structures. They also specify "Maximum Allowable Stresses at Joints in Tensile Zone" of precast and cast-in-place segmental bridge systems for different AASHTO loading groups.

It is clear from the responses that the effects of axial length changes at expansion joints is considered to be the most serious problem by the majority of those states "concerned" with temperature problems. No state includes the temperature gradient effect in its normal design codes. Ten States—Alaska, Colorado, Indiana, New Hampshire, New York, Ohio, Oregon, Pennsylvania, Texas, and Washington—do, however, consider temperature gradient effects for special conditions. Only three of these states furnished the range of temperature gradients used for special conditions. New York used a top to bottom of box gradient of +18°F (10°C) to −9°F (5°C) during stress analysis on two large box superstructures. Pennsylvania, in its 5th draft of "Segmental Bridge Interim Design Specifications," includes a temperature gradient of 40°F (22.2°C). The State of Washington has followed the design recommendations of the Post Tensioning Institute for several major bridge structures. A summary of the design criteria followed is included in Appendix D.

NEW ZEALAND

The New Zealand bridge design criteria consider loading due to variations in the mean temperature of the structure and due to temperature differentials caused by deck heating. The design guidelines require that the cracked, transformed section be used in all calculations involving temperature loadings.

Stresses and movements resulting from variations in the mean temperature of the structure are calculated, based on a temperature variation of ± 20°C (36°F) for concrete structures. The effect of bearing restraint at the superstructure-substructure interface is to be considered in calculating both stresses and movements.

The effect of temperature differentials within the superstructure cross section on both the longitudinal and transverse stresses generated in the structure are also calculated. Temperatures in the cross section are assumed to vary nonlinearly and are considered to be independent of structure type and material. The assumed maximum temperature difference and its variation due to depth depend on the thickness of the blacktop (asphalt) deck surfacing, the total depth of the cross section, and whether the structural element is exposed to the air or only one side (e.g., a box-girder deck) or a solid section exposed to the air on both sides. For webs and decks not above an enclosed cell, the temperature will vary from maximum to minimum as a fifth degree parabola over a depth of 1,200 mm (47.2 in.), measured from the deck surface. It is assumed the soffit temperature is 1.5°C (2.7°F) above minimum at the surface and that it will decrease linearly to a minimum at 200 mm (7.8 in.) into the cross section. For structural cross sections less than 1,400 mm (1,200 mm + 200 mm) (55.1 in.), the effect of deck and soffit temperatures is added. For box girder decks, a linear decrease in temperature at increased depths into the cross section is assumed. The rate of temperature decrease will depend on the thickness of the blacktop surface. These temperature differentials are illustrated in the design specifications included in Appendix D. Deck cooling due to reradiation is not considered.

ENGLAND

The English bridge design specifications consider changes in the average temperature of the bridge as well as differences between the temperatures at various depths within the superstructure cross section. Detailed isothermal maps of maximum and minimum shade air temperatures are used as the basis for calculating temperature loadings. Shade-air temperatures from the maps are adjusted to account for variations in design return period, height above sea level, and local divergence.

Minimum and maximum effective bridge temperatures are calculated from the shade-air temperatures at the bridge site. These vary for the four different types of superstructures defined in the specifications. Effective bridge temperatures are also adjusted to account for the type and amount of deck surfacing. The effective bridge temperature variation is used to determine the forces produced in restraining elements.

Temperatures through the depth of the cross section are assumed to vary nonlinearly. The variation occurs linearly between specified depths. These depths and the amount of temperature variation will depend on the total depth of the section, the type of construction, and the type and amount of deck surfacing. Two conditions are considered. The first condition is unequal temperatures that result from deck heating due to solar radiation. The second condition is unequal temperatures that result from deck cooling due to reradiation.

The English code also specifies the coefficient of thermal ex-

pansion that is to be used for normal concrete. However, a different value is specified for concrete with limestone aggregates.

The English bridge design code uses a limit-states approach, and load factors are specified for temperature loadings in the design of specific elements for the ultimate and serviceability limit states.

GERMANY

The German bridge design code (DIN 1072) provides for variations in the mean temperature of solid concrete bridges as well as for temperature differentials within the cross section.

Variations of +20°C (36°F) and −30°C (54°F) are used to calculate stresses due to thermal expansion and contraction of a bridge superstructure with an assumed construction temperature of 10°C (18°F). The maximum effective mean temperature may be reduced by 5°C (9°F) in structures with elements 70 cm (27.6 in.) or greater in thickness or in structures otherwise protected from rapid temperature fluctuation. Larger temperature variations are considered when calculating potential movement at the bearings.

Temperature variations of ± 5°C (9°F) in a cross section due to unequal heating (or cooling) are also considered in the design of concrete bridges. The temperatures at a cross section are assumed to vary linearly through the depth of the superstructure.

CANADA

In the past, all bridge design in Canada was governed by the AASHTO bridge design specifications, and in many provinces this is still the case. However, two separate efforts to revise bridge design criteria have recently been completed. The province of Ontario has developed a comprehensive bridge design specification based on the limit-states approach. The criteria for determining thermal effects in this code vary considerably from AASHTO's. Another bridge design standard, produced by the Canadian Standards Association (CSA), an independent code-writing body, is not as comprehensive as the Ontario Bridge Code, but it does vary slightly from the AASHTO design specifications. Each of these two design codes is discussed in the following sections.

Ontario

The recently developed Ontario Bridge Code requires bridges to be designed to resist the effects of variations in the average bridge temperature and from deformations caused by temperature differentials within the superstructure. The code also provides requirements to counter the effect of shrinkage and creep which can produce stresses and deformations similar to those caused by temperature effects. Detailed provisions for calculating variations in average bridge temperature are given. Maximum and minimum effective temperatures are assumed to be a specified number of degrees above or below the maximum and minimum daily mean temperatures, respectively. The number of degrees difference depends on the type of superstructure and is adjusted according to the superstructure depth. The variations given in the coefficient of linear thermal expansion are based on the type of aggregate and the method of curing used to produce the concrete.

In noncomposite superstructure types, the effect of a thermal gradient is accounted for by specifying an unrestrained superstructure curvature. Because both radiational heating and cooling of the bridge deck are considered, curvature may occur in either direction. This curvature, which varies according to superstructure depth, is intended to account for only the effects of linear vertical temperature gradients. The curvatures resulting from the thermal gradient effects will produce forces and moments in the restraining elements of continuous bridges.

Canadian Standards Association

The National Standard of Canada, produced by the Canadian Standards Association (CSA), varies from the AASHTO bridge design specifications in that it specifically states that "variation of temperature within a structure" shall be considered when determining stresses or movements caused by thermal effects. However, the document does not give any specific guidance on how this is to be accomplished.

The temperature range to be used in calculating the effective mean temperature within a structure is to be based on weather records from the locality where the bridge is to be constructed. It is recommended that bridge designers make this determination by following the guidelines of the National Building Code of Canada. The CSA standards also mention consideration of member size and thickness in determining temperature fluctuations, but no guidance is offered in this area.

AUSTRALIA

The Australian bridge design code requires that the effect of variation in both mean temperature and temperature differentials within the structure be considered during design. Coefficients of thermal expansion for normal-weight concrete are specified. Placement of bearings and expansion joints will depend on both the assumed mean temperature for design and the temperature at the time of construction.

Average temperature variations are specified in the Australian code. Specific variations depend on the superstructure type and the geographic region. Because concrete superstructures are slower to respond to ambient temperature variations than other superstructure types, the specified average temperature variation for concrete superstructures is less than for other superstructure types.

The code also specifies a bilinear, vertical temperature gradient that provides for a temperature differential of 24°C (43°F) between the top deck surface and the bottom of the superstructure cross section. Because the effect of nonstructural surfacing on this gradient is assumed to be insignificant, it is not considered. The specified temperature gradient is shown in the copy of the code included in Appendix D.

The Australian code also mentions the potential effects of a horizontal temperature gradient through the superstructure cross section, from one side to the other. However, no specific guidance is offered as to when or how this effect should be considered.

JAPAN

The Japanese bridge design specifications consider only the variation in average bridge temperature for the design of concrete bridges, although a temperature gradient from sunny to shady portions of the cross section is required for certain types of steel bridges. The variation in the average bridge temperature to be used in calculating member forces in concrete bridges is dependent on both the bridge site and the type of bridge. A distinction is made between bridges with typical structural elements and those with structural elements over 70 cm (27.6 in.) thick. Only the typical rise and fall in bridge temperatures are specified for these concrete bridge types. The code contains no specific guidance for concrete bridges on how to adjust these typical values to account for bridge site variation, although such guidance is given for steel bridges.

The code specifies the coefficient of thermal expansion to be used, and also specifies a different rise and fall of average bridge temperatures to be used when designing to account for movement at the expansion bearings. This temperature range depends on the type of construction and whether the bridge is located in a region of typical temperature variation or in a cold climate region.

SWEDEN

The Swedish bridge design specifications provide formulas for calculating the maximum and minimum average temperatures in concrete structures. The maximum average temperature is determined from average superstructure thickness only, while the minimum average temperature depends on latitude as well as superstructure thickness. The formulas used to determine these temperatures are based on 80th percentile maximum and minimum temperature measurements. The formulas apply to bridges between 0.1 and 2.0 m (0.33 and 6.6 ft) in thickness. An average superstructure temperature at the time of construction is also specified by the code. The variation between the maximum and minimum average temperatures is used along with the specified temperatures at the time of construction to calculate the stresses and movements caused from longitudinal expansion and contraction of the bridge superstructure.

Temperature distribution in a bridge is assumed to vary linearly through the thickness of the cross section. Both deck heating and deck cooling are considered.

DENMARK

The bridge design procedures used in Denmark take into consideration the effect of the variation in the average temperature of the bridge and the linear variation in temperature through the depth of the cross section. Because Denmark is a small country and the climatic variation within the country is slight, no distinction for bridge location is made. In addition to the variation in temperature through the depth of the superstructure, the code also gives specifications for a temperature variation of 5°C (9°F) through concrete structural members, such as the side wall of a box girder.

The specified variation in the average bridge temperature through the cross section, which also depends on the type of bridge, was basically selected according to the maximum temperature values that were exceeded in 20 percent of the years and the minimum temperature values that were below the minimum annual temperature value for 80 percent of the years. Based on temperature information covering a 115-year period, the average temperature of concrete superstructures is assumed to vary from 25°C (77°F) to −15°C (+5°F).

The bridge designer is to consider both increases and decreases of the outside temperature through the depth of the superstructure when designing a bridge. Similarly, the variation in temperature through any concrete structural member is assumed to increase or decrease from the outside to the inside of the member.

ITALY

The Italian bridge design code provides for temperature variations based on the ambient temperature. A mean effective temperature variation of ±15°C (27°F) for exposed structures and ±10°C (18°F) for nonexposed structures is generally used unless more precise data are available. Usually, unless there is a measurable difference in temperature between various components, the temperature differential within the superstructure is ignored. When a difference in component temperature does exist, a linear variation is assumed.

FRANCE

The French bridge design procedures for thermal effects include consideration of both the effective mean temperature in the superstructure and thermal gradients resulting from deck heating due to solar radiation.

The effective mean temperature in the superstructure is assumed to vary from 30°C (86°F) to −40°C (−40°F). A construction temperature of between 8°C and 14°C (14 and 25°F) is assumed. This will result in thermal strains in the superstructure of 0.0003 for expansion and −0.0004 for contraction. Part of the strain (due to temperature variations of ±10°C) in concrete structures is assumed to occur rapidly. However, because the remainder of the strain is assumed to occur over a period of time, the long-term elastic modulus should be used to determine the resultant stresses. Thermal loadings are multiplied by load factors of 1.0 or 0.6, depending on whether they act in conjunction with permanent or nonpermanent loadings.

The temperature within the cross section of the superstructure is assumed to vary linearly with the highest temperature at the deck surface and the lowest temperature at the bottom of the cross section. The temperature difference is assumed to be 10°C (18°F) if it is superimposed with dead load alone and 6°C (10.8°F) when it is superimposed with other loadings.

CHAPTER FIVE

INTERPRETATION AND APPLICATION—CASE STUDIES

Longitudinal and transverse temperature effects were applied to a selected group of U.S. bridges in this chapter. Four thermal gradients were used for the longitudinal study, and two thermal gradients were used for the transverse study. Comparisons were made between the applied gradients and the analytical results.

LONGITUDINAL TEMPERATURE EFFECTS

Four thermal gradients, shown in Figure 16, were selected for the case studies. These gradients were selected because they are representative of those presented in Chapter Four. They include those specified in the New Zealand, Britrish, and Ontario codes. In addition, the gradient presented in the *Precast Segmental Box Girder Bridge Manual* (*15*) was included because it is somewhat representative of those currently being used in the United States. A summary of the bridges included in these case studies is given in Table 5. The applicable portions of the codes are those pertaining to the positive gradients that occur during the day when there is high solar radiation. For the purpose of clarity, those portions of the codes that applied to the negative gradients were omitted from these case studies.

Plots of top and bottom fiber stress versus the distance longitudinally along the bridge are presented in this section for each of the case studies. In addition, section stresses are included at selected points along the bridge to show the stress variations at different depths.

The plots show that maximum fiber stresses usually occur at the pier or column supports adjacent to the abutments. Changes in superstructure cross sections due to flares in the bottom slab and girder stems and/or haunched superstructures cause significant changes in fiber stresses.

There is little correlation between the magnitudes of the stresses produced by the four thermal loadings evaluated. The temperature gradient assumed by the New Zealand code usually produced the highest stresses for both top and bottom fibers, while the temperature gradient specified in the British code usually produced the lowest bottom-fiber stresses.

In some cases, the presence of columns monolithically connected to the superstructure had a significant effect on the stress pattern. In addition, the characteristic shape of the stress pattern was affected by the presence of internal expansion joint hinges.

Stresses shown at simple supports and at hinges (points of zero moment) are caused by the self-equilibrating stresses that result from nonlinear temperature gradients. These stresses, which do not exist at the member ends, are generally assumed to occur at some distance from the member ends, usually at a distance assumed to be equal to the depth of the member.

The analyses were conducted for bridges assumed to have a coefficient of thermal expansion of 0.000006/°F, uncracked section properties, and no reductions in thermal gradients for surfacing, elevation, etc.

Case 1L—Colorado River Bridge

Selection

This precast, I-girder bridge differs from box girder bridges in that there is no enclosing bottom slab on the T-shaped section. Thus the heat-flow characteristics are different from those of box girders. Also, the cross-sectional properties of this superstructure differ from those of the box girder in that the neutral axis is closer to the slab. Many bridges similar to this type are located throughout the United States. The Colorado River Bridge was selected for study because it is representative of this type of bridge.

Description

This 560-ft-long structure, shown schematically in Figure 17, contains five equal spans. The superstructure is composed of a continuous 7⅛-in.-thick, cast-in-place concrete deck and 7 precast, pretensioned, prestressed concrete I-girders with a depth-to-span ratio of 0.056. Diaphragms are cast around the ends of

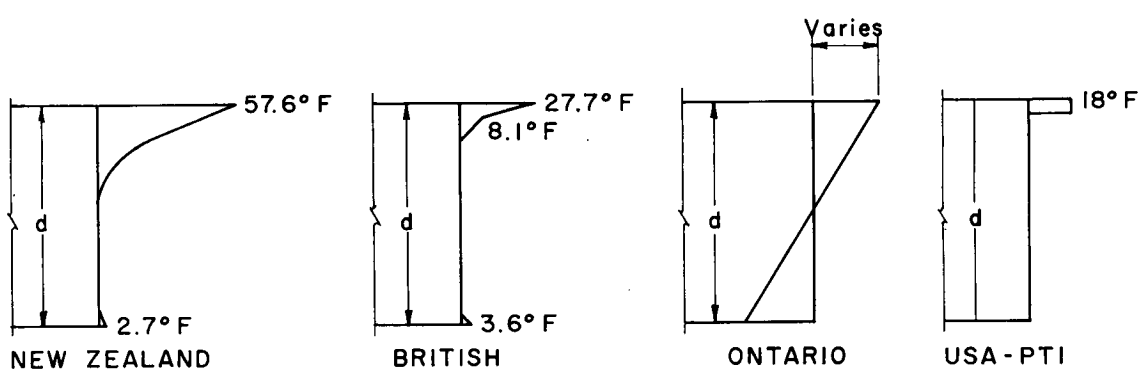

Figure 16. Thermal gradients used for case studies.

Table 5. Summary of bridges included in case studies for longitudinal temperature effects.

CASE NO.	NAME/LOCATION	SUPERSTRUCTURE	SUBSTRUCTURE	LONGITUDINAL DIRECTION LENGTH	DEPTH	DEPTH/SPAN RATIO	NO. SPANS	NO. HINGES	NO. FRAMES	COMMENT
1L	Colorado River Bridge California/Arizona	Precast, prestressed I-girder	Pier Wall	565 ft–6 in.	6 ft–3 in.	0.056	5	0	1	Representative I-girder
2L	West Silver Eagle Rd. Overhead, California	Cast-in-place prestressed box girder	Double Column	750 ft–0 in.	5 ft–0 in.	0.037	6	0	1	Representative box girder
3L	Turkey Run Creek Br. Indiana	Precast, prestressed segmental box girder	Single Column	317 ft–0 in.	9 ft–0 in.	0.057	2	0	1	Segmental cantilever
4L	Kishwaukee River Br. Illinois	Precast, prestressed segmental box girder	Single Column	1,096 ft–0 in.	11 ft–8 in.	0.047	5	0	1	Segmental cantilever
5L	Columbia River Br. Washington	Cast-in-place prestressed segmental box girder	Single Column	1,870 ft–0 in.	9 ft–0 in. min. 24 ft–0 in. max.	0.053	5	0	1	Segmental & haunched cantilever
6L	W. Silver Eagle Rd. OH (Falsework) California	Cast-in-place prestressed box girder	Double Column	750 ft–0 in.	5 ft–0 in.	0.037	6	1	2	Falsework loading
7L	East Connector California	Cast-in-place reinforced box girder	Single Column	1,104 ft–0 in.	6 ft–0 in.	0.055	11	2	3	Multiframe
8L	Miller Creek F-11-AK Colorado	Precast, prestressed segments/box girder	Single Column	445 ft–3 in.	8 ft–0 in.	0.041	3	0	1	Case history

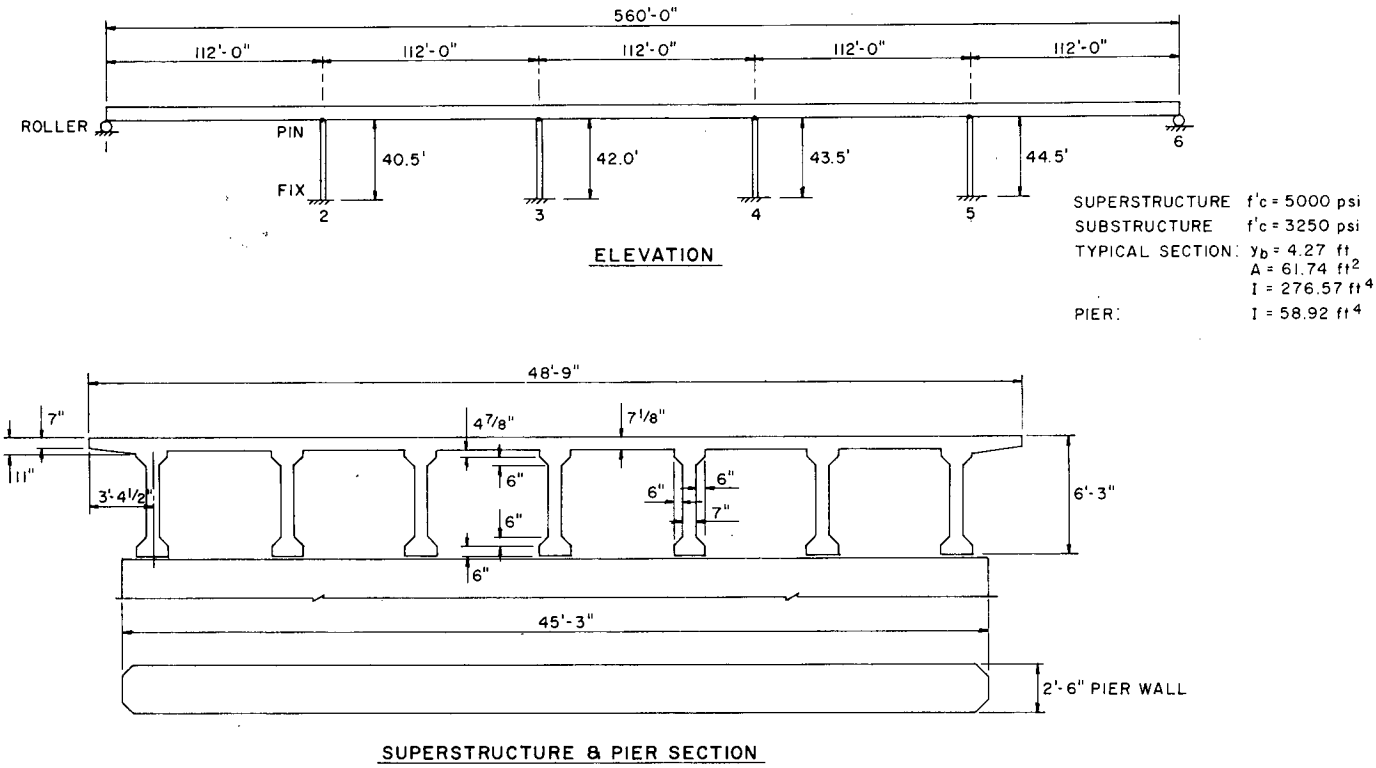

Figure 17. Case 1L—Colorado River Bridge superstructure and substructure details used for analysis.

the precast girders and monolithic with the deck to form a continuous superstructure from abutment to abutment. The substructure is composed of four pier walls, each measuring over 40 ft high and 2.5 ft thick. The piers, which are fixed at the bottom and pinned at the top, are relatively flexible in the longitudinal direction. The seat-type abutments have expansion bearings that allow longitudinal movement. The structure is founded on driven steel piles.

Results

Figures 18 and 19 are plots of top and bottom fiber stresses, respectively, along a typical girder centerline. Because there are no flares in this superstructure, the stress results can be plotted simply by computing the stresses at the supports and then connecting the plotted points with straight lines. The high-tension stresses occurring in the bottom fiber at piers 2 and 5, shown in Figure 19, are caused by the T-shaped superstructure. The Ontario code specifically calls attention to the occurrence of higher bottom fibers in T-beams because of the higher location of the neutral axis.

It is interesting to note that the stresses caused by the axial forces in the superstructure that result from the pier-wall shear restraint are less than 10 psi. Therefore, these axial force stresses are negligible. A structural model allowing freedom of longitudinal movement at the supports in lieu of the pinned pier would have yielded essentially the same results. Shown in Figure 20 are plots of the variation in cross-section stresses with the depth for each of the four gradients considered.

Case 2L—West Silver Eagle Road Bridge and Overhead

Selection

The West Silver Eagle Road Bridge and Overhead was included in the case studies because it is representative of the current trend of bridge designers to eliminate intermediate expansion joint hinges.

Description

This structure, shown schematically in Figure 21, is a six-span, 745-ft-long bridge. The superstructure is a cast-in-place, post-tensioned, prestressed concrete box girder that has a depth-to-span ratio of 0.037. The superstructure has no intermediate expansion joint hinges and is cast monolithic with the columns to form a continuous frame from abutment to abutment. The substructure is composed of five 2-column bents ranging from 25 to 35 ft in height. The columns are pinned at the bottom and fixed at the top. The seat-type abutments have expansion bearings to allow longitudinal movement. The structure is supported on cast-in drilled-hole concrete piles.

Results

Figures 22 and 23 are plots of top and bottom fiber stresses, respectively, along a typical girder centerline. In Figure 23, the

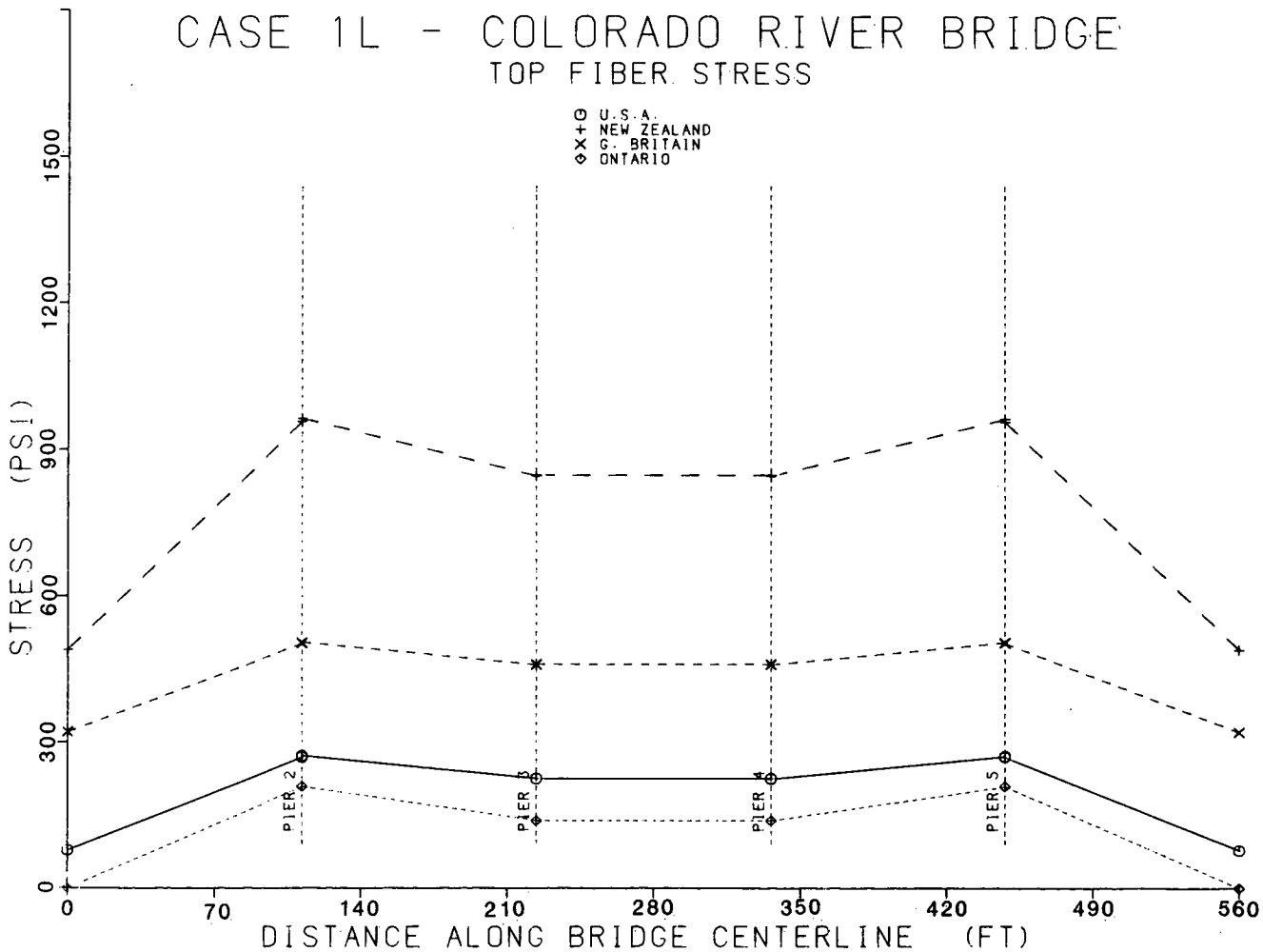

Figure 18. Case 1L—longitudinal variation in top fiber stresses along a typical girder centerline due to positive temperature gradients.

maximum tension and compression stresses are somewhat less than those found at corresponding locations for the T-shaped girder considered in Case 1L. The reason for this difference appears to be due to the additional resistance provided by the bottom slab.

The effect of the monolithic columns is readily apparent at piers 2, 5, and 6. For example, at pier 2 with the New Zealand load, Figure 23 shows that the bottom fiber stresses changed significantly from −446 psi to −326 psi. This is a result of the monolithic connection between the superstructure and the column. The top fiber stresses, shown in Figure 22, are similarly changed. Piers 3 and 4 are not significantly affected because of their close proximity to the superstructure's point of zero movement.

Also evident in the bottom fiber stress shown in Figure 23 is the influence of the relatively modest bottom slab flare. For example, at the right side of span 2 with the New Zealand gradient, the bottom fiber stress changes significantly from −373 psi at the beginning of the flare to −253 psi at the end of the flare. In contrast to the bottom fiber stresses, the top fiber stresses are only slightly influenced by the presence of a bottom slab flare.

Shown in Figure 24 are plots of the variation in cross-section stresses with the depth for each of the four gradients considered.

Case 3L—Turkey Run Creek Bridge

Selection

This bridge was included in the case studies because experimental measurements on the thermal gradients and thermal strains were available (*40*). In addition, the Turkey Run Bridge was among the first of its type in the United States to be constructed by the cantilever method. Because a number of epoxied joints between the precast segments lack mild reinforcement, many engineers have expressed a concern about thermal stresses that could cause serviceability problems at this interface. Realizing these problems, bridge designers are currently evaluating a variety of thermal gradient loads with which to test bridges of this type. The temperature gradients, in turn, result in additional amounts of prestressing steel.

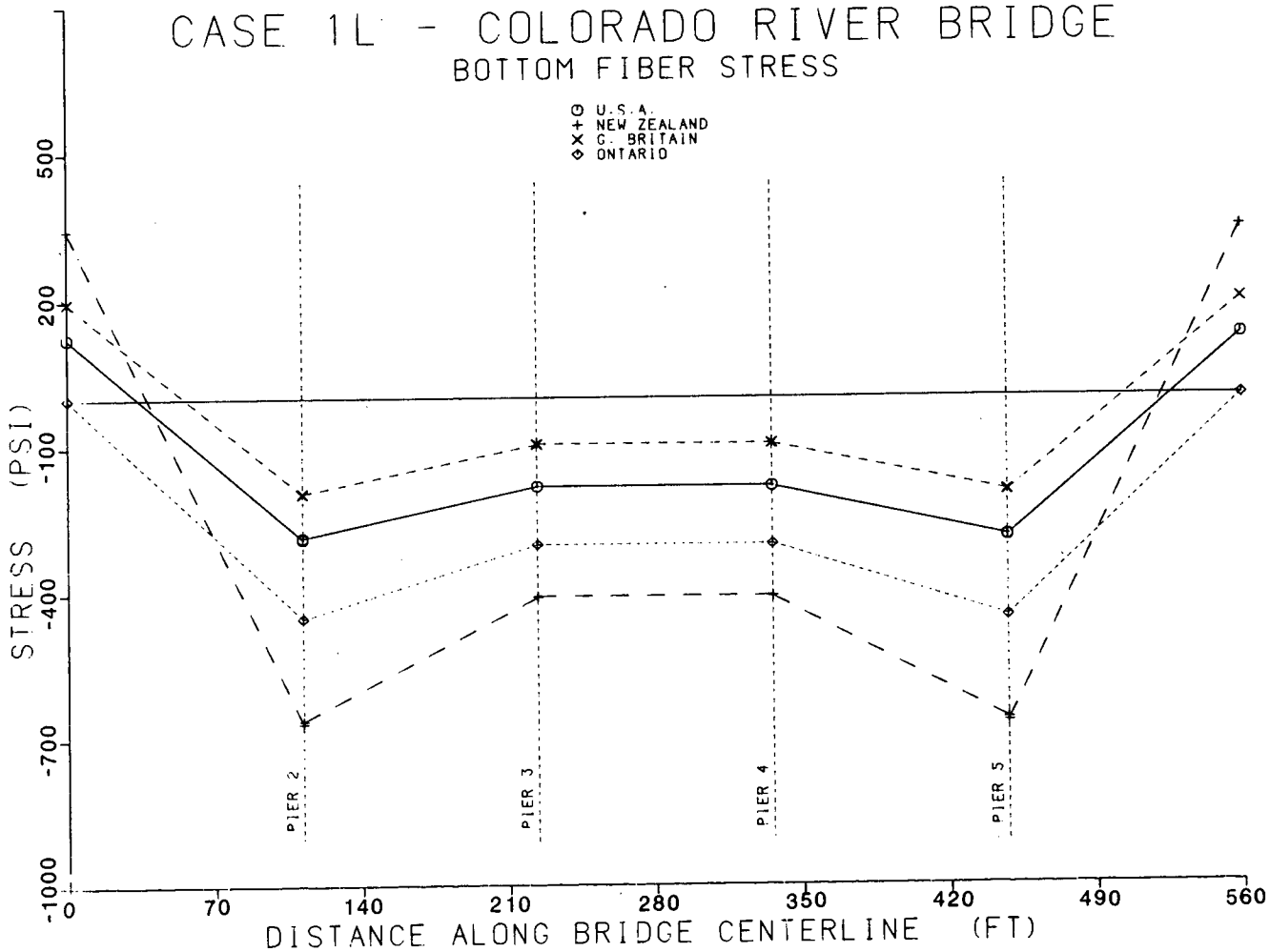

Figure 19. Case 1L—longitudinal variation in bottom fiber stresses along a typical girder centerline due to positive temperature gradients.

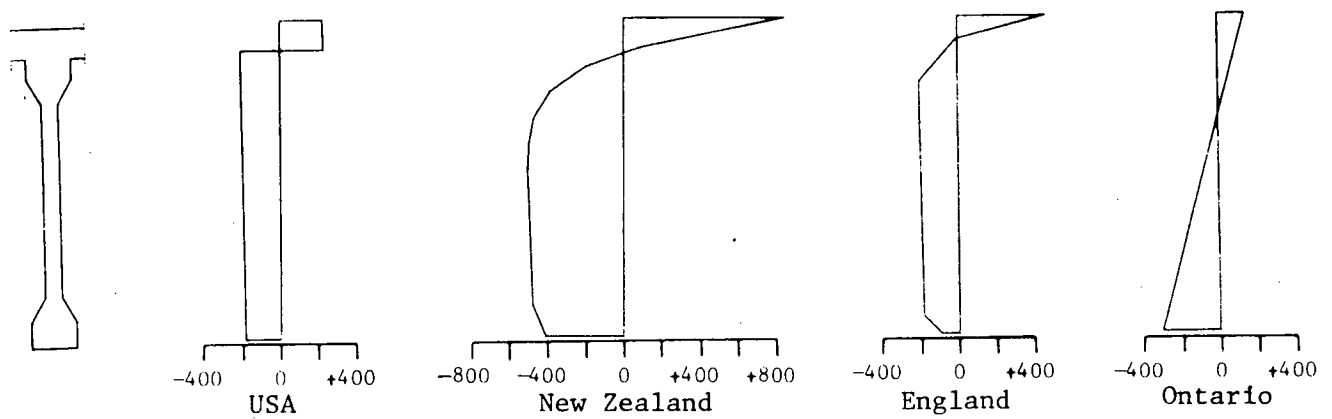

Figure 20. Case 1L—variation in girder cross-section stress with depth due to positive temperature gradients (the − symbol indicates tension and the + symbol indicates compression).

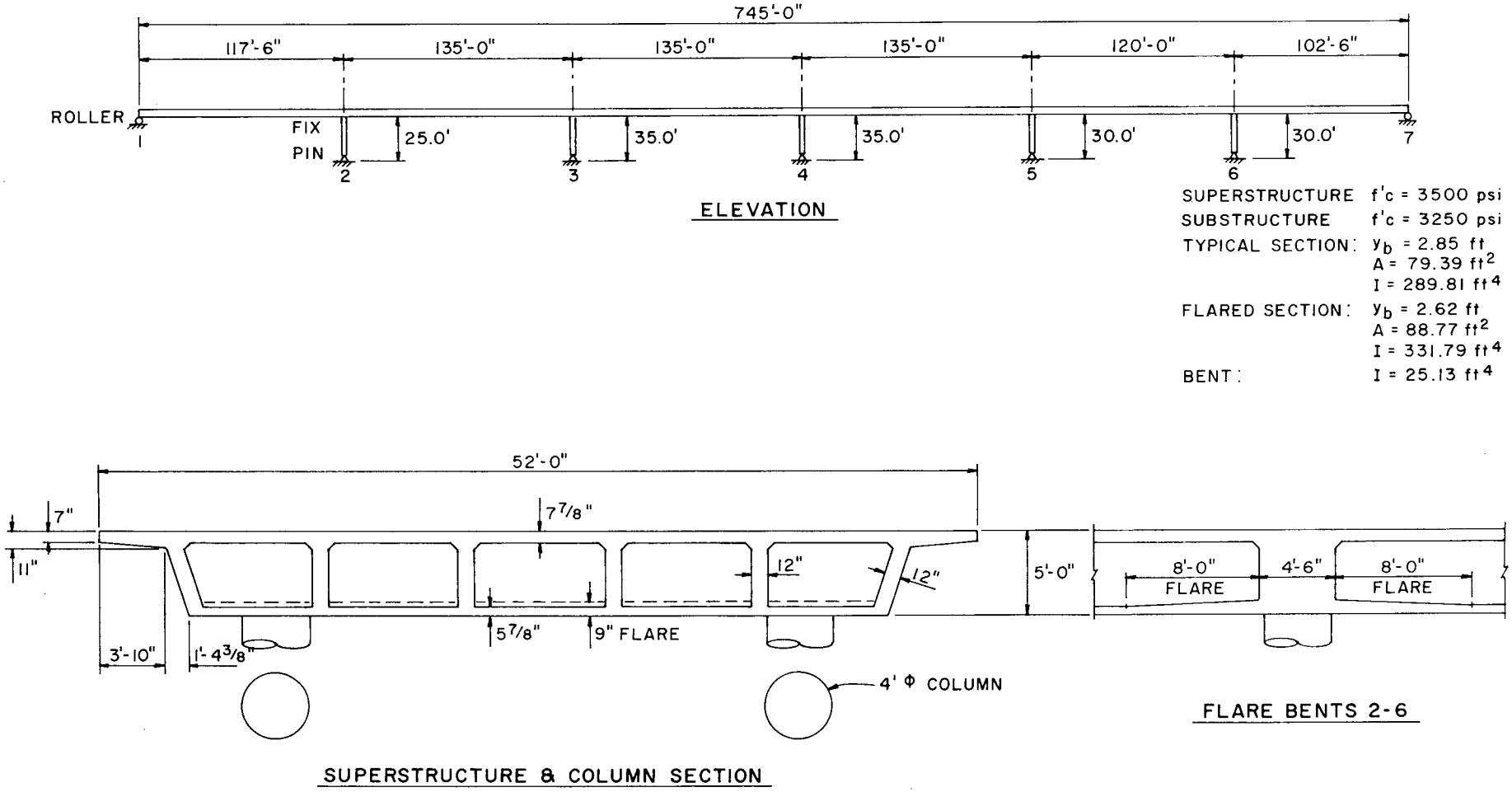

Figure 21. Case 2L—West Silver Eagle Bridge and overhead superstructure and substructure details used for analysis.

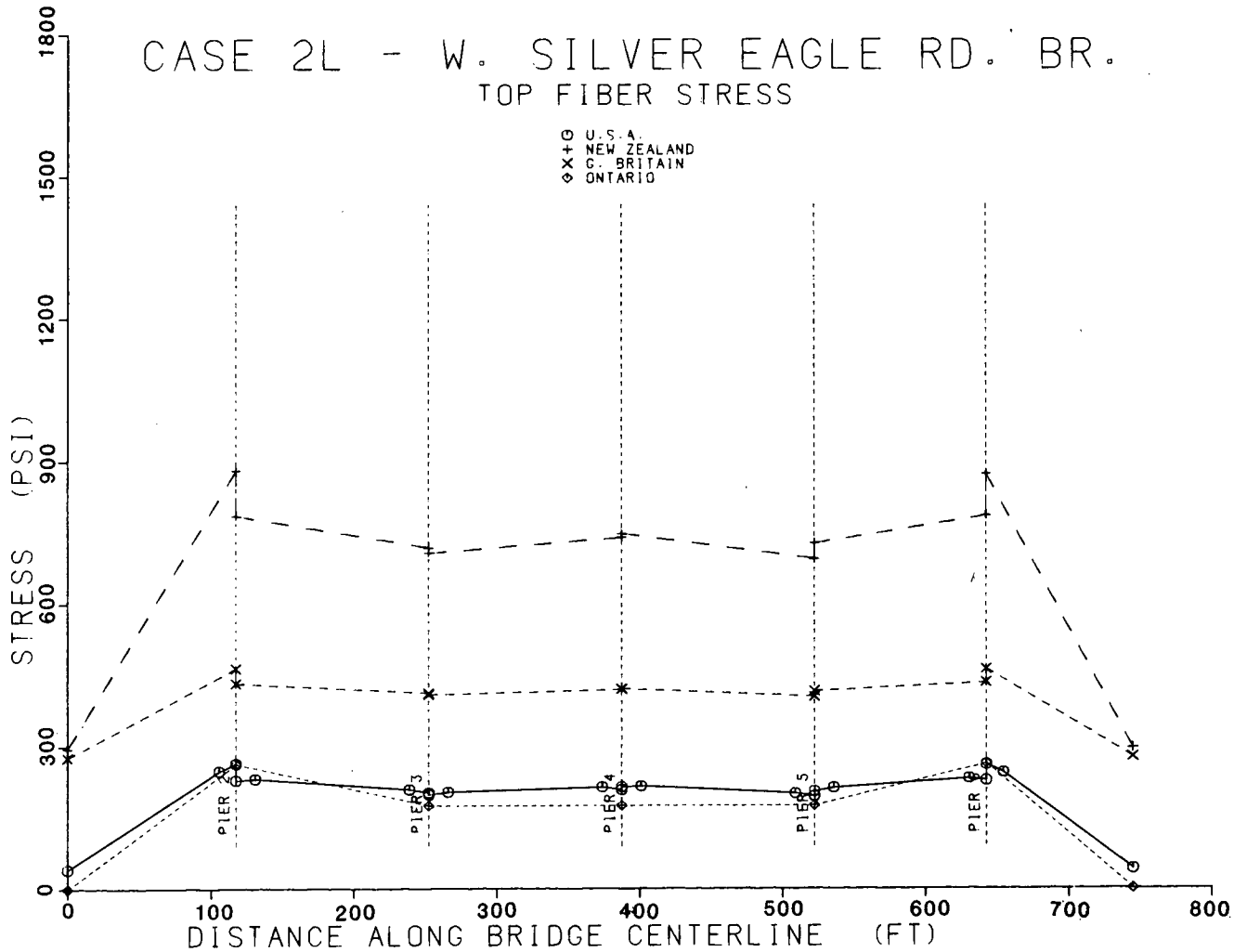

Figure 22. Case 2L—longitudinal variation in top fiber stresses along a typical girder centerline due to positive temperature gradients.

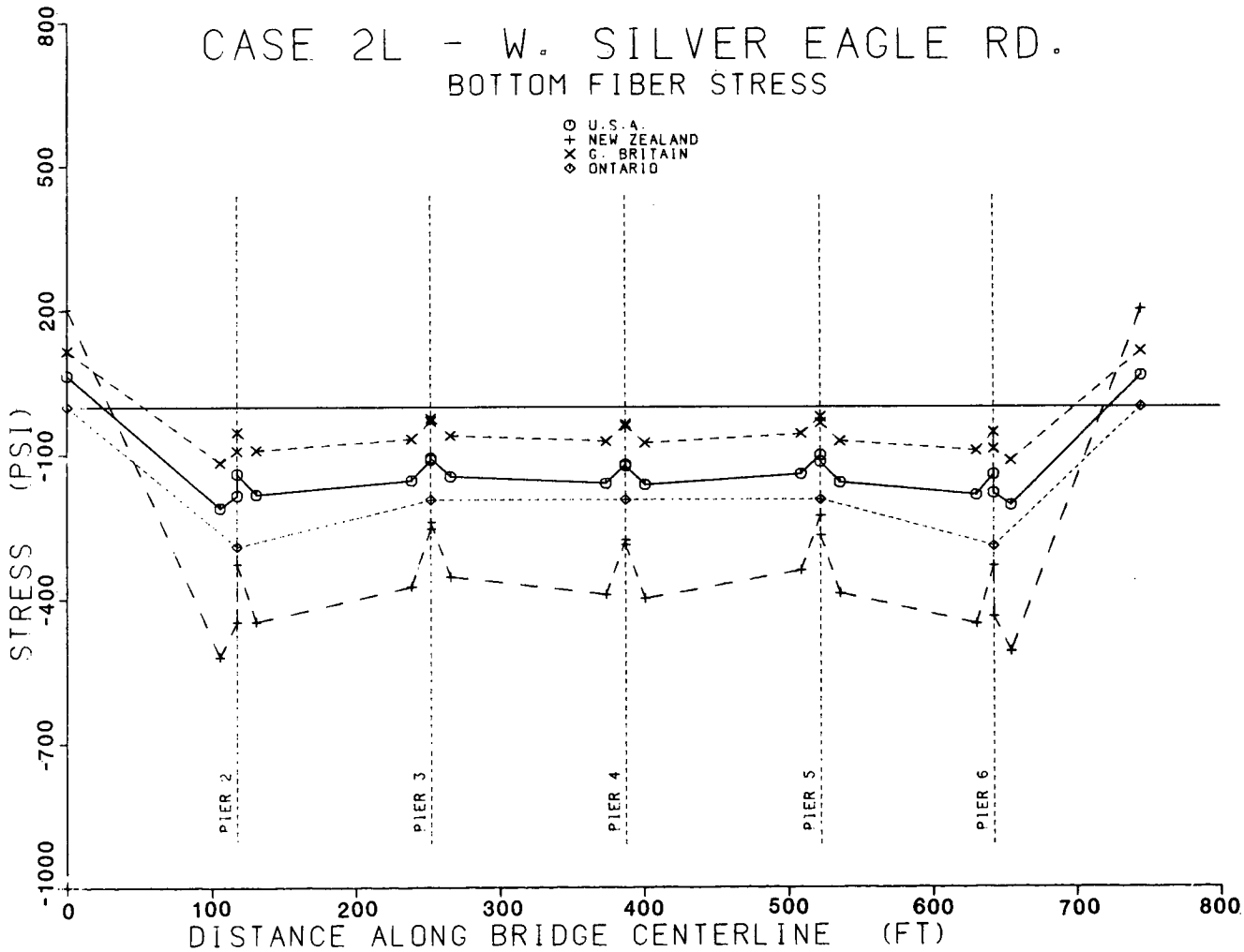

Figure 23. Case 2L—longitudinal variation in bottom fiber stresses along a typical girder centerline due to positive temperature gradients.

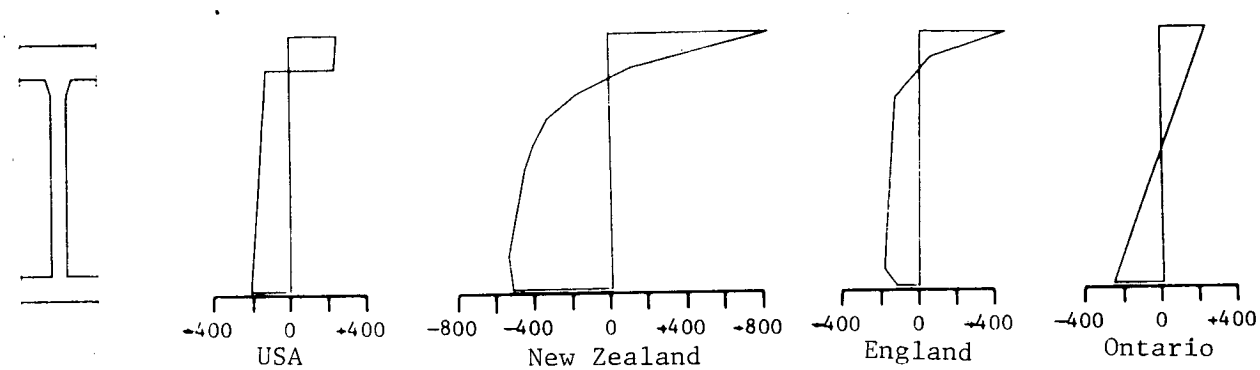

Figure 24. Case 2L—variation in girder cross-section stress with depth due to positive temperature gradients.

Description

This structure, shown schematically in Figure 25, is a two-span, 317-ft-long bridge. The superstructure is a precast, post-tensioned, prestressed concrete segmental box girder constructed by the cantilever method. The superstructure, which is continuous from abutment to abutment, has a depth-to-span ratio of 0.057. The interior support consists of a single column constructed to be fixed against rotation at the bottom and pinned at the top. This column is supported by a spread footing on bedrock. The seat-type abutments, which have expansion bearings to allow for longitudinal movement, are founded on driven steel piles.

Results

Because this structure is symmetrical and contains only two spans, the column will not be affected by axial shortening of the superstructure. Thus, for the purposes of analysis, this column support can be treated as a roller.

Shown in Figure 26 is a comparison of the maximum measured temperature differential with the temperature differentials used for the test cases.

Figures 27 and 28 are plots of top and bottom fiber stresses, respectively, along a typical girder centerline. The fiber stress plots in this case are similar to those for the end spans in Case 2L.

The influence of the bottom slab flare is readily apparent from Figure 28. As with Case 2L, which also had a flared bottom slab, the bottom fiber stresses in this case are significantly changed, while the top fiber stresses remain basically unchanged.

The top slab thickness of this single cell box section also varies transversely, making the computations to approximate the temperature gradient somewhat more tedious and lengthy than for a cross section with a constant slab thickness.

Case 4L—Kishwaukee River Bridge

Selection

The Kishwaukee River Bridge was included in the case studies because temperature data are being recorded as part of a field investigation to determine the time-dependent behavior of segmental, post-tensioned, cantilever concrete bridges. Although the temperature data are not yet available, Shiu, Danile, and Russel (*46*) confirmed that nonlinear temperature gradients similar to those proposed by Emerson (*83*) and Priestley were observed in this structure.

This bridge was one of the first of its type to be constructed in the United States. As with Case 3L, because a number of epoxied joints between the precast segments lack mild reinforcement, many engineers have expressed concern about the possibility of thermal stresses causing serviceability problems at this interface.

Description

This structure, shown schematically in Figure 29, is a five-span, 1,096-ft-long bridge. The superstructure is a precast, post-tensioned, prestressed concrete segmental box girder constructed by the cantilever method. The superstructure, which is continuous from abutment to abutment, has a depth-to-span ratio of 0.047. The interior supports consist of four single-column bents constructed to be fixed against rotation at the bottom. The top of the columns are constructed either to be pinned at the superstructure or to allow for freedom of relative transverse movement. The seat-type abutments have expansion bearings to allow relative longitudinal movement.

Results

Figures 30 and 31 are plots of top and bottom fiber stresses, respectively, along a girder centerline. The fiber stress plots are similar to those of Case 2L, except that the expansion bearings at the tops of the columns eliminate any effect that would occur due to connectivity.

The bottom slab flare, which is longer and thicker than the bottom slab flare in Case 2L, has a significant effect on the bottom fiber stresses.

The British-designed thermal gradient produced bottom-fiber tension stresses that were significantly low, as shown in Figure 31. The reason is that the relatively small bottom portion of that gradient results in a larger effect on the bottom fiber stress.

Case 5L—Columbia River Bridge

Selection

This bridge was included in the case studies because it differs from the precast, cantilever segmental bridges considered in Cases 3L and 4L in that the segments are cast-in-place. In this case, the segments can be easily spliced across the joints with mild, longitudinal reinforcement, thus elminating the epoxy joints between the superstructure segments. Another reason for selecting this bridge is the variation in structure depth caused by the haunches at the interior supports. This bridge was designed according to the Washington State Criteria (see Appendix D) on thermal effects. For longitudinal thermal effects of box girders the criteria specify a temperature increase of 20°F in the top slab. The stresses caused by this increase in temperature are combined with dead load for a service loading. In addition, another service load condition resulting from one-half the temperature gradient (i.e., 10°F) is combined with the dead load and full live load.

Description

This structure, shown schematically in Figure 32, is a five-span, 1,870-ft-long bridge. The superstructure is a cast-in-place, post-tensioned, prestressed concrete segmental box girder constructed by the cantilever method. The superstructure, which is continuous from abutment to abutment, has a depth-to-span ratio of 0.053. The 450-ft main spans are haunched at the supports. The interior supports consist of single columns constructed to be fixed against rotation at the bottom and either fixed against rotation or free to translate with respect to the superstructure at the top. The columns are supported on deep spread footings. The seat-type abutments have expansion bearings to allow longitudinal movement and are founded on driven steel piles.

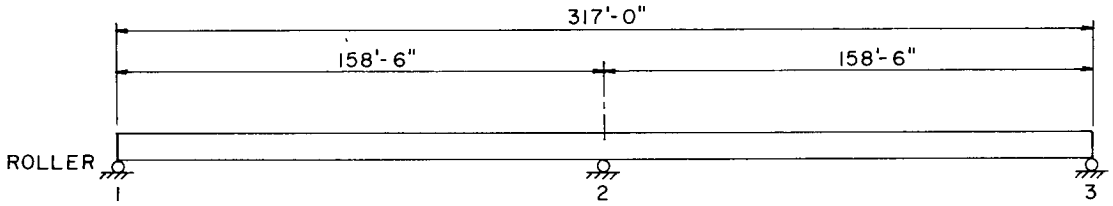

ELEVATION

SUPERSTRUCTURE f'_c = 5000 psi
TYPICAL SECTION: y_b = 5.65 ft
$A = 45.42\ ft^2$
$I = 478.13\ ft^4$
FLARED SECTION: y_b = 5.08 ft
$A = 51.89\ ft^2$
$I = 595.80\ ft^4$

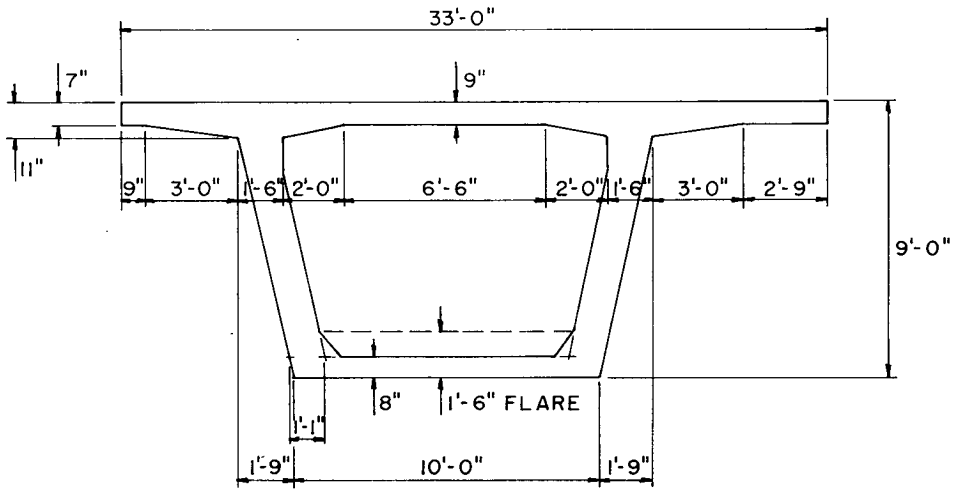

SUPERSTRUCTURE SECTION

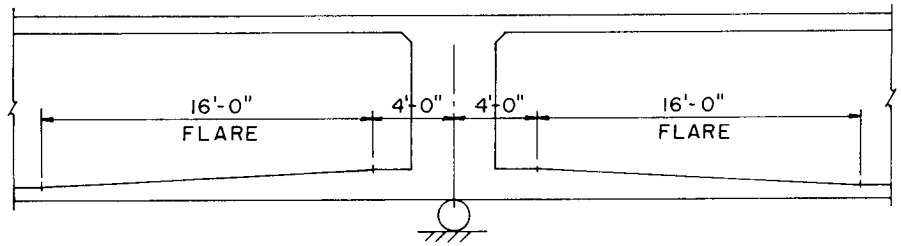

FLARE BENT 2

Figure 25. Case 3L—Turkey Run Creek Bridge superstructure and substructure details used for analysis.

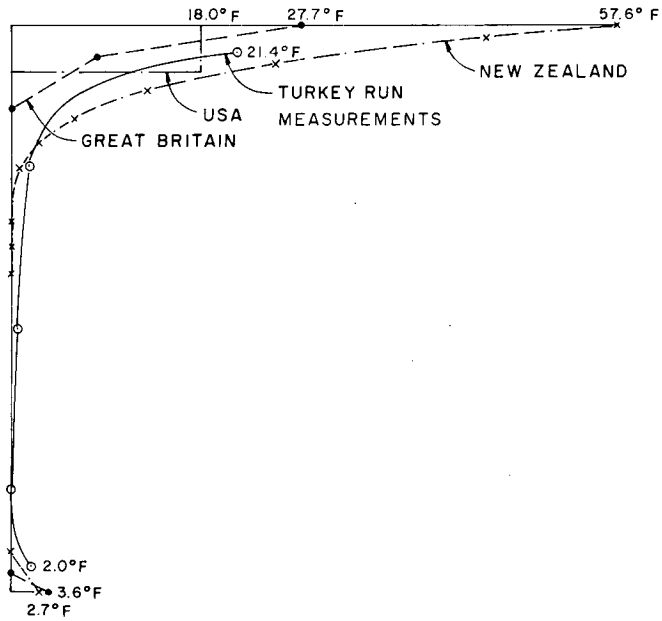

Figure 26. Case 3L—comparison of maximum measured temperature gradient with those used for case studies.

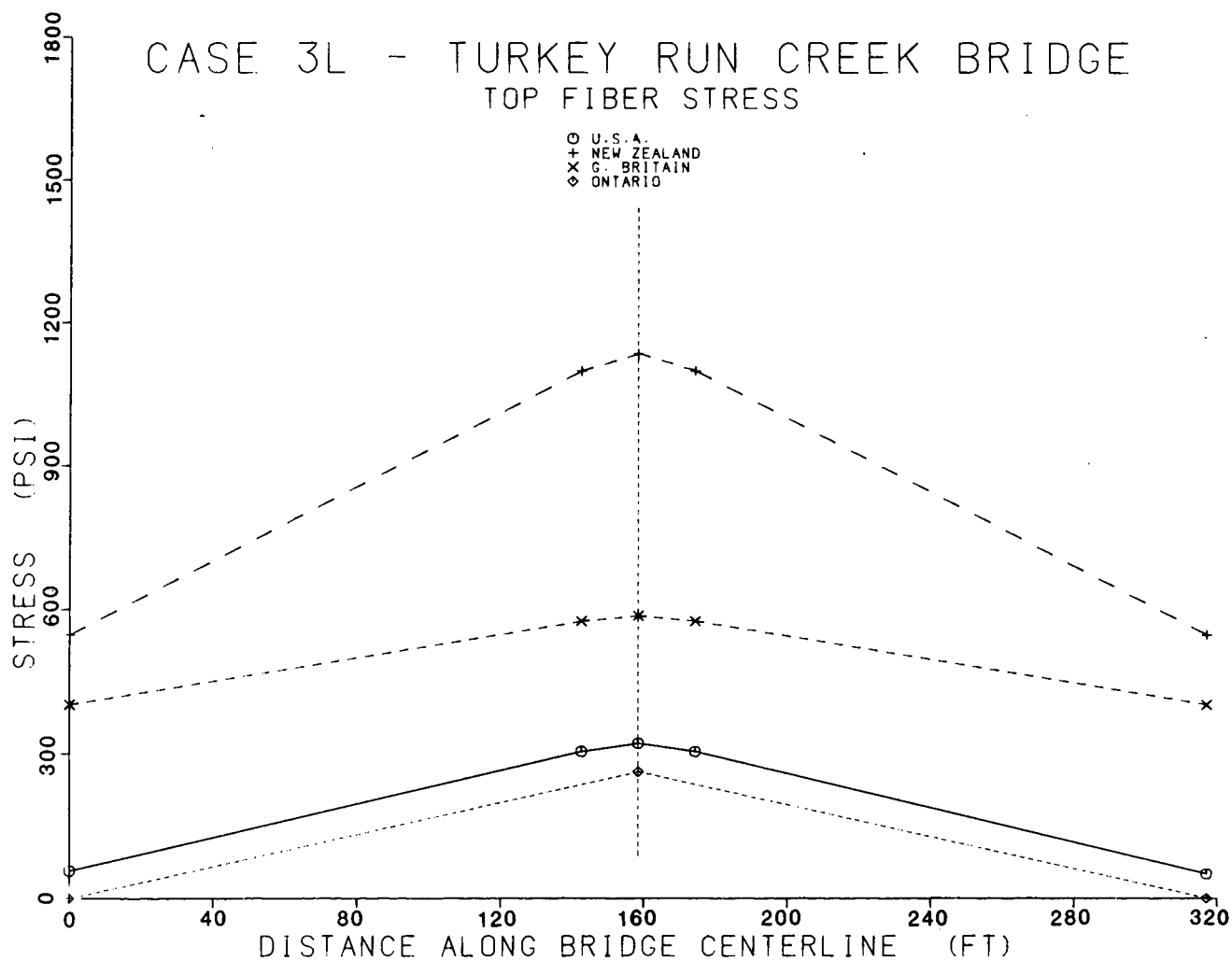

Figure 27. Case 3L—longitudinal variation in top fiber stresses along a girder centerline due to positive temperature gradients.

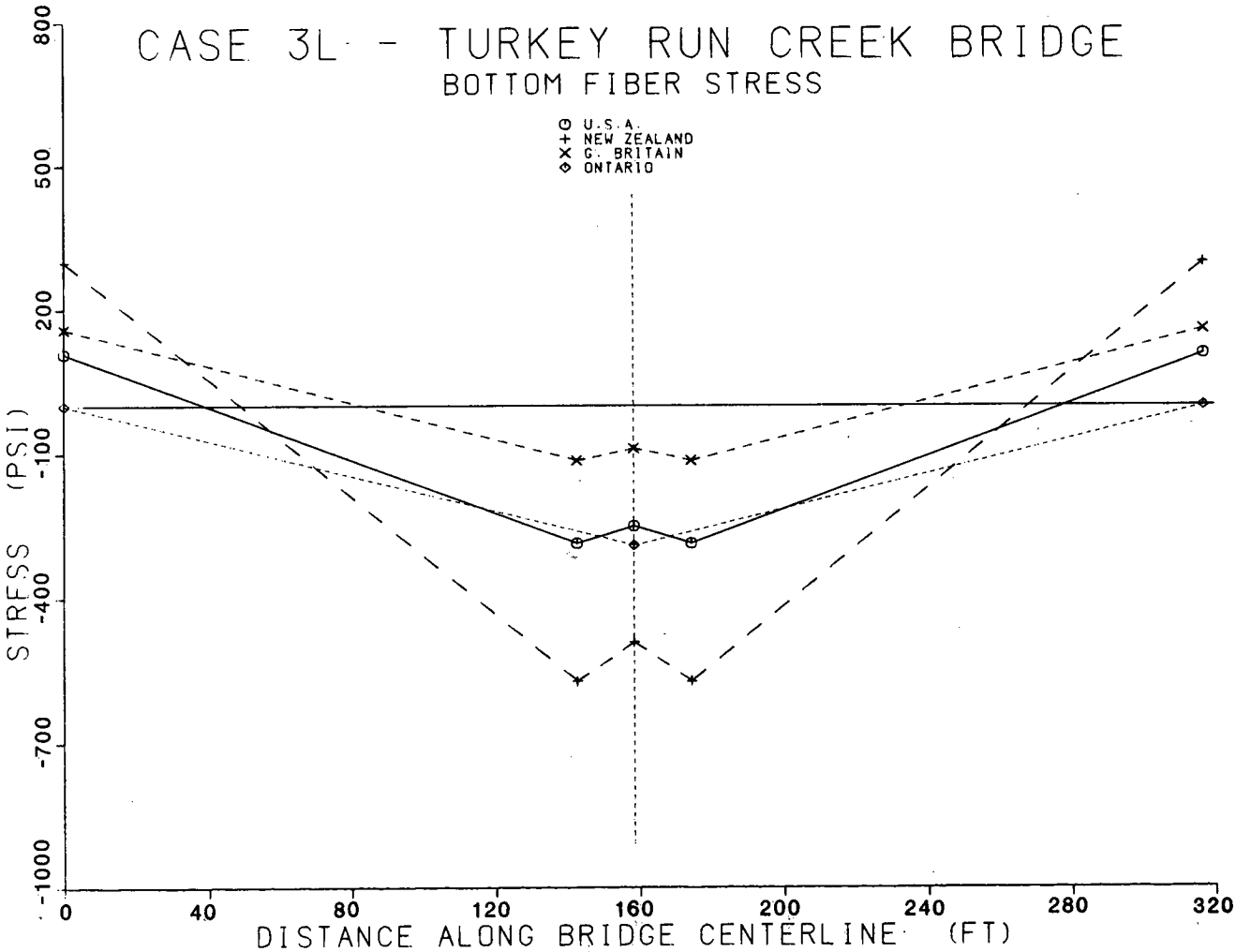

Figure 28. Case 3L—longitudinal variation of bottom fiber stresses along a girder centerline due to positive temperature gradients.

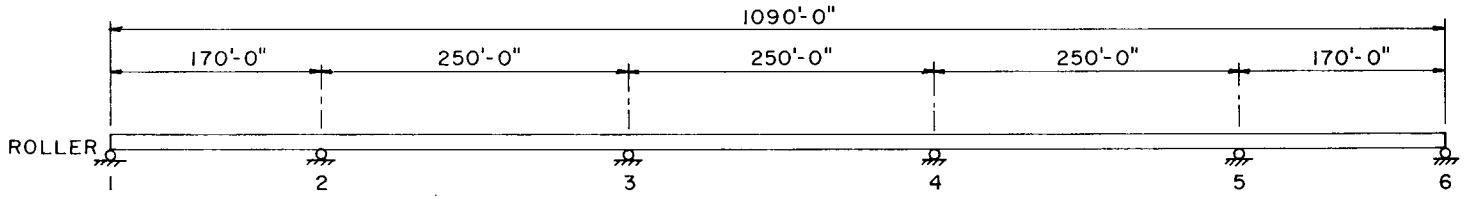

ELEVATION

SUPERSTRUCTURE f'c = 5500 psi

TYPICAL SECTION: y_b = 7.37 ft
A = 79.57 ft^2
I = 1533.60 ft^4

FLARED SECTION: y_b = 6.40 ft
A = 94.12 ft^2
I = 2018.90 ft^4

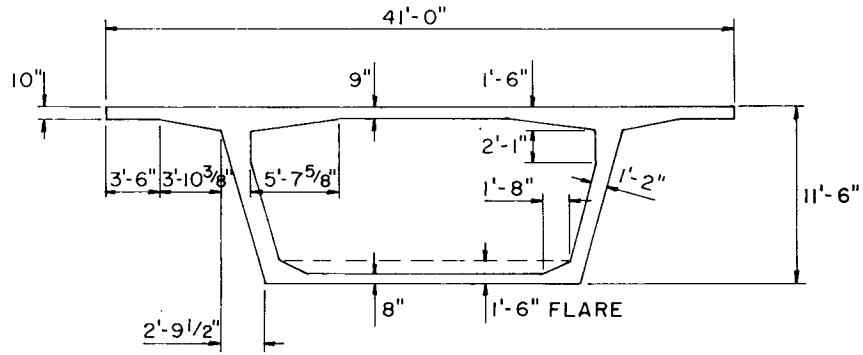

SUPERSTRUCTURE SECTION

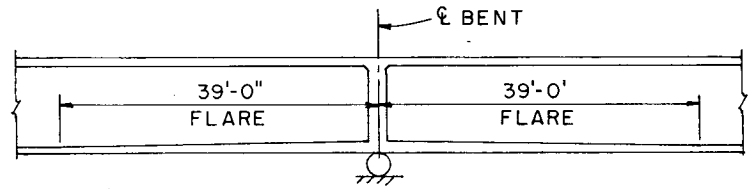

FLARE BENTS 2-5

Figure 29. Case 4L—Kishwaukee River Bridge superstructure and substructure details used for analysis.

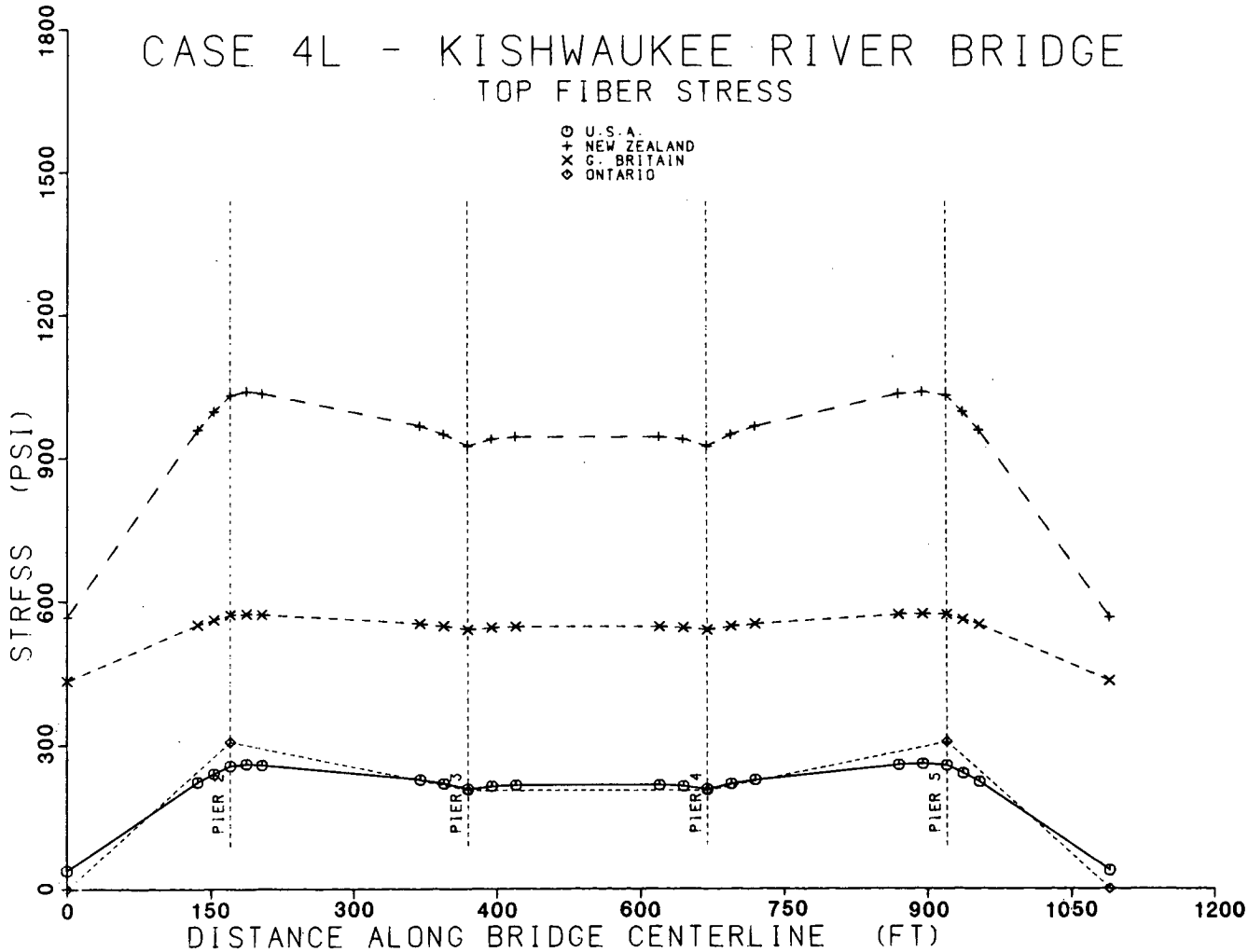

Figure 30. Case 4L—longitudinal variation in top fiber stresses along a girder centerline due to positive temperature gradients.

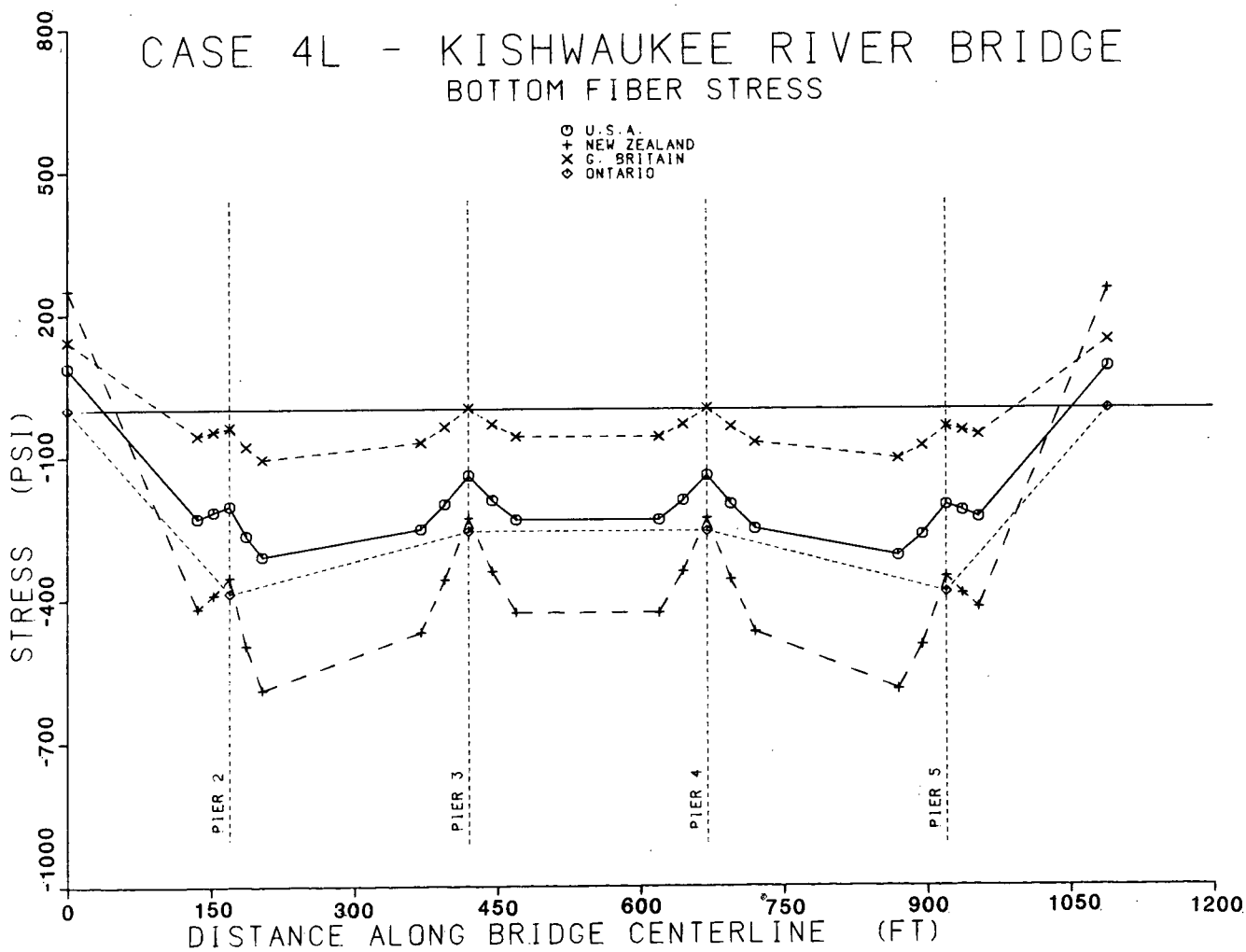

Figure 31. Case 4L—longitudinal variation in bottom fiber stresses along a girder centerline due to positive temperature gradients.

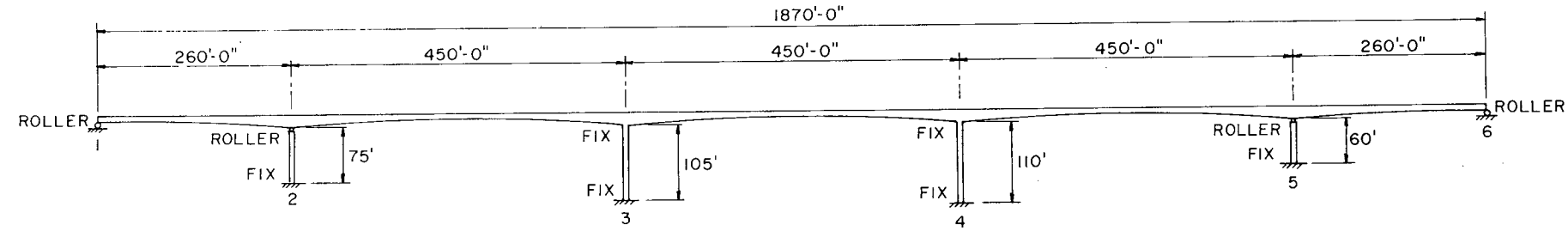

ELEVATION

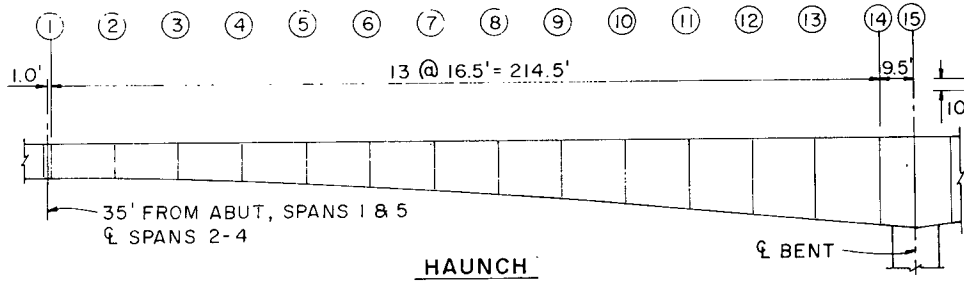

HAUNCH

SECTION	D (ft)	y_b (ft)	A (ft^2)	I (ft^4)
1	9.00	6.00	121.32	1309.84
2	9.19	6.13	121.90	1375.68
3	9.60	6.41	123.23	1524.75
4	10.18	6.79	125.11	1751.09
5	10.90	7.18	129.14	2132.84
6	11.77	7.50	136.75	2775.83
7	12.76	7.85	145.68	3619.63
8	13.87	8.22	155.75	4706.64
9	15.10	8.65	166.35	6060.87
10	16.44	9.13	177.24	7720.86
11	17.89	9.69	187.65	9705.54
12	19.44	10.29	198.45	12109.05
13	21.10	10.95	209.06	14971.47
14	22.85	11.66	219.50	18331.48
15	24.00	11.70	223.10	18540.00

SUPERSTRUCTURE f'c = 5000 psi
SUBSTRUCTURE f'c = 4000 psi

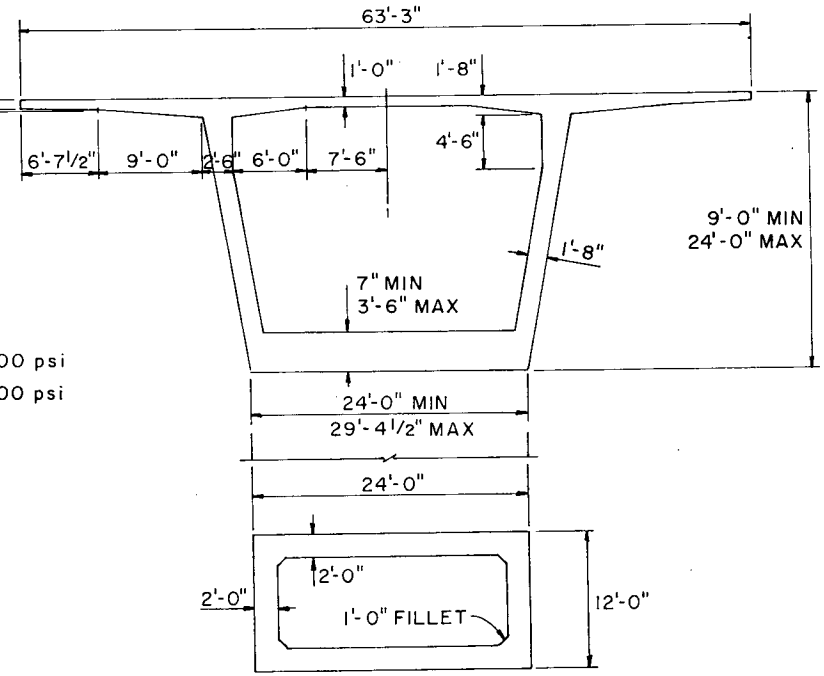

SUPERSTRUCTURE & COLUMN SECTION

Figure 32. Case 5L—Columbia River Bridge superstructure and substructure details used for analysis.

Results

Figures 33 and 34 are plots of top and bottom fiber stresses, respectively, along a girder centerline. The Ontario code was not considered in this case because it was not apparent how this code should be applied to nonprismatic sections. The shape of the fiber stress plots varies significantly from the cases previously considered. It is evident that the effect of the haunch is to magnify the stresses at the midpoint of the span, where the span is least thick. The effect of the haunch on fiber stresses is similar to that of a very long, thick bottom slab flare.

Instead of occurring at the supports, as in Cases 1L through 4L, the maximum stresses for this case occur at midspan. The tensile stresses in the bottom fibers are about twice the magnitude of the previous four cases, as shown in Figure 34.

Because of the magnitude of the tensile stresses in the bottom slab and their location coincident with maximum dead load and live load tensile stresses, it is evident that the design of a bridge of this type should provide for thermal gradient loadings.

Shown in Figures 35 and 36 are plots of the variation in stresses with section depth for the three gradients considered for 9-ft and 24-ft deep sections respectively.

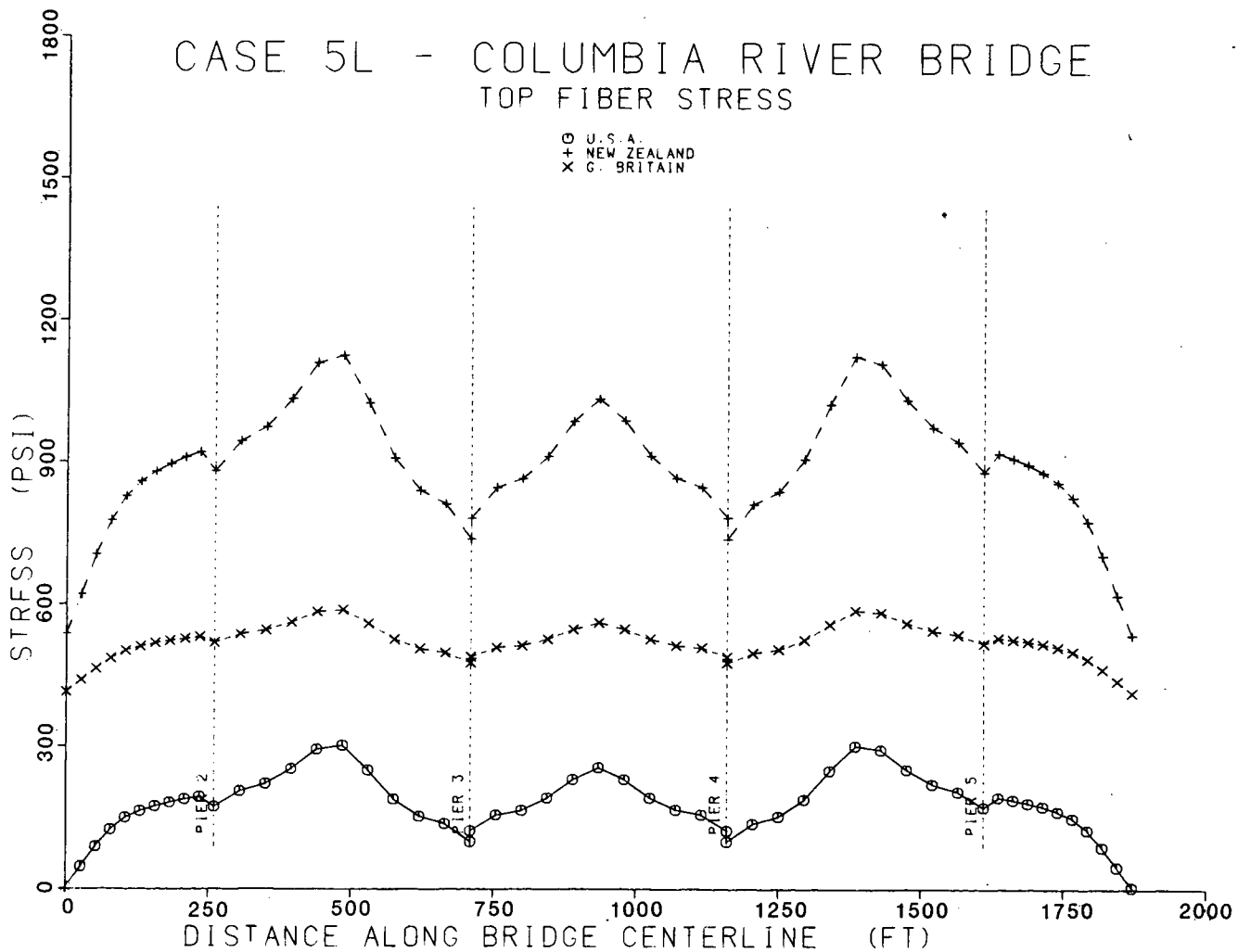

Figure 33. Case 5L—longitudinal variation in top fiber stresses along a girder centerline due to positive temperature gradients.

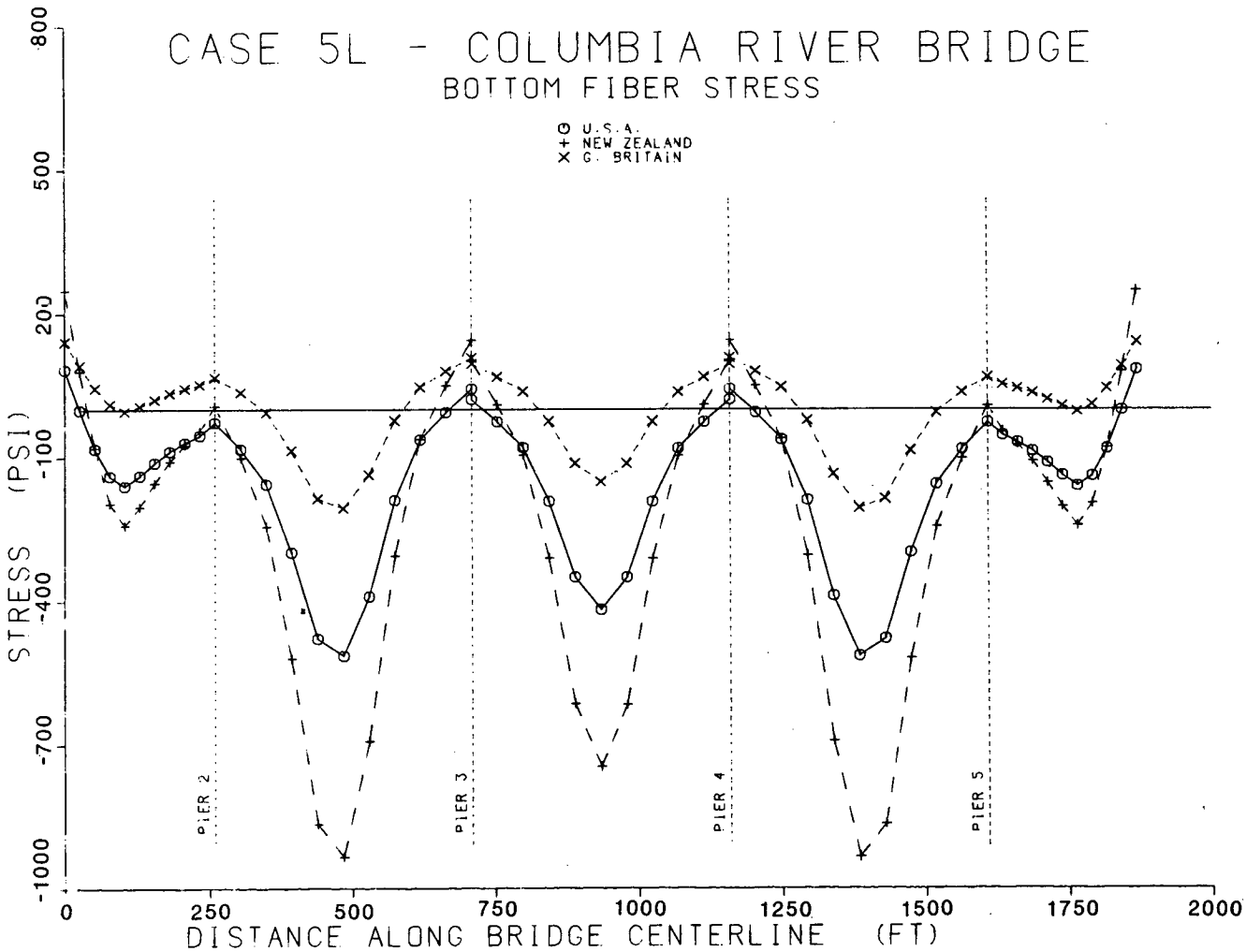

Figure 34. Case 5L—longitudinal variation in bottom fiber stresses along a girder centerline due to positive temperature gradients.

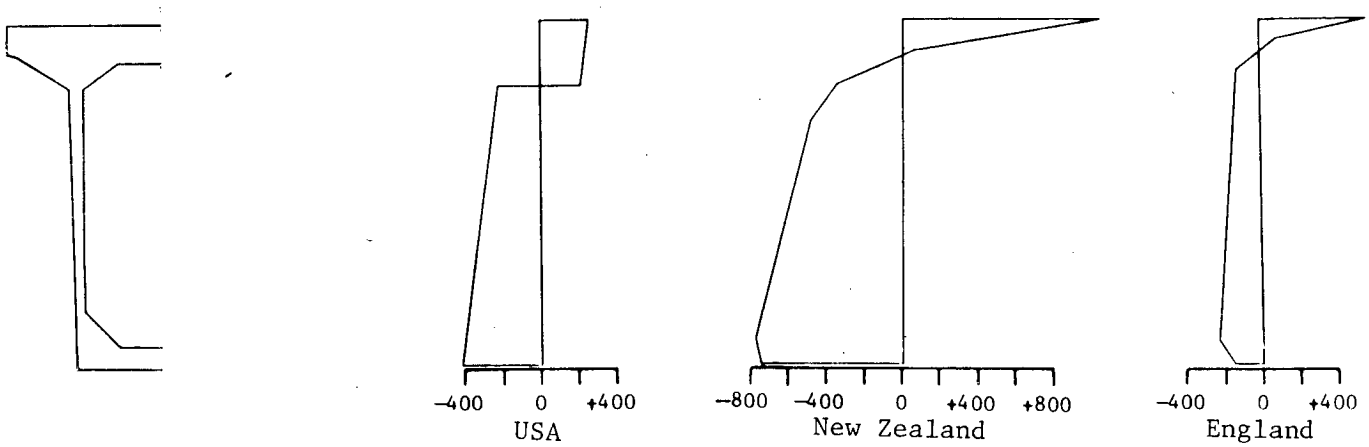

Figure 35. Case 5L—9-ft deep cross section—variation in girder cross-section stresses with depth due to positive temperature gradients (the − symbol indicates tension and the + symbol indicates compression).

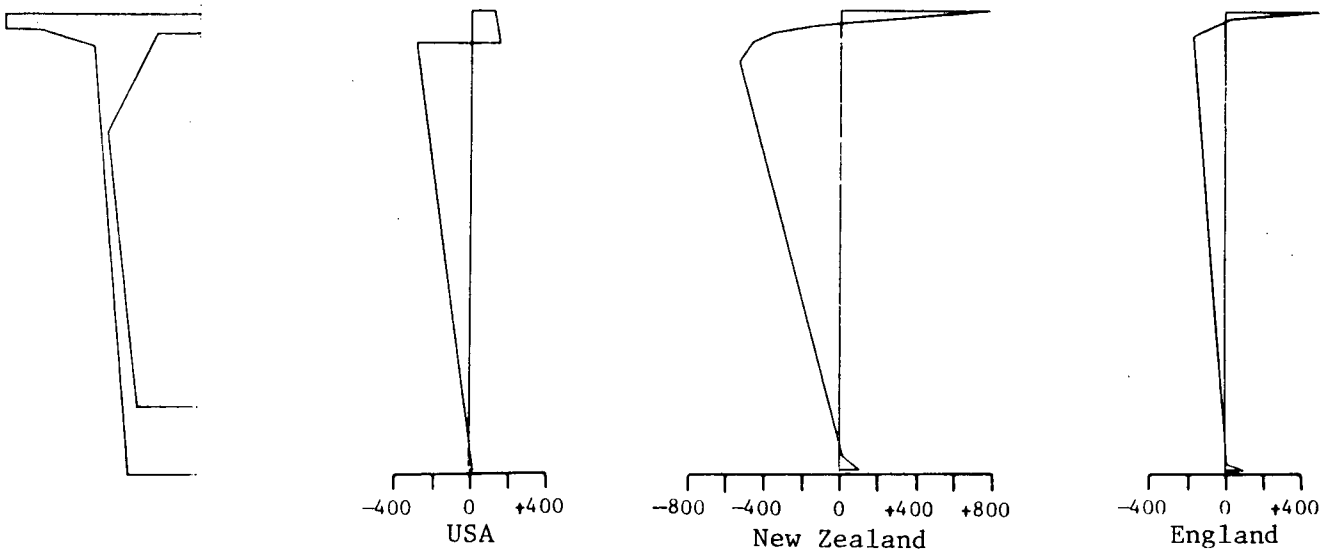

Figure 36. Case 5L—24-ft deep cross section—variation in girder cross-section stresses with depth due to positive temperature gradients (the − symbol indicates tension and the + symbol indicates compression).

Case 6L—West Silver Eagle Road Bridge and Overhead (Falsework)

Selection

The falsework failure that occurred in New Zealand prompted the inclusion of this case study. Huizing, Blakely, and Ramsay (*110*) established that the thermal loading was a probable factor contributing to the falsework failure that occurred on a section of the Karangahape Ramp A Bridge in Auckland, New Zealand. It was concluded that the tendency for longitudinal thermal hogging resulted in the redistribution of loads in the falsework bents, critically increasing the reactions at the extreme supporting bents. The coupling of this thermal effect with similar load redistributions resulting from the stage-prestressing process led to the eventual collapse of the falsework.

Except for an added hinge in span 3, this bridge is identical to Case 2L. The effects of thermal gradient loads were analyzed during an assumed intermediate stage of construction, i.e., shortly after casting the concrete, while one of the frames is still being supported on falsework.

This hypothetical example was selected to evaluate the redistribution of falsework loads caused by thermal gradient strains during construction and to determine if this redistribution might have a significant effect on falsework design. The effect of thermal gradients is similar to the effect of prestressing operations in that they result in a redistribution of falsework support reactions.

Description

This structure, shown schematically in Figure 37, is a six-span, 745-ft long bridge. The superstructure, which has one intermediate expansion joint hinge, is a cast-in-place, post-tensioned, prestressed concrete box girder with a depth-to-span ratio of 0.037. The intermediate supports consist of five 2-column bents ranging in height from 25 to 35 ft. The columns are constructed to be pinned at the bottom and monolithic with the superstructure at the top. The seat-type abutments have expansion bearings to allow longitudinal movement. The bridge is founded on cast-in drilled-hole concrete piles.

Results

The concrete bridge frame, which is assumed to be cured and supported on falsework, was analyzed to determine how it would be affected by the USA design temperature gradient. The falsework reactions, particularly under the expansion joint hinge, were evaluated for overload.

The analysis indicated that the only falsework posts significantly affected by the thermal loads were those at the expansion joint hinge. Depending on the stiffness and redundancy of the remainder of the falsework, the reaction at these posts due to the assumed thermal gradient alone could exceed the reaction at these posts due to dead and live loads. Therefore, if not designed for thermal effects, the posts could be subjected to compression loads in excess of twice their safe capacity. A larger thermal load, such as the thermal gradient used in the New Zealand code, would produce a correspondingly greater overload.

This hypothetical situation seldom occurs in actual bridge construction practice. Nevertheless, falsework failures are a major problem, and it may be appropriate to incorporate provisions for thermal gradient loads into falsework design procedures.

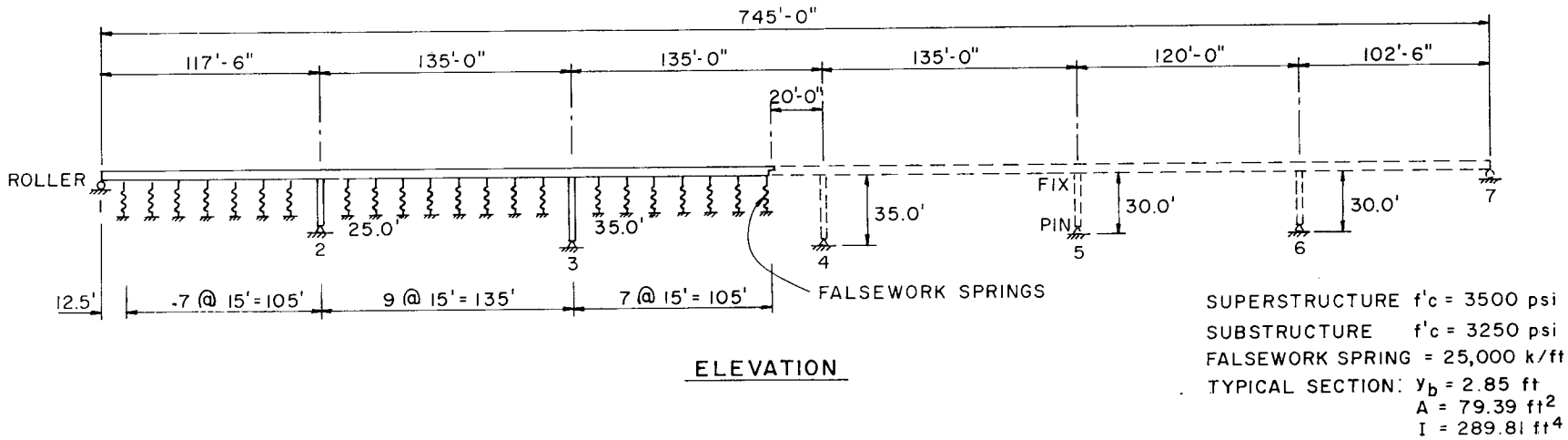

ELEVATION

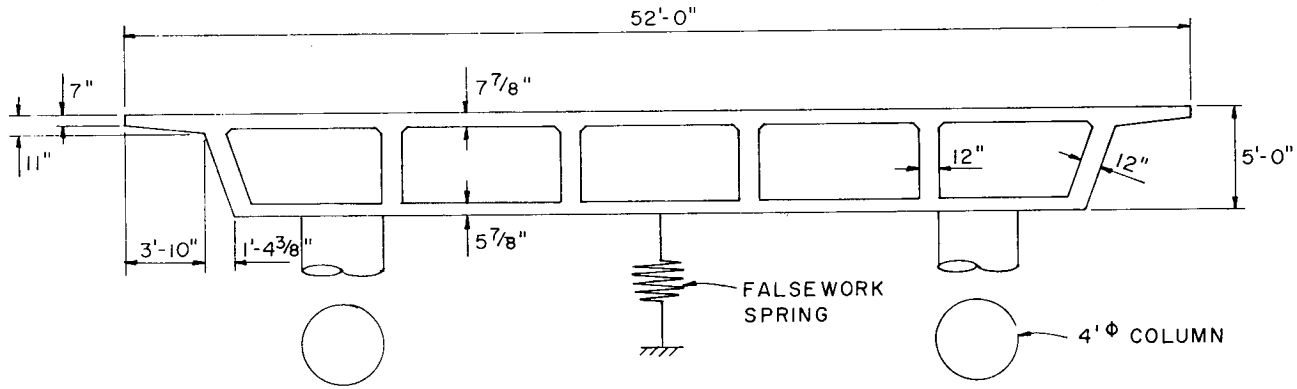

SUPERSTRUCTURE & COLUMN SECTION

Figure 37. Case 6L—falsework—West Silver Eagle Raod Bridge and overhead superstructure and substructure details used for analysis.

Case 7L—East Connector Overcrossing

Selection

The East Connector Overcrossing was selected to evaluate the presence of internal expansion joint hinges which will significantly change the thermal stresses in adjacent members.

Description

This bridge differs from the other cases studied because it contains two intermediate expansion joint hinges and because it is the only reinforced concrete bridge studied. Also, the abutments can be assumed to be pinned instead of fixed at the base of the diaphragm.

This structure, shown schematically in Figure 38, is an eleven-span, 1,104-ft-long bridge. The superstructure, which has two intermediate expansion joint hinges, is a cast-in-place, reinforced concrete box girder with a depth-to-span ratio of 0.055. The intermediate supports consist of ten single-column bents that are constructed to be monolithic with the superstructure and fixed against relative rotation at the footing. The diaphragm-type abutments are assumed to prevent longitudinal movement. The structure is founded on cast-in drilled-hole concrete piles.

Figures 39 and 40 are plots of top and bottom fiber stresses, respectively, along a typical girder centerline. The shape of the fiber stress plots is greatly influenced by the presence of internal expansion joint hinges for a distance of about one span length on either side of the hinge. This is similar to the behavior observed at the abutments in the previous cases.

This structure is somewhat different in that the abutments, rather than being on rollers, are designed to be pinned. This appears to have affected the fiber stresses less than expected. The main reason for this difference is the reversal in the direction of concentrated column moment at the bents adjacent to the abutments.

The normal flexural cracking that can be expected to develop in a reinforced concrete structure such as this will decrease the effective moment of inertia of the superstructure and relieve the fiber stresses shown.

Case 8L—Miller Creek Bridge

Selection

This bridge is similar to Turkey Run Creek (Case 3L). It and several other bridges in the area developed severe cracking problems shortly after completion of construction. Thermal gradient effects are suspected as being one of the causes of this distress.

Description

This structure, shown schematically in Figure 41, is a three-span 455-ft-long bridge. The superstructure is a cast-in-place, post-tensioned, prestressed concrete segmental box girder constructed by the cantilever method. The superstructure, which is continuous from abutment to abutment, has a depth-to-span ratio of 0.041. The interior supports consist of single-column bents on spread footings. The bottoms of the columns are fixed and the tops are pinned. The seat-type abutments have expansion bearings to allow relative longitudinal movement.

Results

The shape and magnitude of the fiber stress plots, shown in Figures 42 and 43, are similar to those of comparable structures previously analyzed, such as Turkey Run Creek and Kishwaukee River. However, the magnitude of the stress results produced by the New Zealand thermal loading was much less than the other structures because of the insulating effect of the relatively thick (2¾-in.) asphalt overlay.

This bridge is of special interest because the structure developed relatively severe cracking in the bottom flange and girder stems at approximately the ¼ and ¾ points of span 2, as shown in Figure 3, a short time after completion of construction. Thermal gradient effects are thought to have been a significant contributing factor to this distress. The crack widths, in fact, were observed to be opening and closing on a daily basis, generally correlating reasonably well with daily temperature fluctuations.

This structure was constructed by the cast-in-place segmental balanced cantilever method. Prestress tendons are typically placed in the bottom slab within the center portion of the span to resist positive bending moments that can result because of creep after the cantilevered portions of the superstructure are tied together. In this bridge, these tendons terminated in the vicinity of the cracking. Several other similar bridges constructed nearby at about the same time have developed similar cracking patterns.

A plot showing dead, prestress, and USA thermal load stresses, as calculated by Figg and Muller Engineers, Inc., of Tallahassee, Florida (*131*), is shown in Figure 44. This plot shows that tensile stresses occur in the bottom fiber at the same location where the cracks developed.

Based on the details of construction and the characteristics of the observed cracking, the reasons for the cracking appear to be some combination of the following:

1. Inelastic redistribution of stress (i.e., increase of positive moment due to creep) was greater than anticipated.
2. Stress concentrations in the prestress anchorage zone.
3. Thermal gradient stresses.

Although the primary cause of the distress cannot be precisely determined, it appears that the inelastic redistribution of stress resulting in an increase of positive moment (reason 1 above) is probably the most important single factor. Local tension stresses caused by prestress anchorages and thermal gradient stresses, although significant, are probably of secondary importance.

The cracking probably could have been avoided by extending the bottom slab prestress tendons, thus anchoring them much closer to bent 2 and bent 3, in zones of high bottom fiber compression.

In summary, it appears that the thermal gradient stresses are not the basic cause of this cracking problem, but are, however, contributing to it.

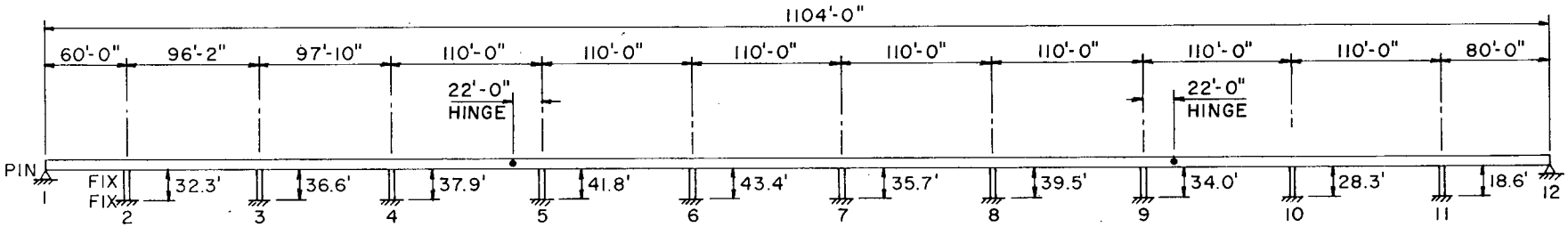

ELEVATION

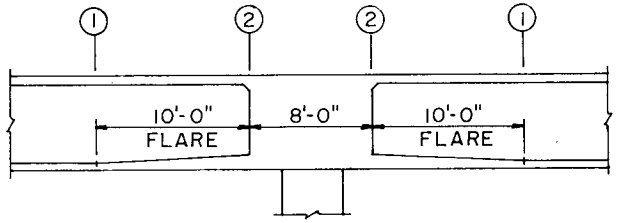

FLARE BENTS 2-4, 6-8 & 10-11

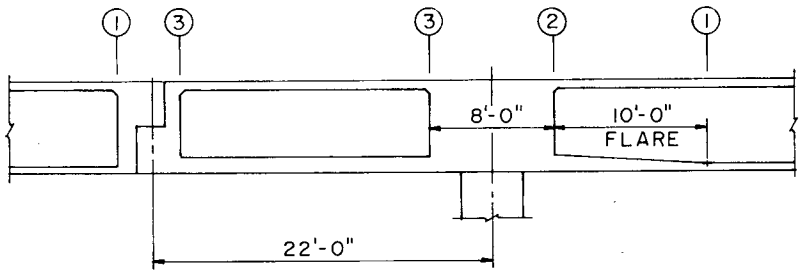

FLARE BENTS 5 & 9

f'c = 3250 psi

SECTION (1): y_b = 3.56 ft, A = 56.91 ft^2, I = 297.22 ft^4

SECTION (2): y_b = 3.04 ft, A = 69.73 ft^2, I = 381.42 ft^4

SECTION (3): y_b = 3.05 ft, A = 73.54 ft^2, I = 387.53 ft^4

BENT I = 35.40 ft^4

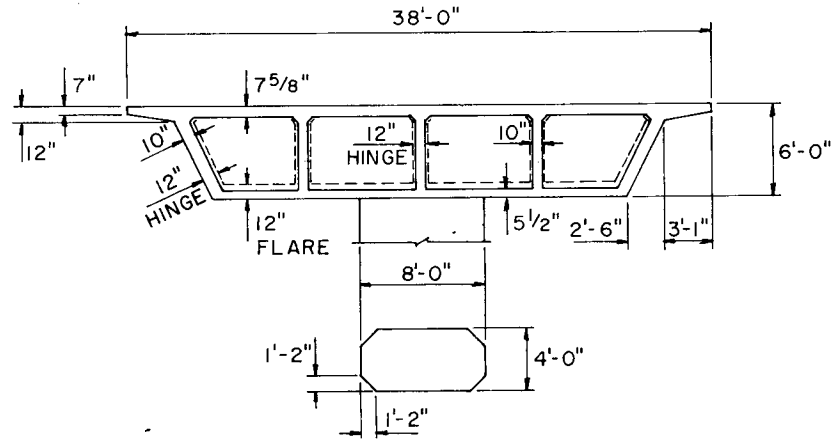

SUPERSTRUCTURE & COLUMN SECTION

Figure 38. Case 7L—East Connector Overcrossing superstructure and substructure details used for analysis.

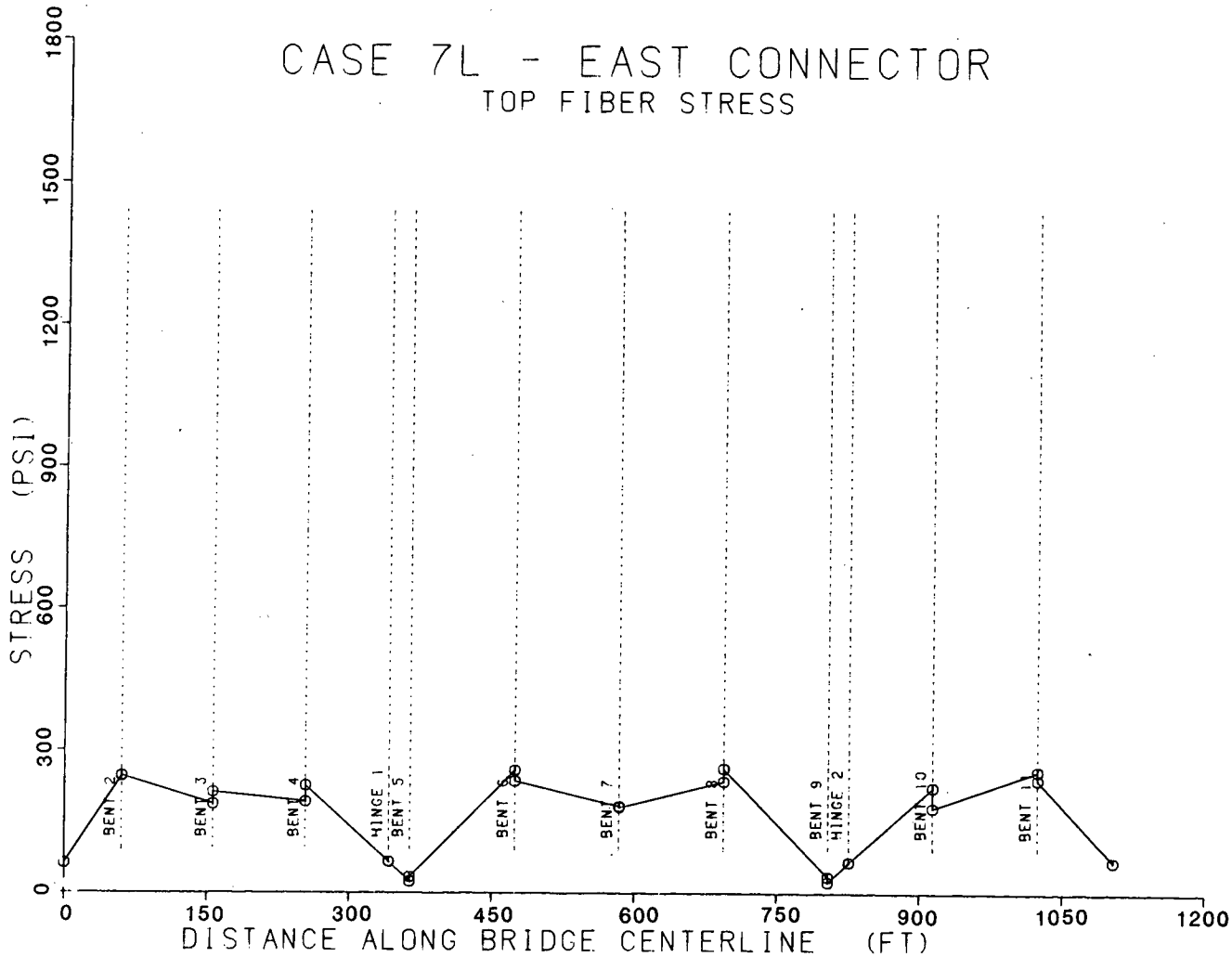

Figure 39. Case 7L—longitudinal variation in top fiber stresses along a typical girder centerline due to positive temperature gradients.

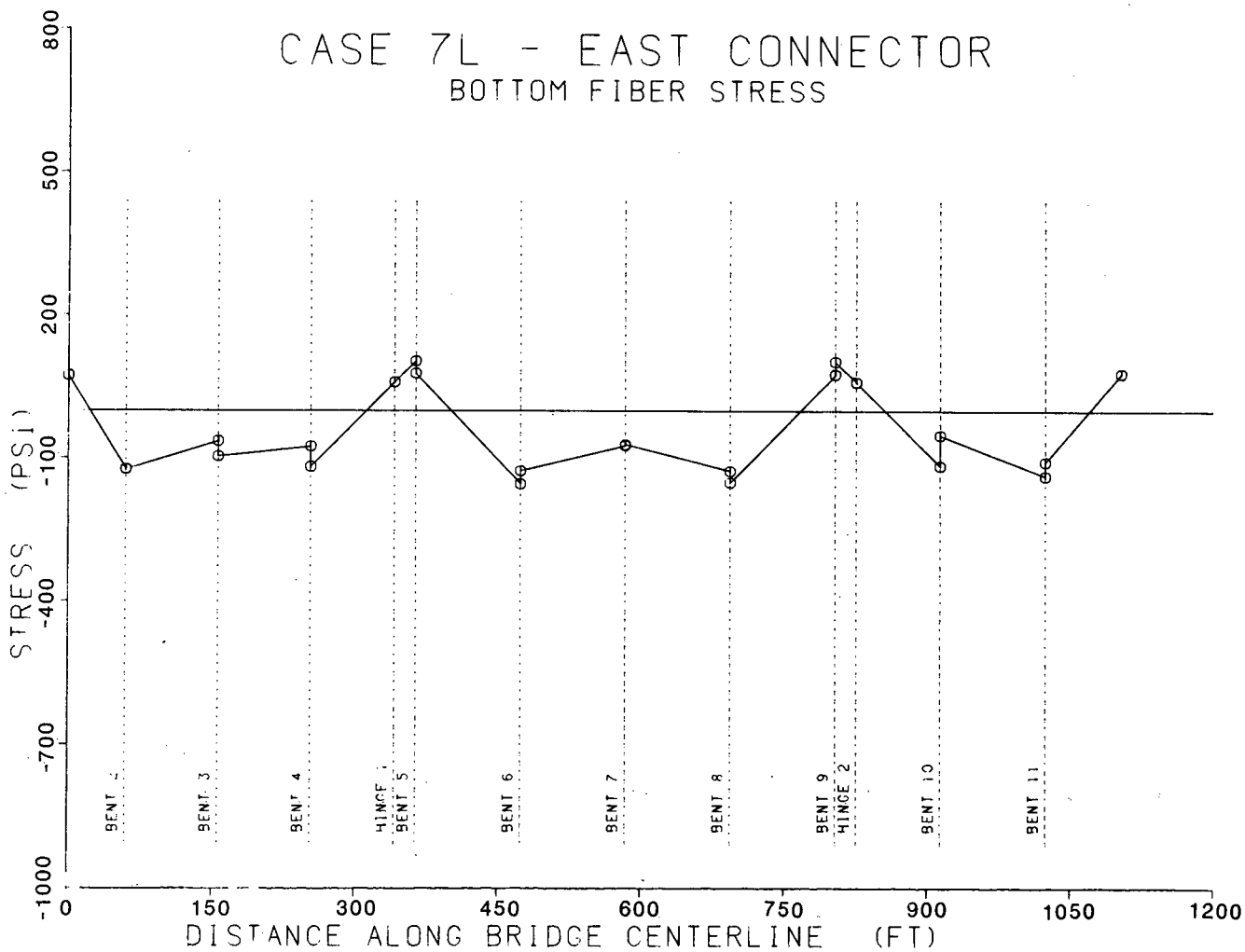

Figure 40. Case 7L—longitudinal variation in bottom fiber stresses along a typical girder centerline due to positive temperature gradients.

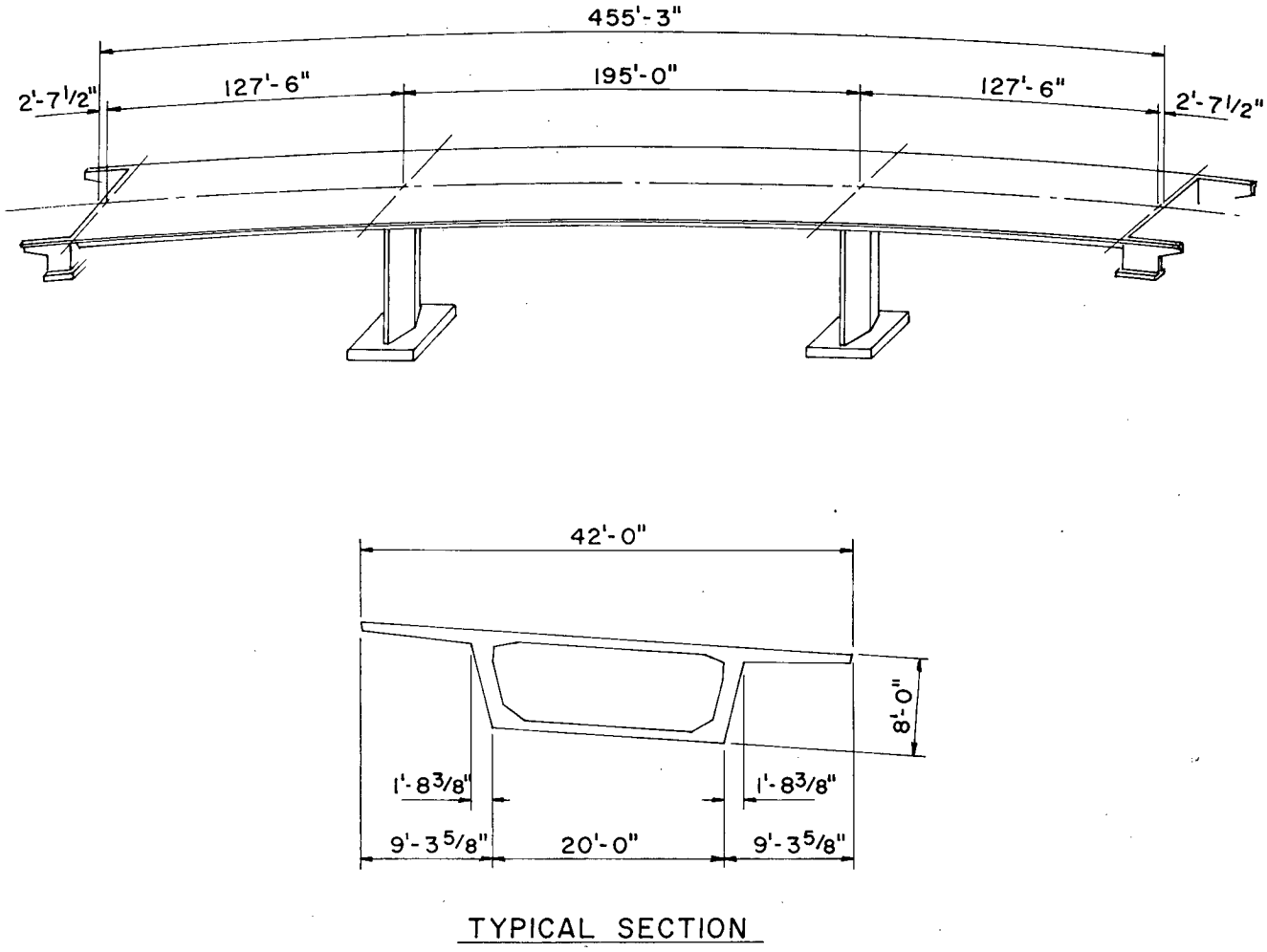

Figure 41. Miller Creek Bridge superstructure and substructure details used for analysis.

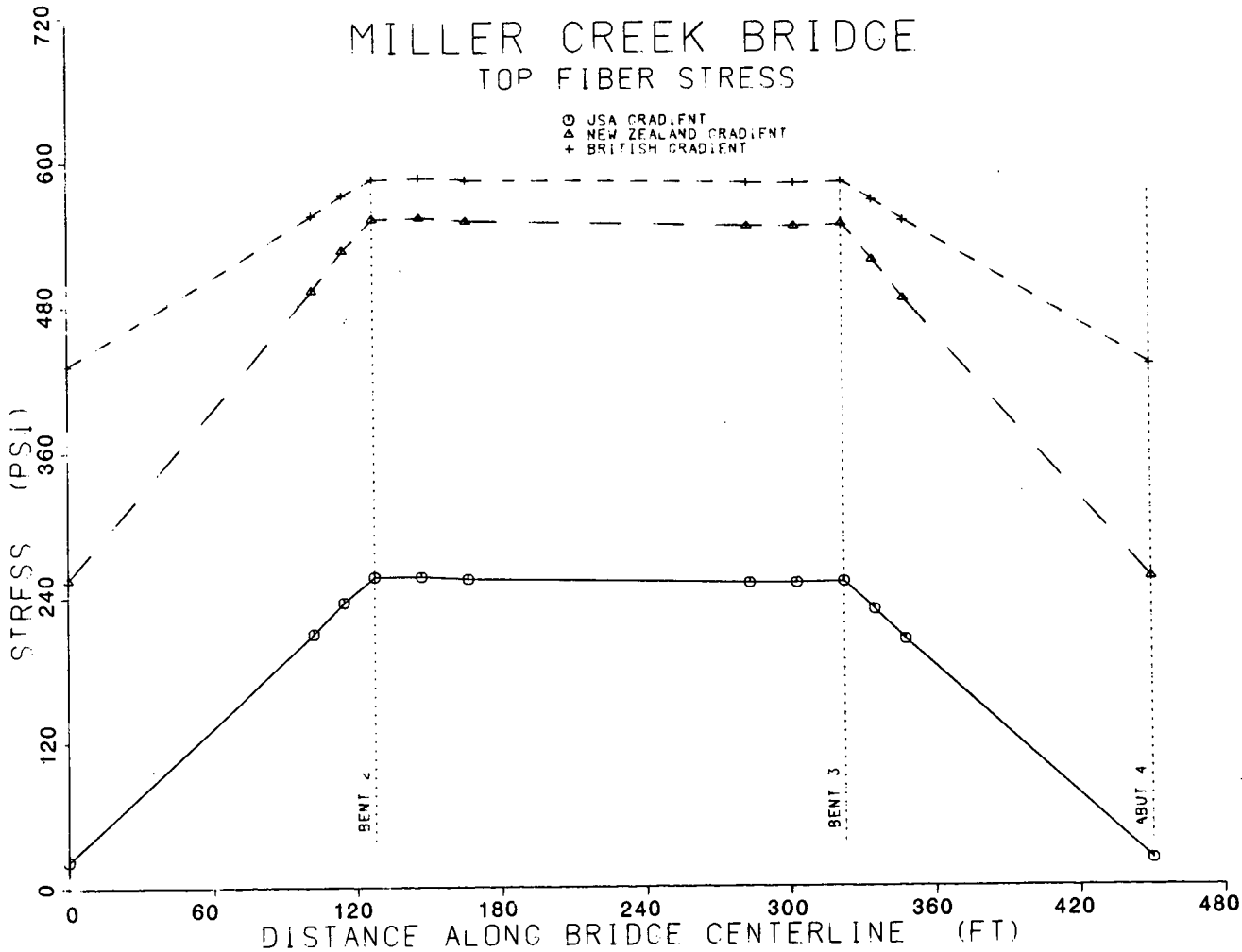

Figure 42. Case 8L—longitudinal variation in top fiber stresses along a girder centerline due to positive temperature gradients.

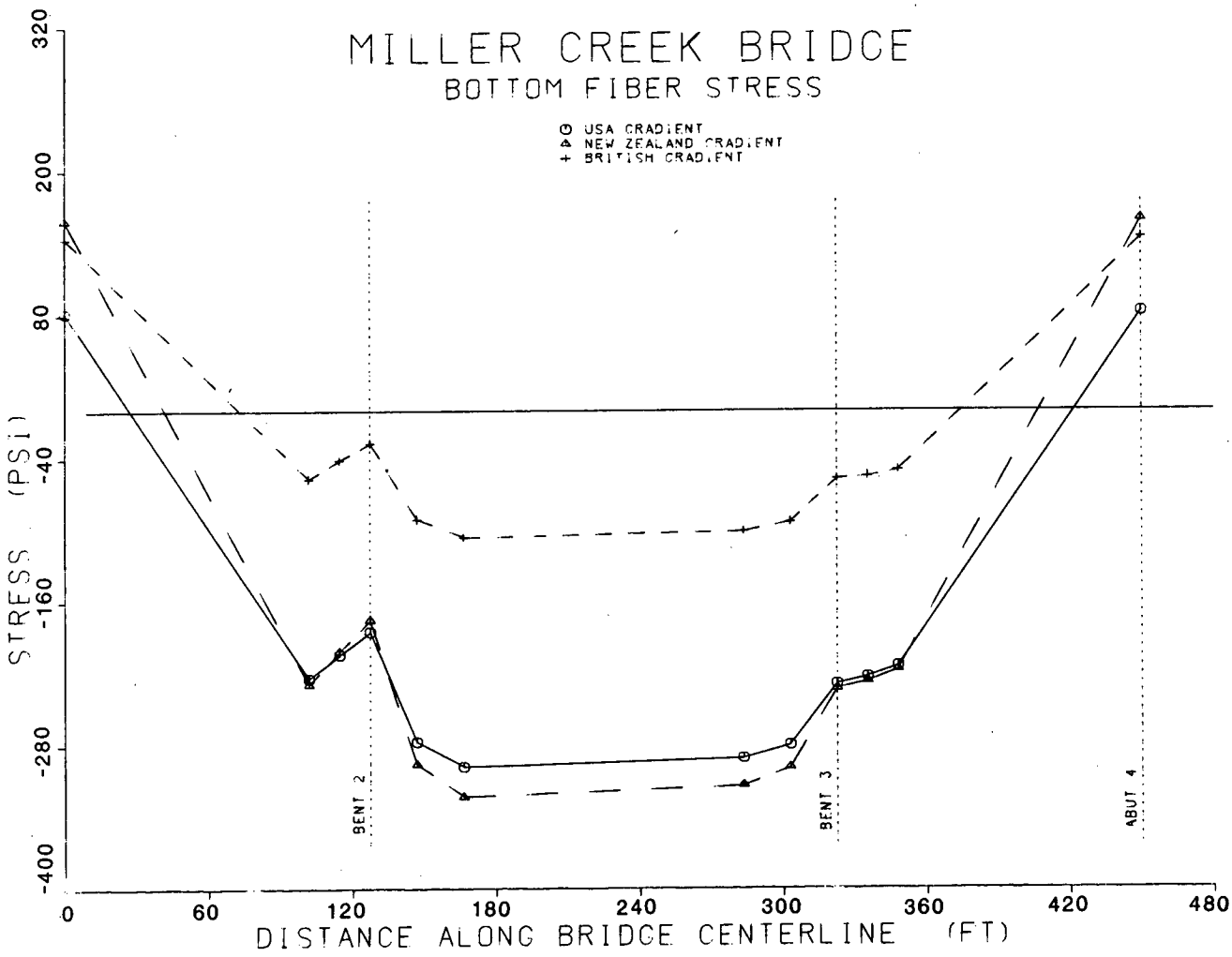

Figure 43. Case 8L—longitudinal variation in bottom fiber stresses along a girder centerline due to positive temperature gradients.

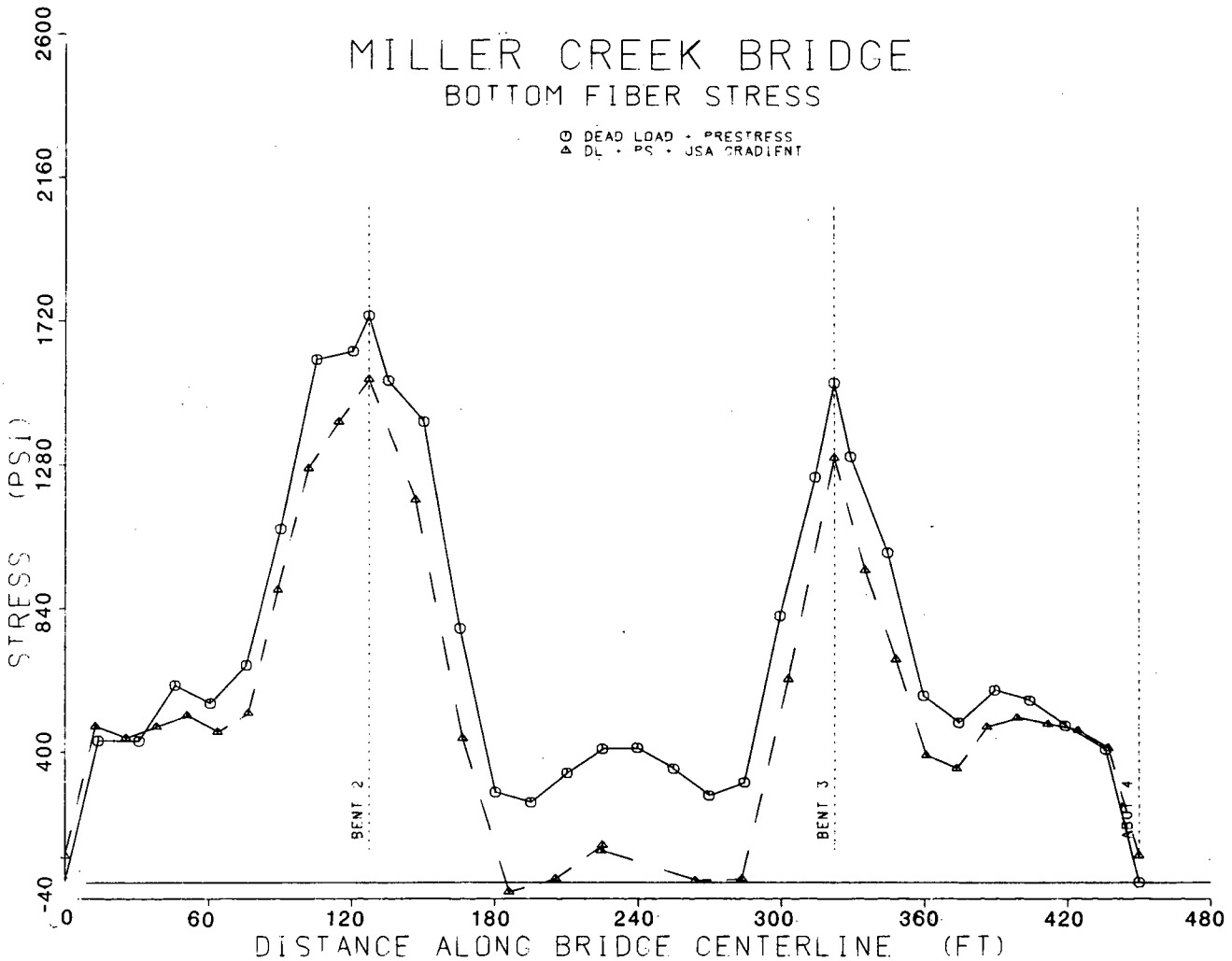

Figure 44. Case 8L—longitudinal variation in bottom fiber stresses along a girder centerline due to combined dead load, positive temperature gradient, and prestressing.

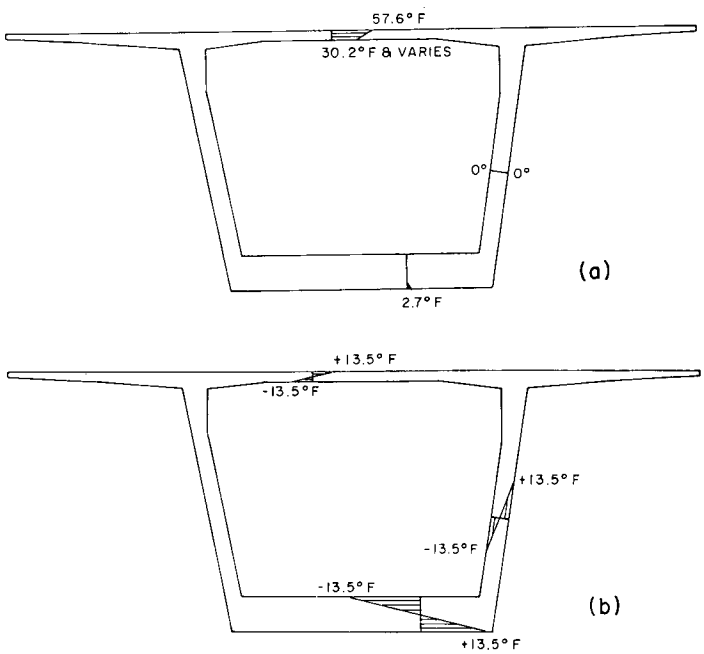

Figure 45. Thermal gradients used in the case studies for transverse temperature effects: (a) from the New Zealand Code, and (b) from Ref. 15.

TRANSVERSE TEMPERATURE EFFECTS

Two thermal gradient loads, shown in Figure 45, were applied to the case studies presented in this section (see Table 6). One load is based on the provisions of the New Zealand code and the other on a 27°F linear temperature gradient imposed around the boundaries of the transverse section, as used in the illustration presented in the *Precast Segmental Box Girder Bridge Manual* (*15*). The temperature gradient used in the New Zealand code is determined only on the basis of top slab heating due to solar radiation. The 27°F linear gradient, which assumes the exterior fibers warmer than the interior fibers, is determined on the basis of either the effect of direct solar radiation heat gain or a rapid increase in ambient temperature. The reverse case, which is based on the interior fibers being 27°F warmer than the exterior fibers, was not considered.

Plots of fiber stresses at the interior and exterior transverse surfaces of both the slab and girder stem elements along the boundary of the transverse section are included in the case studies presented in this section. The plots show the influences of variations in slab and girder thickness on these fiber stresses. Because the two applied loads are based on temperature gradients that are fairly diverse, there is little comparison between the resultant fiber stresses.

The analysis assumes linearly elastic material and uncracked section properties.

Case 1T—Columbia River Bridge (9 Ft Depth)

Selection

This structure was included in the case studies because of the varying cross-sectional dimensions of the superstructure. The 9-ft deep section at midspan that is considered in this case has slab and girder dimensions that are representative of most box girders being constructed. A temperature gradient of ±15°F (8.3°C) was used for the design of this bridge (see Appendix D).

Description

This structure, which is the same structure studied in Case 7L, was investigated for transverse temperature effects at the midspan cross section. This cross section, shown in Figure 46, has a transversely prestressed concrete deck slab with a depth-to-span ratio of 0.056. The slab varies in thickness, as is typical for a single-cell box girder section of this type. The slab on this 63-ft 3-in. wide superstructure spans nearly 30 ft between girders and cantilevers over 16 ft at the overhangs. The sloping girder stems are prestressed vertically and the variable thickness bottom slab is conventionally reinforced.

Designers frequently consider some type of thermal gradient load when designing an optimized cross section such as this.

Results

Figures 47 and 48 are plots of exterior and interior fiber stresses, respectively, in the slab and girder stem elements located along the boundary of the transverse section. The shapes

Table 6. Summary of bridges included in case studies for transverse temperature effects.

CASE NO.	NAME/LOCATION	DECK SLAB	GIRDER WEBS	TRANSVERSE DIRECTION			DEPTH/SPAN RATIO	NO. BAYS	COMMENT
				EXTERIOR GIRDER	WIDTH	DEPTH			
8	Columbia River Bridge (9-ft depth) Washington	Cast-in-place prestressed haunched slab	Prestressed vertically	Sloping	63 ft–3 in.	9 ft–0 in.	0.056	1	Average depth to width proportions
9	Columbia River Bridge (24-ft depth) Washington	Cast-in-place prestressed haunched slab	Prestressed vertically	Sloping	63 ft–3 in.	24 ft–0 in.	0.056	1	Deep and narrow proportions
10	Hamilton Street Bridge Washington	Cast-in-place prestressed haunched slab	Conventionally reinforced	Vertical	78 ft–0 in.	7 ft–0 in.	0.069	3	Shallow and wide proportions

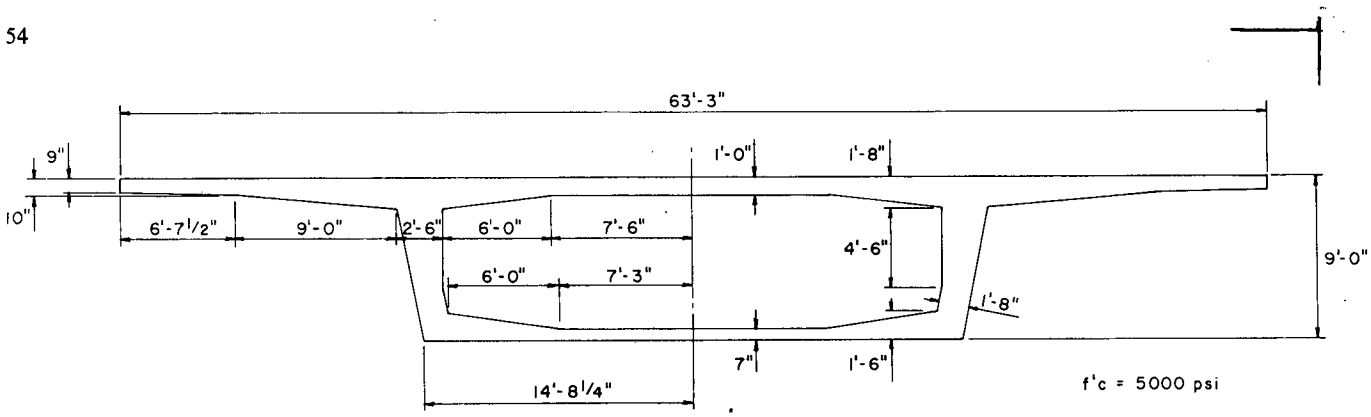

Figure 46. Case 1T—Columbia River Bridge (9 ft depth) superstructure cross-section details used for analysis.

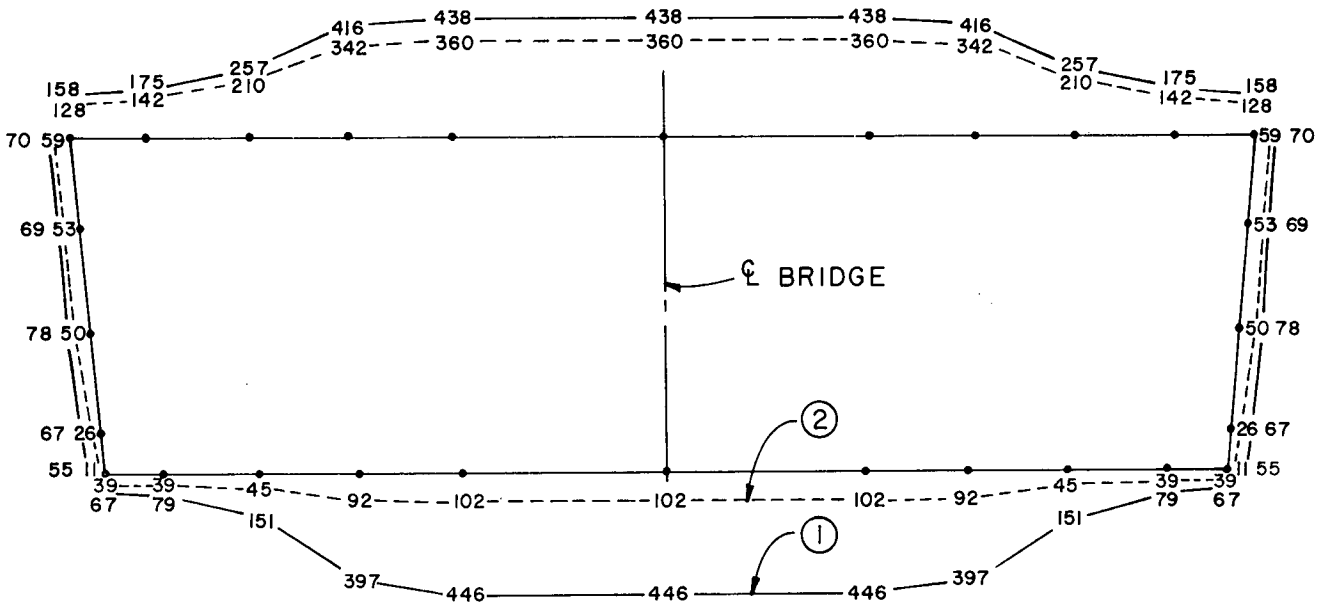

Figure 47. Case 1T—Columbia River Bridge exterior fiber stresses (PSI) at the 9-ft depth section.

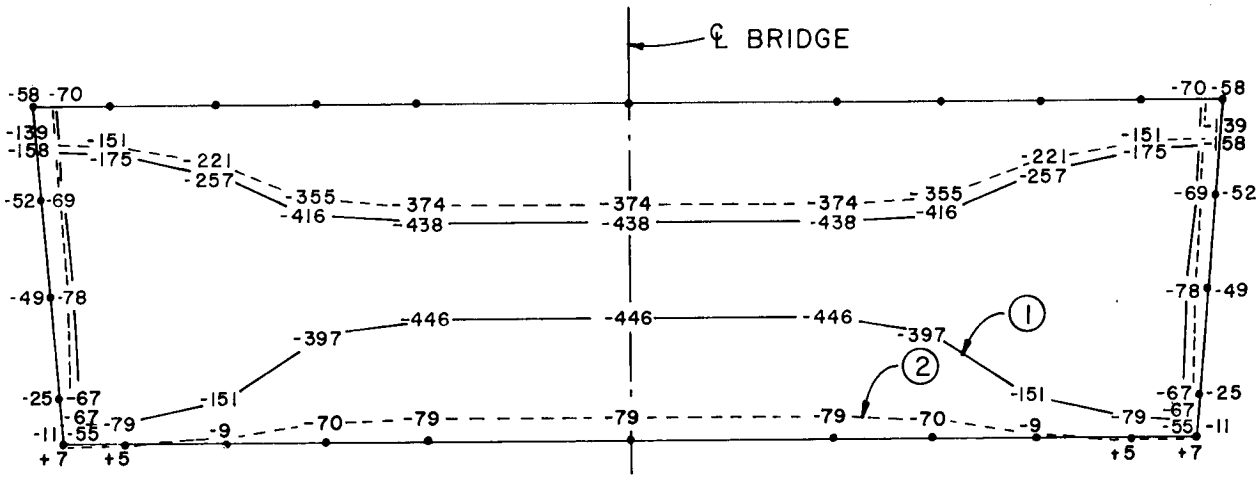

LEGEND

① 27°F GRADIENT

② NEW ZEALAND

Figure 48. Case 1T—Columbia River Bridge interior fiber stresses (PSI) at the 9-ft depth section.

of the fiber stress plots are similar for both load cases. The maximum stresses occur at the thinnest sections of the top and bottom slabs (midspan), while the minimum stresses occur in the girder stems. The largest difference in the magnitude of stresses resulting from these two loadings occurs in the bottom slab.

The cracking that will probably occur in the reinforced concrete bottom slab will substantially reduce the thermal stresses at this location. Smaller stress reductions due to this cracking will also result in the prestressed webs and top slab.

Case 2T—Columbia River Bridge (24 Ft Depth)

Selection

This cross section of the Columbia River Bridge was also considered because of the rather massive slab and girder sections. Particular attention was given to the design of these sections because of the higher thermal stresses caused by the stiffer massive sections connected rigidly to the piers.

Description

This structure, which was investigated in Case 1T for transverse temperature effects at midspan, is investigated here for similar effects at the ends of the span. A cross section from one of the identical ends of the span, shown in Figure 49, has a transversely prestressed concrete deck slab identical in design to the slab at midspan. The sloping webs, which are 24 ft deep at the ends of the span, are prestressed in the direction of the slope. The bottom slab, which is 3 ft 6 in. deep to accommodate compressive stress, is conventionally reinforced.

Results

The effects of the two temperature gradients on the deformations of this cross section are shown in Figures 50 and 51. Figure 50 shows the cross-section deformations caused by the temperature gradient used by New Zealand. The deformation caused by the 27°F linear temperature differential between exterior and interior fibers is shown in Figure 51. In both cases the top slab deflects downward contrary to what would be expected from a positive temperature gradient. This phenomenon can be explained by the overwhelming influence of the relatively stiff bottom slab. When curvatures are induced in the bottom slab due to temperature gradients, the top slab will deflect downward. Even though the positive temperature differentials in the deck slab will tend to cause upward deflection, it is not sufficient to overcome the downward deflection induced by bottom slab curvatures. Therefore, there will be a net downward deflection in the deck slab.

Figures 52 and 53 are plots of exterior and interior fiber stresses, respectively, in the slab and girder stem elements located along the boundary of the transverse section. The shapes of the fiber stress plots for the two load cases are different. The difference occurs mainly in the webs. The change in the web thickness near the top slab appears to have had a significant effect on the stresses produced by the 27°F temperature gradient.

The top-slab stresses are similar in shape and magnitude to those found in Case 1T, indicating that the top slab stresses are not greatly affected by the webs and bottom slab.

The high web stresses resulting from the 27°F temperature gradient appear to be caused by the massive bottom slab. Any flexural cracking in the reinforced concrete bottom slab would greatly relieve these web stresses.

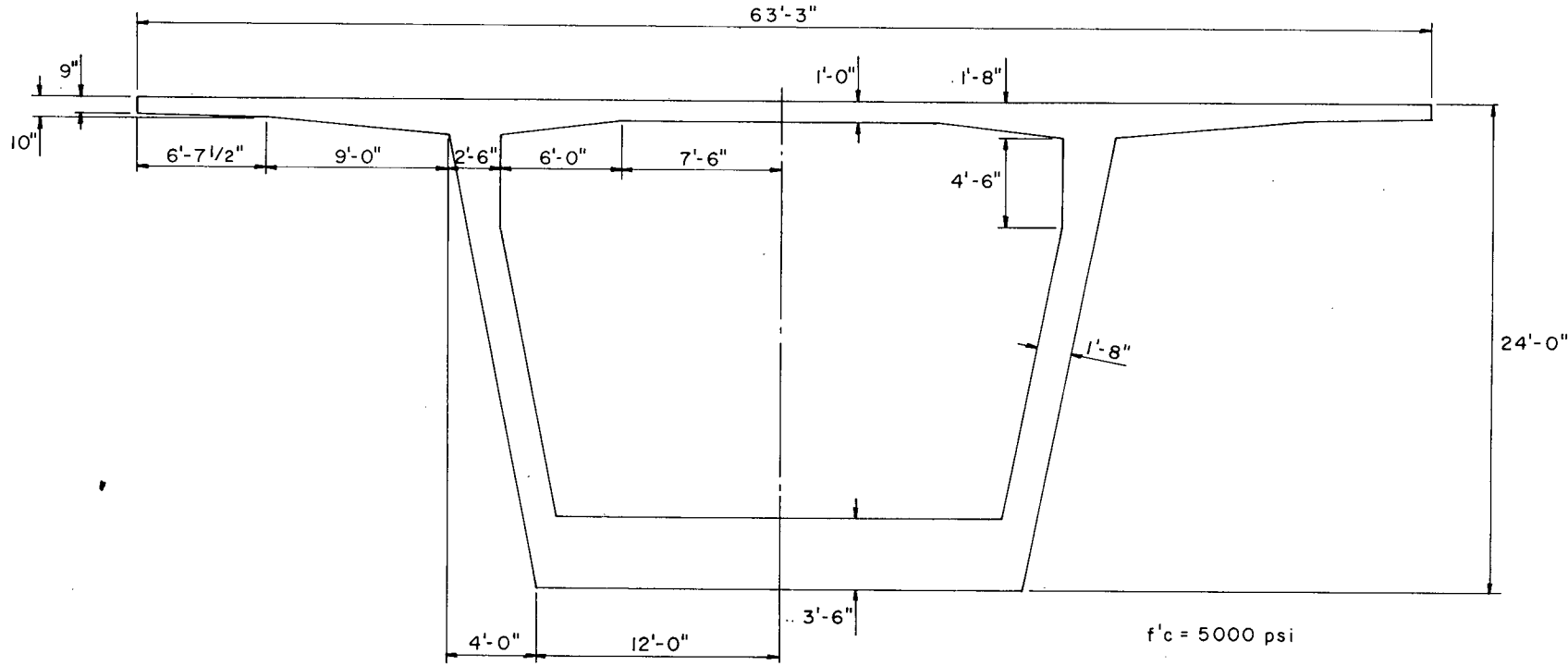

Figure 49. Case 2T—Columbia River Bridge (24-ft depth) superstructure cross-section details used for analysis.

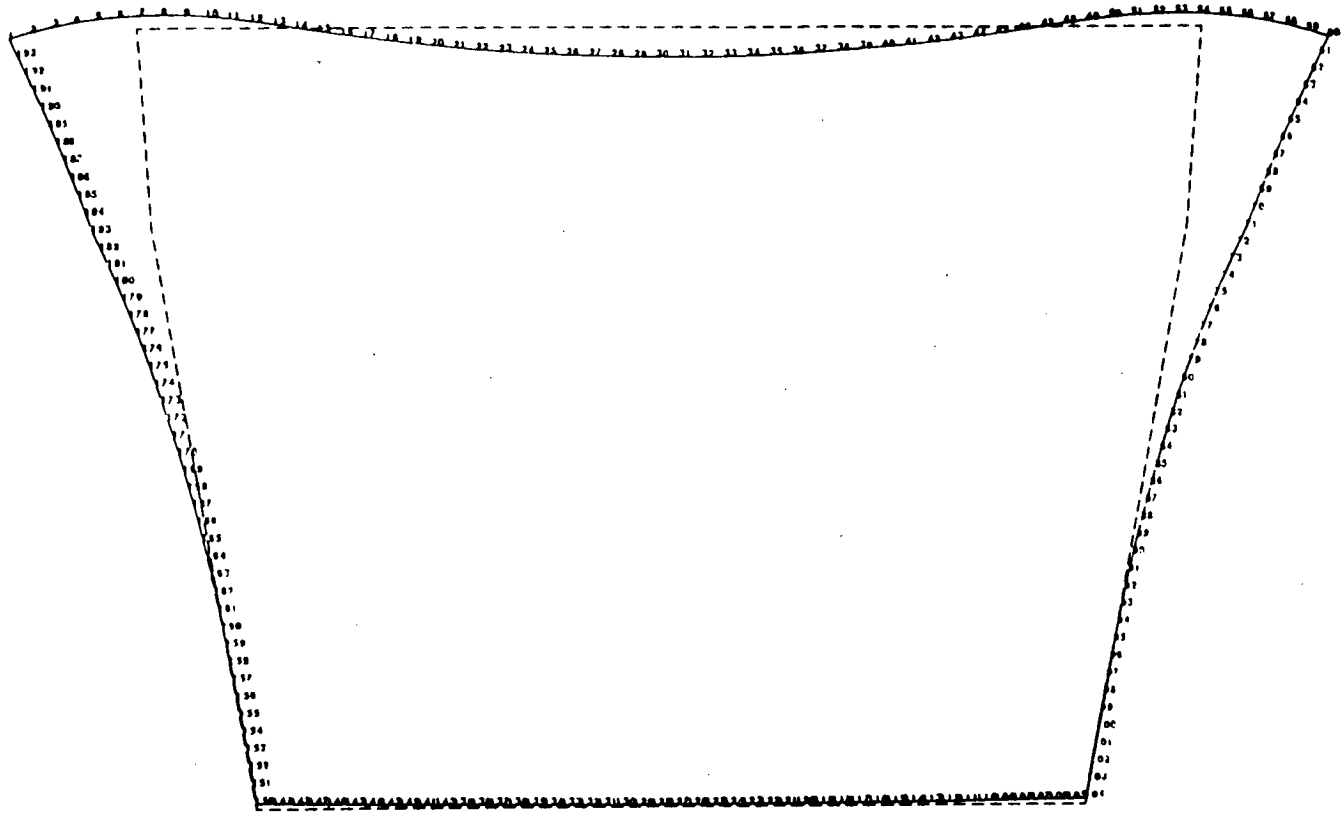

Figure 50. Case 2T—Columbia River Bridge deformations at the 24-ft deep cross section due to the New Zealand temperature gradient.

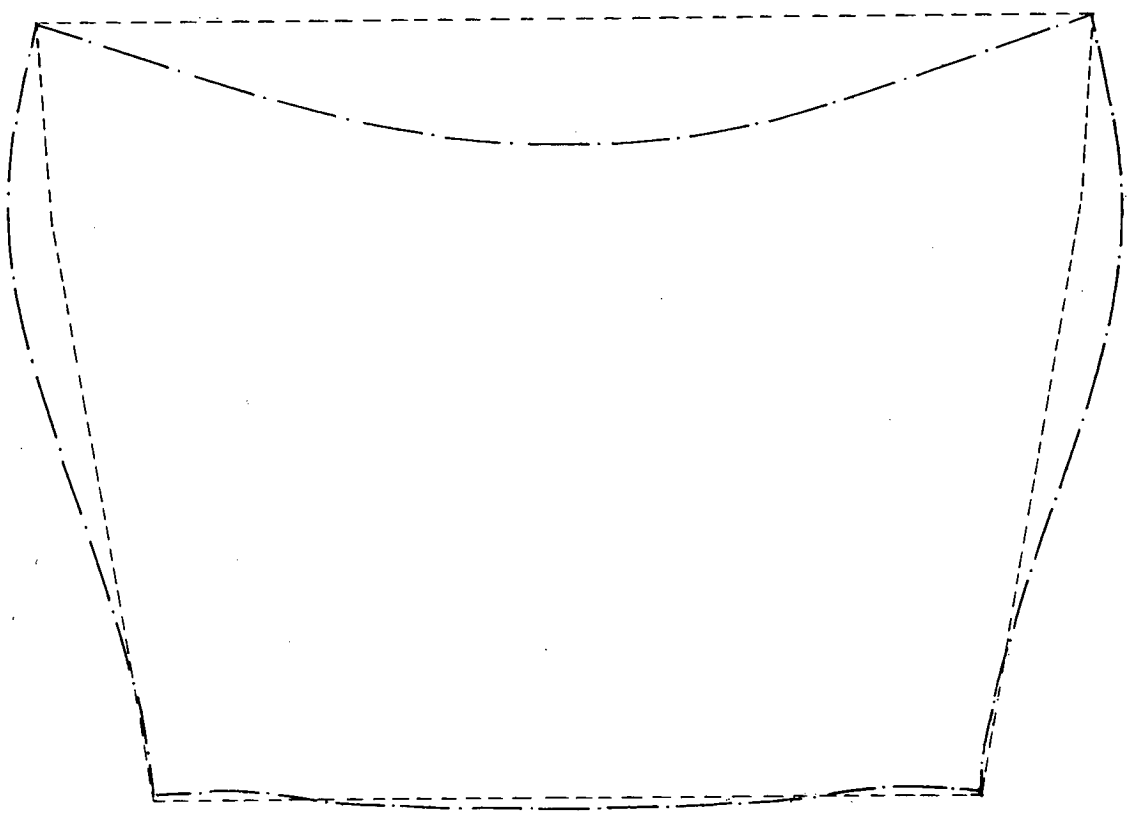

Figure 51. Case 2T—Columbia River Bridge deformations at the 24-ft deep cross section due to a 27°F linear temperature gradient (PTI/PCI) in the members.

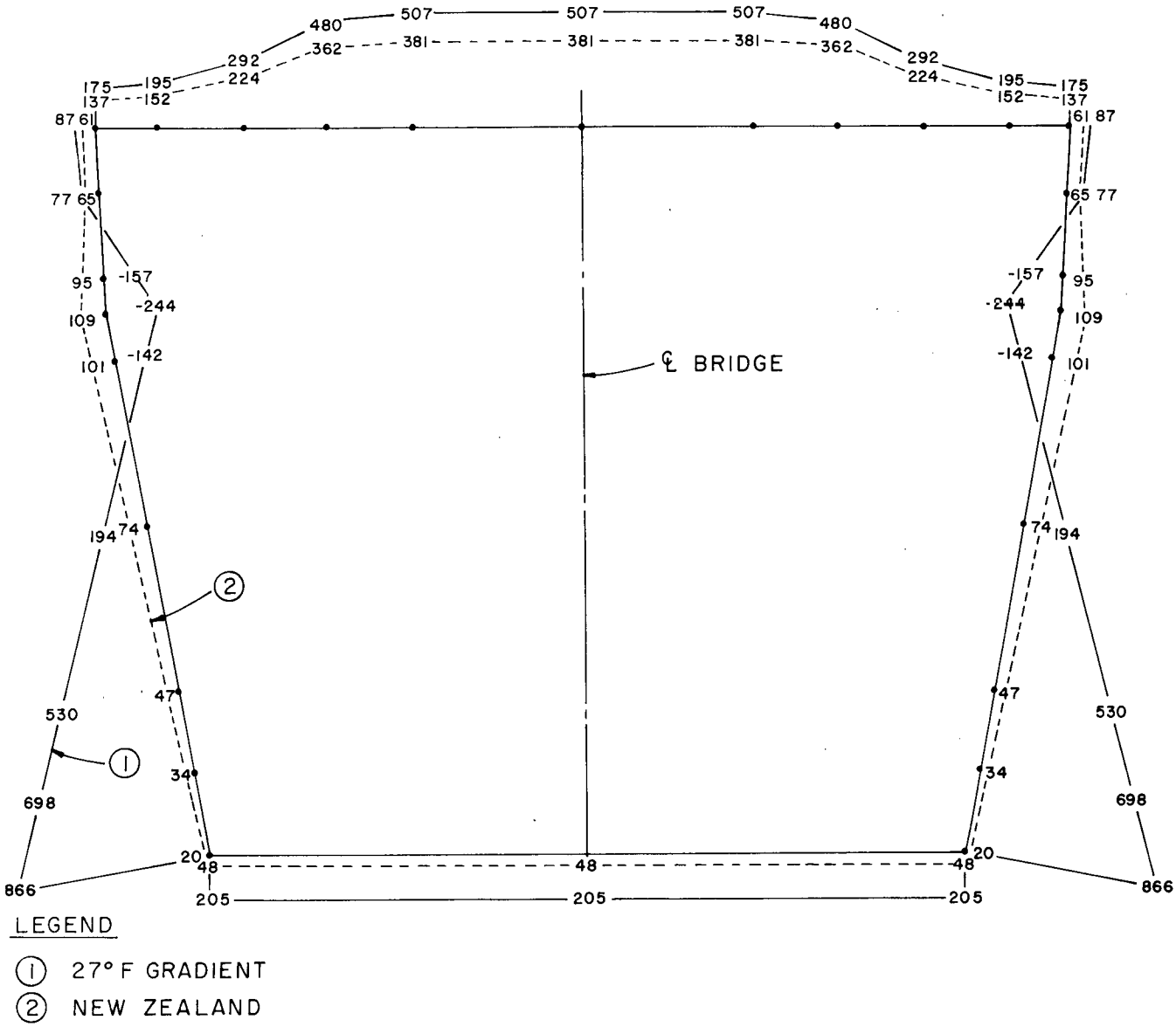

Figure 52. Case 2T—Columbia River Bridge exterior fiber stresses (PSI) at the 24-ft depth section.

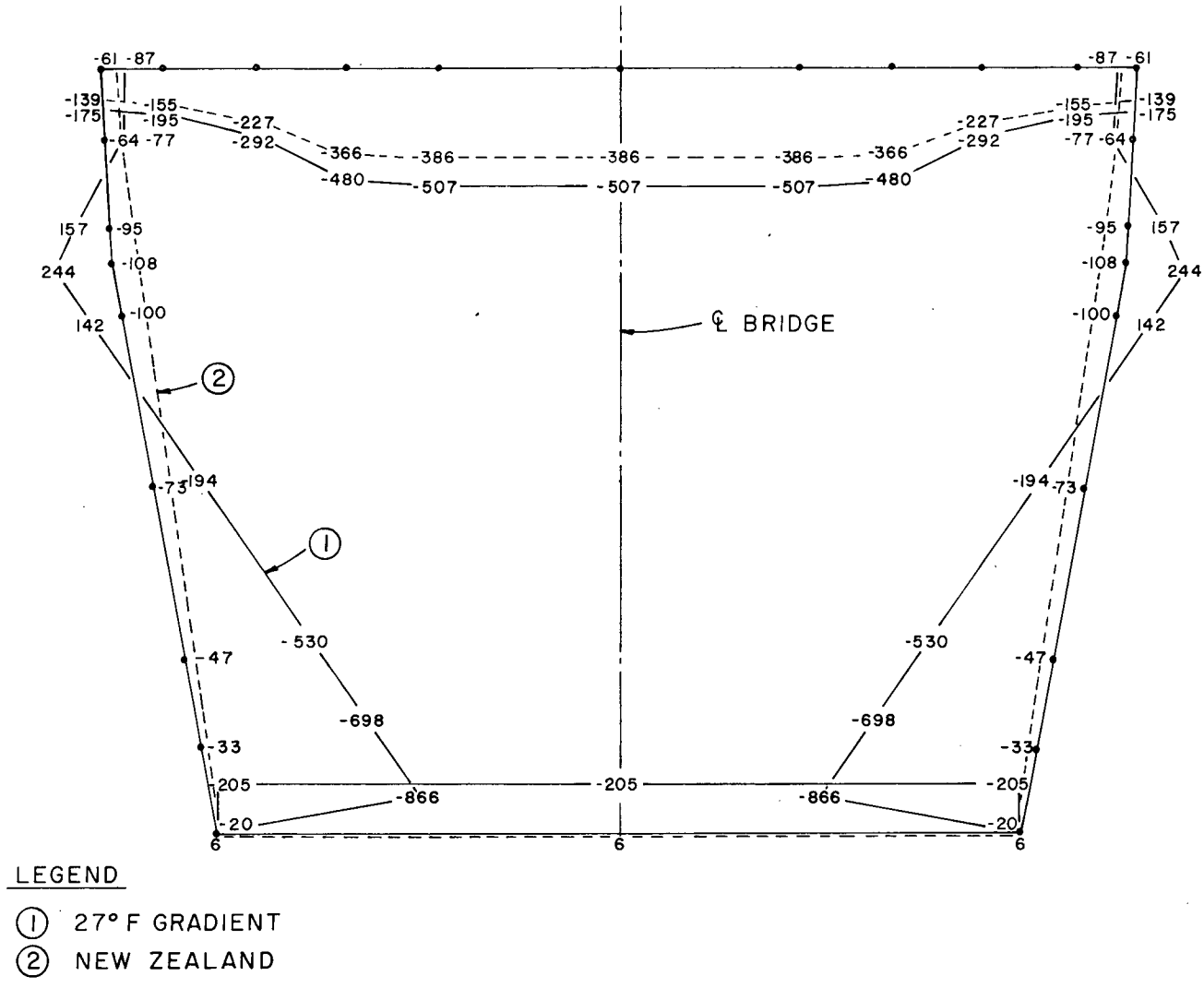

Figure 53. Case 2T—Columbia River Bridge interior fiber stresses (PSI) at the 24-ft depth section.

Case 3T—Hamilton Street Bridge

Selection

This structure was selected because it has a somewhat unusual cross section in that the girders are widely spaced. This superstructure was designed for a transverse gradient of ±15°F (8.3°C) between the inside and outside surfaces of the box section. Frequently designers do consider a thermal gradient load of some type when designing an optimized cross section such as this.

Description

This structure, shown schematically in Figure 54, is a ten-span, 1,467-ft-long bridge. The cross section has a transversely prestressed concrete deck slab with a depth-to-span ratio of 0.069. The slab varies in thickness over the girder webs and has spans measuring approximately 19 ft between girders. Both the vertical girder stems and the variable-thickness bottom slab are constructed of conventionally reinforced concrete.

Results

Figures 55 and 56 are plots of exterior and interior fiber stresses, respectively, in the slab and girder stem elements along the boundary of the transverse section. The shapes of the fiber stress plots for the two load cases are different, except for the top and bottom slabs at the interior cell. Although the fiber stress plots are linear at the constant-thickness webs, they show that the increase in the thickness of the slabs at the girders causes the stresses in the slabs to be moderately magnified. Any flexural cracking in the reinforced concrete webs and bottom slab would greatly relieve the fiber stresses shown. However, that cracking would probably not significantly affect the stresses in the prestressed top slab.

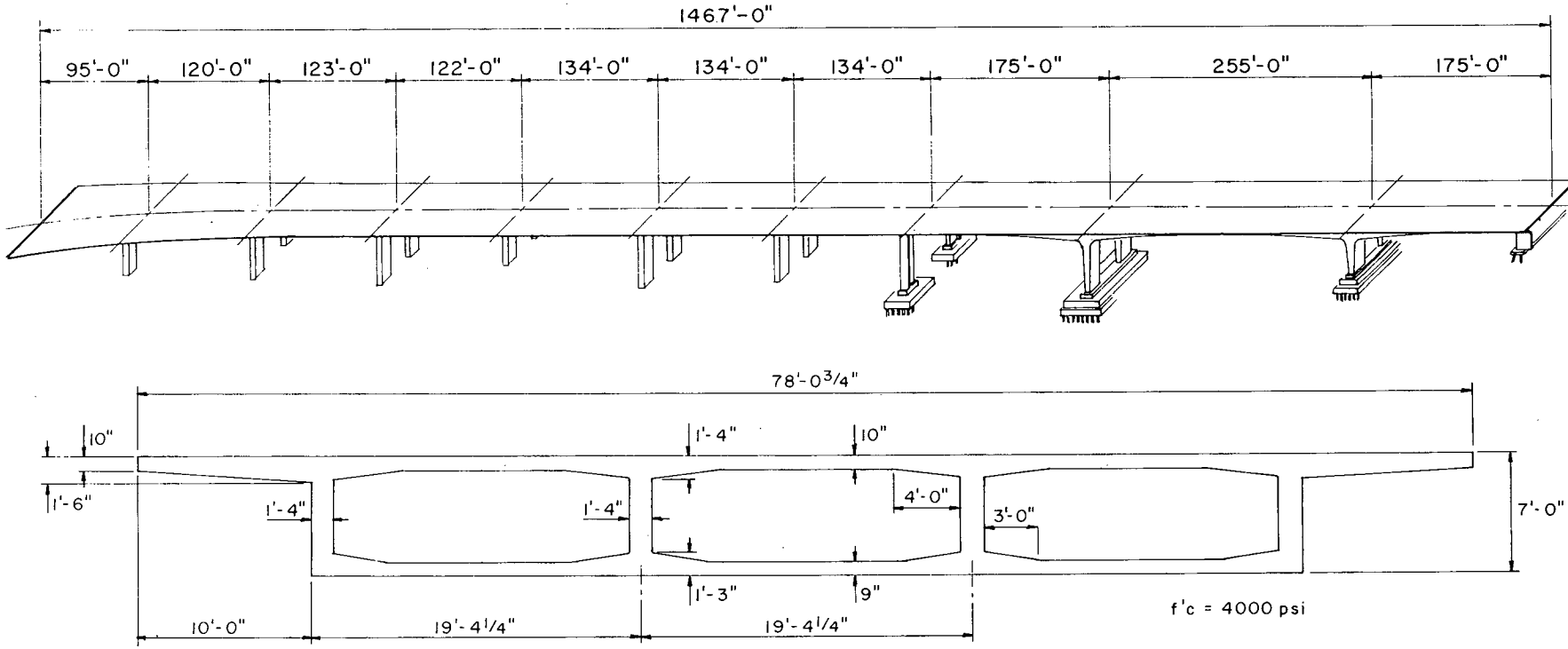

Figure 54. Case 3T—Hamilton Street Bridge superstructure cross-section details used for analysis.

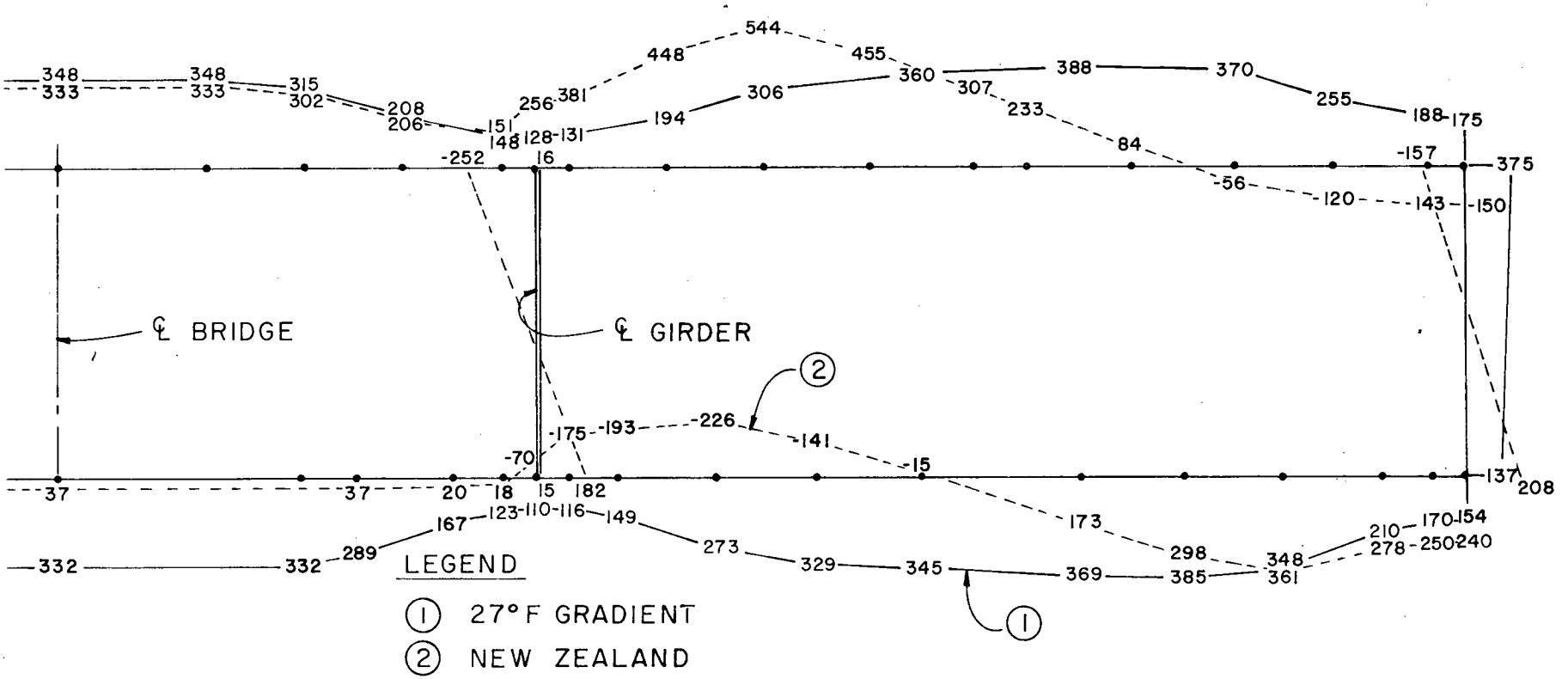

Figure 55. Case 3T—Hamilton Street Bridge exterior fiber stresses (PSI).

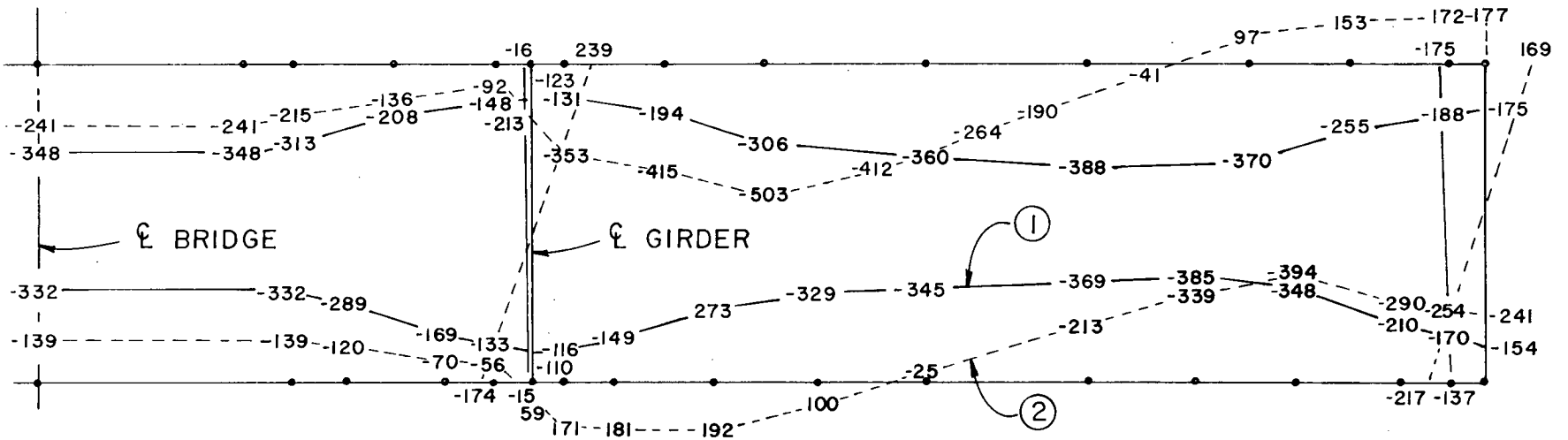

Figure 56. Case 3T—Hamilton Street Bridge interior fiber stresses (PSI).

CONCLUSIONS AND RECOMMENDATIONS

CONCLUSIONS

Chapter Five described several case studies that were conducted to investigate the effect of various assumed thermal gradients on the longitudinal and transverse fiber stresses induced in various types of concrete bridge superstructures. Several conclusions concerning the nature of thermal effects on concrete bridges can be drawn from an assessment of the results of these case studies.

These conclusions are as follows:

1. Although fiber stresses induced in different bridges by any single thermal gradient may vary in magnitude, the stress patterns are generally similar.
2. Changes in cross section have a significant effect on the fiber stresses induced by thermal gradients. In the longitudinal direction, cross-section changes usually consist of haunched girders or flares in the bottom slab. Large variation in girder depth can increase fiber stresses significantly. In the transverse direction, large differences in the transverse stiffness of the cross-section elements will also have a large effect.
3. The calculated fiber stresses were very sensitive to the type of temperature gradient assumed. While some gradients produced similar extreme stresses, the differences in fiber stresses between the extreme fibers were significant. In most cases, this difference was sufficient to affect the requirements for longitudinal reinforcement. This was the case even in the bridges with shorter span lengths. This could be a contributing factor in some cases where concrete cracking has been observed.
4. In the transverse direction a temperature difference can result in transverse stresses significantly different from when such a temperature difference is ignored. These stresses can be realistically predicted by assuming a mean effective temperature in the top deck slab that is greater than the mean temperatures in the remainder of the cross section.
5. Temperature gradients can have a significant effect on the redistribution of falsework loads. Falsework designers should be aware of this fact, especially in light of the falsework failure in New Zealand that is attributed to temperature effects.

RECOMMENDED DESIGN APPROACH FOR THERMAL EFFECTS

Based on the results from the case studies and a review of the design approaches used in other countries, it is apparent that U.S. bridge design requirements should be expanded to include the effects of a thermal gradient. Use of the current AASHTO procedures for considering longitudinal movement, although not based on precise temperature data, has resulted in very few temperature-related problems in concrete bridges even though thermal gradients are often ignored. This may be the case because the current AASHTO criteria for axial temperature effects are too conservative. Therefore, it would also be desirable to include a more accurate method for determining seasonal variations in temperature and the effect of aggregate type and curing methods. The proposed design guidelines, included in Appendix A, were written in light of these observations.

NEED FOR FUTURE RESEARCH

Although research to date has determined the magnitude of temperature differentials in bridge superstructures, the effect of these differentials has not been clearly established. The stresses that would be theoretically developed in a bridge by the observed temperature gradients are inconsistent with the observed performance of these bridges in many cases. There are only a few instances of distress caused by a thermal gradient in bridge superstructures. When distress does exist, it is often in conjunction with other contributing factors, and therefore the relative importance of the thermal effect is not always clear. This fact has led to considerable skepticism among bridge engineers as to the accuracy of, and need for, elaborate thermal design procedures. This is a primary reason why a guide specification is recommended rather than a modification of the AASHTO design specifications.

Field measurements of differential temperatures and thermal stresses through the sections of prestressed concrete box girder bridges clearly indicate significant differences that should be recognized and possibly addressed by the designers of such structures. Heretofore these effects have usually not been considered. The lack of problems is not necessarily indicative of adequate design procedures.

It is possible that bridge structures may have some inherent strength not currently recognized or temperature-induced stresses may not be as high as theoretically predicted. Because most temperature effects result in serviceability problems that do not affect the structural strength of the bridge, more information on the effect of thermal gradients is needed before designers will be totally convinced of the need for elaborate design procedures. Even though very little temperature distress has been observed due to a temperature gradient, the increased use of optimum cross sections in long superstructures makes it imperative to develop accurate methods for considering temperature differentials in the superstructure. Future research should be directed toward this goal.

REFERENCES AND BIBLIOGRAPHY

DESIGN CODES AND PRACTICES

1. *Standard Specifications for Highway Bridges.* 12th ed., American Association of State Highway and Transportation Officials, Washington, D.C. (1977) 496 pp.
2. *Ontario Highway Bridge Design Code and Commentary.* Ontario Ministry of Transportation and Communications, Ontario, Canada (1979).
3. ACI Committee 349. "Reinforced Concrete Design for Thermal Effects on Nuclear Power Plant Structures." *ACI J.*, No. 6, *Proc. V.* 77 (Nov.–Dec. 1980) pp. 399–428.
4. "Thermal Expansion and Contraction." *Tennessee Structures Memorandum-045, SM045-01/07,* Bureau of Highways, Tennessee Dept. of Transportation (Feb. 1982) 5 pp.
5. *Proposal for Design and Load Regulations for Highway Bridges.* Danish Ministry of Transport (Oct. 1977) 20 pp.
6. *NAASRA Bridge Design Specification.* 5th ed., National Association of Australian State Road Authorities (1976) 26 pp.
7. *Specifications for Highway Bridges.*, Japan Road Association Tokyo, Japan (1976) pp. 1–18.
8. State of Washington, Department of Transportation, "Thermal Effects of Design Criteria for the Yakima River Bridges and the Hamilton Street Bridges." NCHRP Project 12-22, FY '81 (Revised Feb. 22, 1982).
9. MENTES, G. A., BHAT, P. D., RANNI, A. I., PAJUHESH, J., and COMMITTEE. "Reinforced Concrete Design for Thermal Effects on Nuclear Power Plant Structures—Discussion." *ACI J.* (Sept.–Oct. 1981) pp. 406–407.
10. "Italian Bridge Design Regulations for Concrete Bridges." Rome, Italy (1980).
11. "Actions Uniforme de la Temparature: Gradient Thermique." (Summary of rules for temperature actions in a bridge) Bagneux, France (1982).
12. BRITISH STANDARDS INSTITUTION, "Steel, Concrete and Composite Bridges, Part I, General Statement." *British Standard BS 5400* Crowthorne, Berkshire, England (1978) 43 pp.
13. *DIN 1072* (German Bridge Design Code). (Nov. 1967).
14. SMITH, A. W., "The Newmarket Viaduct—Part 2: Design Investigations and Specification." *New Zealand Engineering* (Dec. 1965) pp. 498–503.
15. *Precast Segmental Box Girder Bridge Manual.* Post Tensioning Institute and Prestressed Concrete Institute (1978) 116 pp.

PROPOSED DESIGN CODE AND PRACTICES

16. PRIESTLEY, M. J. N., and BUCKLE, I. G., "Ambient Thermal Response of Concrete Bridges." *Road Research Unit Bulletin 42,* Bridge Seminar, 1978, Vol. 2, Road Research Unit, National Roads Board, Wellington, New Zealand, ISSN 0549-0030 (1979) 83 pp.
17. Committee on Loads and Forces on Bridges of the Committee on Bridges, Structural Divsion, "Recommended Design Loads for Bridges." *J. Structural Division,* No. ST7 (July 1981) pp. 1161–1212.
18. CHURCHWARD, A. J., and SOKEL, Y. J., Thermal Responses in Concrete Bridges, Brisbane." *ARRB Proc.,* Vol. 10, Part 3 (1980) pp. 87–93.
19. BRIDGE CONSTRUCTION DIVISION, Structures Department of TRLL, "Bridge Temperatures." *TRLL Supplementary Report 442,* Proceedings of Symposium held at Transport and Road Research Laboratory, Department of the Environment, Department of Transport, Crowthorne, Berkshire, England, ISSN 0305-1315 (Oct. 5, 1977) 5 pp.
20. WHITE, I. G., "Non-Linear Differential Temperature Distributions in Concrete Bridge Structures: A Review of the Current Literature." *Technical Report 525,* Cement and Concrete Association (May 1979) 23 pp.
21. EMERSON, M., "Temperature differences in Bridges: Basis of Design Requirements." *TRRL Laboratory Report 765,* Department of the Environment, Department of Transport, Crowthorne, Berkshire, England, ISSN 0305-1293 (1977) 39 pp.
22. PAJUHESH, J., "Design of Concrete Structures for Thermal Effects." *ACI J.* (Mar.–Apr. 1980) pp. 74–77.
23. RADOLLI, M., and GREEN, R., "Thermal Stress Analysis of Concrete Bridge Superstructures." *Transportation Research Record 607,* Transportation Research Board (1976) pp. 7–13.
24. SINDEL, J. A., "A Design Procedure for Post-Tensioned Concrete Pavements." *Concrete International* (Feb. 1983) pp. 51–57.

IN-SITU THERMAL MEASUREMENTS (AXIAL EFFECTS, RESEARCH FINDINGS, PROPOSED RESEARCH)

25. BURDETTE, E. G., and GOODPASTURE, D. W., "Thermal Movements of Continuous Concrete and Steel Structures." *Research Project No. 77-27-2,* Research Proposal to Tennessee Department of Transportation, Department of Civil Engineering, University of Tennessee (Feb. 1978) 17 pp.
26. MORTLOCK, J. D., "The Instrumentation of Bridges for the Measurement of Temperature and Movement." *TRRL Laboratory Report 641,* Department of the Environment, Crowthorne, Berkshire, England (1974) 53 pp.
27. BLACK, W., MOSS, D. S., and EMERSON, M., "Bridge Temperatures Derived from Measurements of Movement." *TRRL Laboratory Report 748,* Department of the Environment, Crowthorne, Bershire, England, ISSN 0305-1293 (1976) 35 pp.
28. ABDUL-AHAD, R. B., "Effects of Restrained Thermal Movement in a Continuous, Prestressed Concrete Bridge Without Interior Expansion Joints." Ph.D. Dissertation, University of Tennessee (June 1981) 147 pp.
29. "Thermal Movements of Continuous Concrete and Steel Structures." *Research Project No. 77-27-2,* Final Report, Tennessee Department of Transportation (Jan. 1982) 114 pp.

30. HOUDESHELL, D. M., ANDERSON, T. C., and GAMBLE, W. L., "Field Investigation of a Prestressed Concrete Highway Bridge Located in Douglas County, Illinois." Project IHR-93, Documentation Report to State of Illinois Division of Highways, The Structural Research Laboratory, Dept. of Civil Engineering, University of Illinois (Feb. 1972) 64 pp.
31. EMANUEL, J. H., and WISCH, J., "Thermal Stresses Induced in a Composite Model Bridge Structure." Study 75-2, Missouri Cooperative Highway Research Program, Final Report to Missouri State Highway Department, Civil Engineering Department, University of Missouri-Rolla (Aug. 1977) 141 pp.
32. WILLEMS, N., "Experimental Strain Analysis of Continuous Skew Slab Bridge Decks." *Report No. HPR-SCH 71-3-F,* Draft Final Report to State Highway Commission of Kansas, University of Kansas, Center for Research, Inc. (Aug. 1973) 19 pp.
33. WHITE, I. G., and BELCHER, R. D., "Tests to Determine the Magnitude of Temperature Induced Moments in Concrete Structures." Design Research Department, Cement and Concrete Association (Nov. 1980) 16 pp.
34. STEWART, C. F., "Long Structures Without Expansion Joints." Interim Report, California Department of Transportation (June 1967) 10 pp.
35. STEWART, C. F., "Annual Movement Study of Bridge Deck Expansion Joints." Final Report, Bridge Department, Division of Highways, State of California (June 1969) 52 pp.
36. DILLON, E. W., and KISSANE, R. J., "Annual End Movements of Prestressed Concrete Bridges." *Research Report 66,* Final Report, Engineering Research and Development Bureau, New York State Department of Transportation (Oct. 1978) 22 pp.
37. SHIU, K. N., and RUSSELL, H. G., "Instrumentation of Linn Cove Viaduct." FHWA Contract No. DTFH61-80-C-00112, Interim Report to Teng and Associates, Construction Technology Laboratories, Portland Cement Association, Skokie, Illinois (Aug. 1981) 30 pp.

IN-SITU THERMAL GRADIENTS (RESEARCH FINDINGS, PROPOSED RESEARCH)

38. SHIU, K. N., and RUSSELL, J. G., "Instrumentation of Linn Cove Viaduct," FHWA Contract No. DTFH61-80-C-00112, Interim Report to Teng and Associates, Construction Technology Laboratories, Portland Cement Association, Skokie, Illinois (Aug. 1981) 30 pp.
39. THURSTON, S. J., and POTTER, S. M., Measurements of Thermal Crack Widths in a Continuous Prestressed Concrete Bridge." *Central Laboratories Report No. 5-79/10,* Ministry of Works and Development, Gracefield, Lower Hutt, New Zealand (Nov. 1979) 30 pp.
40. WANDERS, S. P., WINSLOW, D. A., and SUTTON, C. D., "Study of the Segmental Box Girder Bridge at Turkey Run: Construction, Instrumentation and Data Collection." Project No. C-36-56T, Interium Report to Indiana State Highway Commission and FHWA, Purdue University (Dec. 17, 1979) 175 pp.
41. CLARK, J. H., and HAWKINS, N. M., "Thermal, Live Load, Creep and Shrinkage Deformations and Stresses in the Denny Creek Bridge." Proposal to the Washington State Department of Transportation (Sept. 1980) 17 pp.
42. EMERSON, M., "Steel Box Bridge Temperatures in Australia and the United Kingdom." *TRRL Supplementary Report 611,* Department of the Environment, Department of Transport, Crowthorne, Berkshire, England, ISSN 0305-1315 (1980) 26 pp.
43. EMERSON, M., "Bridge Temperatures Estimated from the Shade Temperature." *TRRL Laboratory Report 696,* Department of the Environment, Crowthorne, Berkshire, England, ISSN 0305-1293 (1976) 50 pp.
44. EMERSON, M., "Temperatures in Bridges During the Hot Summer of 1976." *TRRL Laboratory Report 783,* Department of the Environment, Department of Transport, Crowthorne, Berkshire, England, ISSN 0305-1293 (1977) 31 pp.
45. EMERSON, M., "Temperatures in Bridges During the Cold Winter of 1978/1979." *TRRL Laboratory Report 926,* Department of the Environment, Department of Transport, Crowthorne, Berkshire, England, ISSN 0305-1293 (1980) 31 pp.
46. SHIU, K. N., DANIEL, J. I., and RUSSEL, H. G., "Time-Dependent Behavior of Segmental Cantilever Concrete Bridges: Progress Report 1978–80 (Kishwaukee River Bridge)." Construction Technology Laboratories, Portland Cement Association, Skokie, Illinois (Dec. 1980) 18 pp.
47. HOFFMAN, P. C., MCCLURE, R. M., and WEST, H. H., "Temperature Studies for an Experimental Segmental Bridge." *Report PTI 8010,* Interim Report to Pennsylvania Department of Transportation, Pennsylvania Transportation Institute, Pennsylvania State University (June 1980) 112 pp.
48. HIRST, M. J. S., "Solar Heating of Bridges." *Australian Road Research,* Vol. 11, No. 2 (June 1981) pp. 28–36.
49. RUSSELL, H. G., "What We Have Learned from Box-Girder Bridges." Paper given at Segmental Concrete Bridge Conference, Kansas City, Construction Technology Laboratories, Portland Cement Association, Skokie, Illinois (1982) 20 pp.
50. THURSTON, S. J., PRIESTLEY, M. J. N., and COOKE, N., "Influence of Cracking on Thermal Response of Reinforced Concrete Bridges." Submitted to ACI for Publication (Nov. 1982) 24 pp.
51. HIRST, M. J. S., "Thermal Loading of Concrete Bridges." International Conference on Short and Medium Span Bridges, Toronto, Canada, Canadian Society for Civil Engineering, *Proc.,* Vol. 1 (Aug. 1982) pp. 115–124.
52. ABDUL-AHAD, R. B., "Effects of Restrained Thermal Movement in a Continuous, Prestressed Concrete Bridge Without Interior Expansion Joints." Ph.D. Dissertation, University of Tennessee (June 1981) 147 pp.
53. "Thermal Movements of Continuous Concrete and Steel Structures." Research Project No. 77-27-2, Final Report, Tennessee Department of Transportation (Jan. 1982) 114 pp.
54. BURDETTE, E. G., and GOODPASTURE, D. W., "Thermal Movements of Continuous Concrete and Steel Structures." Research Project No. 77-27-2, Final Report, Tennessee Department of Transportation (Jan. 1982) 118 pp.
55. RADOLLI, M., and GREEN, R., "Thermal Stresses in Concrete Bridge Superstructures Under Summer Conditions." *Transportation Research Record 547,* Transportation Research Board (1975) pp. 23–36.

56. MAHER, D. R. H., "The Effects of Differential Temperature on Continuous Prestressed Concrete Bridges." *Civil Engineering Transaction,* Institute of Engineers of Australia, Vol. CE12, Part 1, Paper 1795 (April 1970) pp. 29–32.
57. PRIESTLEY, M. J. N., "Effects of Transverse Temperature Gradients on Bridges." *Report No. 394,* Ministry of Works, New Zealand (Sept. 1972).
58. PRIESTLEY, M. J. N., "Temperature Gradients in Bridges—Some Design Consideration." *New Zealand Engineering,* Vol. 27, Part 7 (July 1972) pp. 228–233.
59. PRICE, W. I. J., "Discussion on Paper Entitled Medway Bridge Design by O. A. Kerensky and G. Little and Medway Bridge Construction by M. F. Hansen and J. A. Dunster." Institution of Civil Engineers, *Proc.*, Vol. 31 (June 1965) pp. 162–166.
60. PRIESTLEY, M. J. N., "Linear Heat-Flow and Thermal Stress Analysis of Concrete Bridge Decks." *Research Report No. 76/3*, University of Canterbury, Department of Engineering, Christchurch, New Zealand (Feb. 1976).
61. PRIESTLEY, M. J. N., "Design Thermal Gradients for Concrete Bridges." *New Zealand Engineering,* Vol. 31, Part 9 (Sept. 1976) pp. 213–219.
62. NAROUKA, M., HIRAI, I., and YAMAGUTI, T., "Measurement of the Temperature of the Interior of the Reinforced Concrete Slab of the Shigita Bridge and Presumption of Thermal Stress." Symposium of the Stress Measurements for Bridge and Structures, Japanese Society for the Promotion of Science, *Proc.*, Tokyo, Japan (1957) pp. 106–115.
63. BARBER, E. S., "Calculation of Maximum Pavement Temperatures from Weather Reports." *Highway Research Board Bulletin 168* (1957) pp. 1–8.
64. Zuk, W., "Thermal and Shrinkage Stresses in Composite Beams." *ACI J.,* Vol. 58, No. 3 (Sept. 1961) pp. 327–340.
65. LIU, Y. N., and ZUK, W., "Thermoelastic Effects in Prestressed Flexural Members." *PCI J.*, Vol. 8, No. 3 (June 1963) pp. 64–85.
66. WAH, T., and KIRKSEY, R. E., "Thermal Characteristics of Highway Bridges." *Report HR 12-4*, Final Report, Southwest Research Institute (July 1969).
67. ZUK, W., "Thermal Behavior of Composite Bridges—Insulated and Uninsulated." *Highway Research Record 76* (1965) pp. 231–253.
68. BUCKLE, I. G., "Seasonal Variations in the Thermal Response of a Concrete Box Girder Bridge." *Report No. 286,* Report to the National Roads Board, Department of Civil Engineering, University of Auckland, New Zealand (June 1982) 32 pp.
69. HOFFMAN, P. C., MCCLURE, R. M., and WEST, H. H., "Temperature Study of an Experimental Segmental Concrete Bridge." *PCI J.*, Vol. 26, No. 2 (Mar.–Apr. 1983) pp. 78–97.
70. ELBADRY, M. M., and GHALI, A., "Nonlinear Temperature Distribution and its Effects on Bridges." *IABSE Proc. P-66/83*, ISSN 0377-7278 (Aug. 1983) pp. 169–191.
71. SHIU, K. N., "Seasonal and Diurnal Behavior of Concrete Box-Girder Bridges." Construction Technology Laboratories, Portland Cement Association, Skokie, Illinois, 29 pp.
72. WROTH, C. P., "The Hammersmith Flyover—Site Measurements of Prestressing Losses and Temperature Movements." Institute of Civil Engineers, *Proc.,* Vol. 23 (Dec. 1962) pp. 601–624.
73. POTGIETER, I., and GAMBLE, W. L., "Response of Highway Bridges to Nonlinear Temperature Distributions." *Report No. FHWA/IL/UI-201*, Final Report, University of Illinois (April 1983) pp. 291.
74. BERWANGER, C., "Thermal Stresses in Composite." *J. Institute of Structural Engineers* (Apr. 1974).

TRANSVERSE TEMPERATURE EFFECTS

75. EMANUEL, J. H., and FILLA, M. J., "Transverse Thermal Response of a Composite Bridge." Report, University of Missouri-Rolla, 36 pp.

ANALYTICAL TECHNIQUES

76. FATTAL. S. G., REINHOLD, T. A., and ELLINGWOOD, B., "Analysis of Thermal Stresses in Internally Sealed Concrete Bridge Decks." *Report No. FHWA/RD-80/085*, Center for Building Technology, National Bureau of Standards (Apr. 1981) 116 pp.
77. RAHMAN, F., and GEORGE, K. P., "Thermal Stress Analysis of Continuous Skew Bridges." *J. Structural Division, ASCE*, Vol. 105, No. ST7 (July 1979) pp. 1525–1541.
78. THURSTON, S. J., PRIESTLEY, M. J. N., and COOKE, N., "Thermal Analysis of Thick Concrete Sections." *ACI J.*, No. 5, *Proc. V.* 77 (Sept.–Oct. 1980) pp. 347–357.
79. THURSTON, S. J., "Thermal Stresses in Concrete Structures." Ph.D. Dissertation, No. 78, 78-21, Department of Civil Engineering, University of Canterbury, Christchurch, New Zealand.
80. LEONHARDT, F., "Crack Control in Concrete Structures." *IABSE Surveys*, S-4/77, University of Stuttgart, Germany, 26 pp.
81. EMERSON, M., "Bridge Temperatures for Setting Bearings and Expansion Joints." *TRRL Supplementary Report 479*, Department of the Environment, Department of Transport, Crowthorne, Berkshire, England, ISSN 0305-1315 (1979) 18 pp.
82. EMERSON, M., "Bridge Temperatures in the Arabian Gulf: Theoretical Predictions." *TRRL Supplementary Report 495,* Department of the Environment, Department of Transport, Crowthorne, Berkshire, England, ISSN 0305-1315 (1979) 25 pp.
83. EMERSON, M., "The Calculation of the Distribution of Temperature in Bridges." *TRRL Laboratory Report 561,* Department of the Environment, Crowthorne, Berkshire, England (1973).
84. JONES, M. R., "Bridge Temperatures Calculated by a Computer Program." *TRRL Laboratory Report 702,* Department of the Environment, Crowthorne, Berkshire, England, ISSN 0305-1293 (1976) 42 pp.
85. EMERSON, M., "Extreme Values of Bridge Temperatures for Design Purposes." *TRRL Laboratory Report 744,* Department of the Environment, Crowthorne, Berkshire, England, ISSN 0305-1293 (1976) 50 pp.
86. JONES, M. R., "Calculated Deck Plate Temperatures for a Steel Box Bridge." *TRRL Laboratory Report 760*, Department of the Environment, Department of Transport,

Crowthorne, Berkshire, England, ISSN 0305-1293 (1977) 24 pp.

87. THEPCHATRI, T., JOHNSON, C. P., and MATLOCK, H., "Prediction of Temperature and Stresses in Highway Bridges by a Numerical Procedure Using Daily Weather Reports." *Research Report 23-1*, Interim Report to Texas State Department of Highways and Public Transportation, Center for Highway Research, University of Texas at Austin (Feb. 1977) 165 pp.
88. WILL, K. M., JOHNSON, C. P., and MATLOCK, H., "Analytical and Experimental Investigation of the Thermal Response of Highway Bridges." *Research Report 23-2*, Interim Report to Texas State Department of Highways and Public Transportation, Center for Highway Research, University of Texas at Austin (Feb. 1977) 148 pp.
89. YARGICOGLU, A., and JOHNSON, C. P., "Temperature Induced Stresses in Highway Bridges by Finite Element Analysis and Field Tests." *Research Report 23-3F*, Final Report to Texas State Department of Highways and Public Transportation, Center for Highway Research, University of Texas at Austin (July 1978) 196 pp.
90. ZICHNER, T., "Thermal Effects on Concrete Bridges." C. E. B. Enlarged Meeting—Commission 2—Pavia (Oct. 1981) pp. 292–313.
91. Emanuel, J. H., and HULSEY, J. L., "Thermal Stresses and Deformations in Nonprismatic Indeterminate Composite Bridges (Abridgement)." *Transportation Research Record 607* (1976) pp. 4–6.
92. DILGER, W. H., and GHALI, A., "Temperature Induced Stresses in Composite Box Girder Bridges." Final Report to The Department of Supplies and Services in Ottawa, Civil Engineering Consultants, Calgary, Alberta (Oct. 1980) 179 pp.
93. Chief Designing Engineer (Civil), "Differential Temperature Analysis." *CDP 806/A*, New Zealand Ministry of Works and Development, Wellington, New Zealand (Feb. 1974) 20 pp.
94. HAMBLY, E. C., "Temperature and Prestress Loading." Chap. 11 in *Bridge Deck Behavior*, John Wiley & Sons, Inc., New York (1976) pp. 187–194.
95. HOFFMAN, P. C., MCCLURE, R. M., and WEST, H. H., "Temperature Study of an Experimental Segmental Concrete Bridge." *PCI J.*, Vol. 26, No. 2 (Mar.–Apr. 1983) pp. 78–97.

MATERIALS

96. *Building Movements and Joints.* 1st ed. Portland Cement Association, Skokie, Illinois (1982) 64 pp.
97. *Concrete Manual.* 7th ed., U.S. Department of the Interior, Bureau of Reclamation.

METEOROLOGICAL

98. *Climatic Atlas of the United States.* U.S. Department of Commerce, Ashville, North Carolina (June 1968).
99. "Solar Radiation Energy Resource Atlas of the United States." *SERI/SP-642-1037*, Superintendent of Documents, U.S. Government Printing Office, Washington, D. C. (Oct. 1981) 167 pp.
100. DEPARTMENT OF WATER RESOURCES, "California Sunshine-Solar Radiation Data." *Bulletin 187*, Sacramento, California (Aug. 1978) 110 pp.
101. "Daily Normals of Temperature and Heating and Cooling Degree Day 1941-1970." *Climatography of the United States No. 84*, National Climatic Center, Ashville, N.C.

OTHER RELATED CATEGORIES

102. MOULTON, L. K., GANGARAO, H. V. S., and HALVORSEN, G. T., "Tolerable Bridge Movements." Paper Presented at the Sixth N. W. Bridge Engineers' Seminar, Boise, Idaho (Oct. 7, 1981) 55 pp.
103. ZUK, W., "Jointless Bridges." *FHWA/VA-81-23*, Interim Report to Virginia Department of Highways and Transportation, Virginia Highways and Transportation Research Council, University of Virginia (Nov. 1980) 15 pp.
104. MARSH, J. G., "ARRB Creep and Shrinkage Research; What Has Been Achieved and Where Do We Go from Here?" *ARRB Proc.*, Vol. 10, Part 3 (1980) pp. 267–273.
105. LEONHARDT, F., KOLBE, G., and PETER, J., "Temperaturunterschiede gefahrden Spannbetonbrucke." *Beton-und Stahlbetonbau*, Vol. 60, No. 7, Berlin (July 1965) pp. 157–163.
106. MARSHALL, V., and GAMBLE, W. L., "Time-Dependent Deformations in Segmental Prestressed Concrete Bridges." *Report UILU-ENG-81-2014 SRS-495*, Interim Report to Illinois Department of Transportation, Illinois Cooperative Highway and Transportation Research Program, Phase 3, University of Illinois (Oct. 1981) 251 pp.
107. STRATTON, F. W., ALEXANDER, R. and NOLTING, W., "Cracked Structural Concrete Repair Through Epoxy Injection and Rebar Insertion." *Report FHWA-KS-RD-76-2*, Interim Report, Planning and Development Department, Kansas Department of Transportation (May 1977) 42 pp.
108. STRATTON, F. W., ALEXANDER, R., and NOLTING, W., "Cracked Structural Concrete Repair Through Epoxy Injection and Rebar Insertion." *Report FHWA-KS-RD-78-3*, Final Report, Planning and Development Department, Kansas Department of Transportation (Nov. 1978) 56 pp.
109. LANIGAN, A. G., "The Temperature Response of Concrete Box Girder Bridges." Ph.D, Dissertation, University of Auckland, New Zealand (1973).
110. HUIZING, J. B. S., BLAKELEY, R. W. G. and RAMSAY, G., "Falsework." *New Zealand Engineering*, Vol. 32, No. 1 (Jan. 15, 1977) pp. 2–9.
111. BROWN, G. M., "Thermal Stresses Study of the State of the Art." *Transportation Research Record 607*, Transportation Research Board (1976).
112. SINDEL, J. A., "A Design Procedure for Post-Tensioned Concrete Pavements." *Concrete International, Design and Construction*, Vol. 5, No. 2 (Feb. 1983) pp. 51–57.
113. "Tolerable Movement of Bridge Foundations, Sand Drains, K-Test, Slopes, and Culverts." *Transportation Re-*

search Record 678, Transportation Research Board, 21 pp.
114. DARPAS, G., "Recent Evolution of the Design of the Bridges Built in France by the Cantilever Method." Eleventh Congress of the International Association for Bridge and Structural Engineering, Vienne, France (Sept. 1980) pp. 101–105.
115. BRANSON, D. E., and TROST, H., "Unified Procedures for Predicting the Deflection and Centroidal Axis Location of Partially Cracked Nonprestressed and Prestressed Concrete Members." *ACI J.* (Mar.–Apr. 1982) pp. 119–130.
116. REYNOLDS, J. C., and EMANUEL, J. H., "Thermal Stresses and Movements in Bridges." *J. Structural Division, ASCE* (Jan. 1974).
117. LEONHARDT, F., and LIPPOTH, W., "Folgerungen aus Schaden an Spannetonbrucken" (Conclusions from damage to prestressed concrete bridges). *Beton-und Stahlbetonbau,* Vol. 65, No. 10, Berlin (Oct. 1970) pp. 231–344.
118. MATLOCK, H., PANAK, J. J., VORA, M. R., and CHAN, J. H. C., "Field Investigation of a Skewed, Post-Stressed Continuous Slab Structure." Research Project 3-5-63-56, Interim Study Report, Center for Highway Research, University of Texas, Austin (May 1970).
119. KOOB, M. J., BOGGS, D. W., and HANSEN, J. M., "Field Testing of the Fremont Bridge." *Report No. 78646,* Wiss, Janney, Elstner & Associates, Inc., Northbrook, Illinois (Mar. 1980) 100 pp.
120. KAMADOLI, K. A., "Thermal Stresses in Fremont Bridge Superstructure." Northwest Bridge Engineers' Seminar, Olympia, Washington (Oct. 1983) 27 pp.
121. SCHRECK, P., "The Great Blunder." Lecture 62 at the Annual Committee Meeting, Transportation Research Board, Washington, D.C. (Jan. 1983) 11 pp.
122. LEONHARDT, F., "RiBschaden an Betonbrucken-Ursachen und Abhilfe." *Beton-und Stahlbetonbau,* Vol. 74, No. 2 (Feb. 1979) pp. 36–44.

BRIDGE PLANS AND OTHER RELEVANT INFORMATION

123. California Department of Transportation, "Colorado River Bridge—Contract Plans." San Bernardino County, District 8, Route W614, Bridge No. 54C-349, Sacramento, California (Dec. 1976).
124. California Department of Transportation, "Land Park Underpass—Contract Plans." Sacramento County, District 3, Route I-5, Bridge No. 24-226, Sacramento, California (May 1972).
125. Illinois Department of Transportation, "Kishwaukee Bridge—Contract Plans." Winnebego County, Route 412 (Jan. 1977).
126. Indiana State Highway Commission, "Turkey Run Creek Bridge—Contract Plans." Parke County, State Route 47, Bridge File No. 47-61-6570 (1974).
127. Washington State Department of Transportation, "Hamilton Street Bridge—Contract Plans." City of Spokane, State Route 290, Olympia, Washington (Jan. 1982).
128. Washington State Department of Transportation, "Yakima River Bridges and Approaches—Contract Plans." Benton County, State Route 182. MP 2.94 to MP 3.82, Olympia, Washington (May 1980).
129. FIGG AND MULLER ENGINEERS, INC., "Site Inspection of Miller Creek and Black Gore Bridges." (Aug. 11–12, 1982).
130. State of Colorado, Department of Highways, "Memorandum—In-depth Inspection of the Creeks and Spalls Developing in the Walls and Bottom Slabs of the F-11-AK, F-11-AL Structures over Miller Creek on I70." (July 29, 1982).
131. FIGG AND MULLER ENGINEERS, INC., "Computer Output-Vail Pass, Bridge AK, Miller Creek." (Sept. 29, 1982) pp. 799–807.

APPENDIX A

DESIGN GUIDELINES FOR THERMAL EFFECTS IN CONCRETE BRIDGE SUPERSTRUCTURES

1. PURPOSE OF THE GUIDELINES

These design guidelines include provisions for considering the effects of temperature on reinforced and prestressed concrete bridge superstructures. Temperature effects result from time-dependent fluctuations in the effective bridge temperature or from temperature differentials within the bridge superstructure. All concrete bridges should be designed for temperature effects resulting from time-dependent fluctuations in the effective bridge temperature. Prestressed concrete bridges within a range of span lengths, and with cross sections for which a long-established history of satisfactory performance does not exist, should also be designed for the effects of temperature differentials within the bridge superstructure.

2. EFFECTIVE BRIDGE TEMPERATURES

All concrete bridges shall be designed to accommodate the stresses and movements resulting from a fluctuation in the effective bridge temperature. The values for the anticipated minimum and maximum effective bridge temperatures are dependent on the type of construction and on the minimum and maximum normal air temperatures at the bridge site. The minimum effective bridge temperature shall be obtained from Table A-1, while the maximum effective bridge temperature shall be obtained from Table A-2. Although this report is concerned with concrete bridges, results for effective bridge temperatures in composite and steel structures will be included. Unless more precise local meteorological data are available, the minimum normal air temperature shall be obtained from the map of isotherms included in Figure A-1, and the maximum normal air temperature shall be obtained from the map of isotherms included in Figure A-2.

3. DIFFERENTIAL TEMPERATURES

Provisions shall be made for stresses and movements resulting from differential temperatures within prestressed concrete bridge superstructures when a long-established history of satisfactory performance for similar bridge superstructure does not exist. Both longitudinal and transverse stresses and movements resulting from the positive and negative vertical temperature gradients, described below, shall be considered.

3.1 Positive Temperature Gradients

Vertical temperature differentials within concrete superstructures that result from the solar heating of the deck surface shall be assumed to vary at different depths of concrete, as shown in Figure A-3. This gradient is only applicable to superstructures with a depth greater than 2 ft. Actual temperatures shall be assumed to vary in accordance with the values specified in Table A-3 for the various solar radiation zones and thicknesses of black top surfacing on the bridge deck.

When determining the temperature variations within box girder bridges the values T_2 and T_3 shall be increased by 5°F. Maximum solar radiation zones are shown in Figure A-4.

Table A-1. Correlation between normal daily minimum temperature and minimum effective bridge temperature.

Normal Daily Minimum Temperature °F	Minimum Effective Bridge Temperature Type of Superstructure		
	Concrete °F	Composite °F	Steel Only °F
-30	-3	-12	-43
-25	0	-9	-36
-20	3	-7	-30
-15	5	-4	-24
-10	8	-1	-17
-5	11	2	-10
0	13	4	-5
5	16	9	0
10	19	14	5
15	22	17	11
20	25	22	16
25	29	26	22
30	32	31	27
35	35	36	33
40	38	40	38

Table A-2. Correlation between normal daily maximum temperature and maximum effective bridge temperature.

Normal Daily Maximum Temperature °F	Maximum Effective Bridge Temperature Type of Superstructure		
	Concrete °F	Composite °F	Steel Only °F
55	66	70	91
60	69	74	94
65	73	79	97
70	77	83	101
75	80	88	104
80	84	93	107
85	88	96	110
90	92	99	112
95	95	102	115
100	98	104	116
105	101	105	118
110	105	107	120

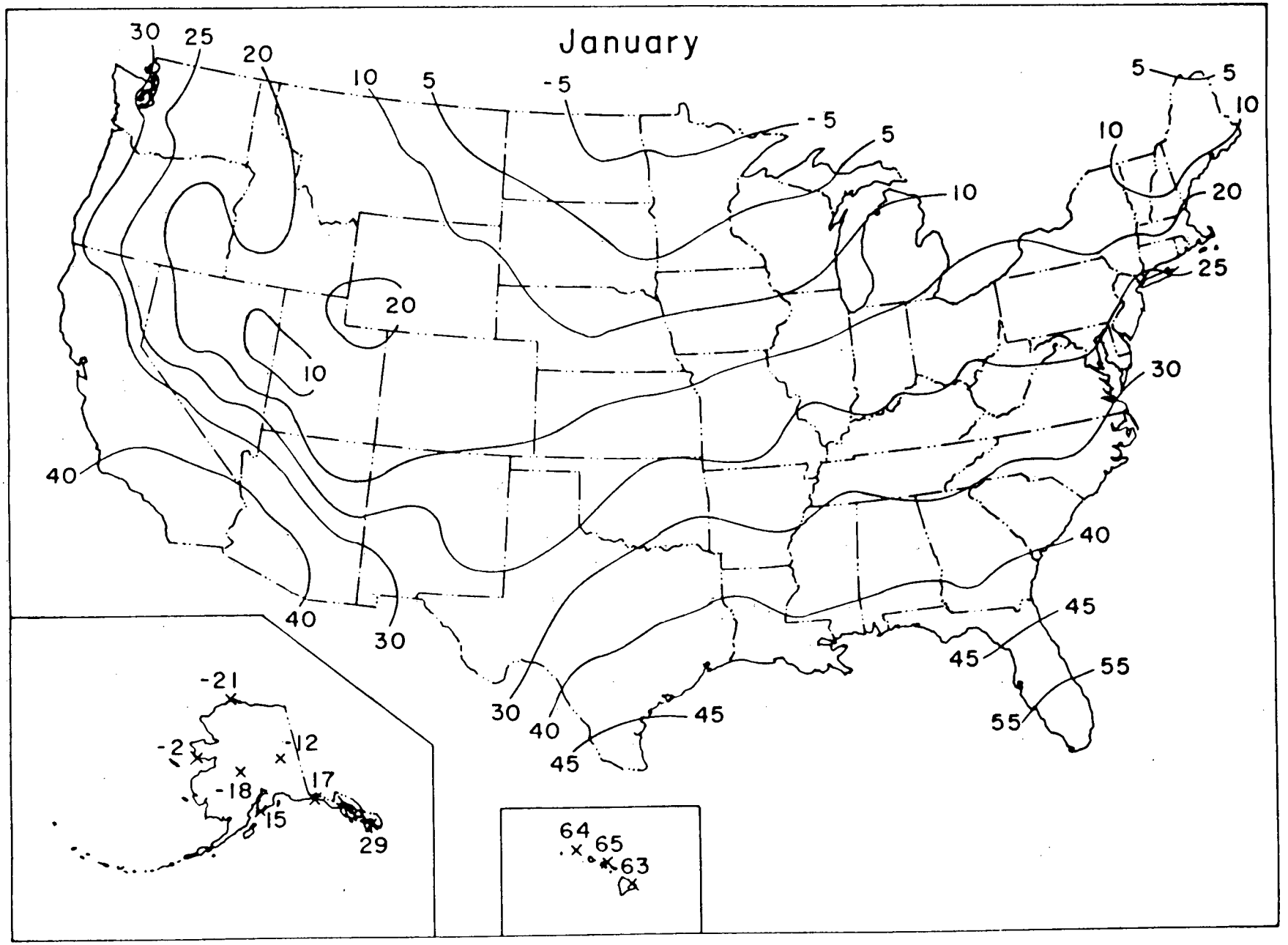

Figure A-1. Normal daily minimum temperature (°F) for January.

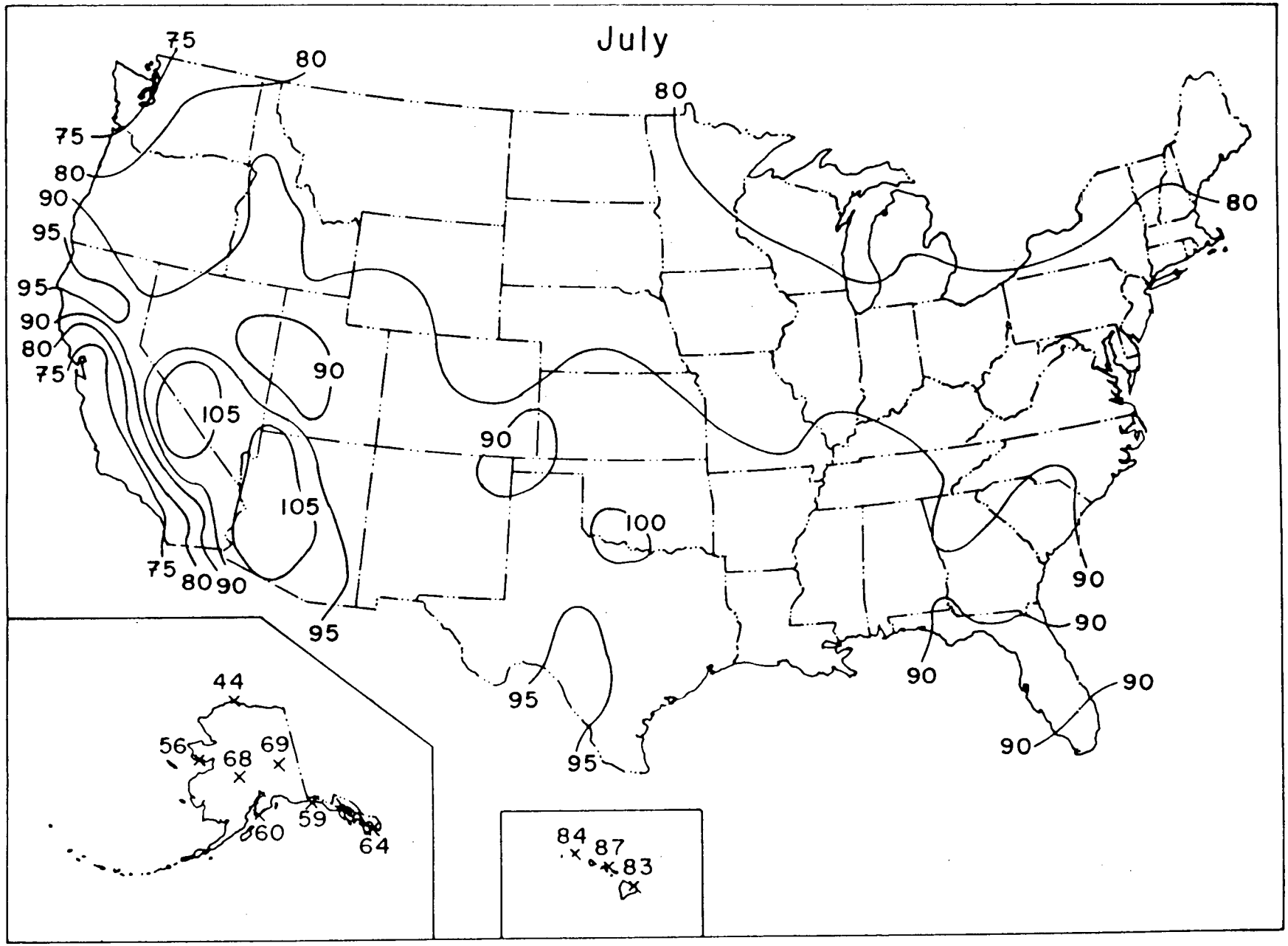

Figure A-2. Normal daily maximum temperature (°F) for July.

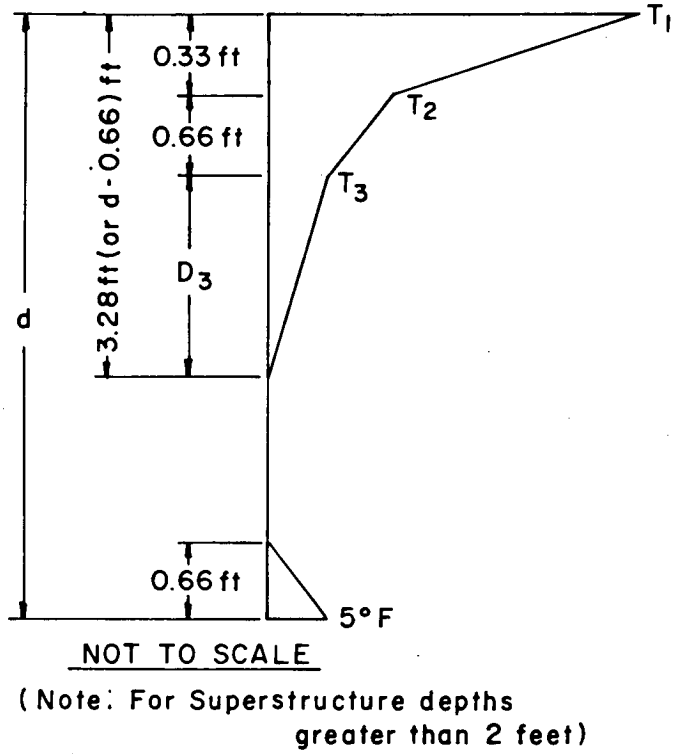

Figure A-3. Positive vertical temperature gradient within superstructure concrete.

Table A-3. Temperature differentials within a concrete superstructure for a positive temperature gradient (see Fig. A-4 for zone map).

Plain Concrete Surface

Zone	T_1 (°F)	T_2 (°F)	T_3 (°F)
1	54	14	5
2	46	12	4
3	41	11	4
4	38	9	3

2 in. Blacktop

Zone	T_1 (°F)	T_2 (°F)	T_3 (°F)
1	43	14	4
2	36	12	4
3	33	11	3
4	29	9	2

4 in. Blacktop

Zone	T_1 (°F)	T_2 (°F)	T_3 (°F)
1	31	9	3
2	25	10	3
3	23	11	2
4	22	11	2

3.2 Negative Temperature Gradients

Temperature differentials within concrete superstructures that result from a rapid cooling of exposed concrete surfaces shall be assumed to vary at different depths, as shown in Figure A-5. This gradient is only applicable to superstructures with a depth greater than 2 ft. Temperatures shall be assumed to vary with the maximum solar radiation zone and the thickness of black top surfacing on the bridge deck, as specified in Table A-4.

4. COEFFICIENT OF THERMAL EXPANSION

The coefficient of thermal expansion used to determine temperature effects shall be based on the type of aggregate to be used, as specified in Table A-5.

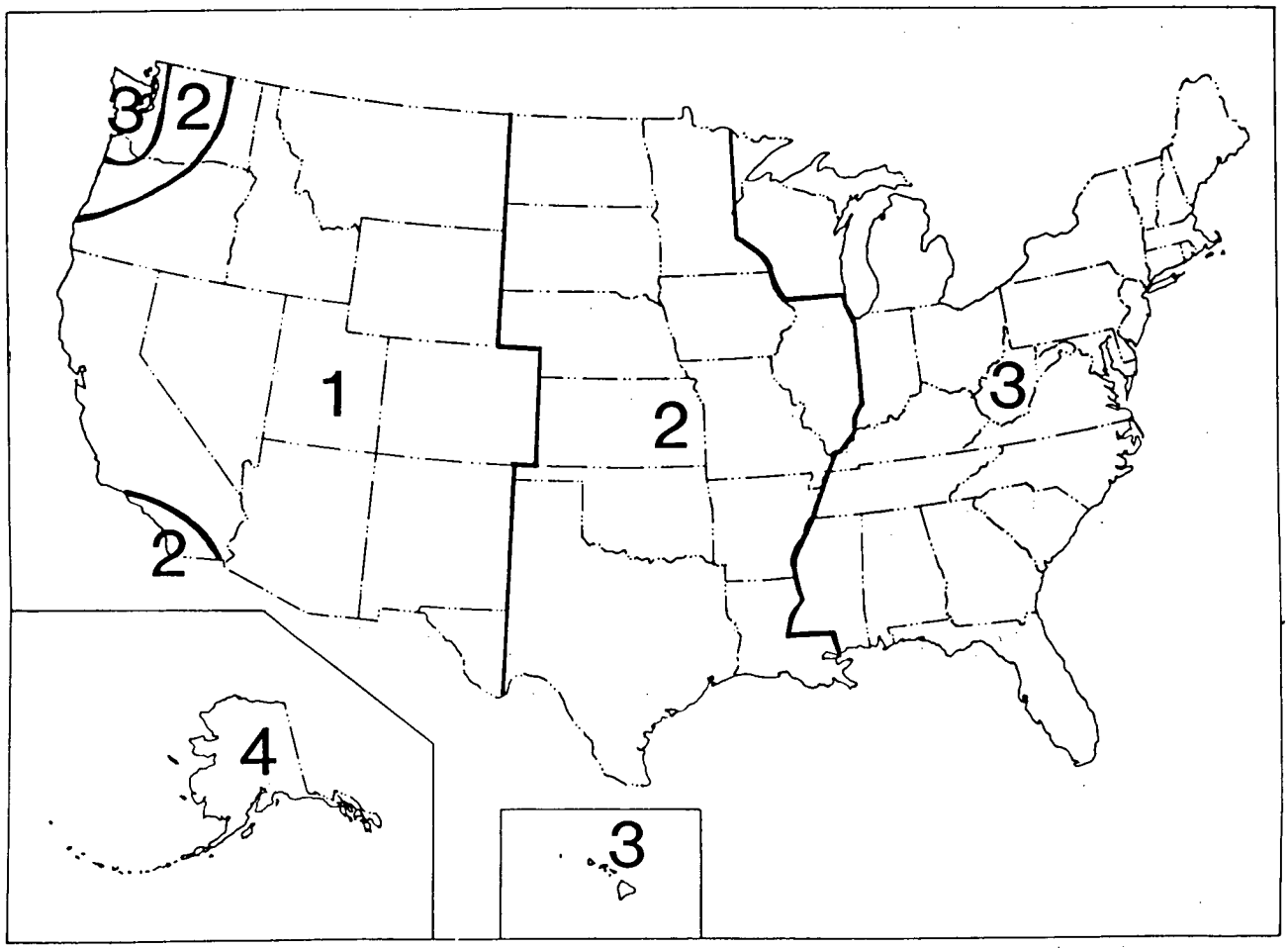

Figure A-4. Maximum solar radiation zones for the United States.

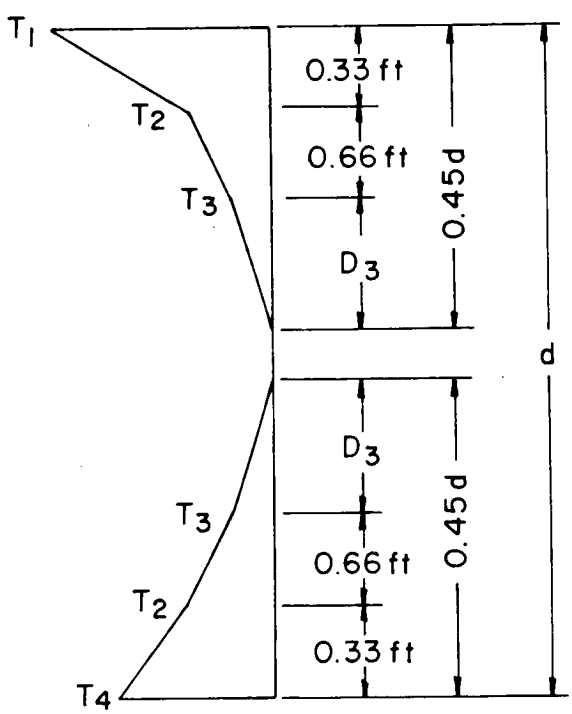

NOT TO SCALE

(Note: For Superstructure depths greater than 2 feet)

Figure A-5. Negative temperature gradient within superstructure concrete.

Table A-4. Temperature differentials within a concrete superstructure for a negative temperature gradient (see Fig. A-4 for zone map).

Plain Concrete Surface

Zone	T_1 (°F)	T_2 (°F)	T_3 (°F)	T_4 (°F)
1	27	7	2	14
2	23	6	2	10
3	21	6	2	8
4	19	5	2	6

2 in. Blacktop

Zone	T_1 (°F)	T_2 (°F)	T_3 (°F)	T_4 (°F)
1	22	7	2	15
2	18	6	2	11
3	17	6	2	10
4	15	5	1	8

4 in. Blacktop

Zone	T_1 (°F)	T_2 (°F)	T_3 (°F)	T_4 (°F)
1	16	5	1	12
2	13	5	1	9
3	12	6	1	8
4	11	6	1	8

Table A-5. Coefficient of thermal expansion based on aggregate type (thermal coefficient of concrete based on fine and coarse aggregates).

AGGREGATE TYPE	THERMAL COEFFICIENT OF CONCRETE* (0.000001 per °F)
Quartzite	7.1
Quartz	6.4
Sandstone	6.5
Gravel	6.9
Granite	5.3
Dolerite	5.3
Basalt	5.0
Marble	2.4-4.1
Limestone	4.0

*Based on fine and coarse aggregates

5. ANALYSIS PROCEDURES

An analysis of temperature effects shall be performed to determine the stresses and movements expected to result from temperature-induced strains within specified elements of the bridge superstructure. The effects of structure continuity shall be included when analyzing both the effects of fluctuations in the effective bridge temperature and the effects of temperature differentials in the superstructure. Note, however, that for standard prestress concrete cross sections within a range of span lengths having a long-established history of satisfactory performance, the designer has the option of waiving the detailed analysis of temperature differential effects.

APPENDIX B

COMMENTARY ON DESIGN GUIDELINES FOR THERMAL EFFECTS IN CONCRETE BRIDGE SUPERSTRUCTURES

1. APPLICABILITY OF THE GUIDELINES

All bridges are subjected to stresses and/or movements resulting from temperature variation. Although time-dependent variations in the effective bridge temperature have caused problems in both reinforced and prestressed concrete bridges, detrimental effects caused by temperature differentials within the superstructure have occurred, thus far, only in prestressed bridges.

Except in extreme cases, concrete bridges will not suffer a sudden loss of strength as a result of temperature changes. The

primary detrimental effect from temperature variation is the formation of unacceptable cracks in the concrete that reduce the serviceability of the bridge. Strength loss may eventually result if these cracks contribute to accelerated deterioration. Safety could be affected if the deterioration were to escape detection, as might be the case if prestress strands concealed from inspection were to corrode. Because the total elimination of cracks in concrete bridges is not possible, these guidelines are designed to limit temperature-induced cracking to acceptable levels.

Although these guidelines do not specifically address falsework loads and temperature differentials resulting from the heat of hydration in thick members, they will be useful in determining those effects. Heat of hydration cooling can be an important cause of cracking, such as in the case of curing and/or cooling of the top deck slab which is cast on top of the previously constructed bottom slab and/or stems which provide restraint against movement.

2. EFFECTIVE BRIDGE TEMPERATURES

Fluctuations in effective bridge temperatures result in expansion and contraction of the superstructure. These movements, in turn, induce stresses in supporting elements such as columns or piers, and result in horizontal movement of the expansion joints. The magnitude of these stresses and movements on a given bridge depends on the range of temperature variation and the temperature of the bridge at the time of construction. These guidelines establish the criteria for determining the minimum and maximum bridge temperatures that can reasonably be expected. For bridge designers to determine the amount of expansion and contraction that can be expected to occur on a given bridge to be built in a given location, they will need to assume an effective temperature at the time of construction.

2.1 Bridge Temperature Response

Emerson established a method for estimating minimum and maximum effective bridge temperatures based on the geographical distribution of minimum and maximum shade temperatures throughout the United Kingdom (*19*). The procedures established by Emerson were subsequently incorporated into British Standard BS 5400. Because the range of minimum and maximum temperatures for the United States is larger than that reported for the United Kingdom, it was necessary to extrapolate some of the curves relating effective bridge temperatures to minimum and maximum shade temperatures. Minimum temperatures for the United States range from −30°F to 40°F, as compared to a minimum temperature range of −11°F (−24°C) to 23°F (−5°C) for the United Kingdom. The extrapolated portions of the minimum temperature range presented by Emerson are shown in Figure B-1. Maximum temperatures for the United States range from approximately 55°F to 110°F, as compared to a maximum temperature range of 75°F (24°C) to 100°F (38°C) for the United Kingdom. The extrapolated portions of the maximum temperature range are also shown in Figure B-1. The values given in Tables B-1 and B-2 are based on these curves. Note that adjustments in the effective bridge temperature are not required for bridge surfacing.

2.2 Minimum and Maximum Air Temperatures

The isotherms used for the minimum and maximum air temperature are taken from charts published in the "Climatic Atlas of the United States" (*98*). The minimum air temperatures were obtained from the normal daily minimum temperatures for the month of January, while the maximum air temperatures were obtained from the normal daily maximum temperatures for the month of July. These isotherms are based on average daily records for the 30-year period from 1931 through 1960. Although data are available that list the extreme daily minimum and maximum temperatures in the United States for a given period of time, there is no readily available published information that lists the duration in days that these extreme temperatures have occurred. Since bridges require 2 to 3 days to respond to a given minimum or maximum temperature, additional data on the actual duration are required. In the "Climatography of the United States No. 84," minimum and maximum extremes for each day are averaged for the years 1941 through 1970 (*101*). Maximum extreme temperatures occurring at 20 randomly selected stations were compared with the iso-

Table B-1. Correlation between normal daily minimum temperature and minimum effective bridge temperature.

Normal Daily Minimum Temperature	Minimum Effective Bridge Temperature Type of Superstructure		
°F	Concrete °F	Composite °F	Steel Only °F
-30	-3	-12	-43
-25	0	-9	-36
-20	3	-7	-30
-15	5	-4	-24
-10	8	-1	-17
-5	11	2	-10
0	13	4	-5
5	16	9	0
10	19	14	5
15	22	17	11
20	25	22	16
25	29	26	22
30	32	31	27
35	35	36	33
40	38	40	38

Table B-2. Correlation between normal daily maximum temperature and maximum effective bridge temperature.

Normal Daily Maximum Temperature	Maximum Effective Bridge Temperature Type of Superstructure		
°F	Concrete °F	Composite °F	Steel Only °F
55	66	70	91
60	69	74	94
65	73	79	97
70	77	83	101
75	80	88	104
80	84	93	107
85	88	96	110
90	92	99	112
95	95	102	115
100	98	104	116
105	101	105	118
110	105	107	120

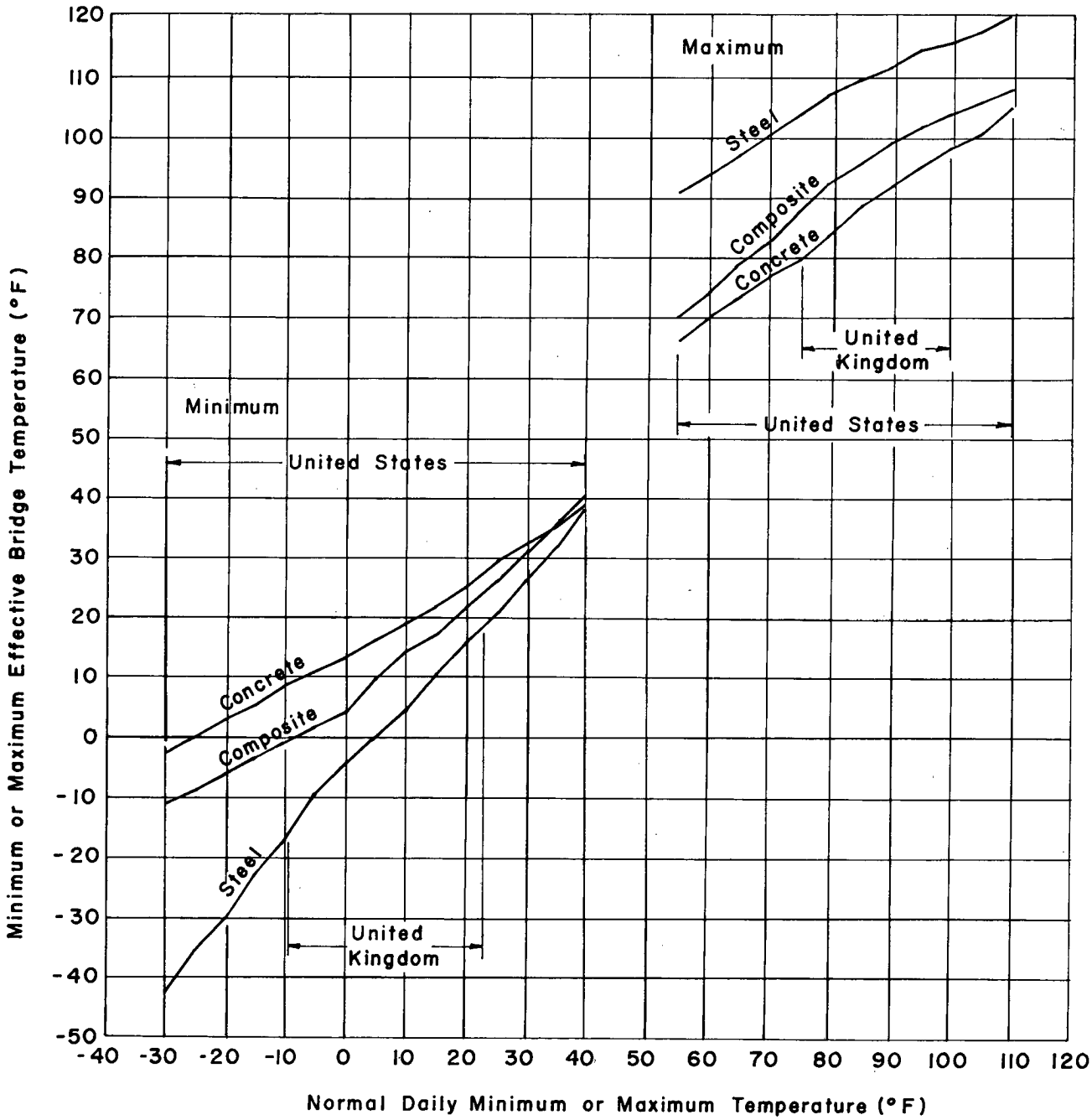

Figure B-1. Correlation between minimum or maximum temperature and minimum or maximum effective bridge temperature.

therms for the normal daily maximums and found to agree within 6°F. Minimum extreme temperatures were also compared with the isotherms for the normal daily minimums and found to agree within 6°F. Initially, it was thought that the extremes on a day-to-day basis (averaged over the 30-year period from 1941 through 1970) would be substantially different from those obtained from the isotherms. On the basis of this comparison, it may be concluded that the isotherms selected will yield fairly accurate approximations of the minimum and maximum extremes for the United States. Local meteorological data may be more applicable in mountainous areas, coastal areas, urban areas, and sheltered, low-lying areas where frost pockets may develop. It is recommended that local meteorological data rather than isotherms be used for unusually large or complex bridges located in regions where extreme temperature conditions are known to occur.

3. DIFFERENTIAL TEMPERATURES

Variations in temperature at different depths of the superstructure caused by solar radiation effects may result in significant temperature-induced fiber stresses. These stresses are induced in two ways. The first way occurs when bending moments are generated in continuous spans as a result of the differences between the deformations in the top and bottom fibers. These deformations will cause a deflection in the superstructure; stresses result when this deflection is restrained by structure continuity. The second way in which stresses are induced is when nonlinear temperature variations through the depths of the section cause initially plane sections of the superstructure to become distorted. Because shallow superstructures have not been adversely affected in the past by temperature differentials, design thermal gradients were developed for superstructures with depths greater than 2 ft.

Most typical structures have not experienced difficulties because of temperature differentials. Recently, however, concrete bridge designs have become more sophisticated. As a result, span lengths have increased and designers have kept superstructure weights at a minimum. This has resulted in a reduction of reserve strength for temperature-induced stresses, a reduction which has caused unacceptable cracking in some bridge superstructures. Much of this unacceptable cracking could have been avoided had the designer accurately considered the effects of differential temperatures.

Bridges can be protected from excessive temperature-induced stresses in several ways. One method is to resist the tensile force produced by the tensile stresses by providing a sufficient quantity of mild reinforcement in the zone of tension. Stresses in reinforcement should be limited to $0.6 f_y$ for crack control. Extra prestressing steel may also be used. However, it is recommended that the designer not rely on the tensile strength of concrete.

3.1 Positive Temperature Gradients

Positive temperature gradients occur when solar radiation, large diurnal temperature variations, and/or low wind speed conditions produce a higher temperature in the bridge deck. Each of these individual weather conditions varies throughout the United States, and they can combine to produce extreme positive temperature distributions in concrete bridge superstructures in some locations. Experimental data from 26 SOLMET stations in the United States were used to compute the maximum temperature differences of a 2-m (6.56-ft) deep concrete bridge structure (*73*). In order to obtain solar radiation zones in the United States these temperature differences were superimposed on solar radiation contours for the month of July (*99*). The maximum solar radiation zones for an unsurfaced deck, a 50-mm (2-in.) blacktop deck, and a 100-mm (4-in.) blacktop deck are shown in Figures B-2, B-3, and B-4, respectively. The United States has been divided into four climatic zones (see Fig. B-5), each reflecting the maximum expected positive temperature gradients expected for its geographical area. The temperature variations in these four categories, as shown, shall be assumed to occur throughout the deck and girder members. The positive temperature gradient was based on studies done in Illinois (*73*). A simplification of the New Zealand fifth order temperature distribution was shown to be a good approximation by using straight-line segments from lower bound and upper bound temperature differences at the SOLMET stations in Brownsville, Texas, and Phoenix, Arizona, respectively. Basically the gradient was composed of three linear curves at the top portion of the deck. In order to obtain temperature differences in the United States average maximum temperature differences were computed over each solar radiation zone to obtain T_1. Temperature differences for Zone 4 were obtained by extrapolation.

Because of the effect of the enclosed air cavity in concrete box girder bridges, the temperature in the deck above the cavity will be slightly different than in an exposed deck. Measurements made by researchers at the University of Illinois have shown that box girder deck temperatures above the girder stems do not vary significantly from those in the deck above the cell (*73*). Modifications to the design temperature gradients for box girders are required to account for this phenomenon. Although the temperatures in the cantilevered deck overhang and the center of the girder stems are not likely to be significantly altered by the presence of the enclosed air cavity, a uniform temperature gradient may be applied to the entire cross section of a box girder bridge for the sake of simplicity. This practice will lead to thermal stress distributions very similar to those obtained if unadjusted thermal gradients were used in the overhangs and the webs.

3.2 Negative Temperature Gradients

Negative temperature gradients may occur when a bridge superstructure that had obtained a high temperature during the day experiences a reduction in temperature caused by a cool night. For convenience, the design negative temperature gradient in these recommendations is related to the temperatures and distances used for the design positive gradient. The shape of the negative gradient is based on the negative gradient proposed in British Standard BS 5400.

4. COEFFICIENT OF THERMAL EXPANSION

Several researchers have investigated the effect of aggregate type on the coefficient of thermal expansion for concrete. The values given in Table B-3 are averages of values reported in the literature.

5. ANALYSIS PROCEDURES

Several techniques exist for determining the effects of temperature-induced strains on a bridge structure. The following assumptions are made when performing thermal stress analyses using the one-dimensional beam theory.

1. The material is homogeneous and exhibits isotropic behavior.
2. Material properties are independent of temperature.
3. The material has linear stress-strain and temperature-strain relations. Thus, thermal stresses can be considered independently of stresses or strains imposed by other loading conditions, and the principle of superposition holds.
4. The Navier-Bernoulli hypothesis that initially plane sections remain plane after bending is valid.
5. The temperature varies only with depth, but is constant

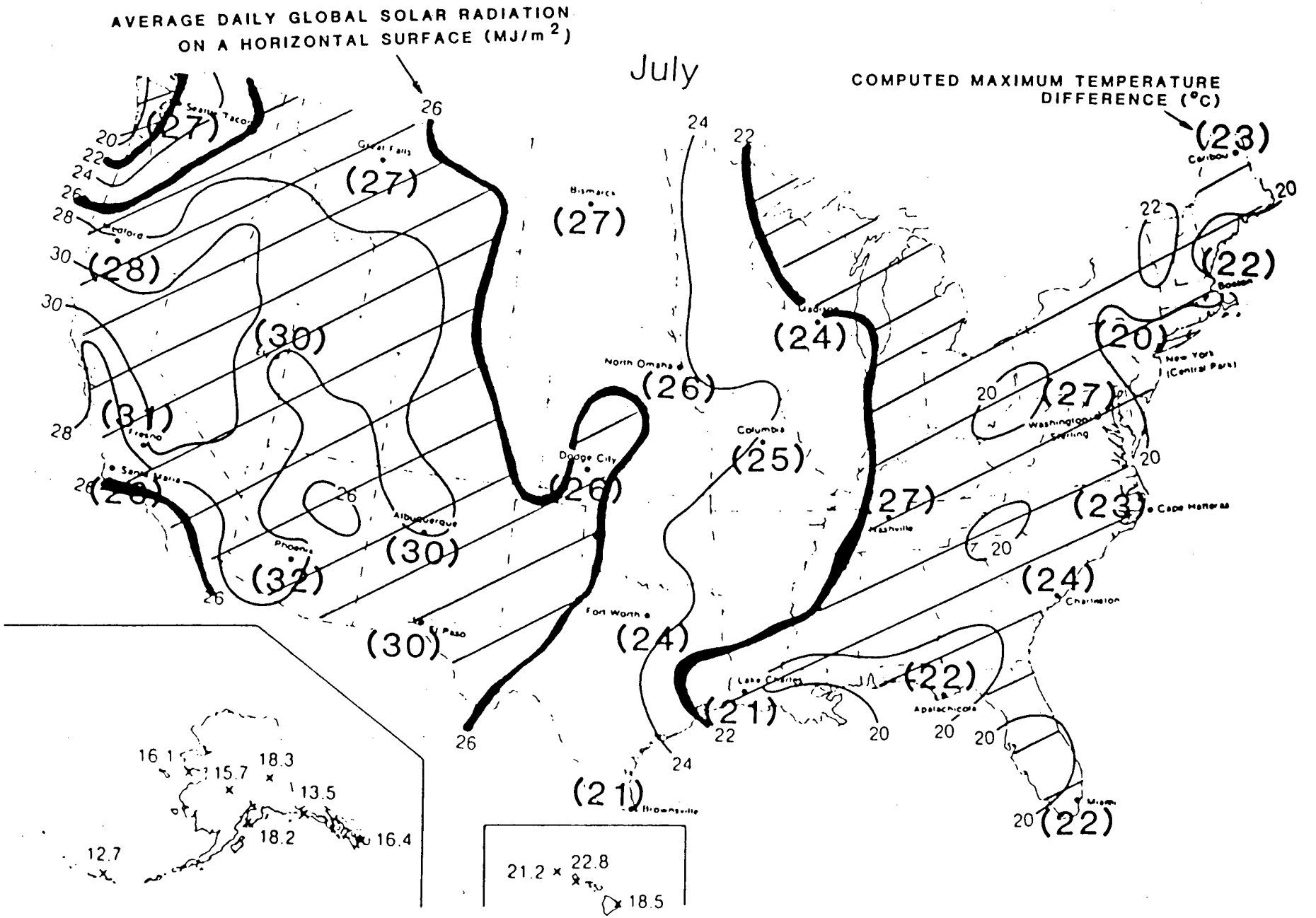

Figure B-2. Maximum solar radiation zone for a 2-m (6.56-ft) deep bridge structure (unsurfaced).

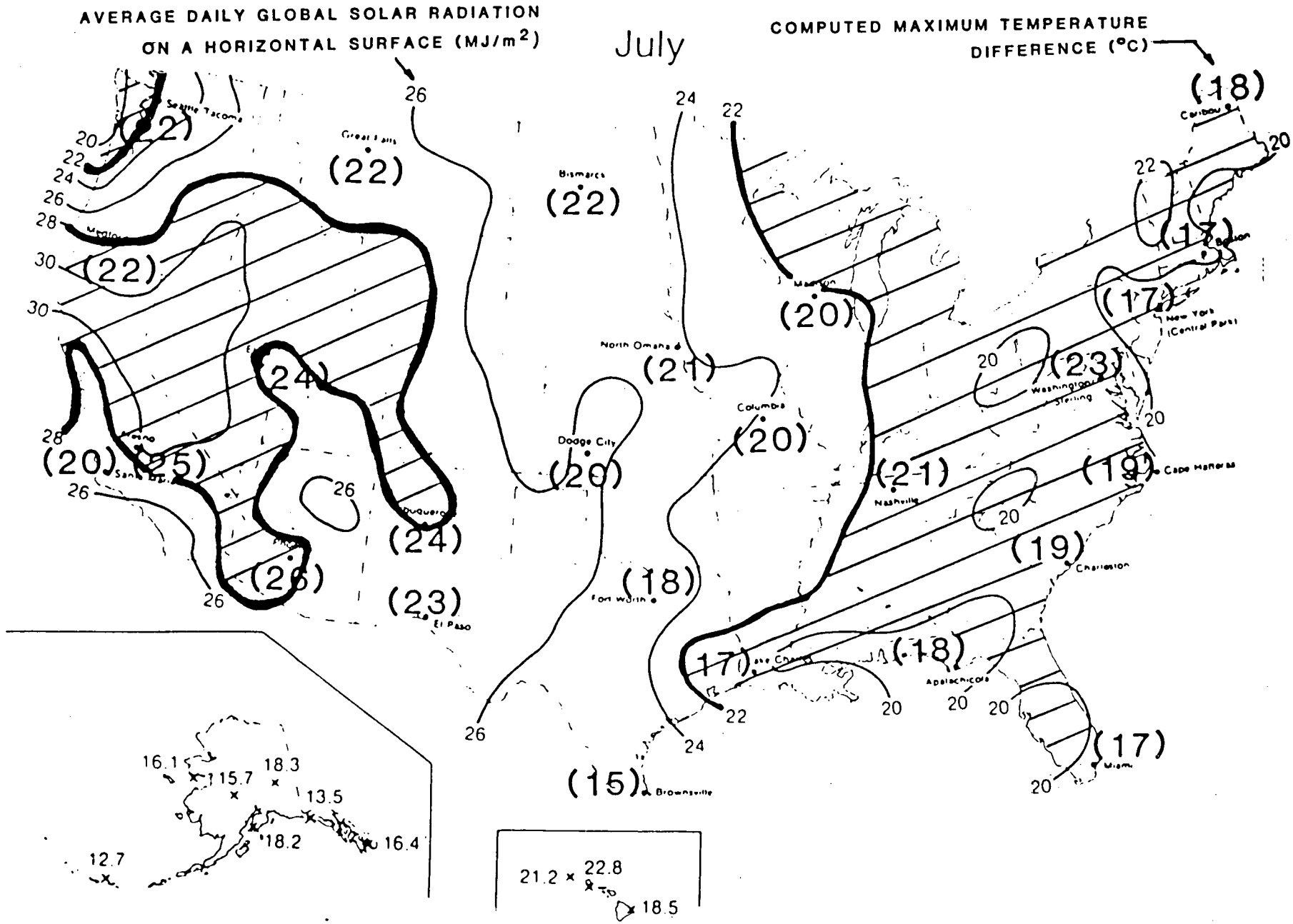

Figure B-3. Maximum solar radiation zone for a 2-m (6.56-ft) deep bridge structure with a 50-mm (2-in.) blacktop.

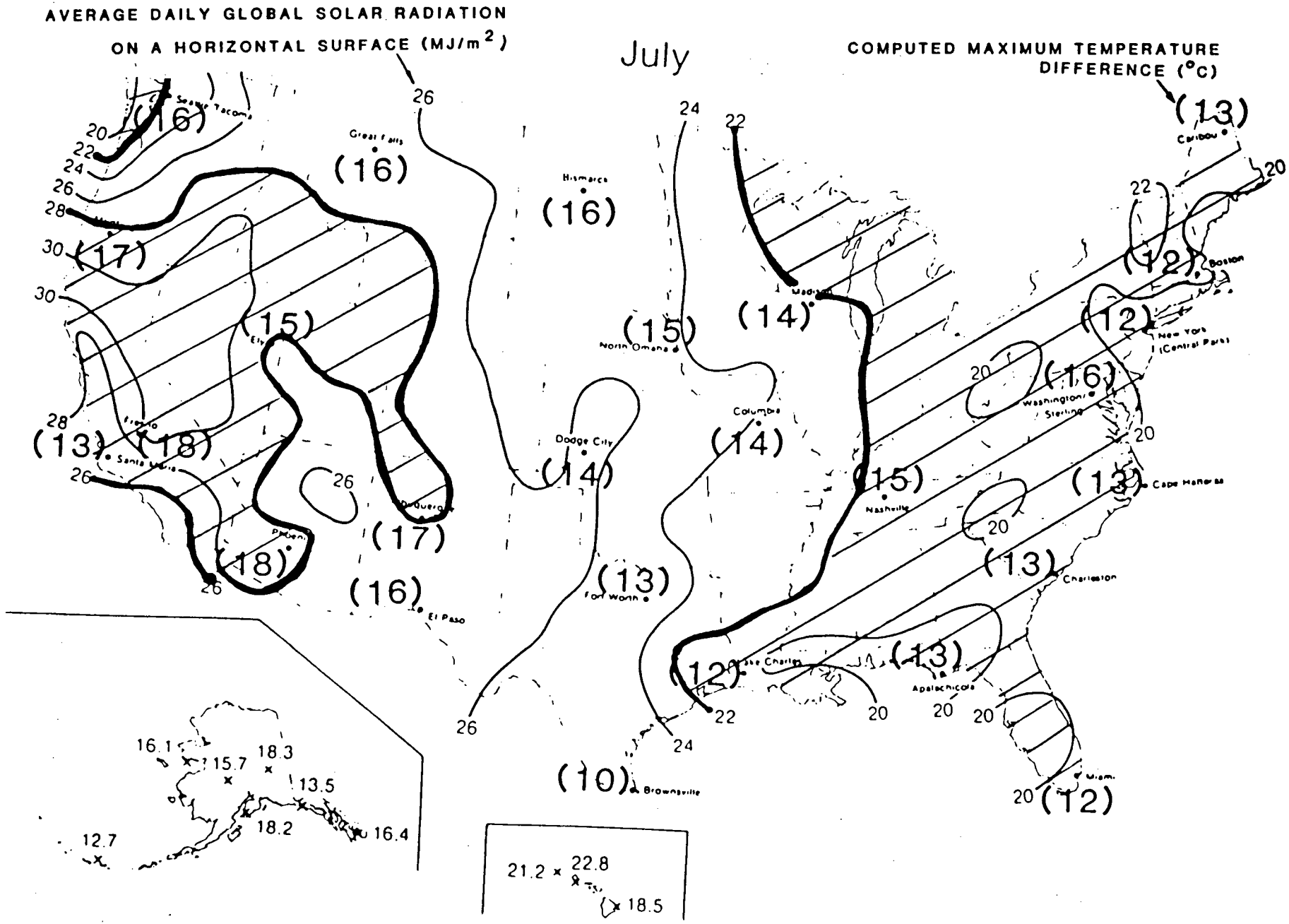

Figure B-4. Maximum solar radiation zone for a 2-m (6.56-ft) deep bridge structure with a 100-mm (4-in.) blacktop.

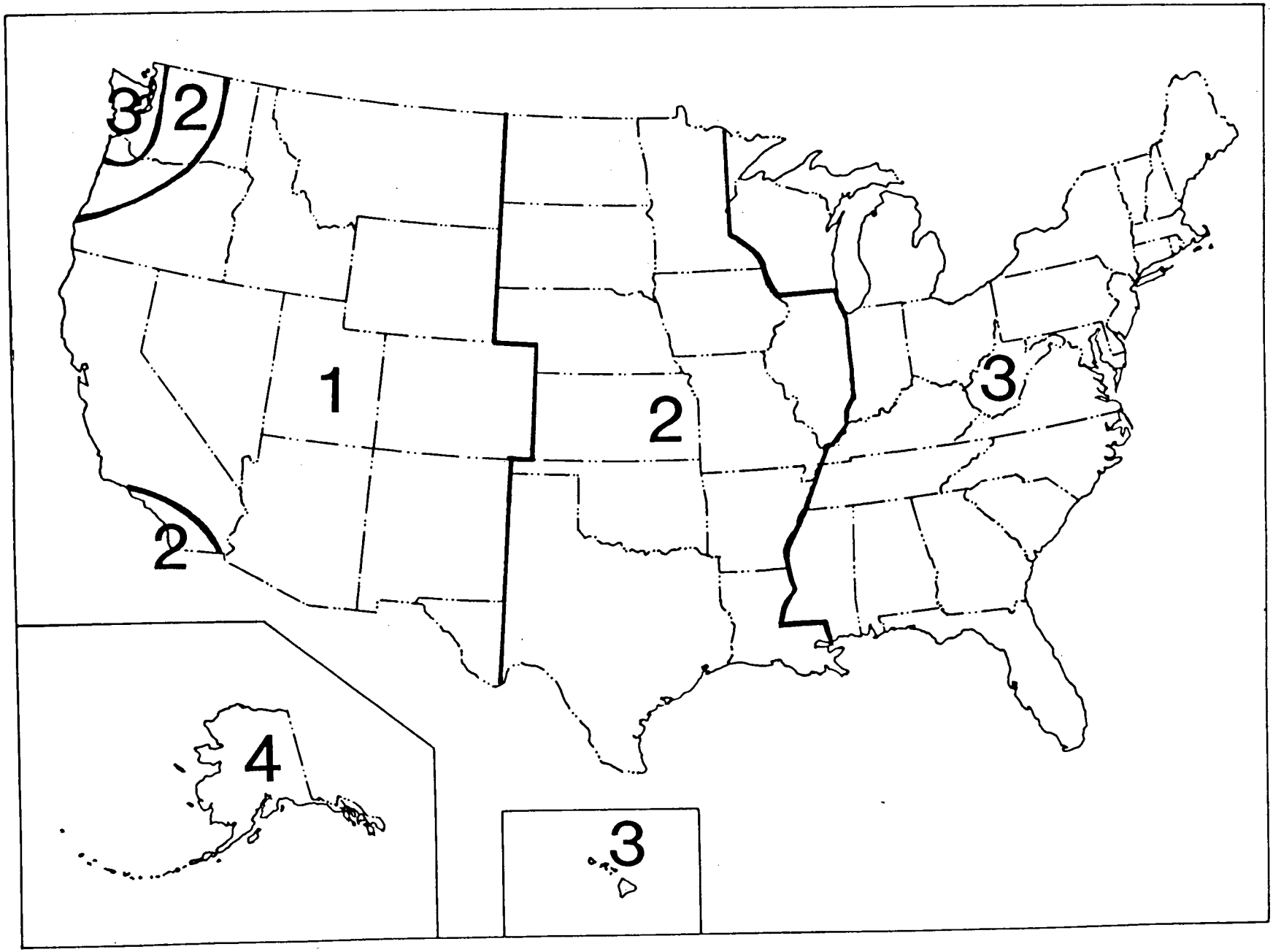

Figure B-5. Zones of maximum solar radiation for the United States.

at all points of equal depth (except those points over an enclosed cell).

6. Longitudinal and transverse thermal responses of the bridge superstructure can be considered independently and the results superimposed; i.e., the longitudinal and transverse thermal stress fields are assumed to be uncoupled.

This final assumption simplifies the analysis, particularly for such complex section geometries as box girders. Because of this assumed uncoupling of the responses, the theory and analysis techniques for longitudinal and transverse thermal stresses are generally treated separately.

Perhaps the most troublesome analysis most designers are likely to encounter is the analysis of the effects of temperature differentials on the longitudinal fiber stresses induced in prestressed bridge superstructures. This analysis is typically accomplished by first assuming that the free ends of the bridge superstructure are restrained from both translation and rotation. Thermal stresses will be induced throughout the depth of the cross section according to the following equation:

$$\sigma\,(Y) = EcT(Y)$$

where $\sigma\,(Y)$ = longitudinal stress at a fiber located a distance Y from the center of gravity of the cross section; E = elastic modulus; c = coefficient of thermal expansion; and $T(Y)$ = temperature at a depth Y.

These stresses will result in axial forces and bending moments at the restrained ends of the superstructure. The response of an unrestrained bridge structure to a given temperature gradient may be obtained by superimposing on the stresses and deformations in the restrained bridge the stresses and deformations resulting from equal and opposite axial forces and bending moments applied at the free ends of the bridge. In some computer programs, this can be done by applying equivalent prestress forces to simulate the stresses induced at the restrained end of the bridge.

Table B-3. Coefficients of thermal expansion based on aggregate base (thermal coefficient of concrete based on fine and coarse aggregates).

AGGREGATE TYPE	THERMAL COEFFICIENT OF CONCRETE* (0.000001 per °F)
Quartzite	7.1
Quartz	6.4
Sandstone	6.5
Gravel	6.9
Granite	5.3
Dolerite	5.3
Basalt	5.0
Marble	2.4-4.1
Limestone	4.0

*Based on fine and coarse aggregates

APPENDIX C

WORKED EXAMPLE PROBLEMS

EXAMPLE 1

Problem

A three-span pedestrian overcrossing, which is shown in Figure C-1, has been built in Albuquerque, New Mexico. The effective bridge temperature at which the bridge was restrained was approximated at 57°F. The deck surface is plain. Determine the expansion up to the maximum effective bridge temperature, the contraction down to the minimum effective bridge temperature, and the longitudinal stress distribution through the superstructure due to the temperature gradients.

Solution

1. *Determine the expansion up to the maximum effective bridge temperature:*

(a) Step 1: Determine the normal daily maximum temperature at the given location from Figure C-2.

Maximum Temperature = 90°F

(b) Step 2: Determine the maximum effective bridge temperature from Table C-1.

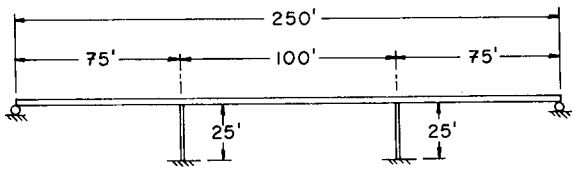

ELEVATION

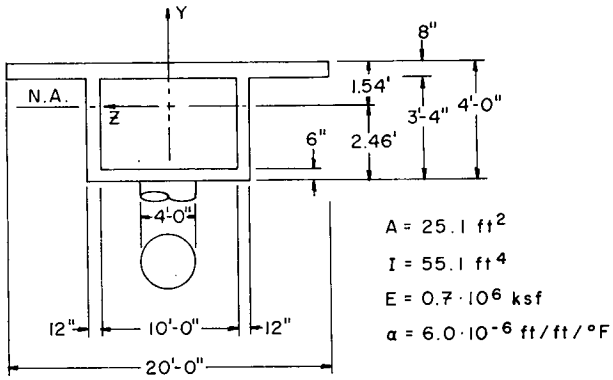

SUPERSTRUCTURE AND COLUMN CROSS SECTION

Figure C-1. Elevation and superstructure cross section of Example 1.

Table C-1. Correlation between normal daily maximum temperature and maximum effective bridge temperature.

Normal Daily Maximum Temperature °F	Maximum Effective Bridge Temperature Type of Superstructure		
	Concrete °F	Composite °F	Steel Only °F
55	66	70	91
60	69	74	94
65	73	79	97
70	77	83	101
75	80	88	104
80	84	93	107
85	88	96	110
90	92	99	112
95	95	102	115
100	98	104	116
105	101	105	118
110	105	107	120

Maximum Effective Bridge Temperature = 91.8°F

(c) Step 3: Calculate the expansion up to the maximum effective bridge temperature.

$$\text{Expansion} = L\alpha\Delta T$$
$$= (250\text{ ft})(6.0 \times 10^{-6}\text{ ft/ft/°F})(92°\text{F} - 57.0°\text{F})$$
$$= 0.0525\text{ ft} = 0.0630\text{ in.}$$

2. *Determine the contraction down to the minimum effective bridge temperature:*

(a) Step 1: Determine the normal daily minimum temperature at the given location from Figure C-3.

Minimum Temperature = 25°F

(b) Step 2: Determine the minimum effective bridge temperature from Table C-2.

Minimum Effective Bridge Temperature = 29°F

(c) Step 3: Calculate the contraction down to the minimum effective bridge temperature.

$$\text{Contraction} = L\alpha\Delta T$$
$$= (250\text{ ft})(6.0 \times 10^{-6}\text{ ft/ft/°F})(29°\text{F} - 57.0°\text{F})$$
$$= -0.0420\text{ ft} = -0.504\text{ in.}$$

3. *Determine the longitudinal stress distribution through the superstructure due to the temperature gradients:*

(a) *Positive Gradient Stress Distribution*

- Step 1: Determine the maximum solar radiation zone at the bridge site from Figure C-4.

Albuquerque, NM: Zone 1 (Plain concrete)

- Step 2: Determine the temperature gradient from Figure C-5. The temperature distribution is shown in Figure C-6. Note that 5°F has been added to T_2 and T_3 for the box girder section.
- Step 3: Determine the thermally induced stresses assuming a totally restrained structure. In general, the thermally induced stresses are computed using Eq. 2 in Chapter Three:

$$\sigma_t(Y) = E\alpha T(Y)$$
$$= (0.7 \times 10^6\text{ ksf})(6.0 \times 10^{-6}\text{ ft/ft/°F})\,T(Y)$$
$$= 4.20\,T(Y)$$

The thermally induced stress distribution is shown in Figure C-7.

- Step 4: Determine the restraining axial stress. Using Eq. 3 in Chapter Three gives:

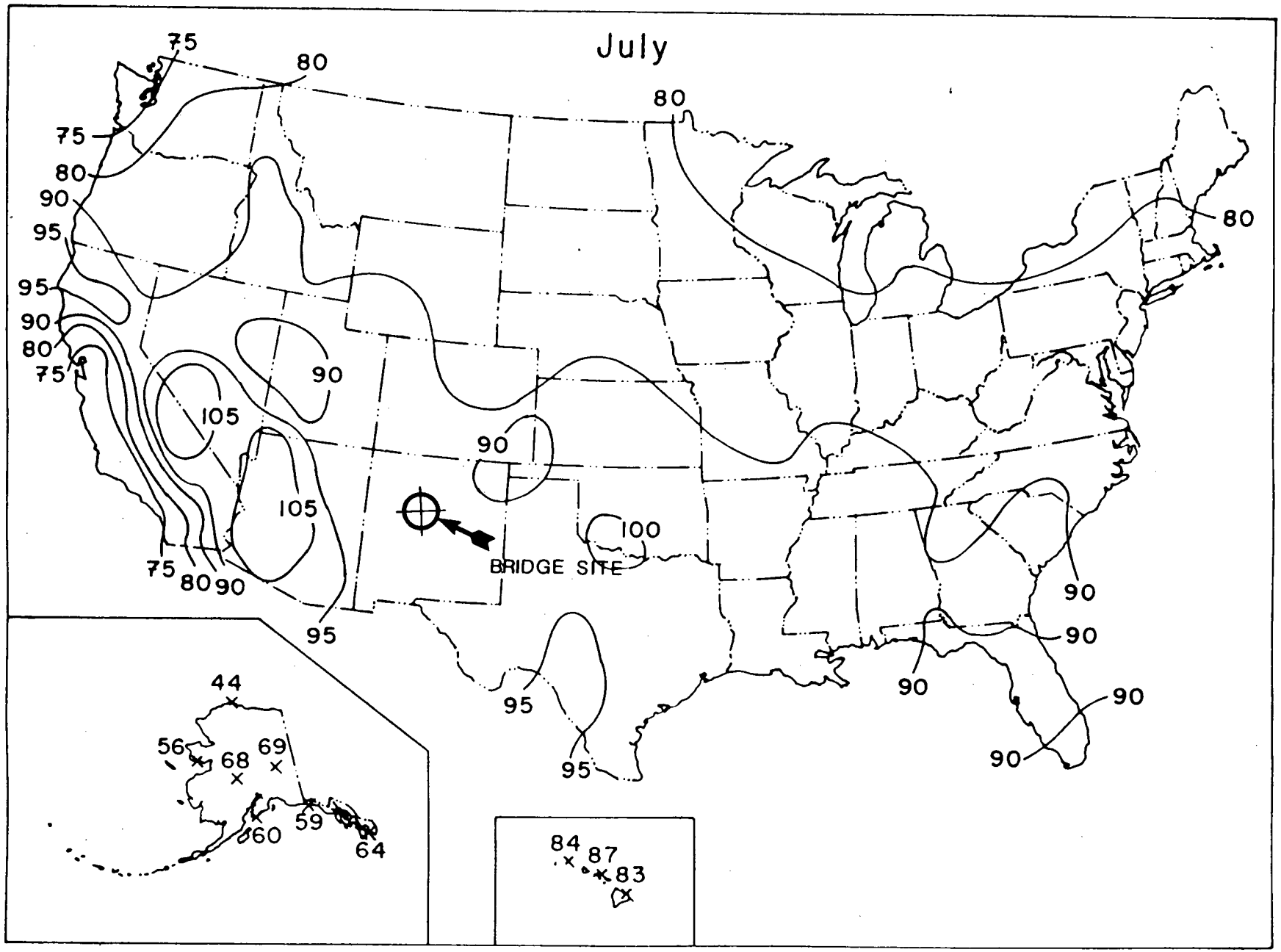

Figure C-2. Normal daily maximum temperature (°F) for July.

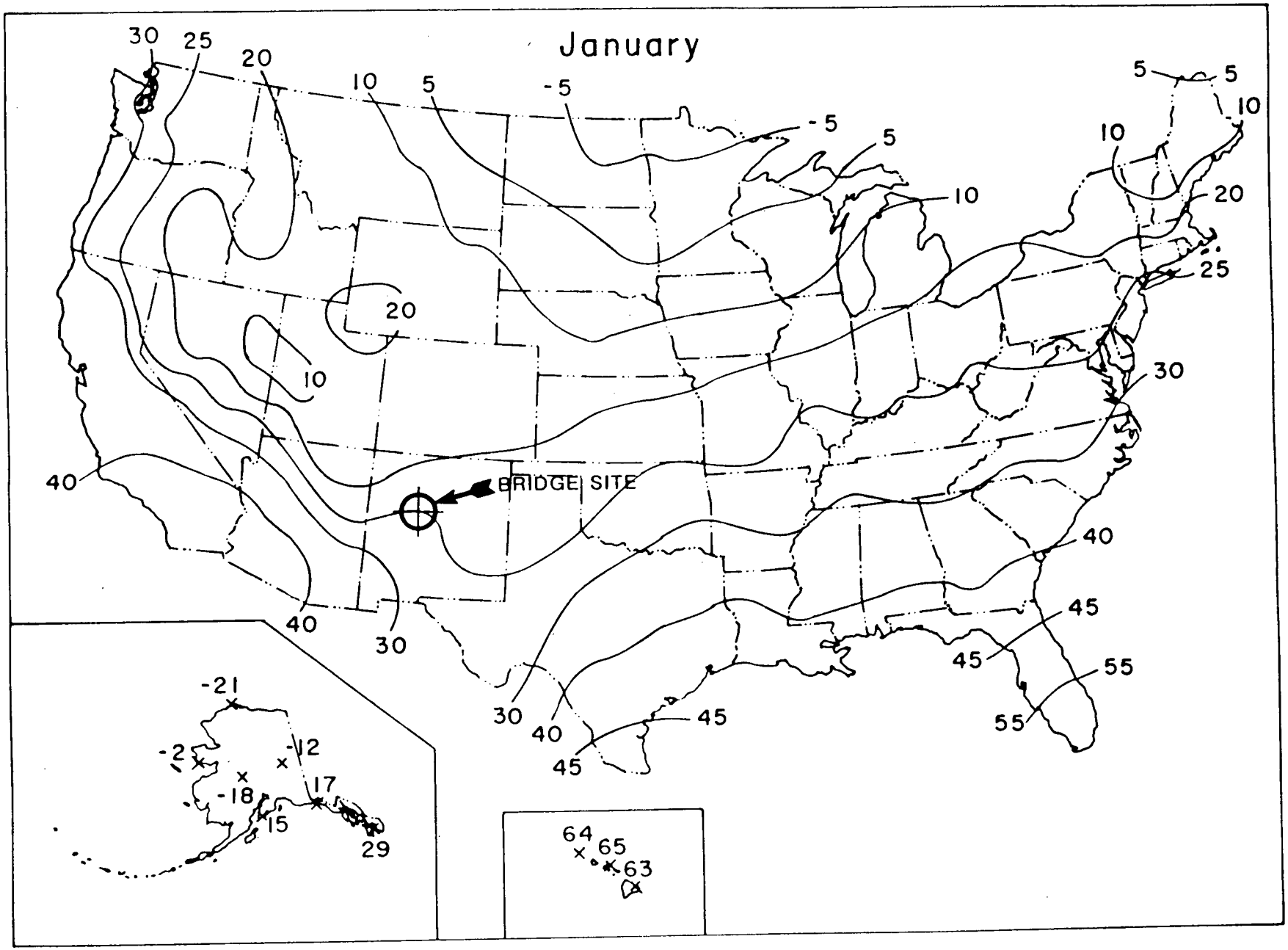

Figure C-3. Normal daily minimum temperature (°F) for January.

$$P = \int E\alpha T(Y)\, b(Y)\, dY = \int \sigma_t(Y)\, b(Y)\, dY$$

$$= \int_{-2.46}^{-1.96} [-31.84\,(Y + 1.80)]\,(12')\, dY$$

$$+ \int_{-1.96}^{-1.80} [-31.84\,(Y + 1.80)]\,(2')\, dY$$

$$+ \int_{-1.74}^{0.55} [18.35\,(Y + 1.74)]\,(2')\, dY$$

$$+ \int_{0.55}^{0.87} [57.29\,(Y - 0.55) + 42.00]\,(2')\, dY$$

$$+ \int_{0.87}^{1.21} [57.29\,(Y - 0.55) + 42.00]\,(20')\, dY$$

$$+ \int_{1.21}^{1.54} [445.45\,(Y - 1.21) + 79.80]\,(20')\, dY$$

$$= 78.33 + 0.82 + 96.23 + 32.75 + 476.49 + 1011.80$$

$$= 1696.41 \text{ k}$$

The restraining axial stress is found using Eq. 4 in Chapter Three. Noting that the cross-sectional area of the member is given by

$$A = \int_Y b(Y)\, dY = 25.1 \text{ ft}^2$$

where

$$\sigma_P(Y) = \frac{P}{A} = \frac{1696.41 \text{ k}}{25.1 \text{ ft}^2} = 67.6 \text{ ksf} = 469.3 \text{ psi}$$

- Step 5: Determine the restraining bending stress. The restraining end moment is evaluated from Eq. 5 in Chapter Three:

$$M = \int E\alpha T(Y)\, b(Y)\, Y dY = \int \sigma_t(Y)\, b(Y)\, Y dY$$

$$= \int_{-2.46}^{-1.96} [-31.84\,(Y + 1.80)]\,(12')\, Y\, dY$$

$$+ \int_{-1.96}^{-1.80} [-31.84\,(Y + 1.80)]\,(2')\, Y\, dY$$

$$+ \int_{-1.74}^{0.55} [18.35\,(Y + 1.74)]\,(2')\, Y\, dY$$

$$+ \int_{0.55}^{0.87} [57.29\,(Y - 0.55) + 21.00]\,(2')\, Y\, dY$$

$$+ \int_{0.87}^{1.21} [57.29\,(Y - 0.55) + 42.00]\,(20')\, Y\, dY$$

Table C-2. Correlation between normal daily minimum temperature and minimum effective bridge temperature.

Normal Daily Minimum Temperature °F	Minimum Effective Bridge Temperature Type of Superstructure		
	Concrete °F	Composite °F	Steel Only °F
-30	-3	-12	-43
-25	0	-9	-36
-20	3	-7	-30
-15	5	-4	-24
-10	8	-1	-17
-5	11	2	-10
0	13	4	-5
5	16	9	0
10	19	14	5
15	22	17	11
20	25	22	16
25	29	26	22
30	32	31	27
35	35	36	33
40	38	40	38

$$+ \int_{1.21}^{1.54} [445.45\,(Y - 1.21) + 79.80]\,(20')\, Y\, dY$$

$$= -177.08 - 1.55 - 20.53 + 23.56 + 499.30 + 1417.91$$

$$= 1741.61 \text{ k-ft}$$

The bending moments in the superstructure are found by applying the end restraining moments and axial forces to the abutments and performing a structural analysis. Only moments and axial forces at the ends of the superstructure are needed to restrain a prismatic superstructure (i.e., constant cross section along the length). The moments and axial forces obtained from a structural analysis are shown in Figure C-8.

The bending stresses due to the restraining moment are obtained from Eq. 5. Noting that the moment of inertia for the cross section is given by

$$I = \int_Y b(Y)\, Y\, dY = 55.1 \text{ ft}^4$$

which gives

$$\sigma_m(Y) = \frac{MY}{I}$$

$$\text{Abut 1: } \sigma_m(Y) = \frac{1742 \text{ k-ft}}{55.1 \text{ ft}^4} Y = 31.6\, Y \text{ ksf}$$

$$= 219.5\, Y \text{ psi}$$

$$\text{Bent 2: } \sigma_m(Y) = \frac{98 \text{ k-ft}}{55.1 \text{ ft}^4} Y = 1.8\, Y \text{ ksf}$$

$$= 12.4\, Y \text{ psi}$$

$$\sigma_m(Y) = \frac{674 \text{ k-ft}}{55.1 \text{ ft}^4} Y = 12.2\, Y \text{ ksf}$$

$$= 84.9\, Y \text{ psi}$$

- Step 6: Determine the self-equilibrating stresses. The self-equilibrating stresses are obtained by adding the negative of the restraining axial and bending stresses to the thermally induced stresses determined assuming a fully restraining structure, as shown in Figure C-9.

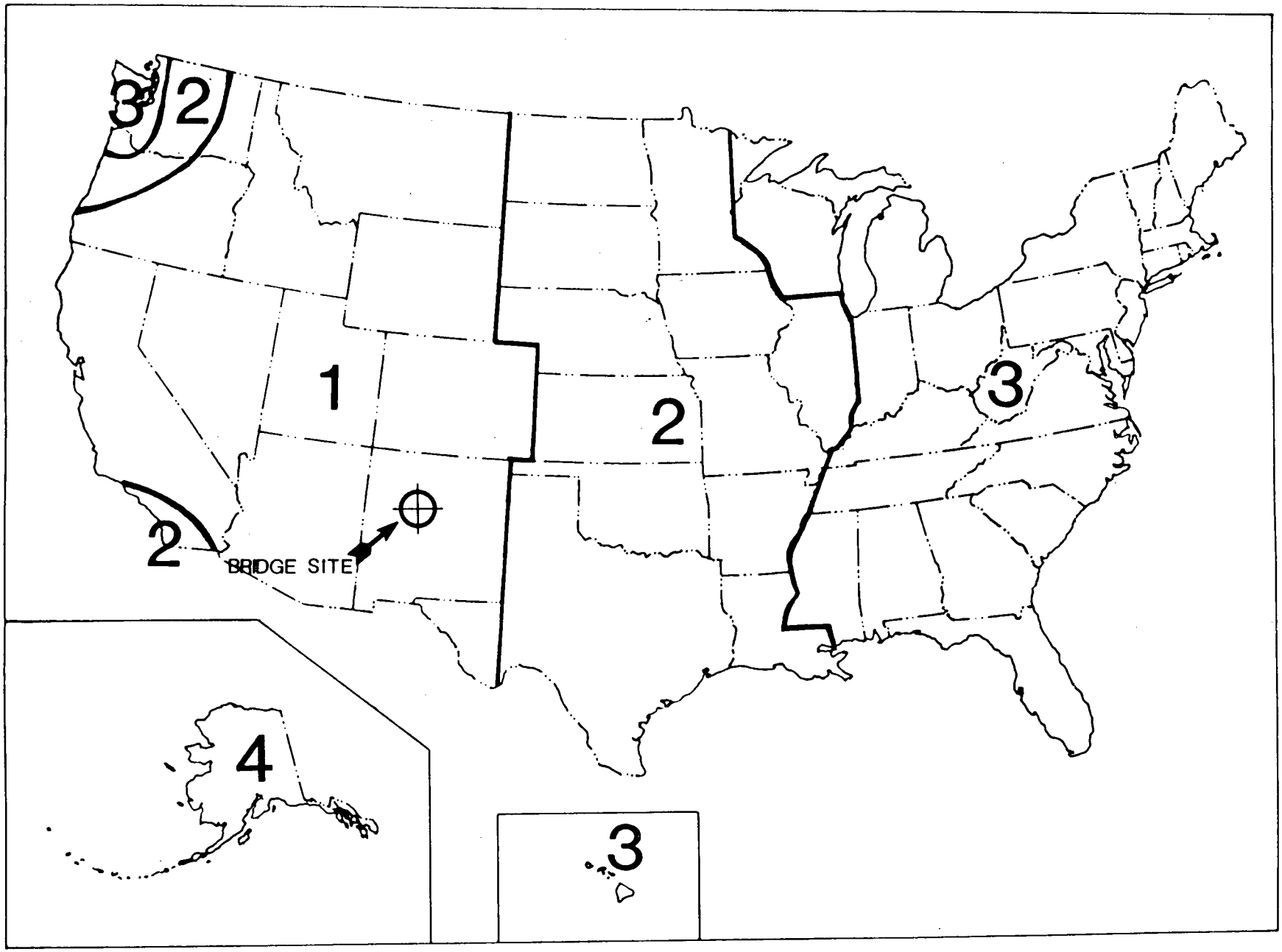

Figure C-4. Maximum solar radiation zones for the United States.

(b) *Negative Gradient Stress Distribution*

- Step 1: Determine the solar radiation zone at the bridge site from Figure C-4.

  Albuquerque, NM: Zone 1 (Plain concrete)

- Step 2: Determine the temperature gradient from Figure C-10. The temperature distribution is shown in Figure C-11.
- Step 3: Determine the thermally induced stresses assuming a totally restrained structure. The thermally induced stresses are computed identically to those of the positive gradient:

$$\sigma_t(Y) = 4.20\ T(Y)$$

  This stress distribution is shown in Figure C-12.
- Steps 4 through 6 are identical to those presented in the positive gradient section.

Figures C-13 and C-14 show the top fiber stress and bottom fiber stress along the superstructure. These results are compared to another method which applied fictitious prestress forces to simulate the stresses induced at the restrained end of the bridge. The two methods give close comparison. This method of applying fictitious prestress forces will be presented in Example 2.

EXAMPLE 2

Problem

The West Silver Eagle Bridge, which was analyzed in Chapter Five, will be used for this example, This structure, shown in Figure C-15, is a six-span 745-ft long bridge. The bridge is located in Zone 1 and assumed to have a plain concrete surface. Young's modulus is 3,350 ksi and the coefficient of thermal expansion is 6.0×10^{-6} in./in./°F. Determine the amount of reinforcement needed to resist the thermal stresses. The method used to calculate the self-equilibrating stresses was the equivalent prestress method.

Solution

1. *Positive Gradient Stress Distribution*

(a) Step 1: Determine the temperature gradient from Chapter Three. The temperature distribution is shown in Figure C-16.

(b) Step 2: Determine the thermally induced stresses assuming a totally restrained structure. The thermally induced stresses are computed using Eq. 2.

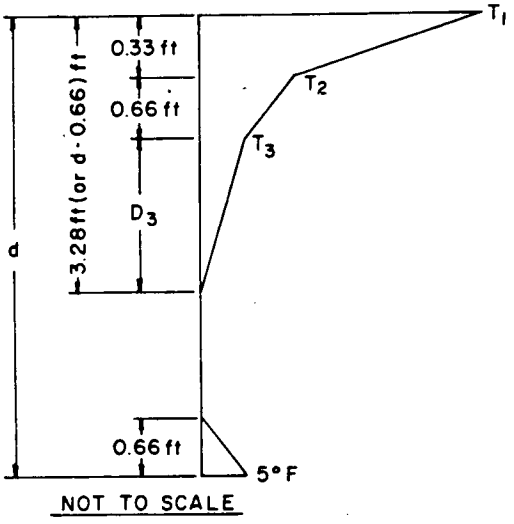

Plain Concrete Surface

T_1 (°F)	T_2 (°F)	T_3 (°F)
54	14	5
46	12	4
41	11	4
38	9	3

2 in. Blacktop

T_1 (°F)	T_2 (°F)	T_3 (°F)
43	14	4
36	12	4
33	11	3
29	9	2

4 in. Blacktop

T_1 (°F)	T_2 (°F)	T_3 (°F)
31	9	3
25	10	3
23	11	2
22	11	2

Figure C-5. Positive temperature gradient for a concrete bridge superstructure.

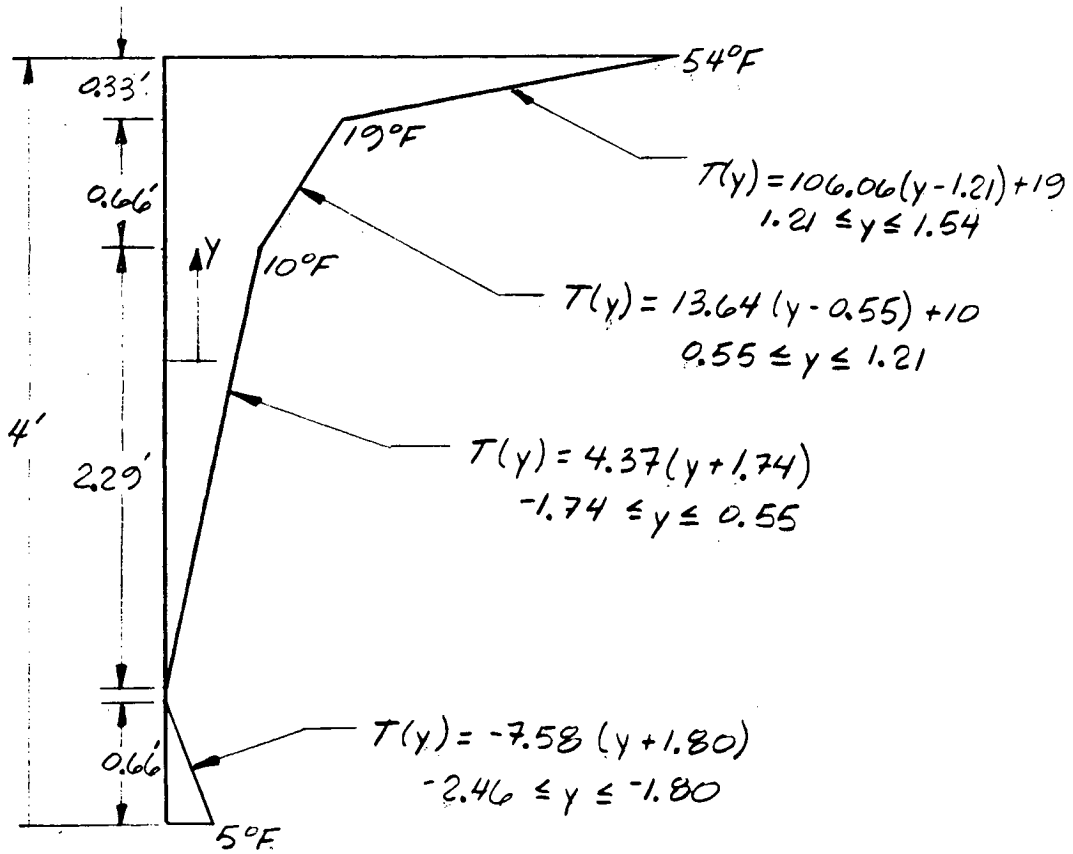

Figure C-6. Temperature distribution for a positive temperature gradient.

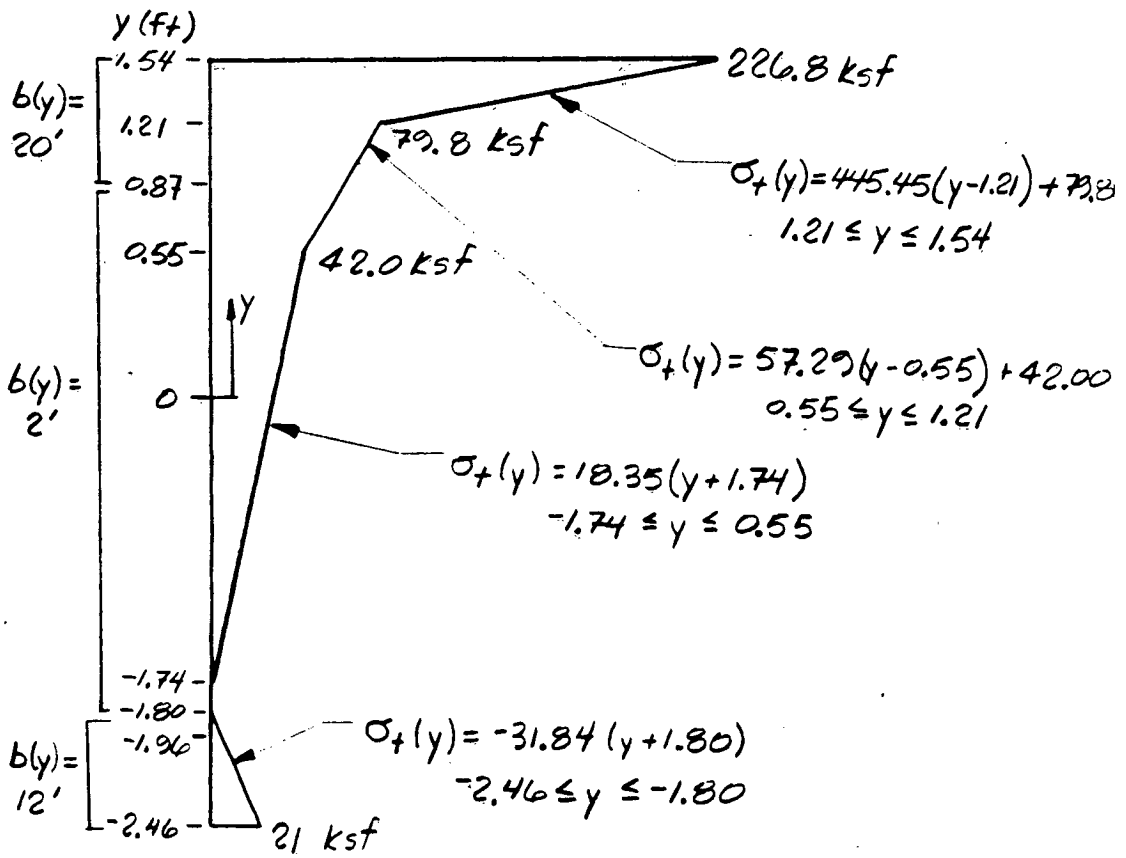

Figure C-7. Thermally induced stress distribution.

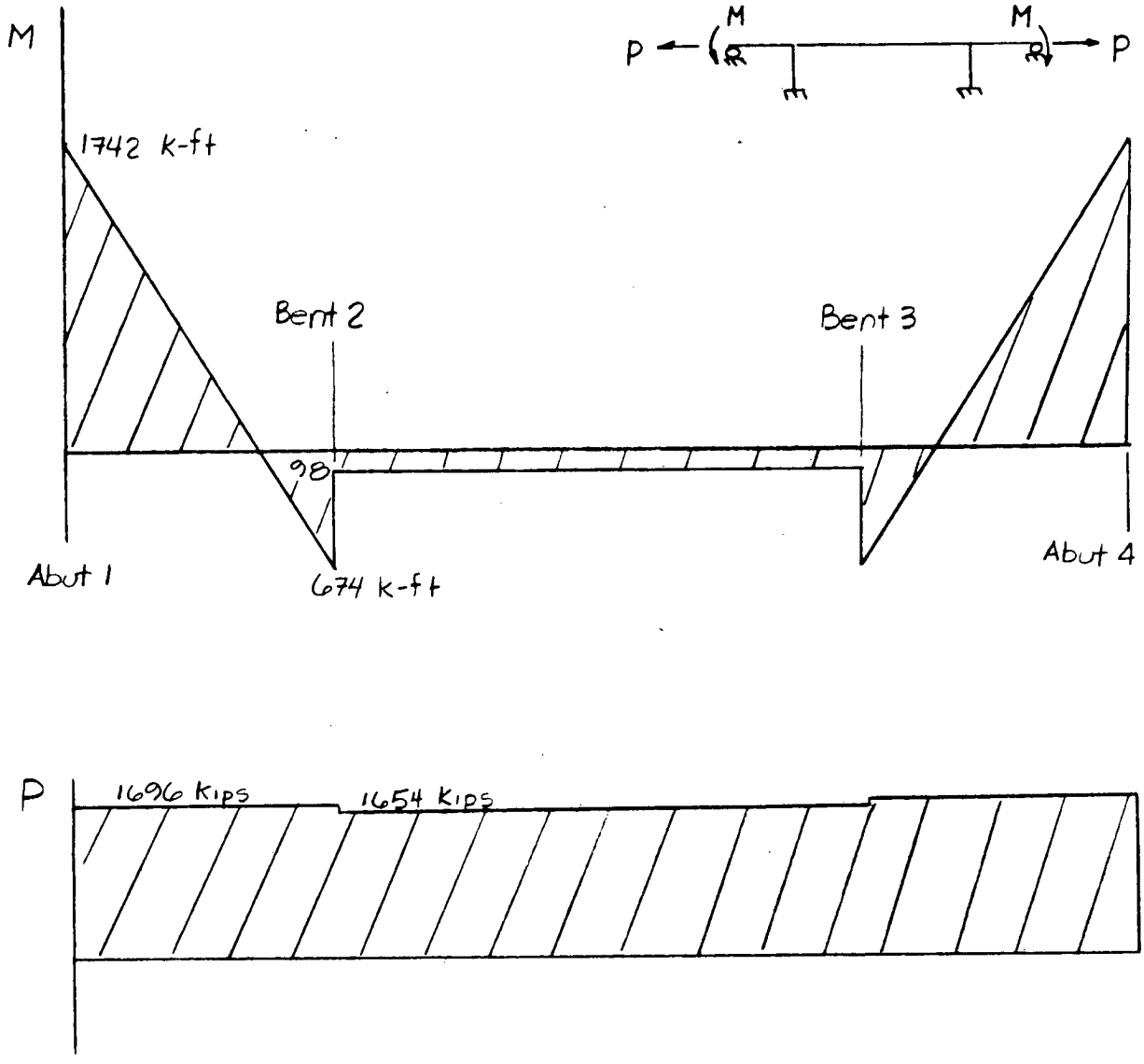

Figure C-8. Moment and axial force diagram due to end restraining forces.

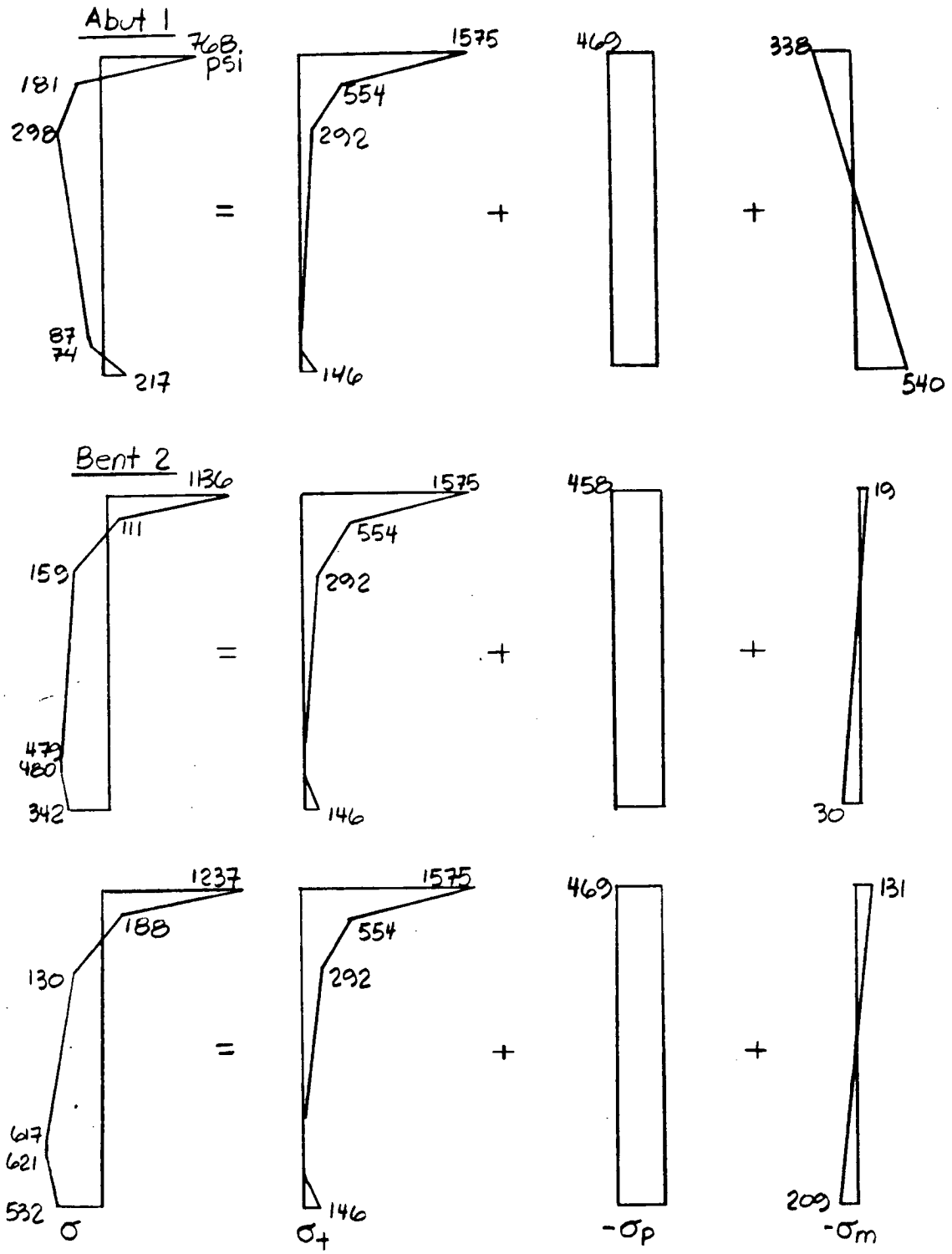

Figure C-9. Self-equilibrating stresses.

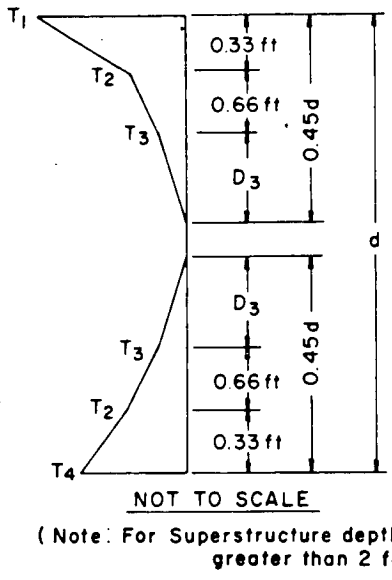

Plain Concrete Surface

T_1 (°F)	T_2 (°F)	T_3 (°F)	T_4 (°F)
27	7	2	14
23	6	2	10
21	6	2	8
19	5	2	6

2 in. Blacktop

T_1 (°F)	T_2 (°F)	T_3 (°F)	T_4 (°F)
22	7	2	15
18	6	2	11
17	6	2	10
15	5	1	8

4 in. Blacktop

T_1 (°F)	T_2 (°F)	T_3 (°F)	T_4 (°F)
16	5	1	12
13	5	1	9
12	6	1	8
11	6	1	8

Figure C-10. Negative temperature gradient for a concrete bridge superstructure.

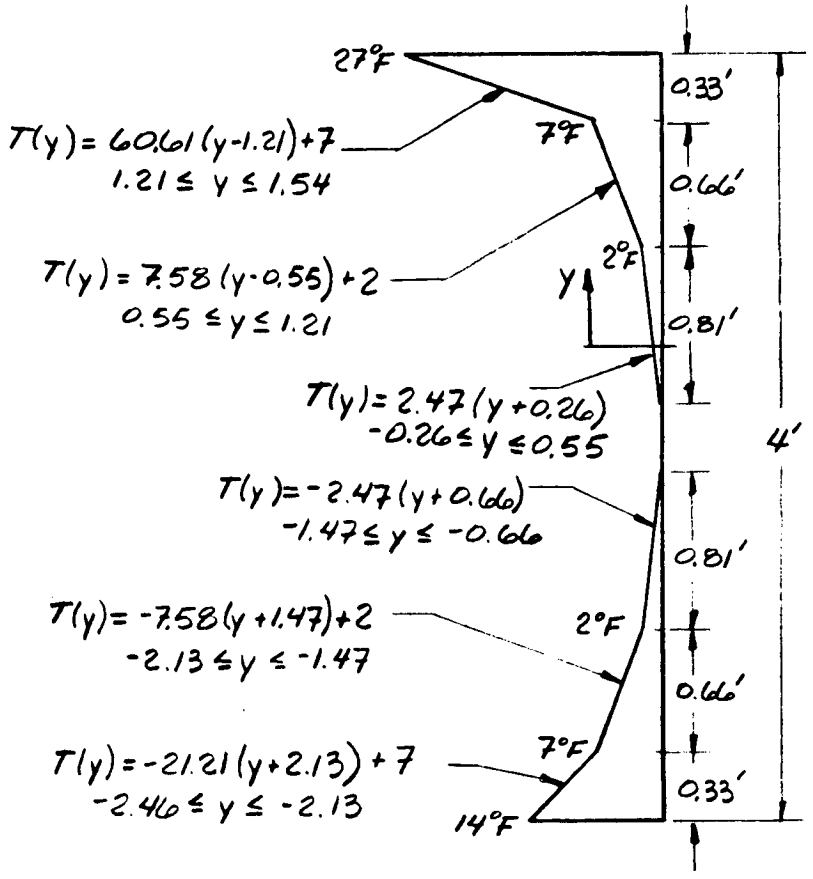

Figure C-11. Temperature distribution for a negative temperature gradient.

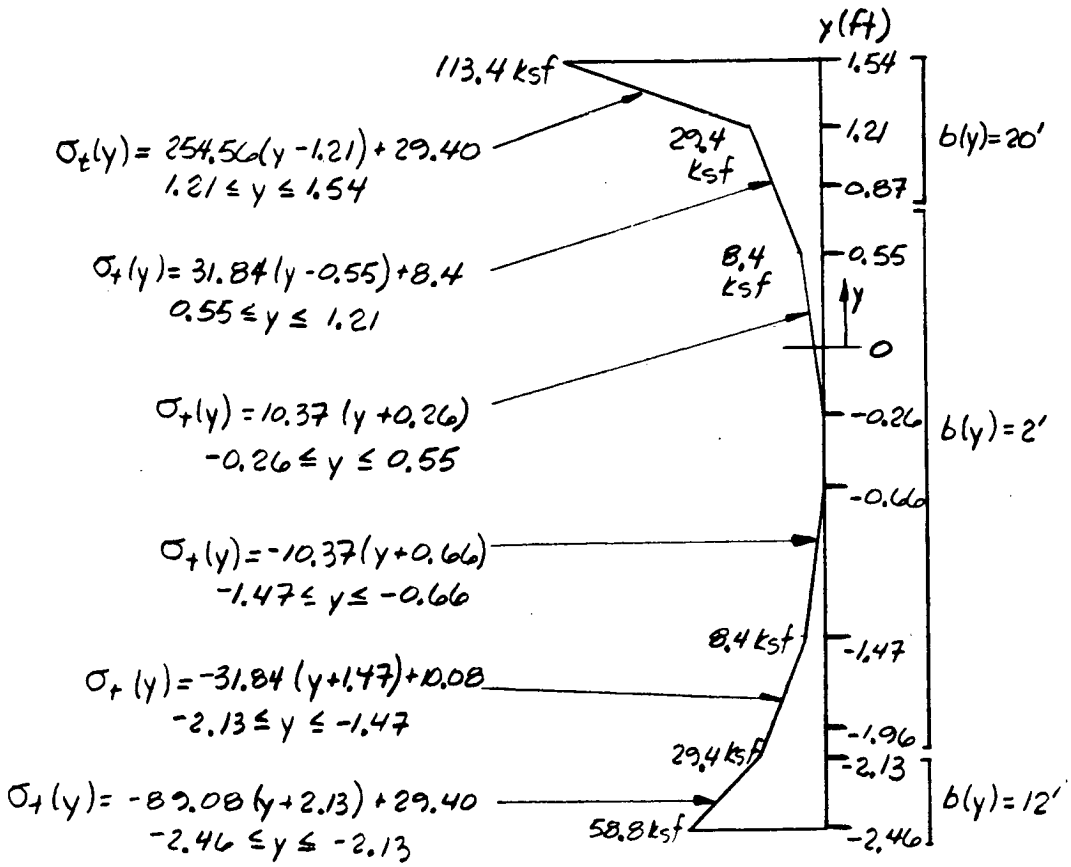

Figure C-12. Thermally induced stress distribution.

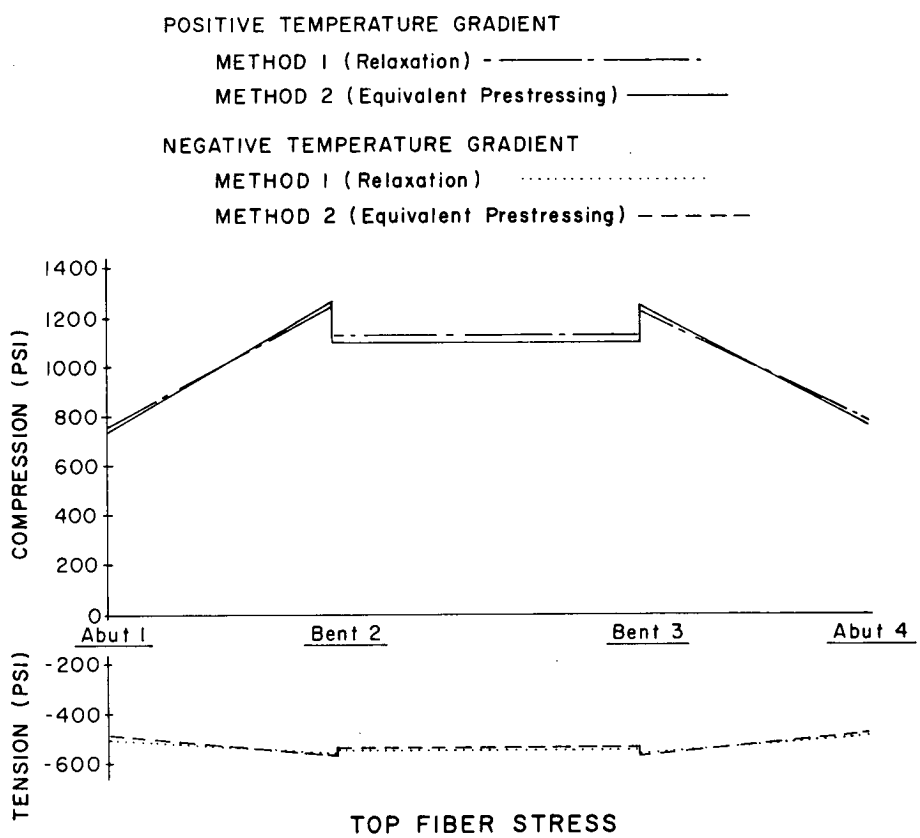

Figure C-13. Top fiber stress.

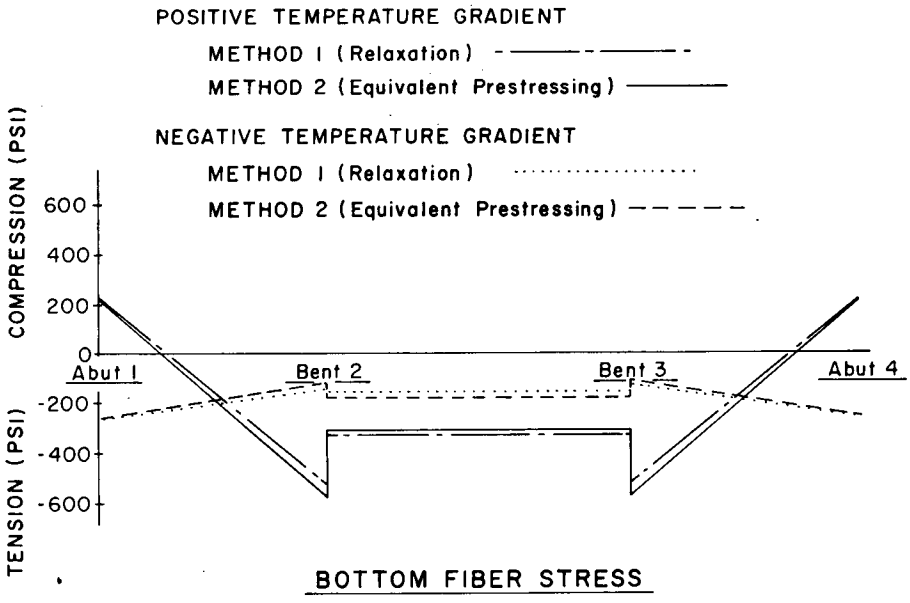

Figure C-14. Bottom fiber stress.

$$\sigma_t(Y) = E\alpha T(Y)$$
$$= (3350 \text{ ksi})\,(6.0 \times 10^{-6} \text{ in./in./°F})\,T(Y)$$
$$= 0.02010\,T(Y)$$

Table C-3 gives the thermally induced stresses for the relevant temperatures shown in Figure C-16.

(c) Step 3: Determine the equivalent prestress forces. The equivalent prestress forces, P_f, are shown schematically in Figure C-17 and the P-jack forces, P_j, which were used in a plane frame prestress program, are given in Table C-4.

(d) Step 4: Apply the equivalent prestress forces to the superstructure and calculate the self-equilibrating stresses by adding the negative of the results from the equivalent prestress method to the thermally induced stresses assuming a fully restrained structure. Table C-5 gives the self-equilibrating stresses at selected points along the superstructure. For illustrative purposes a selected self-equilibrating stress distribution at 0.9 point of span 1 is shown in Figure C-18.

2. *Negative Gradient Stress Distribution*

(a) Step 1: Determine the temperature gradient from Chapter Three. The temperature distribution is shown in Figure C-19.

(b) Step 2: Determine the thermally induced stresses assuming a totally restrained surface. The thermally induced stresses are computed using Eq. 2:

$$\sigma_t(Y) = E\alpha T(Y)$$
$$= (3350 \text{ ksi})\,(6.0 \times 10^{-6} \text{ in./in./°F})\,T(Y)$$
$$= 0.02010\,T(Y)$$

Table C-6 gives the thermally induced stresses for the relevant temperatures shown in Figure C-19.

(c) Step 3: Determine the equivalent prestress forces. The equivalent prestress forces, P, are shown schematically in Figure C-20 and the P-jack forces, which were used in a plane frame prestress program, are given in Table C-7.

(d) Step 4: Apply the equivalent prestress forces to the superstructure and calculate the self-equilibrating stresses by adding the negative of the results from the equivalent prestress method to the thermally induced stresses assuming a fully restrained structure. Table C-8 gives the self-equilibrating stresses at selected points along the superstructure.

(e) Step 5: Evaluate the amount of reinforcement required.

- *Top Fiber Stresses*

The top fiber stresses along the superstructure are shown in Figure C-21. The point of control, which is found by inspection, is at 0.0 point of span 4. The final stress distribution at this location (shown in Figure C-22) is determined by adding the temperature effects to the dead, prestress, and live load effects. The amount of reinforcement is calculated as follows:

$$T = \left\{\left(\frac{0.719 + 0.190}{2}\right) + \left(\frac{0.190 + 0.043}{2}\right)\right\} \text{ ksi}$$
$$\times\ 0.33' \times 52' \times 144 \text{ in.}^2/\text{ft}^2$$
$$= 1.411 \text{ kips}$$

$$A = \frac{1{,}411 \text{ k}}{36 \text{ ksi}} = 39.2 \text{ in.}^2$$

Existing Reinforcement (for M_u) = 0.00 in.
Existing Long. Reinforcement = #5 (total 39) + #4 (total 63)
= 24.7 in.^{2}.

Need 14.5 in.^{2} more reinforcement.

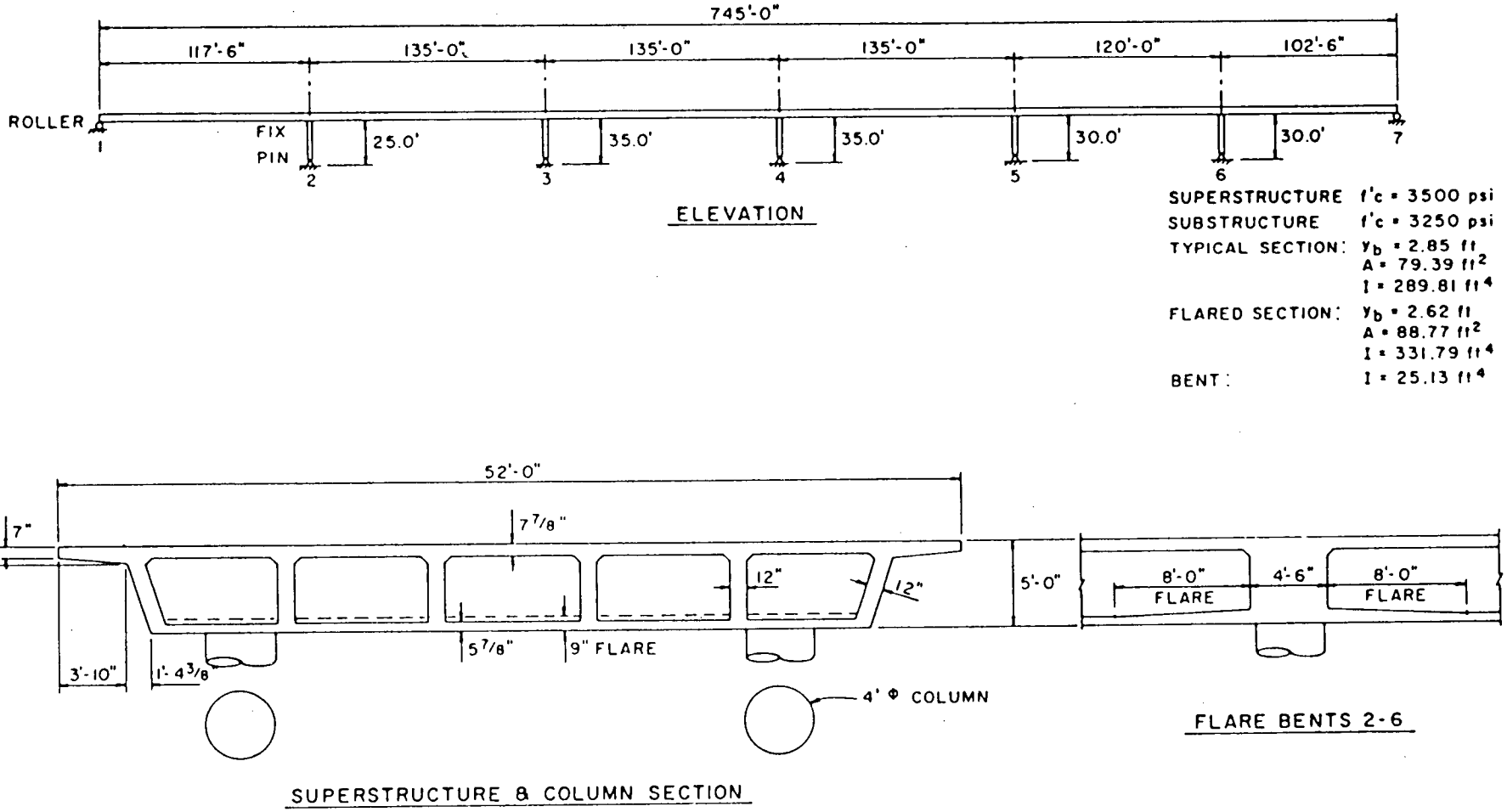

Figure C-15. Case 2L—West Silver Eagle Bridge and overhead superstructure and substructure details used for analysis.

- *Bottom Fiber Stresses*
  The bottom fiber stresses along the superstructure are shown in Figure C-23. The point of control is from the positive gradient curve at 0.5 point of span 4. The final stress distribution at this location (shown in Figure C-24) is determined by adding the temperature effects to the dead, prestress, and live load effects. The amount of reinforcement is calculated as follows:

$$T = \left[\frac{0.267 + 0.220}{2}\right] \text{ksi} \times 0.49' \times 41.8' \times 144 \text{ in.}^2/\text{ft}^2$$

$$= 718 \text{ kips}$$

$$A_s = \frac{718 \text{ k}}{36 \text{ k/in.}^2} = 19.9 \text{ in.}^2$$

Existing Reinforcement = #5 (total 28) = 8.7 in.^{2}
Need 11.2 in.^{2} more reinforcement.

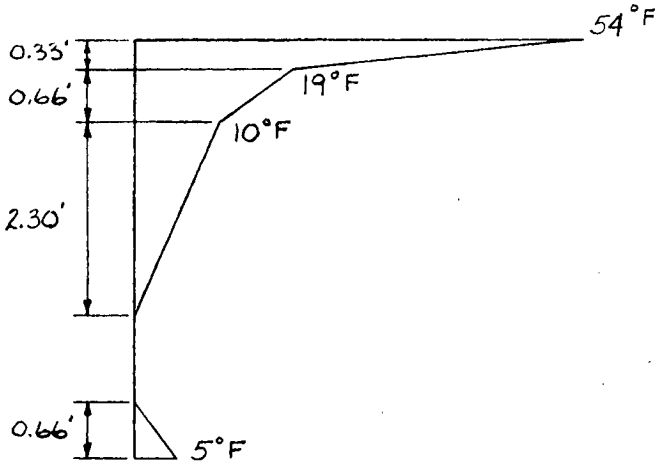

Figure C-16. Temperature distribution for a positive temperature gradient.

Table C-3. Thermally induced stresses for the positive gradient.

T(°F)	σ_t(psi)
54	1085
19	382
10	201
5	101

Table C-4. P-Jack used in the prestress program.

Path	Average Stress (psi)	Area (in^2)	P_f (k)	P_j (k)
1	352	2,471	870	879
2	382	2,471	944	954
3	45	2,471	111	112
4	292	2,471	722	729
5	45	285	13	14
6	201	285	57	58
7	100	1,987	199	201
8	13	147	2	2
9	26	2,936	76	77
10	38	2,936	112	113

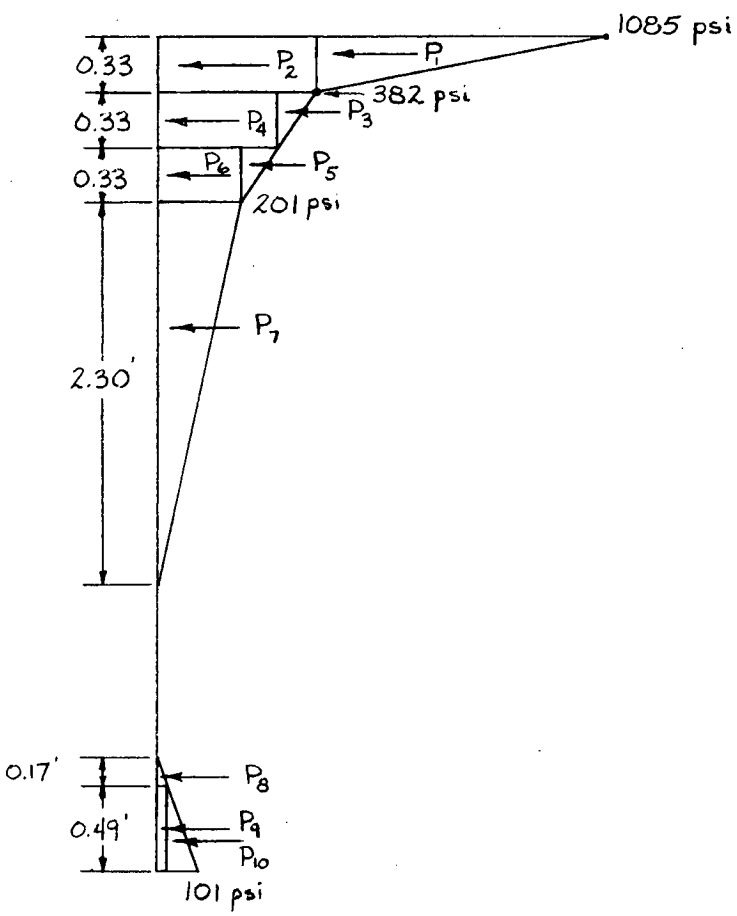

Figure C-17. Equivalent prestress forces.

Table C-5. Self-equilibrating stresses.

		TOP FIBER				BOTTOM FIBER			
Span	Point	Fully Restrained (psi)	Negative Prestress (psi)	Axial Correction (psi)	Self-Equil. Stresses (psi)	Fully Restrained (psi)	Negative Prestress (psi)	Axial Correction (psi)	Self-Equil. Stresses (psi)
	0.0	1085	-487	0	598	101	54	0	155
1	0.9	1085	-195	0	890	101	-336	0	-235
	1.0	1085	-172	0	913	101	-290	0	-189
	0.0	1085	-232	4	857	101	-224	4	-119
2	0.1	1085	-227	4	862	101	-293	4	-188
	0.9	1085	-254	4	835	101	-258	4	-153
	1.0	1085	-265	4	824	101	-189	4	- 84
	0.0	1085	-272	4	817	101	-181	4	- 76
3	0.1	1085	-263	4	826	101	-246	4	-141
	0.9	1085	-249	4	840	101	-266	4	-161
	1.0	1085	-254	4	835	101	-201	4	- 96
	0.0	1085	-250	4	839	101	-206	4	-101
4	0.1	1085	-245	4	844	101	-270	4	-165
	0.9	1085	-269	4	820	101	-238	4	-133
	1.0	1085	-279	4	810	101	-173	4	- 68
	0.0	1085	-258	3	830	101	-196	3	- 92
5	0.1	1085	-248	3	840	101	-266	3	-162
	0.9	1085	-225	3	863	101	-295	3	-191
	1.0	1085	-231	3	857	101	-225	3	-121
	0.0	1085	-178	0	907	101	-284	0	-183
6	0.1	1085	-200	0	885	101	-330	0	-229
	1.0	1085	-487	0	598	101	54	0	155

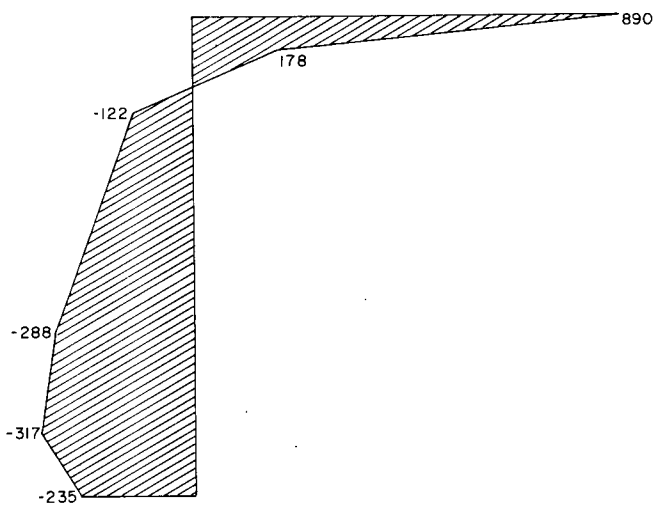

Figure C-18. Self-equilibrating stresses at 0.9 point of span 1.

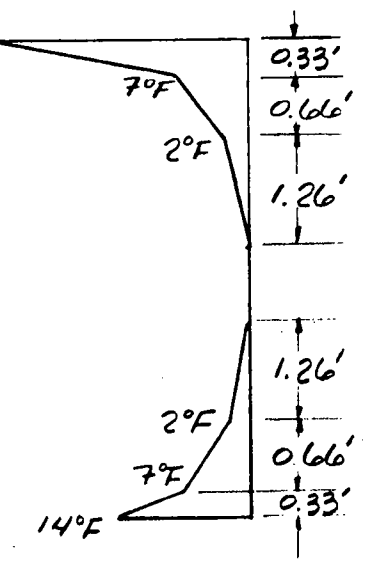

Figure C-19. Temperature distribution for a negative temperature gradient.

Table C-6. Thermally induced stresses for the positive gradient.

T(°F)	∇_t(psi)
27	-543
7	-141
2	-40
14	-289

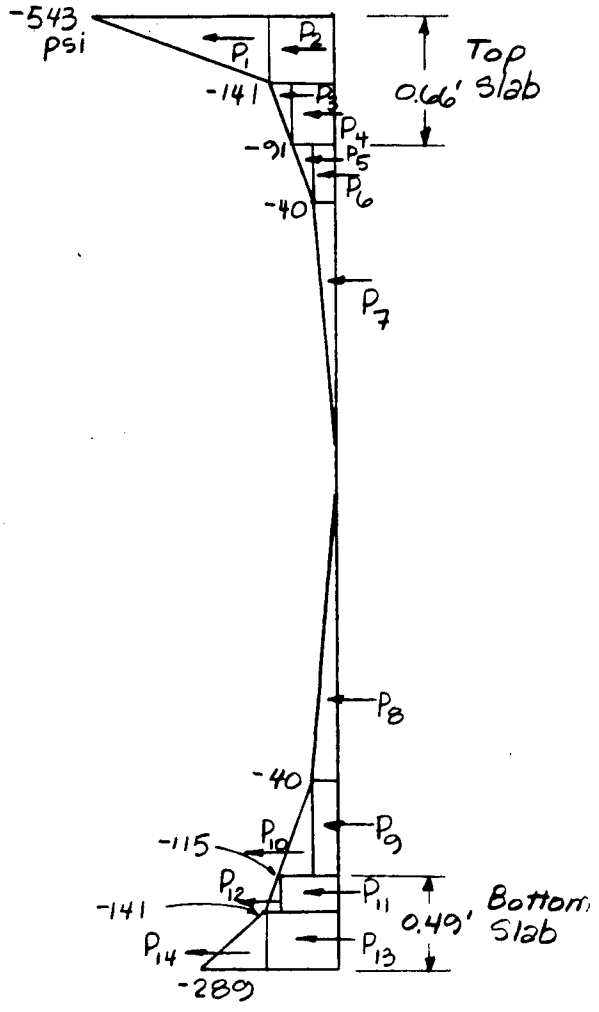

Figure C-20. Equivalent prestress forces.

Table C-7. P-Jack forces used in the prestress program.

Path	Average Stress (psi)	Area (in^2)	P_f (k)	P_i (k)
1	201	2,471	497	502
2	141	2,471	348	352
3	25	2,471	62	63
4	91	2,471	225	227
5	25	285	7	7
6	40	285	11	11
7	20	1,089	22	22
8	20	1,089	22	22
9	40	432	17	17
10	38	432	16	16
11	115	963	111	112
12	13	963	13	13
13	141	1,986	280	283
14	74	1,986	147	148

Table C-8. Self-equilibrating stresses.

		TOP FIBER				BOTTOM FIBER			
Span	Point	Fully Restrained (psi)	Negative Prestress (psi)	Axial Correction (psi)	Self-Equil. Stresses (psi)	Fully Restrained (psi)	Negative Prestress (psi)	Axial Correction (psi)	Self-Equil. Stresses (psi)
1	0.0	-543	190	0	-353	-289	111	0	-178
1	0.9	-543	137	0	-406	-289	182	0	-107
1	1.0	-543	137	0	-406	-289	144	0	-145
2	0.0	-543	166	-2	-379	-289	112	-2	-179
2	0.1	-543	160	-2	-385	-289	152	-2	-139
2	0.9	-543	151	-2	-394	-289	164	-2	-127
2	1.0	-543	155	-2	-390	-289	124	-2	-167
3	0.0	-543	161	-2	-384	-289	117	-2	-174
3	0.1	-543	156	-2	-389	-289	157	-2	-134
3	0.9	-543	154	-2	-391	-289	160	-2	-131
3	1.0	-543	159	-2	-386	-289	120	-2	-171
4	0.0	-543	157	-2	-358	-289	122	-2	-169
4	0.1	-543	153	-2	-392	-289	162	-2	-129
4	0.9	-543	160	-2	-385	-289	153	-2	-138
4	1.0	-543	165	-2	-380	-289	113	-2	-178
5	0.0	-543	152	-1	-392	-289	128	-1	-162
5	0.1	-543	148	-1	-396	-289	168	-1	-122
5	0.9	-543	159	-1	-385	-289	153	-1	-137
5	1.0	-543	165	-1	-379	-289	113	-1	-177
6	0.0	-543	139	0	-404	-289	141	0	-148
6	0.1	-543	140	0	-403	-289	179	0	-110
6	1.0	-543	190	0	-353	-289	111	0	-178

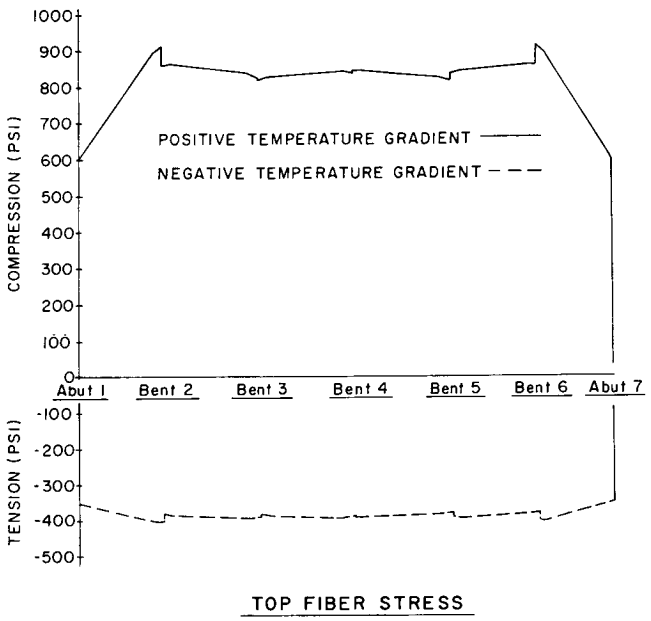

Figure C-21. Top fiber stresses for Example 2.

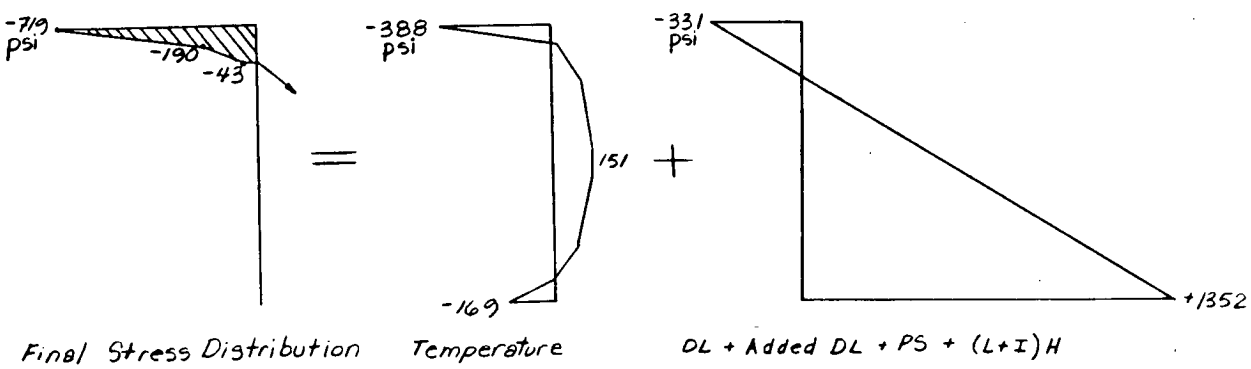

Figure C-22. Final stress distribution.

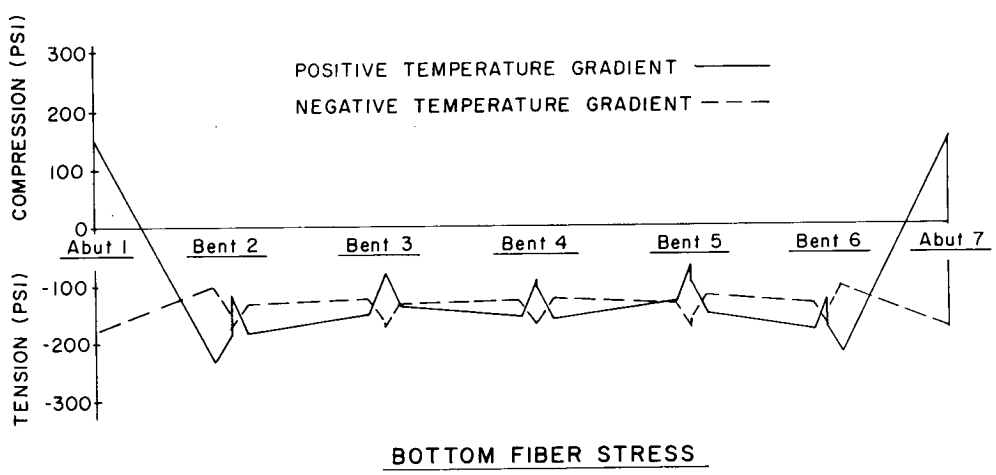

Figure C-23. Bottom fiber stresses for Example 2.

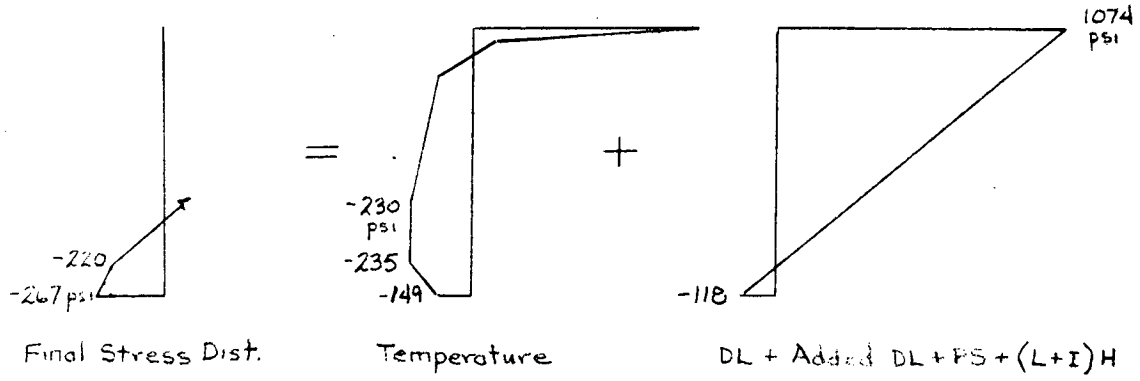

Figure C-24. Final stress distribution.

APPENDIX D AND APPENDIX E

Appendix D, "Summary of Bridge Design Codes of Different Countries," and Appendix E, "Alternative Analysis Procedures for Calculating Thermally Induced Longitudinal Stresses," are not published herewith but are contained in the agency final report as submitted to the sponsors, and are available on a loan basis on request to the Director, Cooperative Research Programs.

THE TRANSPORTATION RESEARCH BOARD is a unit of the National Research Council, which serves the National Academy of Sciences and the National Academy of Engineering. The Board's purpose is to stimulate research concerning the nature and performance of transportation systems, to disseminate information that the research produces, and to encourage the application of appropriate research findings. The Board's program is carried out by more than 270 committees, task forces, and panels composed of more than 3,300 administrators, engineers, social scientists, attorneys, educators, and others concerned with transportation; they serve without compensation. The program is supported by state transportation and highway departments, the modal administrations of the U.S. Department of Transportation, the Association of American Railroads, the National Highway Traffic Safety Administration, and other organizations and individuals interested in the development of transportation.

The National Research Council was established by the National Academy of Sciences in 1916 to associate the broad community of science and technology with the Academy's purposes of furthering knowledge and of advising the Federal Government. The Research Council has become the principal operating agency of both the National Academy of Sciences and the National Academy of Engineering in the conduct of their services to the government, the public, and the scientific and engineering communities. It is administered jointly by both Academies and the Institute of Medicine.

The National Academy of Sciences was established in 1863 by Act of Congress as a private, nonprofit, self-governing membership corporation for the furtherance of science and technology, required to advise the Federal Government upon request within its fields of competence. Under its corporate charter the Academy established the National Research Council in 1916, the National Academy of Engineering in 1964, and the Institute of Medicine in 1970.

TRANSPORTATION RESEARCH BOARD
National Research Council
2101 Constitution Avenue, N.W.
Washington, D.C. 20418

ADDRESS CORRECTION REQUESTED